5-2023

Physical Model of Rainwater Along Roadway Filter Strip

Ryan C. Eberhard
Utah State University

PHYSICAL MODEL OF RAINWATER ALONG ROADWAY FILTER STRIP

by

Ryan C. Eberhard

A thesis submitted in partial fulfillment
of the requirements for the degree

of

MASTER OF SCIENCE

in

Civil and Environmental Engineering

Approved:

John D. Rice, Ph.D., P.E., G.E. Major Professor	Brian M. Crookston, Ph.D., P.E. Committee Member
Brady R. Cox, Ph.D., P.E. Committee Member	D. Richard Cutler, Ph.D. Vice Provost of Graduate Studies

UTAH STATE UNIVERSITY

Logan, Utah

2023

ABSTRACT

Physical Model of Rainwater Along Roadway Filter Strip

by

Ryan C. Eberhard, Master of Science

Utah State University, 2023

Major Professor: Dr. John Rice
Department: Civil and Environmental Engineering

The purpose of this research was to investigate infiltration rates of rainwater into a roadside filter strip. The findings of this study were intended to be used by the Utah Department of Transportation in their design of stormwater retention. A testing apparatus was designed and constructed to simulate rainfall runoff and infiltration on a 3-foot by 20-foot inclined slope during the 80th percentile 24-hour rainstorm event in Utah. The model was used to test six different surface soil configurations at three slope inclinations.

The six testing configurations consisted of a 19-inch thick soil layer. The initial tests were run on 19 inches of embankment fill and successive tests were conducted on 15 inches of embankment fill beneath 4 inches of topsoil. Two types of topsoil were tested each with bare soil and with vegetation cover that had grown for a minimum of 42 days. One configuration included scarifying the top 6 inches of the embankment material overlain with topsoil. Each configuration was tested at three inclinations of 6:1, 4:1, and 2:1 (horizontal to vertical). Each test was subjected to a simulated storm event of ½ inches of rain over a 2-hour period.

The variation in the top 4 inches of soil resulted in the most significant changes to the amount of infiltration while the slope had little effect on infiltration for the two topsoil materials. The addition of vegetation resulted in increased amounts of infiltration as did the scarifying beneath the topsoil. After further testing, the results of this study will be used to update the Utah Department of Transportation's Best Practices Manual for estimating rainfall infiltration.

(181 pages)

PUBLIC ABSTRACT

Physical Model of Rainwater Along Roadway Filter Strip

Ryan C. Eberhard

The purpose of this research was to investigate infiltration rates of rainwater into a roadside filter strip. The findings of this study were intended to be used by the Utah Department of Transportation in their design of stormwater retention. A testing apparatus was designed and constructed to simulate rainfall and infiltration on an inclined slope during the 80th percentile 24-hour rainstorm event in Utah. The model was used to test six different surface soil configurations at three slope inclinations. Each test was subjected to a simulated storm event of ½ inch of rain over a 2-hour period. The variation in the top 4 inches of soil resulted in the most significant changes to the amount of infiltration, while the slope had little effect on infiltration for the two topsoil materials. The addition of vegetation resulted in increased amounts of infiltration as did the scarifying beneath the topsoil.

ACKNOWLEDGMENTS

This study was funded by the Utah Department of Transportation and I would like thank them for the opportunity I have had to work on this research project for them. Special thanks to the Utah Water Research Lab for the use of their facilities and equipment for the duration of this project. I would like to thank Dr. John Rice and Dr. Brian Crookston for the opportunity I have had to work and learn from them. I am grateful for the knowledge and skills I have gained throughout this project.

I would like to thank Mom, Dad, Megan, and Nicole for their support throughout my time at Utah State University. A special thanks to Brett for his willingness to help me even on weekends. Thanks to Dr. Zac Sharp and all the shop workers at the UWRL who have helped, encouraged, and supported me while I have had the opportunity to work at the UWRL.

Ryan C. Eberhard

CONTENTS

Page

LIST OF TABLES

Page

LIST OF FIGURES

Page

LIST OF ABBREVIATIONS

AASHTO	American Association of State Highway and Transportation Officials
ASTM	American Society for Testing and Materials
ATS	Amended Topsoil
BMP	Best Management Practice
EF	Embankment Fill
LL	Liquid Limit
MS4	Municipal Separate
NCHRP	National Cooperative Highway Research Program
NRCS	National Resources Conservation Service
PI	Plasticity Index
PL	Plastic Limit
R	Ripped Material
SWRC	Soil Water Retention Curve
TS	Topsoil
UDOT	Utah Department of Transportation
USCC	US Compost Council
VWC	Volumetric Water Content

CHAPTER I

INTRODUCTION

1.1 Problem Statement

Water is a valuable resource in arid environments where there is little rainfall. Residential and commercial developments create impermeable surfaces which prevent stormwater infiltration and increase evaporation. The purpose of this study is to limit runoff to control stormwater flows. The Utah Department of Transportation is required to retain the 80th percentile 24-hr storm in their BMP designs when obtaining MS4 permits (UDOT 2021). UDOT currently has several different BMPs which aid in achieving the volume reduction goals.

A filter strip is one of the BMPs commonly used along roadways. The design of filter strips and specifically the embankment material and topsoil materials of the filter strips became the focus of the conducted research. The current design process has several steps where generalizations are made about the soils.

The NCRS soil survey map (NCRS 2022) is first used to estimate a permeability factor of the native soil. A field infiltration test should be conducted later in the analysis to provide a more accurate infiltration value. The infiltration value obtained from the field infiltration tests should be used with caution due to the variability of soils. UDOT conducted several field infiltration tests in one area, prior to this study, which resulted in a large spread of infiltration values (J. Erdman, personal communication, 2020).

Once an infiltration value is assumed the NCHRP spreadsheet tool (NCHRP 2021) is used to calculate the volume reduction capability of a particular rainstorm. An infiltration rate is assumed by selecting which hydrologic soil group best represents that material. The soil group is also found by using the NCRS soil survey map. The assumed infiltration rate from the spreadsheet, initial permeability factor from the NCRS soil survey map, and the infiltration rates from field infiltration tests are compared and engineering judgment is used to decide what infiltration value should be used in the design of the BMP.

The current process results in uncertainty in the design infiltration rate due to the assumptions about the soil and soil properties. One way the uncertainty has been decreased is by performing the field infiltration tests. The field infiltration tests could still result in uncertainty due to the variability of soil.

1.2 Objective

The objective of this research is to determine an infiltration rate design value for a roadside filter strip. The infiltration rates were found based on the gradation of the embankment material, two different overlaying topsoils, vegetation, and a variety of embankment inclinations. The testing procedures and how each of these factors were used to determine an infiltration rate are described in Chapter 3.

CHAPTER II

LITERATURE REVIEW

The purpose of this section is to review published literature on the topics of interest of this study. The topics include infiltration, matric suction potential, the effects of vegetation, and the UDOT Stormwater Quality Design Manual. Assumptions were made based on the provided information as well as certain expectations of how the different variables of the experiment would perform.

2.1 Infiltration

Infiltration is the process of surface water flowing into the ground. There are several factors which affect infiltration in a filter strip. “Design variables that may influence VFS function include slope (both longitudinal and lateral), density of vegetation, type of vegetation, infiltration rate of the underlying soil, compaction of filter strip soils, and the ratio of catchment area to filter strip area” (Winston et al. 2012).

Infiltration can also be limited by highly contrasting soil layers (USDA 2017). Amendments to soil have been used to increase infiltration. Amendments to the soil are meant to increase the saturated hydraulic conductivity of soil and allow for higher infiltration capacities. “The incorporation of compost into decomposed granite roadcuts can be used as a method to increase infiltration and reduce overland flow, particularly during the time before vegetation is established” (Curtis and Claassen 2007). Although

having differing soil layers can allow for increased infiltration, the matric suction potential of the contrasting soil layers can be a factor in infiltration volumes.

2.2 Matric Suction

The matric suction of a soil is the tensile forces between water and soil particles which can be thought of as a negative capillary force. Lu and Zhang (2019) discussed the effects of matric suction on sorption potential of soil. Fig. 1 provides an overview of how the matric suction varies with water content. The SWRC varies for different soils and therefore the matric suction will be different. Lu (2016) discovered that finer soils require higher VWC in order for the matric suction to approach zero. The addition of water is what will reduce the matric suction potential. However, capillary barriers can form at soil interfaces and absorption of water will decrease (Stormont et al. 1999).

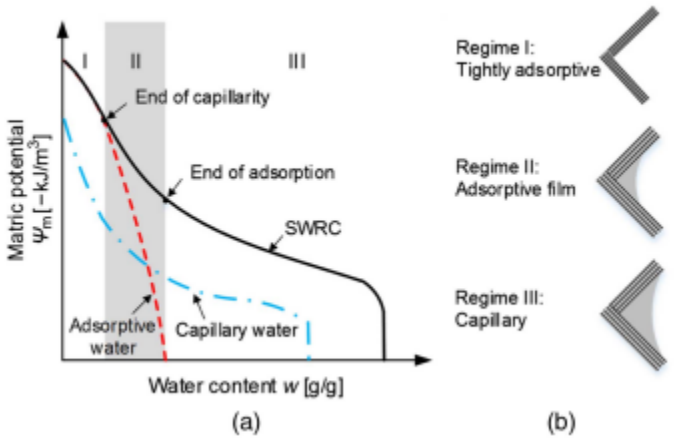

Fig. 1. (a) Generalized soil water retention curve; and (b) soil water retention regimes. (Reprinted from Lu 2016, © ASCE).

A breakthrough head at the soil interface is defined as the suction head at which water begins to flow into an underlying soil. The breakthrough head is dependent on the

two soils at the interface. Stormont et al. (1999) conducted experiments with varying soils above a coarse soil layer. The finer soils above the coarse soil layer had a higher suction head and required higher moisture content to break through the capillary barrier at the interface. A soil with a lower suction head will allow infiltration at lower moisture content and allow infiltration to begin earlier than a soil with a high suction head.

The matric suction can be affected by the type of soil and also amendments/ treatments to the soil. “Matric suction decreased rapidly after the rainfall began and increased slowly during dry days. In non-vegetation cover area, more rapid variation of matric suction was observed at shallower depths. There was a higher increase of matric suction in non-vegetation cover. This is due to less evaporation induced by higher humidity and lower temperature near the surface in the vegetation area” (Kim and Lee 2010).

2.3 Vegetation Effects

The use of vegetation has been known to increase the rate of infiltration which can lead to an increase suction in the subsurface due to plant root absorption (Oorthuis et al. 2021). A study was done by Ted Hartsig and Andy Szatko (2012) in which infiltration rates were compared between two bioretention gardens. Measurements were taken at locations with native soil and an amended sand-compost soil mix. The results of the study indicated that the amended soil increased the infiltration rates. It was also noted that infiltration was greater where there was vegetation compared to just the native soil (Hartsig and Szatko 2012).

A study was done by Zhao et al. (2019) which investigated the effects of vegetation and rainfall intensity on a slope. The vegetation cover reduced runoff and sedimentation. This led to a conclusion that “land cover reduces the sediment load by effectively intercepting rainfall runoff, increasing the surface roughness of the soil, and promoting rainfall infiltration” (Zhao et al. 2019).

2.4 UDOT Stormwater Quality Design Manual

The UDOT Stormwater Quality Design Manual outlines several BMP designs. The BMP designs are put in place in order for UDOT to obtain MS4 permits for construction of highways and other roadways. “BMPs may achieve one or more objectives, including conveyance of flows, runoff volume reduction and treatment” (UDOT 2021). Sections 4.1 and 4.2.1. overview the methodology of BMPs as well as designs for filter strips.

Filter strips are designed for volume reduction and also treatment of stormwater. The volume reduction is calculated using the NCHRP spreadsheet tool. The current process consists of inputting the geometry of the filter strip and the class (A-D) of embankment material which will be used in construction. A runoff coefficient used to determine the volume reduction is calculated based on the amount of added impervious area to a site. The tool is then able to calculate the amount of volume reduction based on the inputs. The manual also provides design criteria for the filter stirp design. A filter strip must be a minimum of 15 ft in length with slopes no steeper than 4:1 (H:V). Vegetation should cover at least 70% of the treatment area (UDOT 2021).

This study is meant to help improve the design of filter strips by determining runoff values based on gradation of the soil rather than the amount of impervious area in the design. The study will investigate the effect of vegetation and a steeper inclination than the current maximum design slope.

CHAPTER III

EXPERIMENTAL METHODS

The purpose of the experimental methods chapter is to provide ample details so further testing can be replicated. The section outlines the soil classifications, design and construction of the testing apparatus, and the testing procedures. The construction and testing for this study were performed at the UWRL.

3.1 Soil Classifications

An embankment material was provided by UDOT for testing. The material was sieved through a ¾-in. sieve before any material testing occurred or before the material was placed in the experimental devices. A modified proctor test was run on the provided material in accordance with ASTM D1557-87. The results were $\gamma_{d,max}$ = 136.1 pcf and w_{opt} = 7.0%.

Tests were performed in a laboratory to determine the embankment material soil classification. Several gradation tests were performed on various samples of the embankment material in accordance with ASTM D2487-17. The LL, PL, PI, and clay fractions were found using ASTM D4318-17 and ASTM D7928-21. The laboratory tests resulted in an AASHTO soil classification of A-2-4(0), LL = 26, PL = 20, PI = 6, with 9% clay.

Tests were performed in a laboratory to determine the soil classification for the topsoil. A gradation test was performed on a sample of the topsoil in accordance with ASTM D2487-17. The LL, PL, and PI were found using ASTM D4318-17. The

laboratory tests resulted in an AASHTO soil classification of A-4(0), LL = 27, PL = 20, PI = 7, with 9% clay. A summary of the embankment fill and topsoil properties are shown in Fig. 2.

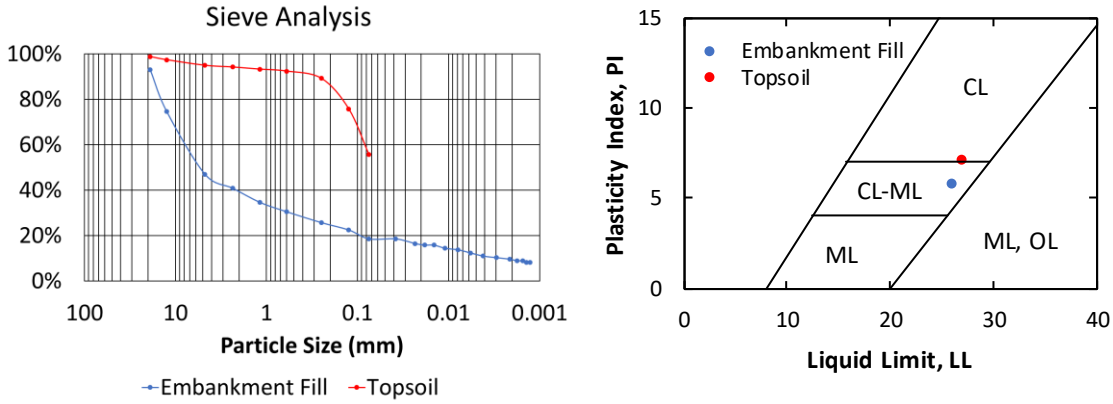

Fig. 2. Embankment fill and topsoil gradations and Atterberg limits.

3.2 Design and Construction

A testing apparatus was constructed to model infiltration of surface water a roadway embankment at varied slope inclinations. Specific criteria for the experimental configurations were developed through discussions with UDOT employees. The criteria consisted of a soil depth of 19 in., a width of 3 ft, and a length of 20 ft. Sheet flow from the roadway above the slope also needed to be included in the model because the design was for a roadside filter strip. A roadway width of 20 ft was modeled. The inclination of the apparatus also needed to vary between a 6:1, 4:1, and 2:1 (horizontal to vertical). The current UDOT design manual has a limit of maximum slope to be 4:1. The addition of the 2:1 slope was incorporated to see what effect the increased slope had on runoff and infiltration and if steeper inclinations would be allowable in filter strip designs.

The initial design consisted of a 20-ft by 3-ft by 2-ft (L x W x H) sheet metal box with 4-in. box beam running along the perimeter of the box and u-shaped channel iron brackets running along the side and bottom of the box (Fig. 3**)**. The box beam and vertical section of the u-shaped brackets were designed to resist the lateral loads of the soil and prevent the testing apparatus from deforming while being lifted. The u-shaped brackets were also designed to limit the amount of deflection in the bottom of the box due to the weight of soil the apparatus would hold.

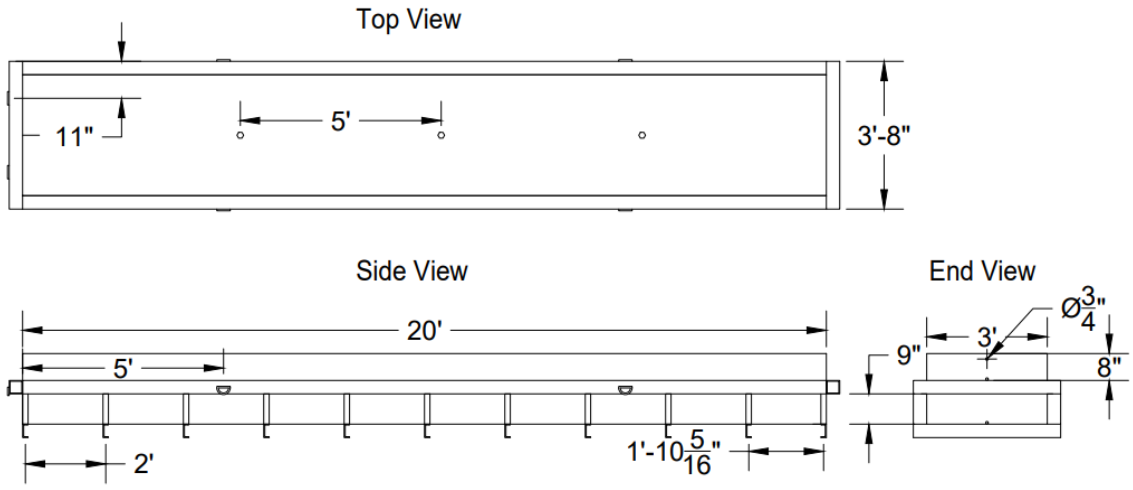

Fig. 3. Soil container portion of the testing apparatus design.

Calculations were performed to determine the weight of the soil. An assumption about the unit weight of the soil was made because a sample of soil was not available during the design phase of the study. A common embankment material consists of sands and gravels with little fines. Therefore, a total unit weight of 125 pcf was assumed. The weight of the soil was calculated to be about 12000 lbs based on the assumed unit weight of the soil and the dimensions of the apparatus. This weight was then used to determine the dimensions of the structural steel.

The main concern became designing for allowable deflections due to the large weight of soil. The allowable deflection in the bottom and side panels of the box was to be no more than ¼-in. The thickness of the metal panels, the size of channel iron, and the spacing of the U-shaped brackets were varied to meet this allowable deflection requirement. The final design consisted of 3/16-in. metal panels, 4-in. wide channel iron, and a bracket spacing of 2 ft.

The initial design consisted of 6 in. of topsoil and 13 in. of embankment fill for a total depth of 19 in. The 4-in. box beam was to be placed 9 in. above the bottom panel so the top of the box beam would be level with the top of the embankment fill. The construction of the apparatus began after the designs were finished.

The U-shaped channel iron brackets were first welded and then laid out at 2-ft spacings. The bottom metal panel was then placed on the bracket layout and then the brackets and panel were leveled to the same height using surveying equipment. It was important the bottom section was completely level when welding to prevent the apparatus from becoming deformed and nonuniform.

Each bracket was then attached to the bottom panel with 2-in. welds at a 1-ft spacing. The side panels were then set in place and attached with 2-in. welds at 6-in. spacing. The 4-in. box beam frame was then placed on the channel iron brackets and welded to the side panels and channel iron. D-rings were then welded on the sides of the box beam to provide lifting locations for the entire apparatus. Continuous waterproof welds were made along the inside of the panels to form a rectangular box.

Holes with a ¾-in. diameter were drilled at the toe of the apparatus to provide a place where runoff and infiltration data could be collected. Three holes were drilled to

provide data for surface runoff, infiltration through the topsoil, and infiltration through the entire embankment. This construction process was repeated to construct an additional testing apparatus (Fig. 4).

Fig. 4. Photo of completed apparatuses with installed drain.

A supporting frame was then designed for one testing apparatus to rest on and enable changing the slope inclination. The frame needed to allow for the inclination of the apparatus to change and a minimal amount of deflection. The design consisted of legs and crossbeams constructed out of 4-in. box beam with diagonal supports constructed of ¼-in. by 2-in. angled steel (Fig. 5 and Fig. 6).

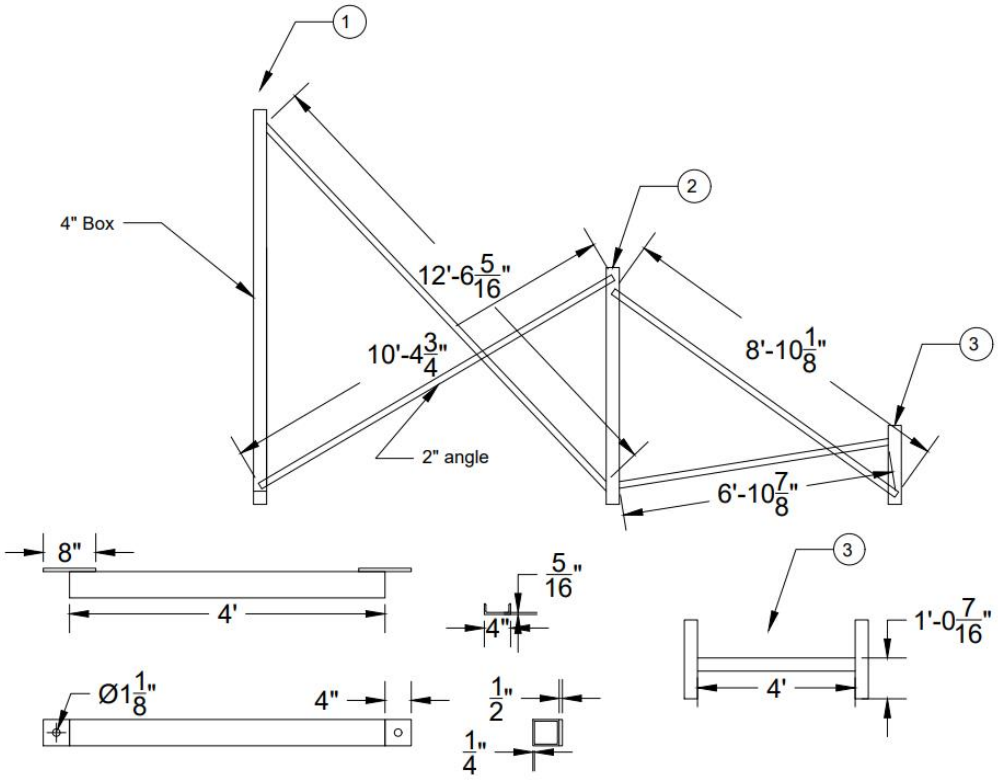

Fig. 5. Drawing of support structure (side view).

The apparatus was designed to pivot on the crossbeam of the shortest leg. The other two crossbeams would be raised to the desired inclination and bolted with 1 1/8-in. bolts to the frame legs. The movable crossbeams consisted of a 4-in. box beam with ½-in. steel plates welded on the ends of the box beam to provide a place for the crossbeam to be bolted to the frame legs. Holes were drilled on the legs at inclinations of 6:1, 4:1, 3:1, and 2:1. The 3:1 inclination was never used in testing due to later changes to the number of desired configurations. The calculated deflection in each of the crossbeams was 1/16-in.

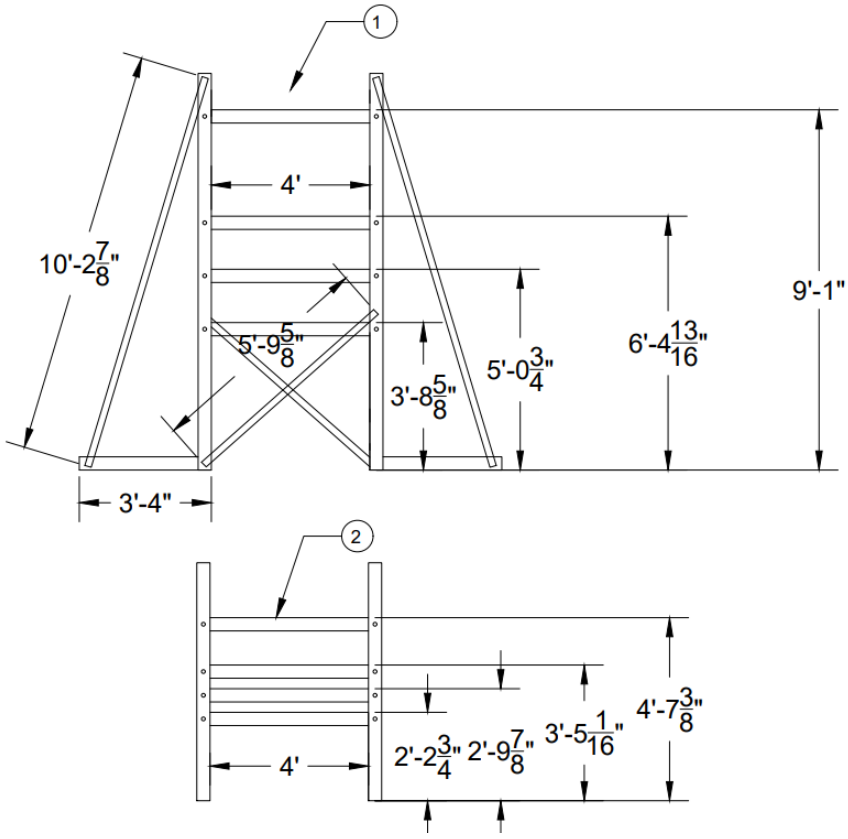

Fig. 6. Drawing of support structure (front view).

Initially, only one frame was constructed for testing to begin. Another frame was constructed six months later to allow both testing apparatuses to be used at the same time. An embankment material was provided by UDOT for testing after the frame was built. The embankment material consisted of material with a diameter greater than ¾-in. This oversized material needed to be filtered out of the soil. A large ¾-in. sieve was constructed due to the large amounts of soil that needed to be processed. The sieving was done by laying the sieve over the testing apparatus and then dumping soil on the sieve with a skid loader (Fig. **7**). The soil was then moved around by hand and any oversized

material was discarded. This process was repeated until there was approximated 8 in. of material in the apparatus.

Fig. 7. Sieving material into apparatus.

A modified proctor test (ASTM D1557-87) was performed and the results are given in section 3.1. Water was added to the loose 8 in. of soil and mixed using a rotary tiller to reach an optimum water content of 7%. Reaching the desired water content was estimated by feeling how well the soil compacted by hand and then by using engineering judgment. A jumping jack compactor was then used to compact the material to a relative density of 90% of the modified proctor.

A nuclear gauge was calibrated and used in accordance with ASTM D7759-18 and ASTM D6938-17. A surface density measurement was taken in three locations inside the apparatus to determine if the soil was uniformly compacted to a relative density of 90%. The soil surrounding the density measurement was compacted again if the results of the density measurement were too low (Fig. 8). This process was repeated for an additional two layers until the total soil depth was 19 in. Two carry deck cranes were used to lift the apparatus into the supporting frame.

Fig. 8. Compaction and testing of material in apparatus.

SoilVUE10 soil moisture sensors from Campbell Scientific with six sensor locations were then installed into the embankment fill (Fig. 9). The sensors measured permittivity, temperature, and electrical conductivity to calculate VWC. Special care was taken during the installation process of the sensors so that the sensor coils would not become damaged. A soil auger bit was used on a hand drill to drill a pilot hole. The hole would also be used for the soil sensor to be screwed into place. Due to the amount of gravel in the material, the pilot hole was larger than the soil sensor. The sensor could no longer be screwed in properly. Having voids around the sensor would provide inaccurate infiltration data.

Fig. 9. Apparatus on support structure and installation of soil moisture sensor.

The pilot hole was expanded to a diameter of 6 in. The soil sensor was placed in the middle of the hole and material was compacted around the sensor. A 10-lb slide hammer (the hammer used in ASTM D1557-87) was used to compact material around the

senor. The hammer was dropped until the surrounding soil was just as compacted as the rest of the embankment material. This method of installation was repeated for each soil sensor that was to be installed in the testing apparatus.

Two soil moisture sensors were initially installed with 6 2/3-ft spacing. After a few tests were performed, another soil sensor was installed to provide more data. The three sensors were now spaced at 5-ft increments. The sensor protruded out of the ground 2 in. so measurements occurred at depths of 2, 6, 10, 14, and 18 in.

A watering system was then designed to simulate a rainstorm in Utah. The 80th percentile, 24-hr storm was determined to be 0.5 in. in 2 hours. Running a 24-hr test with only allowing 0.5 in. of water to fall on the soil was not feasible. The testing period was lowered to 2 hrs with still 0.5 in. of water being added. Constantly running water for the 2-hr duration with only allowing 0.5 in. of rainfall was also not feasible. The sprinklers would need to form a mist if the water was to be constantly running which would result in significant evaporation and an unknown amount of water actually reaching the soil surface. Different rainfall intensities and rates were experimented with and the final design was the main water supply would be turned on for 7 seconds every minute. This allowed for a low intensity to provide infiltration and reduce erosion. An overhead sprinkler system was designed to distribute the water uniformly over the entire soil surface.

A PVC frame was built and attached to the testing apparatus to layout a sprinkler system for simulating a rainstorm. The sprinkler system included 13 sprinklers with equal spacing. Each sprinkler was connected to a one-way valve that was used to prevent water from draining out of the system when the main water was turned off. Each of the one-

way valves was then connected to a primary pipe which led to the main water supply (Fig. 10). Pressure gauges and a pressure reducer were used because the main water supply had high pressures up to 80 psi. A solenoid valve was attached and programed to automatically open and close the valve producing 7 seconds of spray every minute.

Fig. 10. Watering system pipe network.

A platform was designed to model sheet flow coming from a 20-ft wide roadway onto the filter strip (Fig. 11). The purpose of the platform was to provide uniform sheet flow and therefore did not need to extend the entire design roadway length of 20 ft. The watering system consisted of 12 sprinklers evenly spaced over a width of 3 ft. The

sprinklers were all attached to another one-way valve which was connected to the primary pipe. A thin piece of sheet metal with a bent section was placed on the platform with the bent section in contact with the soil. The metal piece was installed to help produce a uniform sheet flow and reduce the amount of contact erosion from the sheet flow to the soil surface.

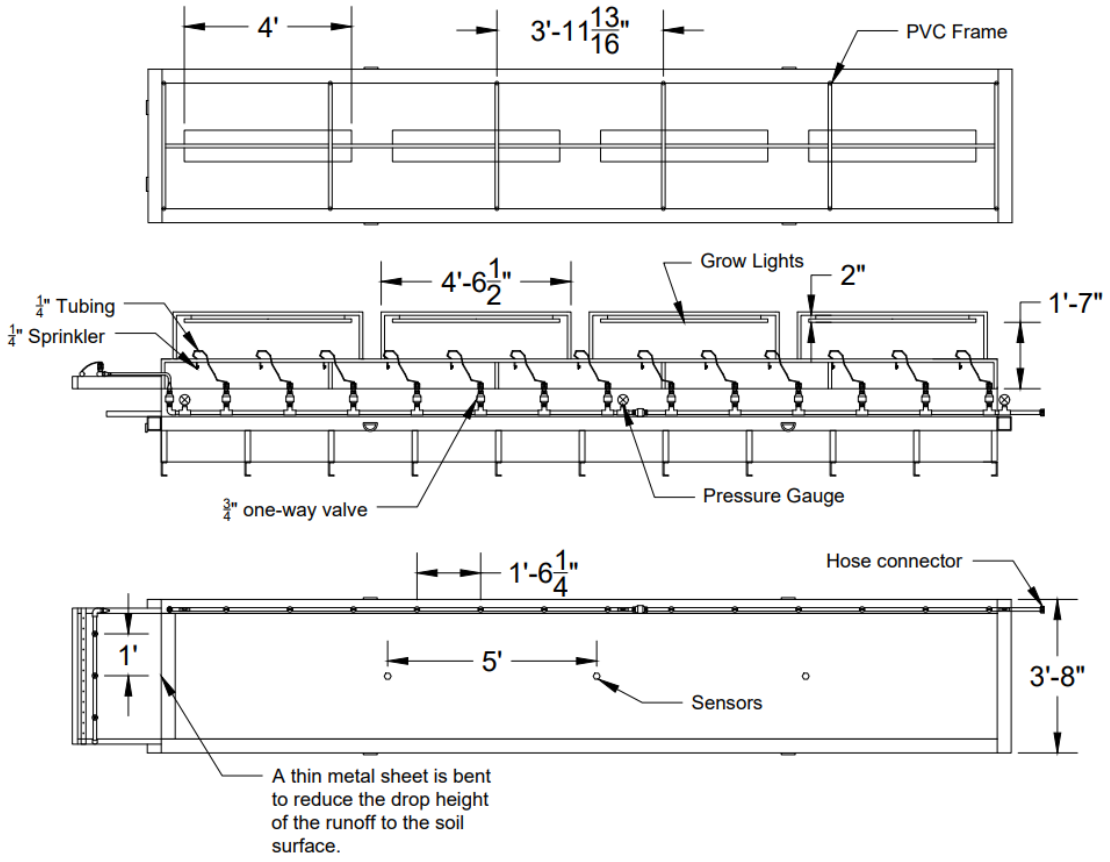

Fig. 11. Drawing of grow light placement (top), grow lights and watering system (middle), and sensor location with sheet flow runoff design (bottom).

Two of the testing configurations included the addition of vegetation. A typical seed mix used along filter strips in Utah was provided by UDOT along with a seed application rate of 26.96 lbs/acre. The application rate was converted into units of

grams/ft^2 and the seed mix was measured with a digital scale to the appropriate weight. The seed mix was then evenly spread over the surface of the soil. A thin layer of peat moss was then spread over the seed mix to assist in the growth of the vegetation (Fig. 12).

Fig. 12. Application of seed mix and peat moss.

Grow lights were hung from PVC frames which were attached to the PVC frame used for the sprinkler system (Fig. 11). The ideal amount of light for growing conditions was 16 hrs. A programable power-strip controlled the duration of light on the vegetation.

The seeds and vegetation were watered every 2-3 days to keep the soil and peat moss damp. The plants grew for a minimum of 6 weeks before testing began.

The data was collected using a Campbell Scientific CR1000x data logger. The data logger was connected to each soil sensor and to the solenoid valve. A program was written to collected VWC readings every 2 min and to open/close the solenoid for 7 seconds every minute for the 2-hr test. The collected data could be viewed in real time on the screen of a connected laptop computer. The laptop computer and an external hard drive were used to store the data for future processing.

3.3 Testing Procedure

A testing procedure was developed so experiments could be replicated and meaningful data could be obtained. Special care was taken when setting up the experiments to the same standards as previous experiments. The following section outlines what steps were taken to ensure reliable data could be collected.

The first step taken prior to performing the next test was setting the testing apparatus to the correct inclinations. One carry deck crane was used to lift half of the testing apparatus (Fig. 13). The two cross beams on the support frame were unbolted, moved to the correct location, and bolted into the support frame legs. The testing apparatus was then carefully lowered onto the cross beams.

Fig. 13. Changing inclination of testing apparatus.

Resetting the testing surface was done by compacting and leveling the material. The surface was scarified to a depth of 6 in. to begin creating a uniform testing surface. Material was added to the testing apparatus to fill any voids that may have formed from erosion and from the scarifying. A 2-in. by 4-in. piece of lumber was used to level the surface for an overall depth of 19 in. of testing material. A handheld tamper was then used to tamp the added material in place. The tamping was performed until the material had been sufficiently compacted comparable to the underlying material.

Bulldozer tracks were then added to the surface to replicate a dozer or other large equipment that may drive over the material after compaction. The tracks spread the width of the apparatus and had a spacing of 6 in. The tracks were ½-in. deep with a width of ¼-in. The tracks were formed by hammering a small section of angle iron into the surface material.

The cables were checked to make sure all connections were tight between the sensors and data logger. Preliminary data collection by the data logger was started to make sure all sensors were reporting data and that the solenoid worked properly. The main water was then connected to the sprinkler system. The testing surface and sheet flow area were then covered with a clear plastic to calibrate the sprinkler system (Fig. 14). Care was taken to make sure water was not added to the surface material during the calibration process. The water supply was then turned on and the calibration process began.

Fig. 14. Calibration of watering system.

The 13 surface sprinklers were individually calibrated by using 100 mL graduated cylinders to measure the amount of water spraying from the sprinkler. The water would be turned on for 7 sec every minute. Each sprinkler was adjusted to the appropriate rate to provide a uniform rain shower over the testing surface for the 7 sec interval. All the sheet flow system sprinklers were calibrated together. Individual sprinkler rates were altered until the desired flow was met. The main water was turned off and the plastic covering was removed.

The main water supply was turned back on and the primary data collection began. Volumetric water content (VWC) data was recorded every 2 min on the laptop computer while runoff and infiltration data were simultaneously being collected every 2 min. The runoff and infiltration data were collected by gathering the stormwater from the three different drains which were installed at the toe of the testing apparatus.

The runoff and infiltration volumes were measured using a graduated cylinder and the volumes were recorded on a piece of paper. The main water supply was turned off and data collection stopped after the 2-hr experiment period. All data from the experiment was then processed using Excel spreadsheets. Each configuration consisted of three tests at 6:1, 4:1, and 2:1 inclinations.

An extra experiment was performed for the starting slope for a configuration. The first experiment resulted in higher volumes of infiltration than the following experiments because the top 4-in. of soil was either dry or consisted of a new material. The extra test allowed the soil to reach an equilibrium moisture content. The moisture content became the starting point for the rest of the experiments for the configuration. Drainage occurred over the space of a few days until the soils had reached an equilibrium moisture content and another experiment could be performed. An equilibrium moisture content was reached when no significant VWC changes were noticed after allowing the system to drain over several days.

CHAPTER IV

RESULTS AND DISCUSSION

4.1 Data Processing

A data processing procedure was followed once experimental data was collected. The raw, collected VWC data from the soil moisture sensors was plotted on a graph to show how VWC readings changed with time (Fig. 15). A similar legend connotation was used for many of the graphs. S#_##cm denotes which sensor the data came from (1 for top sensor, 2 for the middle sensor, and 3 for the sensor near the toe of the apparatus) and at what depths the data point was taken (varies between 10-50 cm). A raw VWC vs time graph for every experiment can be found in Appendix A.

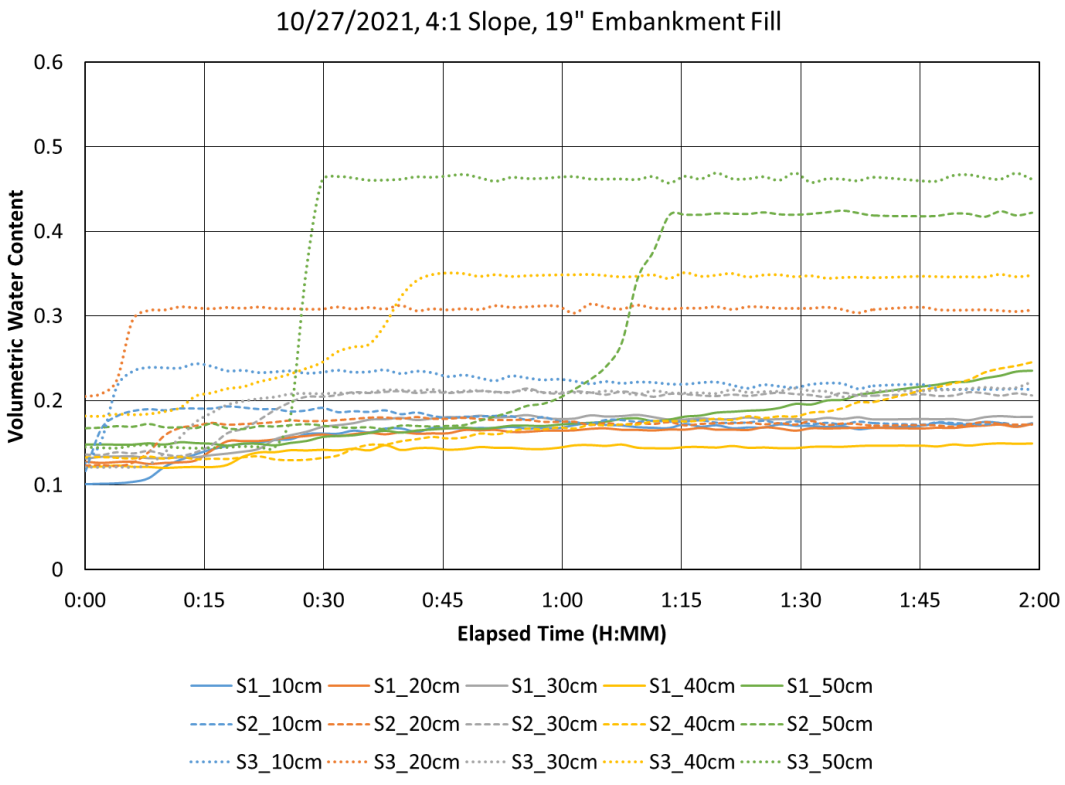

Fig. 15. Sample 2-hr raw VWC reading vs. time graph.

Each raw VWC vs time graph was evaluated. Sometimes there were fluctuations and noise in the sensor data. The noise did not provide an accurate representation of the data and had to be edited to provide a meaningful plot. The data was edited using engineering judgment and based on how similar readings had acted in previous experiments. A few irregularities were discovered while reviewing the data. The deepest part of a sensor would show a change in VWC before some of the previous sensors (Fig. 16). Sensor 3 showed an increase in VWC before sensor 2 and then the bottom readings on sensor 2 at a depth of 50 cm (19.5 in.) showed an increase of VWC before a depth of 40 cm. This suggests that a backfilling process was occurring. The stormwater would flow through the system to the bottom of the apparatus and would backfill along the flow paths instead draining out of the apparatus.

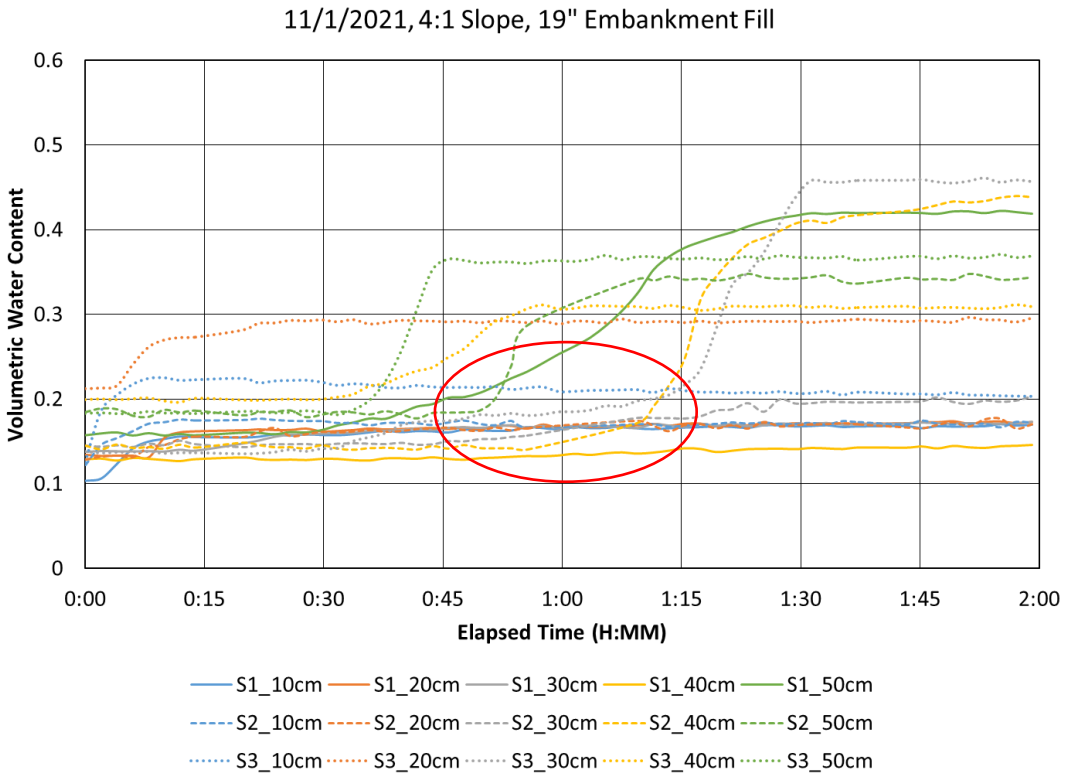

Fig. 16. VWC vs. time graph showing irregularities in collected VWC data.

Due to the non-uniformity and high gravel content of the soil, it is thought that preferential flow paths were present in the fill allowing flow to reach the bottom of the box, and certain sensor depths showed an increase in moisture content before shallower depths. In this specific case, water flowed to the bottom of the box and began to backfill to the lower sensors (Fig. 17). This occurrence would not be expected in field conditions unless there was an impermeable layer underneath the filter strip and a cutoff wall was installed at the toe of the filter strip.

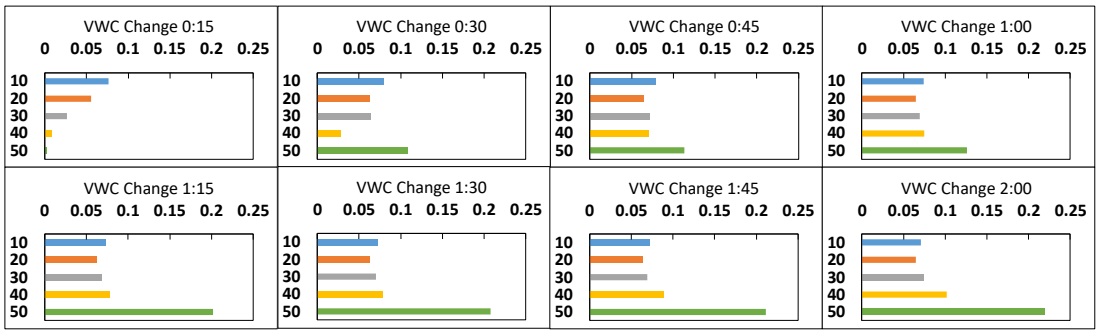

Fig. 17. Change in VWC in 15-min intervals for the configuration of 19-in. embankment fill at a 4:1 inclination.

Fig. 17 shows average increases in VWC for all three soil moisture sensors. The system behaved as expected within the first 15 minutes. The top section had the highest VWC increase and subsequent layers showed less changes in VWC with increasing depth. At 30 minutes into the test the bottom sensor reading showed a large increase in VWC change. This was assumed to be the result of the backfilling process. Over time, the second to lowest sensor reading then showed increased VWC changes amounts than exceeded readings at shallower depths.

The collected runoff and infiltration volumes were then recorded in an Excel spreadsheet and plotted on a graph. A cumulative precipitation line was also plotted to show the rate at which water was added and cumulated in the system. The infiltration and runoff volumes were then converted into a mass for a future evaluation. A phase diagram was used to derive the calculations used to change VWC to a mass of water (Eq. 1-4) so a comparison could be made between the VWC sensor data and the collected runoff volumes.

VWC is defined as:

$$VWC = \frac{V_w}{V_t} \quad (1)$$

Where V_w is the volume of water and V_t is the total volume. The change in VWC (ΔVWC) is defined as:

$$\Delta VWC = VWC - VWC_{initial} \quad (2)$$

Where VWC is the VWC in question and $VWC_{initial}$ is the initial VWC reading. The change in weight of water for a given time increment ($\Delta W_{w,i}$) is defined by using a phase diagram as:

$$\Delta W_{w,i} = \Delta V_w \gamma_w = V_t \gamma_w \Delta VWC \quad (3)$$

Where V_t is the total volume, γ_w is the unit weight of water and ΔVWC is the change in VWC from Eq. 2. The changes in the final weight of water for a given time increment ($\Delta W_{w,f}$) is defined as:

$$\Delta W_{w,f} = \Delta W_{w,i} - \Delta W_{w,i-1} \quad (4)$$

Where $\Delta W_{w,i}$ is the change in weight of water for a given time increment and $\Delta W_{w,i-1}$ is the weight of water for the previous given time increment.

A few assumptions were made about the sensor data when converting to a mass. The volume assumed for one sensor depth reading was V_t = 6.33 cubic ft and remained constant. This was done by assuming the sensor data points represented 15 equally divided sections (3 sensors with 5 readings per sensor for a total of 15 readings). The constant volume assumption can be made because the materials did not consist of expansive materials and therefore no significant volume change would occur.

The changes in final mass of water ($\Delta W_{w,f}$) were then summed for all readings at a given time period to provide a cumulative mass for the entire system. The cumulative mass for the 2-hr duration was then compared with infiltration and runoff mass. This procedure resulted in the calculated mass being different than the measured mass applied during the test.

A correction coefficient (α) needed to be calculated for the calculated mass to be equal to the measured mass. This was done by assuming an α value then using Eq. 5 instead of Eq. 3 to find a new measured total infiltration where, $\Delta W_{w,ic}$ is the corrected change in weight of water for a given time increment. The α value was varied until the calculated infiltration from the sensor data was equal to the total measured infiltration from the collected runoff data. The corrected sensor cumulative infiltration was then plotted on a graph with the runoff infiltration along with the cumulative precipitation line (Fig. 18). The cumulative precipitation line shows the constant rate at which water was applied to the system. A sensor and runoff infiltration graph for each configuration and inclination can be found in Appendix C.

$$\Delta W_{w,ic} = \alpha V_t \gamma_w \Delta VWC \tag{5}$$

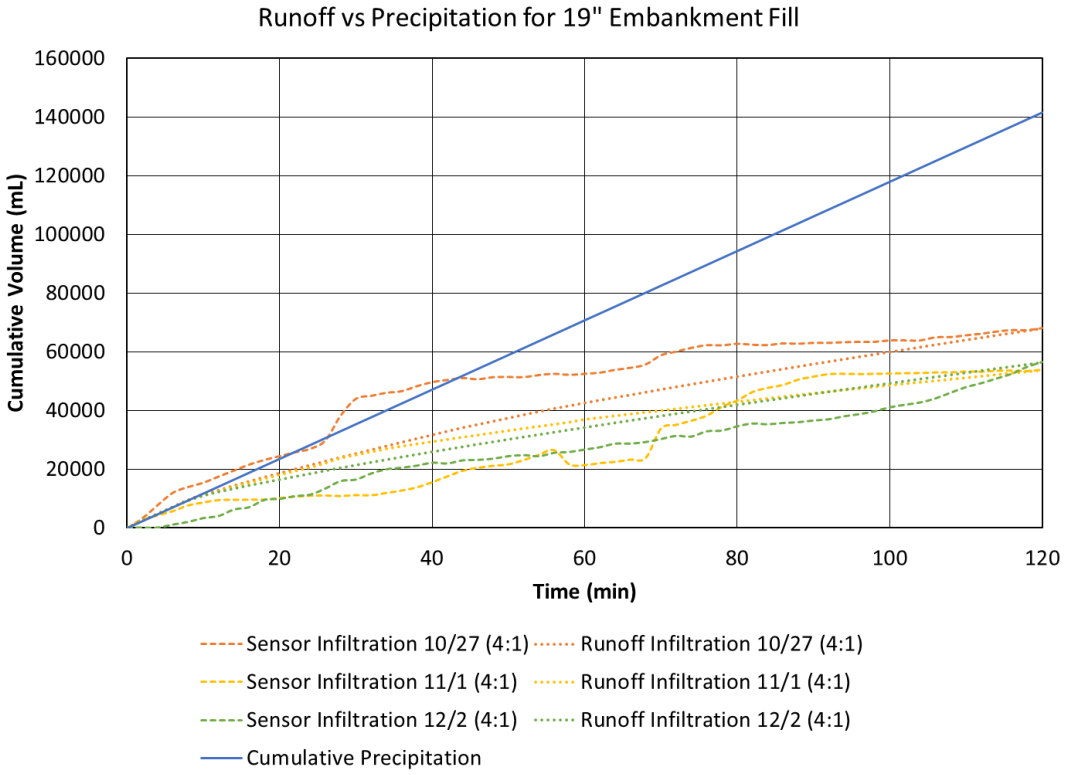

Fig. 18. Cumulative infiltration volumes vs time graph showing cumulative precipitation line, cumulative sensor infiltration, and cumulative runoff infiltration for three tests at a 4:1 slope on 19-in. of embankment fill.

The sensor infiltration curve for the 10/27 test at times crossed above the cumulative precipitation line. This is a result of the fluctuation in subsurface water flow. Water could have flowed into voids around the sensor. The voids are caused by gravel or other coarse material particles being in contact with the sensor. The voids may have initially been filled with fine material and then internally eroded away to create the increase in VWC. The void also may have closed or been filled with fine material as experiments were conducted.

Voids can be filled by groundwater carrying fine particles into void spaces and the fine particles block the flow path. The voids could also be closed due to expansion and contraction of soil. The dilation and contraction of the soils is less likely to occur for the given configuration where there are little expansive clays in the embankment material. The closing of the void would result in a different preferential flow path forming in the subsurface. Since proceeding experiments did not show a similar behavior in Fig. 18, it is assumed that the voids near the sensor were closed during the test.

A correction coefficient was found for each of the 60 experiments and are shown in Table D-1 in Appendix D. The correction coefficients varied slightly for configurations with little infiltration and varied much more for configurations with more infiltration. One reason for this occurrence could be caused by how similar the infiltration amounts were when compared to all experiments in one configuration. The configurations with little infiltration produced similar time vs VWC graphs which meant little variation in correcting to the actual amount of measured infiltration. The correction coefficient did not directly correlate to amount of infiltration such that a higher amount of infiltration did not result in a higher correction coefficient.

The correction coefficients were always less than 1. There could be several reasons why the coefficients were less than 1. The sensors could have measured higher changes in moisture content due to voids around the sensor. The sensors also may have needed a calibration process to be done for each particular configuration. Another reason for the coefficients being less than 1 could be the assumption that the entire 6.33 ft^3 volume had the same VWC as reported by the sensor. Although steps were taken to make the soil and watering uniform, the soil is not homogenous and flow on and through soil is

not perfectly uniform. Preferential flow paths form and water will travel through the path of least resistance. This results in some areas having higher VWC than other areas.

A corrected VWC vs time graph was then plotted (Fig. 19). Corrected VWC vs time graphs for each experiment can be found in Appendix B. Determining the corrected VWC was found by converting the corrected $\Delta W_{w,f}$ back to a VWC by using Eq. 1-4. The corrected VWC vs time graphs showed the correction method mainly affected the sensor points that had a large change in VWC. This is because the correction coefficients were applied to the change in VWC rather than the actual VWC readings. The initial VWC was not changed because the purpose of the correction method was to adjust the change in VWC to equal the measured amounts of runoff.

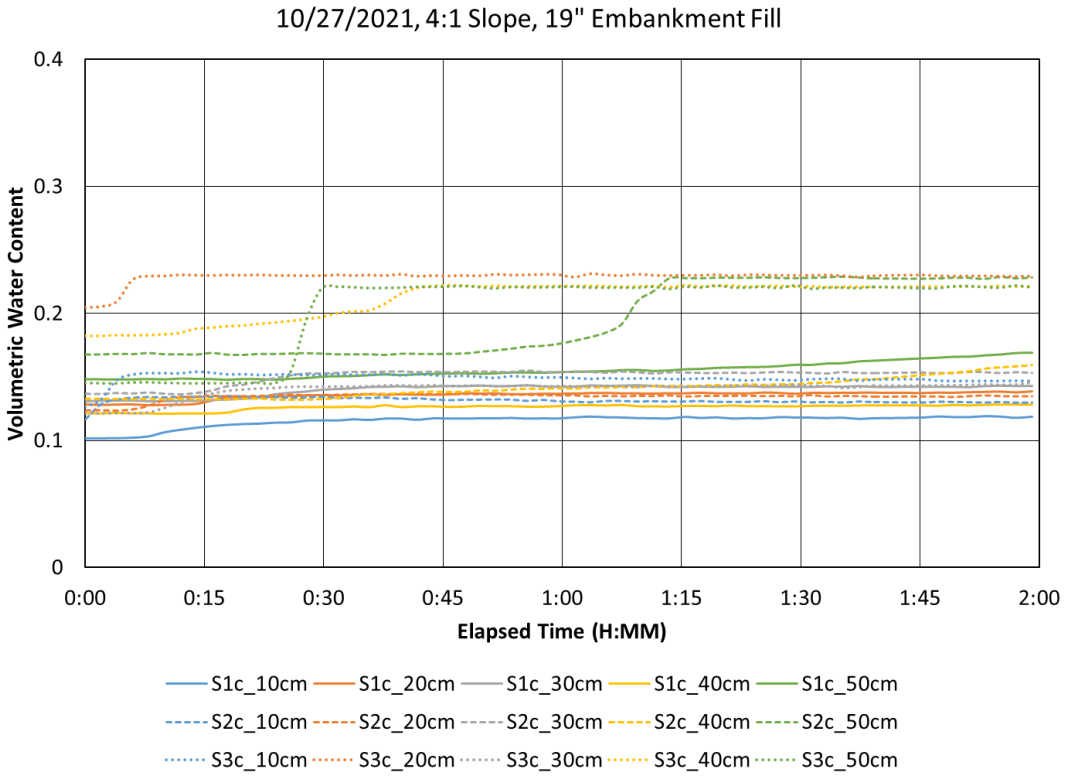

Fig. 19. Corrected VWC vs time graph.

A summary table was created for each configuration with the associated tests for a given inclination (Fig. 20). The summary table consists of the configuration details, date of when the experiment was conducted, the apparatus inclination, volume of infiltration based on the water balance calculations and measurements described above, volume of infiltration per square foot of area, and plots of change in VWC at every depth for each sensor. Summary tables for every configuration and inclination can be found in Appendix E. The summary tables can be useful to quickly compare how each configuration and associated inclination performed.

	Date	Slope	Vol_{infl} (ft^3)	Vol_{infl}/A (ft^3/ft^2)	VWC Change			
					Top Sensor	Middle Sensor	Bottom Sensor	Average
Configuration 1 (19" Embankment Fill)	10/27/2021	4:1	2.401	0.040	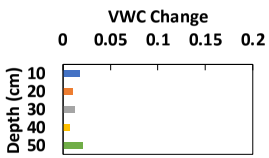	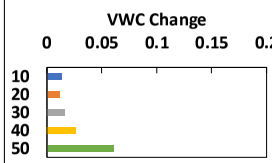	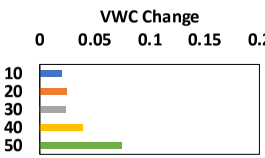	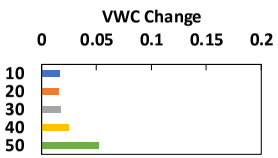
	11/1/2021	4:1	1.903	0.032	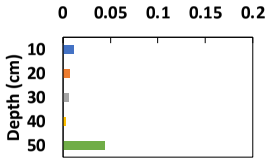	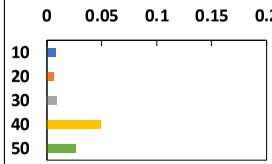	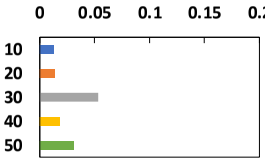	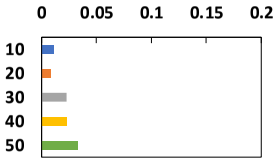
	12/2/2021	4:1	1.990	0.033	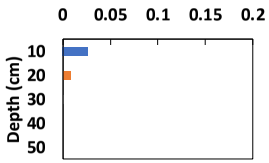	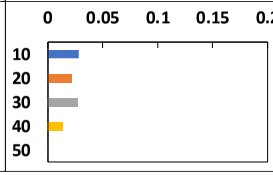	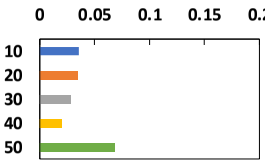	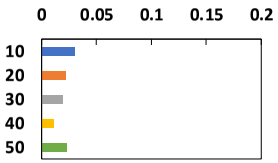

Fig. 20. Summary table of configuration 1 with a 4:1 inclination.

4.2 Soil Effects

4.2.1 Embankment Fill

The embankment fill was a A-2-4(0) silty gravel sand according to the AASHTO classification index. The embankment fill consisted of a large portion of gravel material and a small amount of low plastic fines. The large portions of gravel allowed for higher amounts of infiltration due to larger void spaces than what would be found in a clean sand. The large void spaces could be caused by two gravel particles being in contact with one another or with a soil moisture sensor. The contact between gravel and soil moisture sensor would result in a higher VWC reading than what would be expected if the soil was uniformly distributed. Adjustments described in section 4.1 were made to account for the higher VWC readings.

The large void spaces increased the chance of internal erosion and migration of fine soil particles through the subsurface. Evidence of this was found where VWC readings would increase more at a certain sensor depth than a reading at the same sensor depth at a later conducted experiment. The correction coefficient calculated in the data processing procedure accounts for the increases in VWC that may not have been representative of the system.

4.2.2 Topsoil

The intended purpose of the topsoil was to increase the amount of infiltration. The topsoil was a A-4 (2) silty soil according to the AASHTO classification index. The combination of large amounts of fine soils and slight compaction allowed for the potential of increased infiltration. The first experiment for the 4-in. topsoil configuration

resulted in nearly all the stormwater being infiltrated into the topsoil. Less water was infiltrated into the entire system as further experiments were conducted (Fig. 21). Stormwater was infiltrating mainly in the topsoil while very little water reached the embankment material.

	Date	Slope	Vol_{infl} (ft^3)	Vol_{infl}/A (ft^3/ft^2)	VWC Change			
					Top Sensor	Middle Sensor	Bottom Sensor	Average
Configuration 2 (15" Embankment Fill 4" Topsoil)	11/16/2021	6:1	4.911	0.082	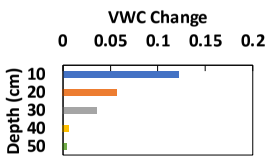	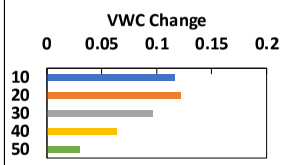	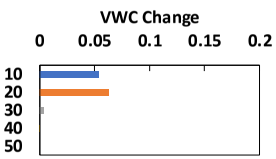	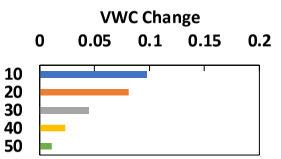
	11/19/2021	6:1	1.535	0.026	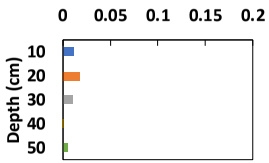	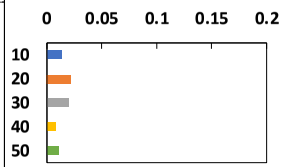	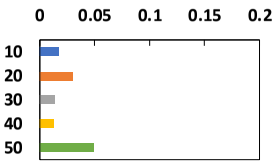	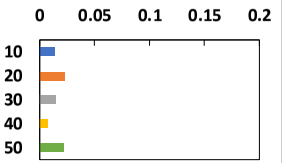
	11/22/2021	6:1	0.349	0.006	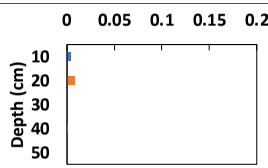	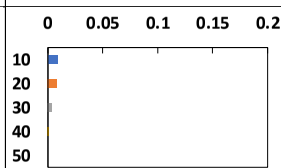	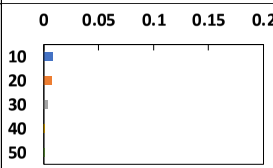	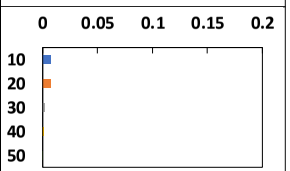
	1/6/2022	6:1	0.284	0.005	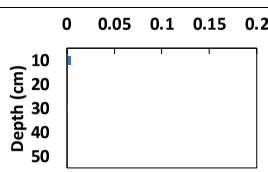	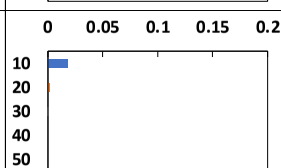	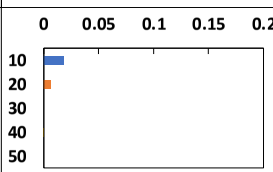	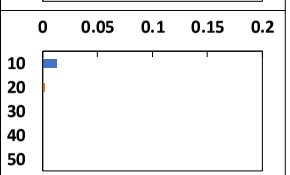

Fig. 21. Summary table showing variation in infiltration in the first experiment due to the wetting of dry soil.

The topsoil behaved similar to a sponge where the topsoil retained water and would not let the water infiltrate into the embankment fill. This phenomenon is related to the matric suction potential of the soil which is discussed in section 4.2.5 of this chapter. The addition of the topsoil resulted in lower infiltration volumes compared to the configuration with just embankment fill (Fig. 22).

The topsoil configuration resulted in approximately a 70% average decrease in infiltration volume from the base configuration. The experiments were conducted several days apart to allow time for the topsoil to reach an equilibrium VWC. The equilibrium VWC was approximately 5% below the VWC at which the topsoil would stop infiltrating water and the stormwater became runoff. Only 8-13% of the entire storm event was infiltrated with the use of just topsoil. The inclination had very little effect on the amount of infiltration. The addition of the topsoil material was only beneficial for the first rainstorm event. The further storm events resulted in large amounts of runoff.

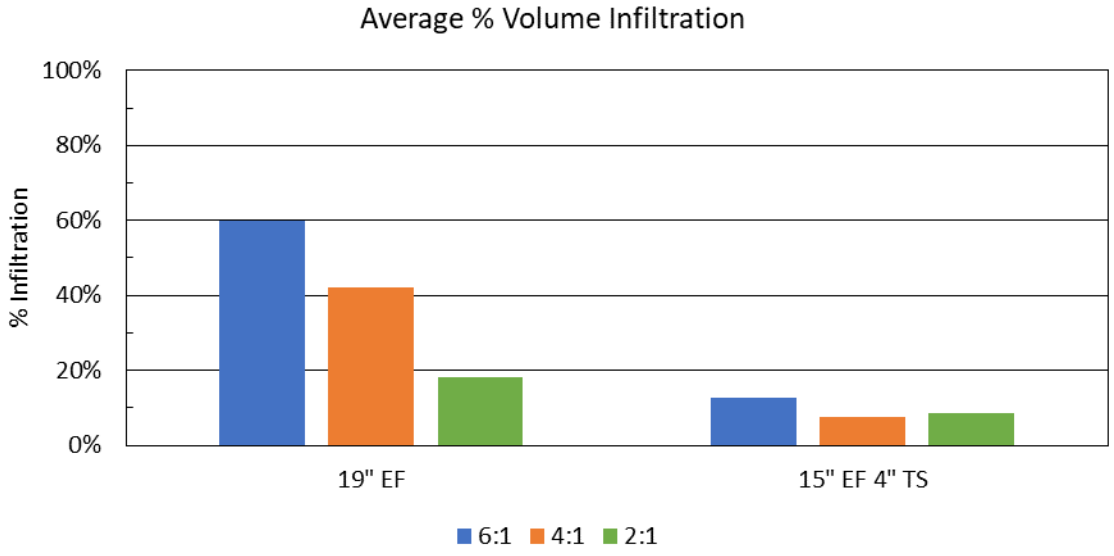

Fig. 22. Infiltration comparison of embankment fill only and embankment fill with 4 in. of topsoil.

4.2.3 Amended Topsoil

The amended topsoil consisted of the topsoil described in section 4.2.2 of this chapter and a compost mixture. The compost mixture came from the Salt Lake Valley Compost site and was USCC certified. The mixture consisted of 20% compost and 80% topsoil based on the dry weight of the materials. The materials were well mixed before placement and compaction in the testing apparatus.

The amending of the topsoil resulted in an increased amount of infiltration over the initial topsoil. The amended soil infiltrated 240% more stormwater on average when compared to the topsoil configuration (Fig. 23). Infiltration, however, decreased in the embankment fill as the experiments progressed. The matric suction of the amended topsoil was still too large to allow water to flow to the embankment material. The amended topsoil was able to capture and retain more stormwater than just the topsoil because of the compost. The compost amendment had large amounts of organic material which increased the amounts of voids in the topsoil. The larger voids allowed for a higher water capacity.

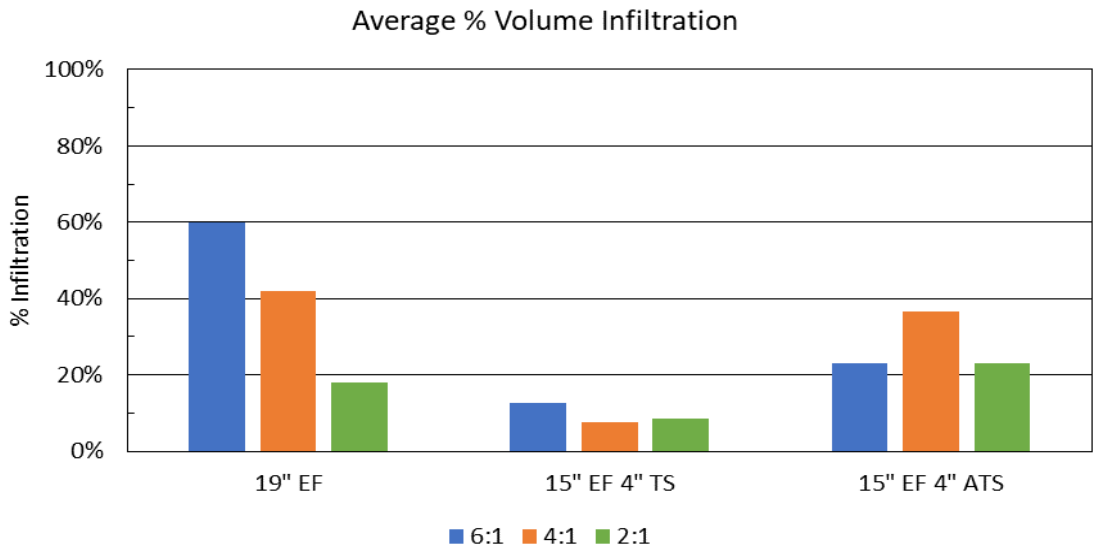

Fig. 23. Infiltration comparison of only embankment fill, embankment fill with 4 in. of topsoil, and embankment fill with 4 in. of amended topsoil.

The experiments began at a 4:1 inclination. The first two experiments resulted in nearly all the stormwater being infiltrated into the system. The amended topsoil captured a majority of the sheet flow runoff at the top of the testing apparatus for the first experiment. Infiltration from the sheet flow mainly occurred at the top and middle sensor and no infiltration was recorded in the embankment material at the lowest sensor (Fig. 24).

	Date	Slope	Vol_{infl} (ft^3)	Vol_{infl}/A (ft^3/ft^2)	VWC Change			
					Top Sensor	Middle Sensor	Bottom Sensor	Average
Configuration 4 (15" Embankment Fill 4" Amended Topsoil)	1/19/2022	4:1	5.000	0.08333	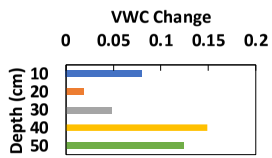	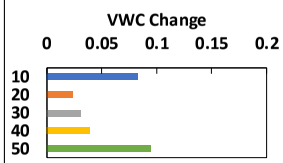	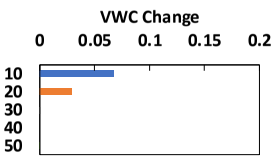	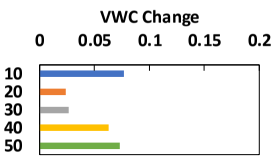
	1/22/2022	4:1	4.112	0.06854	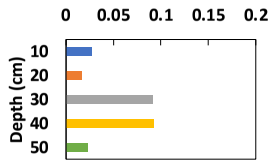	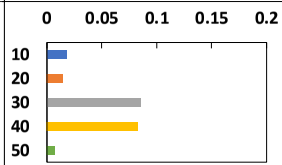	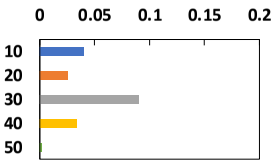	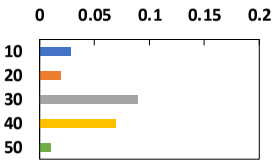
	1/25/2022	4:1	2.796	0.04659	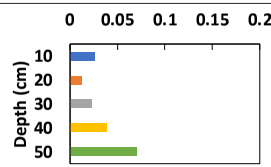	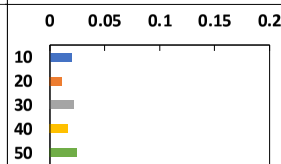	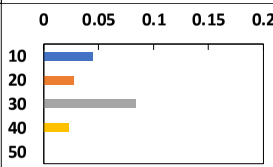	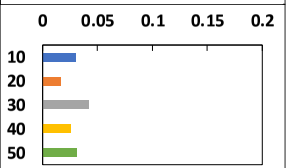
	1/28/2022	4:1	1.836	0.0306	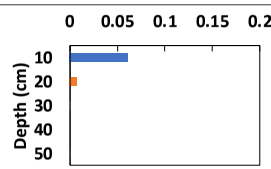	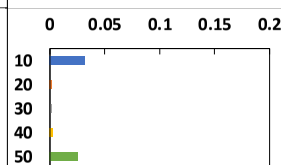	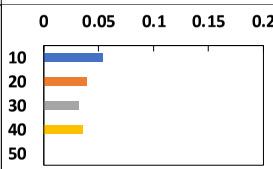	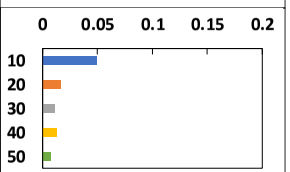

Fig. 24. Summary table showing variation in infiltration between sensors.

4.2.4 Ripping Material

The top 4 in. of topsoil was removed so the embankment material could be scarified. A handheld demolition jackhammer was used to create a 6-in. deep rip through the material (Fig. 25). The scarifying method used was performed to replicate how material would be ripped using dozer ripper blades. Two rips ran parallel to the sides of the apparatus with a 2-ft spacing between the two rips. Several rips were then made perpendicular to the two long parallel rips at a spacing of 1-ft.

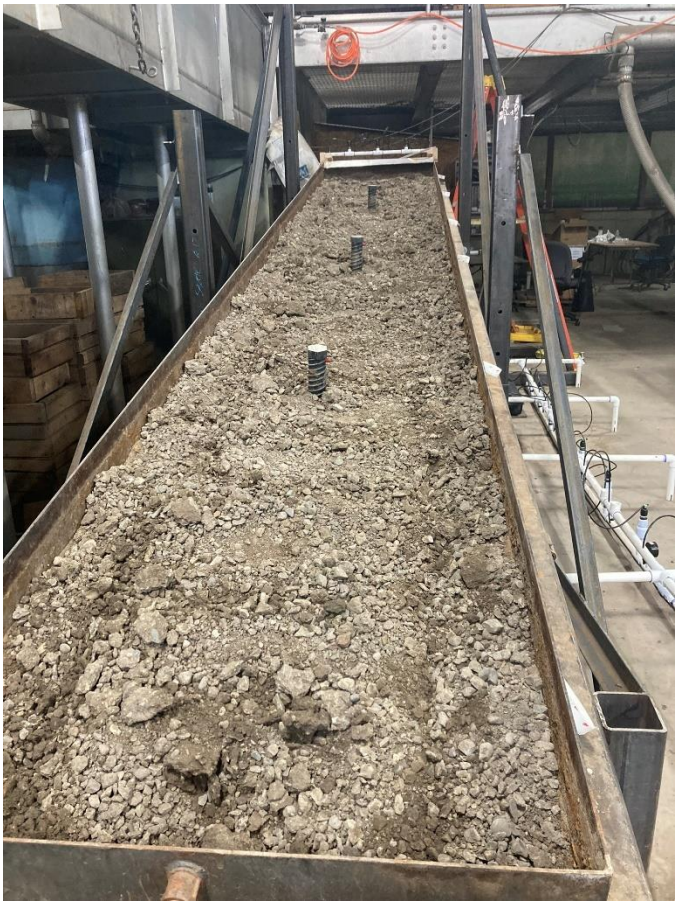

Fig. 25. Photo of ripped embankment material.

Ripping the material allowed for the topsoil to mix with the embankment material which prevented a smooth continuous interface from forming. The loose, ripped material

allowed for the topsoil to get into the voids of the loose material. This mixing could be seen when the topsoil was removed at the conclusion of the experiments (Fig. 26). The cohesive topsoil created a bond to the loose embankment material. This mixing allowed for the groundwater to flow through the topsoil and into deeper parts of the embankment material.

Fig. 26. Photo of topsoil and embankment fill bonding.

The ripping of the underlying embankment material resulted in larger amounts of infiltration (Fig. 27). The configuration with the ripped material increased the average amount of infiltration by approximately 400% on average for each inclination. This proved to be an effective treatment for increasing the amount of infiltration. One concern

of ripping material was determining if the ripped sections would remain open after the wetting and drying of the soil over a long period of time.

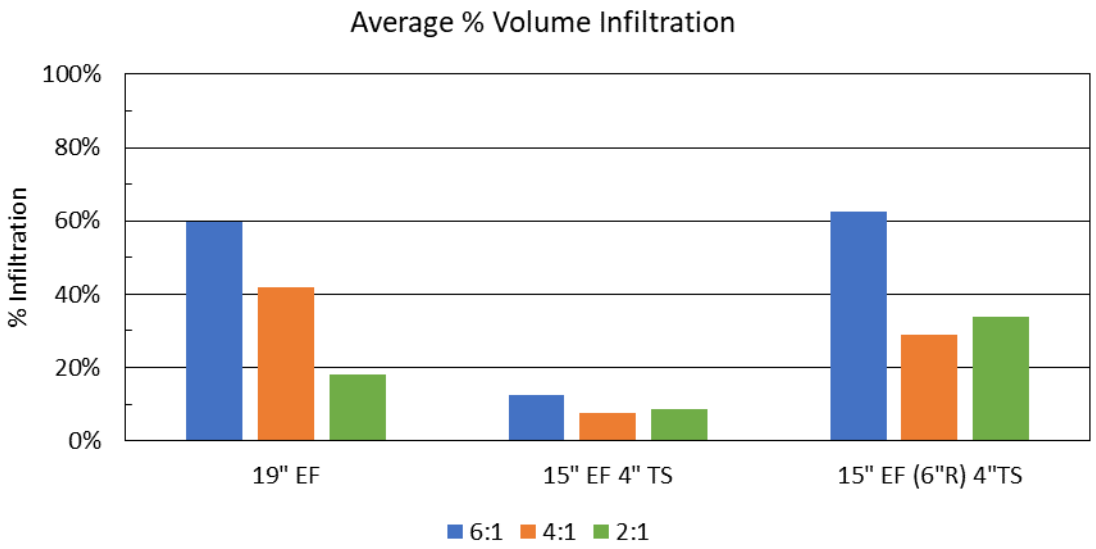

Fig. 27. Infiltration comparison of only embankment fill, embankment fill with 4 in. of topsoil, and embankment fill with 6 in. of ripped material and 4 in. of topsoil.

The experiments with ripped material began at a 6:1 inclination and ten experiments were conducted over a space of 51 days. The experiments concluded with an 11th experiment at a 6:1 inclination to determine how infiltration compared to the initial tests when the rips were opened. There was a 9% decrease in infiltration between one of the initial 6:1 inclination experiments and the final experiment at the 6:1 inclination. This suggests that the rips were slowly closing. The closing could be caused by the wetting and drying of the soil. Water flows through the voids in the material and the pore pressures can cause the voids to expand. The migration of fine soils through the voids could lead to the voids clogging. When the soil dries, negative pore pressures cause the soil particles to consolidate. This mainly occurs in the fine soils. Compaction of the

topsoil can cause the rips to compact and close. It would be expected for the rips to close if any type of vibratory or dynamic compaction methods are performed on the surface.

4.2.5 Matric Suction Effects

Tests with topsoil observed a soil interface was formed between the underlying embankment fill and topsoil. This is believed to be due to a capillary barrier forming from the matric suction of the soil. This interface was partly caused by the dense compaction of the embankment fill. The compaction did not allow for the embankment material and topsoil to mix well. The matric suction is primarily a function of pore water and pore air pressures and can be thought of as a negative capillary suction force. The topsoil and amended topsoil behaved similar to a sponge and did not allow water to pass through to the embankment material.

There was a high matric suction in the topsoil and amended topsoil layers. The compost in the amended topsoil seemed to reduce the matric suction and allowed for more water to infiltrate the embankment fill below resulting in a higher water storage capacity for the test configuration. However, there was still a high enough matric suction in the amended topsoil to prevent groundwater from flowing into the lower embankment material.

Increasing the moisture content would decrease the matric suction potential due to the increase force of the water acting on the pore spaces. The topsoil and amended topsoil reached a VWC at which no more water would be absorbed which resulted in there not being enough force from the water to breakthrough the matric suction. The amended

topsoil had a higher maximum absorption VWC which allowed for more water to break through into the underlying embankment fill.

The creation of rips in the embankment materials allowed for the topsoil particles to mix with the embankment material to create a more uniform soil. This allowed for a more continuous seepage flow path through the topsoil into the underlying embankment material. The topsoil still had a high matric suction in areas where there were no rips and had to drain laterally to where a rip in the embankment was located.

The addition of vegetation also improved infiltration by providing a flow path along the roots through the topsoil to the embankment material. Some roots were seen to extend into the embankment layer and therefore allow for a continuous flow from the surface to the lower embankment fill layer.

4.3 Slope Effects

Each configuration was tested using three different inclinations. The current UDOT BMP design manual limits the design of filter strips to a maximum inclination of 4:1. Based on this design parameter, it was expected that the 2:1 slope would provide little infiltration and large amounts of runoff compared to the 4:1 and 6:1 inclinations. An average percent volume infiltration value was found for each configuration and inclination and plotted on a bar graph (Fig. 28).

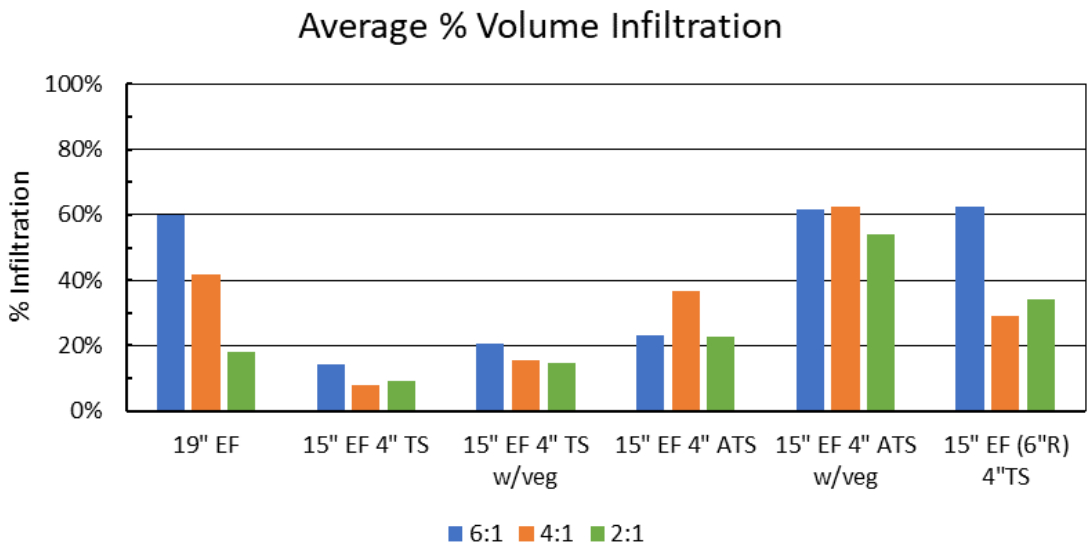

Fig. 28. Comparison of infiltration for all configurations.

The configuration of just embankment fill provided the largest variation in average percent volume infiltration for the three varying slopes. The percent volume infiltration decreased by approximately 20% each time the inclination got steeper. A similar pattern of decreasing infiltration with increased inclination was expected for the proceeding configurations.

The five proceeding configurations did not behave in a similar manner to the first configuration. The replacement of a new material created an interface between the two materials. The interface caused a decrease in infiltration due to the matric suction of the material as described in section 4.2.5 of this chapter. The different inclinations for the five last configurations showed little impact on the amount of infiltration. Looking at Fig. 28 showed the slope had little effect on the infiltration rates for each configuration.

The configuration with 15 in. of embankment fill and 4 in. of amended topsoil showed that the 4:1 inclination allowed for the most infiltration. Not enough experiments

were performed at the 4:1 inclination to give an accurate representation of how the material would perform. The experiments for this configuration began at a 4:1 inclination rather than the 6:1 inclination. The amended topsoil retained a lot of the stormwater over the first four experiments due to the amended topsoil being dry. If more experiments were performed at the 4:1 inclination, it would be expected that the amount of infiltration would be similar to the infiltration amounts at the 6:1 and 2:1 inclinations.

4.4 Vegetation Effects

Topsoil vegetation was grown for 48 days before testing was performed. Three samples of the vegetation were taken at day 32 to measure the growth of the roots. The samples were taken at 21-24 in., 119-122 in., and 178-181 in from the bottom of the test box. The samples were collected by driving a Shelby tube through the topsoil. The sample was then pushed from the Shelby tube and cut open to observe the root growth. The longest observed root reached 2-½ in down in the topsoil. A similar procedure was repeated after all the tests had concluded. Ten samples were taken at evenly vertically spaced intervals and evaluated (Fig. 29).

Fig. 29. Root growth through the topsoil before (left) and after (right) testing.

A few observations were made about the difference between the initial and final root growth. Initial root growth was shallow and did not extend to the embankment fill while post-testing root growth showed a few more root systems extending to the embankment fill. Root systems extended horizontally more than vertically through the topsoil. The infiltration volumes were averaged at each slope for the topsoil and topsoil with vegetation configurations. The difference in infiltration volume was then calculated (Table 1). The addition of vegetation to the topsoil resulted in an average increase of infiltration by 66%.

Table 1. Infiltration comparison of topsoil and topsoil with vegetation.

Slope	TS Vol_{infl} (in.)	TS w/Veg Vol_{infl} (in.)	ΔVol_{infl} (in.)	% Vol Change
6:1	0.145	0.207	0.005	43.5%
4:1	0.078	0.154	0.006	97.0%
2:1	0.092	0.145	0.004	58.1%

Vegetation was grown for 45 days on the amended topsoil before testing began. Three samples were taken on day 34 to measure the growth of the roots. A similar procedure was followed as described in the previous section. Ten samples were collected at the end of testing and analyzed (Fig. 30).

Fig. 30. Root growth through the amended topsoil before (left) and after (right) testing.

A few observations were made about the difference between the initial and final root growth with the amended topsoil. A few roots extended to the embankment fill at the time of initial sampling. Post-testing root growth showed several root systems extending

to the embankment fill. The infiltration volumes were once again averaged and compared (Table 2). The addition of vegetation to the amended topsoil resulted in an average increase of infiltration by 125%.

Table 2. Infiltration comparison of the amended topsoil and amended topsoil with vegetation.

Slope	ATS Volume of infiltration (in.)	ATS w/Veg Volume of infiltration (in.)	Change in Volume of infiltration(in.)	% Volume Change
6:1	0.230	0.616	0.385	167.1%
4:1	0.367	0.627	0.260	70.8%
2:1	0.230	0.540	0.310	135.1%

Overall, the addition of vegetation increased infiltration in each configuration and slope. The amended topsoil allowed for deeper root growth. There were significantly more root systems that reached the embankment fill in the compost mix configuration compared to the topsoil configuration. The deeper root systems allowed for more infiltration into the embankment material and therefore increased the capacity of infiltration. The roots into the embankment material created voids at the soil interface where water could flow. The voids at the soil interface were too large for the matric suction of the soils to have a full effect on the infiltrated water.

4.5 NCHRP Tool

The NCHRP spreadsheet tool (NCHRP 2021) was used to determine the infiltration rates based on the runoff data from the tests of different configurations. The NCHRP tool can be used to calculate runoff reduction for several different BMPs. A BMP was selected and design values were inputted into the tool for a runoff reduction

calculation to be made. A description of the process used to find the infiltration rates is shown below.

1. The Northern Mountains – Echo Dam region in Utah was selected as the project location. The 80th percentile, 24 storm depth (in.) was changed to 0.5 in. instead of the default 0.42 in. This was done because all the testing was conducted using a 0.5 in. storm in a 2-hr duration.
2. A Dispersion (natural-engineered) VRA type was selected based on the guidance given in the UDOT 2021 Stormwater Quality Manual (see section 4.2.1 of the manual).
3. A total tributary area of 4 acres was used. This was done to increase the precision of what the infiltration rate should be. The imperviousness of tributary area was then set to 50% to represent the same conditions as the testing conditions.
4. The tributary area soil type was assumed to be Class B (silt loam).
5. A long-term runoff coefficient (R_v) was calculated (Eq. 6). The water quality volume (WQV) used comes from the runoff data from the testing. The depth (d) of the storm is 0.5 in. and the area (A) is 120 ft^2. The calculated R_v was then used rather than the one provided in the spreadsheet.

$$R_v = \frac{WQV}{dA} \tag{6}$$

6. The effective dispersion footprint area was then set to 2 acres which is 50% of the total tributary area.

7. Two different effective amended soil depths of 0 in. and 3 in. were used. This was done to see how the amended soil affected the infiltration rates.
8. The infiltration rate was then varied until the VRA volume reduction was 99.9% or the highest percentage before the VRA volume reduction was 100%. This was done because varying the infiltration rate to a volume reduction of 100% resulted in a large spread of values that did not seem reasonable.

In step 5 a runoff factor was calculated from test data rather than using the provided R_v value in the spreadsheet. The provided R_v is found using Eq. 7 where A_{imp} is the impervious area. This R_v value only considers the amount of impervious area and does not consider soil properties. Using this equation would result in a constant R_v = 0.16. Calculating R_v values from test data provided a more accurate value of what runoff would be expected (Table 3).

$$R_v = 0.225(A_{imp}) + 0.05 \; where \; A_{imp} \leq 55\%$$
$$R_v = 1.14(A_{imp}) - 0.371 \; where \; A_{imp} > 55\% \quad (7)$$

Table 3. Calculated runoff coefficients (R_v) from runoff data.

Runoff Coefficients			
Configuration	**6:1**	**4:1**	**2:1**
19" EF	0.59, 0.62, 0.59	0.48, 0.38, 0.4	0.23, 0.20, 0.16, 0.13
15" EF 4" TS	0.31, 0.07, 0.06	0.08, 0.09, 0.06	0.14, 0.07, 0.06
15" EF 4" TS w/veg	0.25, 0.17	0.19, 0.12, 0.15	0.14, 0.14, 0.16
15" EF 4" ATS	0.34, 0.21, 0.14	0.37	0.33, 0.17, 0.19
15" EF 4" ATS w/veg	0.58,0.65	0.63, 0.68, 0.58	0.48, 0.64, 0.5
15" EF (6" R) 4" TS	0.66,0.6	0.29, 0.29	0.37, 0.34, 0.31

The infiltration rates calculated from the NCHRP spreadsheet tool are shown in Tables 4 and 5 with associated graphs (Fig. 31 and Fig. 32). Some infiltration rates are not included because the data was not representative of the actual conditions. The main reason for the data not being representative is due to the wetting of the soil at the beginning of a configuration. Typically, only 1 or 2 data sets were discarded for each configuration.

Table 4. Infiltration rates without amended soil implemented in NCHRP tool.

Configuration	6:1 Slope	4:1 Slope	2:1 Slope
19” EF	0.5, 0.5, 0.5	0.49, 0.48, 0.48	0.44, 0.43, 0.41, 0.37
15” EF 4” TS	0.47, 0.25, 0.2	0.28, 0.31, 0.2	0.38, 0.25, 0.2
15” EF 4” TS w/veg	0.45, 0.4	0.43, 0.36, 0.4	0.38, 0.38, 0.41
15” EF 4” ATS	0.47, 0.44, 0.38	0.48	0.47, 0.4, 0.43
15” EF 4” ATS w/veg	0.5, 0.5	0.5, 0.5, 0.5	0.49, 0.5, 0.49
15” EF (6” R) 4” TS	0.5, 0.5	0.46, 0.46	0.48, 0.47, 0.47

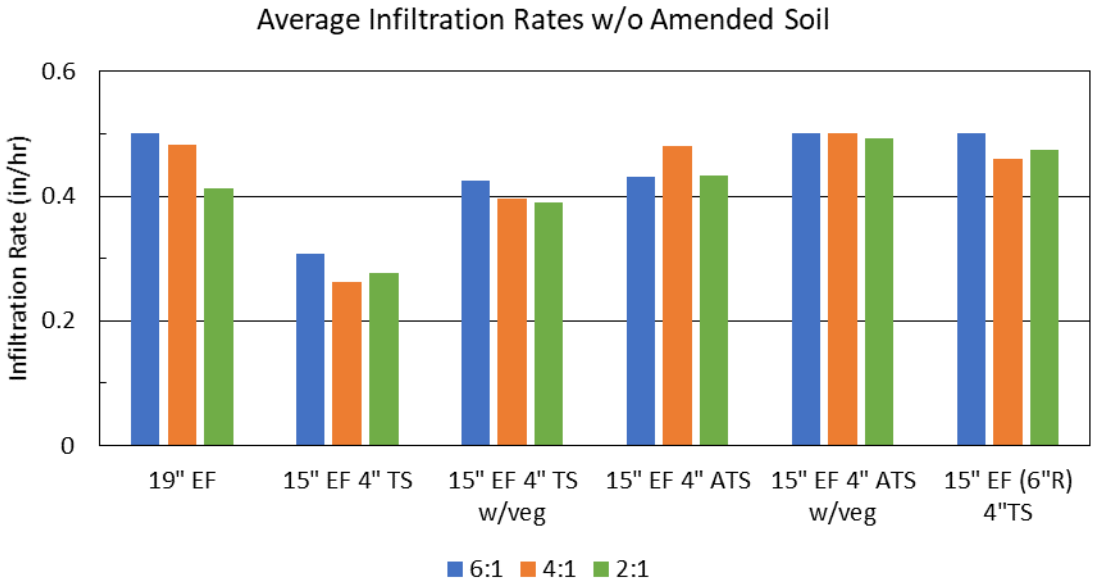

Fig. 31. Average infiltration rates without amended soil implemented in NCHRP tool.

Table 5. Infiltration rates with amended soil implemented in NCHRP tool.

Configuration	6:1 Slope	4:1 Slope	2:1 Slope
19” EF			
15” EF 4” TS	0.1, 0.09, 0.08	0.09, 0.09, 0.08	0.1, 0.09, 0.08
15” EF 4” TS w/veg	0.13, 0.1	0.1, 0.1, 0.1	0.1, 0.1, 0.1
15” EF 4” ATS	0.15, 0.1, 0.1	0.16	0.15, 0.1, 0.1
15” EF 4” ATS w/veg	0.18, 0.18	0.18, 0.18, 0.18	0.17, 0.18, 0.17
15” EF (6” R) 4” TS	0.18, 0.18	0.14, 0.14	0.16, 0.15, 0.15

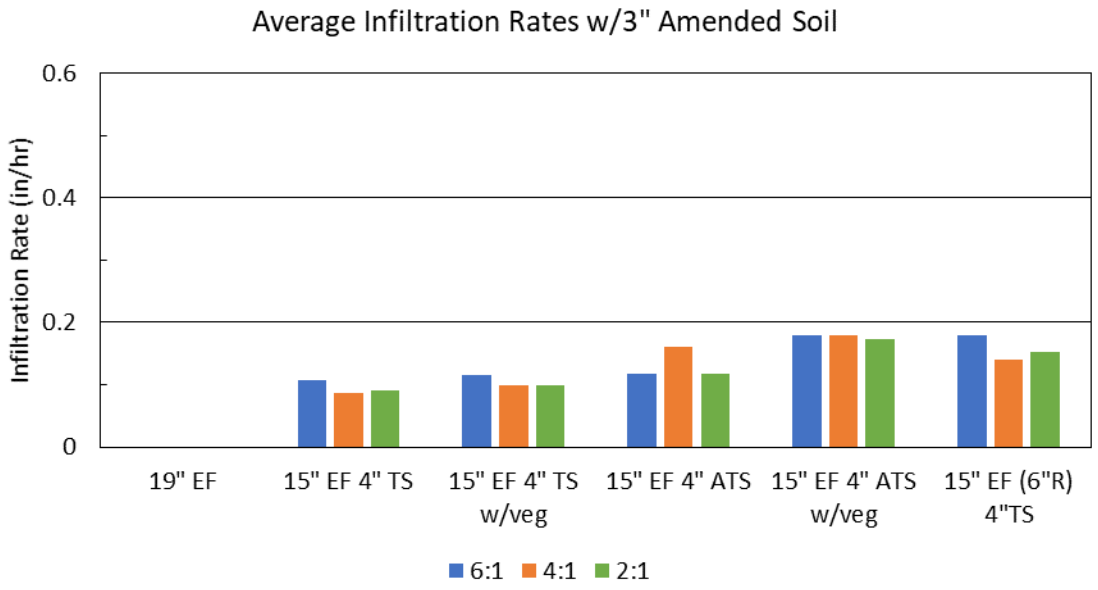

Fig. 32. Average infiltration rates with amended soil implemented in NCHRP tool.

The use of 3 in. amended soil in the NCHRP spreadsheet resulted in smaller infiltration rates than the calculations with no amended soil layer. This was surprising because it was expected that the addition of an amended soil or topsoil would increase infiltration rates. There are assumptions made in the spreadsheet about the amended soil which are never clear. The equations were all locked and no information was given on the properties of the amended soil. One possible interpretation of the data is the low infiltration rates infer that most of the runoff is stored in the amended soil and the

underlying material will have a lower infiltration rate based on the duration and intensity of the storm.

CHAPTER V

CONCLUSION

5.1 Summary

UDOT is required to capture stormwater from the 80th percentile 24-hr storm. Reducing runoff is done by designing various stormwater BMPs near impermeable structures. A filter strip is a common BMP used along roadways to collect stormwater runoff from roads. The design of filter strips became the focus of this research and specifically how the materials and inclinations of the filter strip affected infiltration rates during an 80th percentile 24-hr storm event. A physical model of a filter strip was constructed to test different configurations of soils at various inclinations.

A series of experiments were performed to determine infiltration rates for various configurations consisting of embankment fill, topsoil, an amended topsoil, and vegetation. The six different configurations were 19-in. embankment fill, 15-in. embankment fill with 4-in. of topsoil, 15-in. embankment fill with 4-in. of topsoil and vegetation, 15-in. embankment fill with 4-in. of amended topsoil, 15-in. embankment fill with 4-in. of amended topsoil and vegetation, and 15-in. embankment fill with 6-in. rips and 4-in. of topsoil. Several experiments were conducted at 6:1, 4:1, and 2:1 inclinations for each configuration.

VWC was measured using three soil moisture sensors and runoff/infiltration volumes were collected and measured as each experiment was performed. The VWC readings and runoff measurements were processed to determine how infiltration occurred during the storm event. Adjustments were made to the VWC readings to match the

measured amount of infiltration from the collected runoff volumes. Infiltration rates were then calculated using the NCHRP spreadsheet tool.

5.2 Key Findings

In summary, some configurations performed better than others. The maximum amount of infiltration was 63% of the 80th percentile 24-hr storm which was collected from the configuration of 15-in. embankment fill and 4-in. of amended topsoil with vegetation. The factors that affected infiltration included inclinations, matric suction of the topsoil, vegetation, and the ripping of the underlying embankment fill.

The inclination of the filter strip was a contributing factor on the amount of infiltration for the configuration with only embankment fill. The 6:1 inclination resulted in the most infiltration due to the lower velocity of the surface water. The 2:1 inclination resulted in the least amount of infiltration. There was an average decrease of 20% in VWC between the 6:1 to 4:1 and 4:1 to 2:1 inclinations. The use of just one material reduced the number of factors that could prevent infiltration. Due to the matric suction of the topsoil and amended topsoil, the inclination of the filter strip had little effect on how much infiltration occurred.

The addition of a topsoil over the embankment fill resulted in a capillary barrier forming at the interface of the two materials due to the matric suction of the topsoil. The matric suction of the soil became a major factor in the amount of infiltration. The topsoil and amended topsoil which was used had a high matric suction and did not allow for much infiltration. The topsoil was meant to increase infiltration, but actually reduced the

amount of infiltration. Further research needs to be conducted in order to find a suitable topsoil for the embankment material that will increase infiltration.

The addition of vegetation and sacrificing the embankment material were two methods found to reduce the matric suction and increase infiltration into the lower embankment layer. Vegetation cover allowed for water to flow through around the vegetation roots and into the embankment fill. The vegetation also acted as a barrier to surface flow and therefore slowed down the velocity of the surface water which allowed more time for the surface water to be infiltrated into the soil. There was a 66% increase in infiltration with the addition of vegetation on the topsoil and a 120% increase in infiltration with the addition of vegetation on the amended topsoil when compared to the configurations with only topsoil and amended topsoil.

Ripping the embankment material allowed for the loose soil to mix with the topsoil. This reduced the area where a distinct interface could form and prevent infiltration due to the matric suction of the topsoil. Creating rips in the embankment material resulted in higher increases of infiltration compared to the configurations of just topsoil and topsoil with vegetation. There was a 290% average increase in infiltration due to the scarifying of soil compared to the configuration of embankment material and topsoil with no scarifications. The rips, however, may close over long periods of time which will reduce the amount of infiltration into the system.

The NRCHP spreadsheet tool was used to calculate infiltration rates for the different configurations. Only using the provided values in the spreadsheet resulted in a lower calculated infiltration rates compared to when the recorded data was entered in the spreadsheet. Calculating the runoff coefficient (R_v) from the collected runoff data

provided a more representative infiltration rate for the given soil conditions. The R_v value was now a factor of soil properties and not just amount of impervious area.

5.3 Future Research

Further research will be conducted on various embankment materials and topsoils. The UDOT section 02056 specification for embankment, borrow, and backfill allows for materials consisting of soils with AASHTO classifications of A-1-a through A-4 to be used as borrow material. The current testing consisted of an A-2-4 (0) material which falls near the middle of the range of acceptable classifications for borrow material in an embankment. The future testing will consist of soils near the ends of the specified range.

A different topsoil and amended topsoil will be used in further research in an effort to mitigate the matric suction of the topsoil. This will allow for more retention in the topsoil and more infiltration into the embankment material. Small scale soil column experiments will be conducted to test different topsoil materials. The experiments are meant to find a suitable topsoil that will allow infiltration into the embankment material.

The further research will provide a wide range of data to be used by UDOT in their current designs for filter strips and other stormwater management practices. Interpolations can be performed between the wide range of experimental data points in order to determine design infiltration rate values based on the gradation of the embankment material that will be used in construction.

REFERENCES

Basche A.D., and DeLonge MS. 2019. “Comparing infiltration rates in soils managed with conventional and alternative farming methods: A meta-analysis.” *PLoS ONE* 14(9): e0215702. https:// doi.org/10.1371/journal.pone.0215702

Berland et al. 2017. “The role of trees in urban stormwater management.” *Landsc Urban Plan.* 162: 167–177. doi:10.1016/j.landurbplan.2017.02.017.

Bingqin Zhao et al. 2019. “Effects of Rainfall Intensity and Vegetation Cover on Erosion Characteristics of a Soil Containing Rock Fragments Slope.” *Advances in Civil Engineering* Volume 2019. Article ID 7043428. https://doi.org/10.1155/2019/7043428.

Braga, A., M. Horst, and R. G. Traver. 2007. “Temperature Effects on the Infiltration Rate through an Infiltration Basin BMP.” *J. Irrig. Drain Eng.,* 133(6): 593-601. https://doi.org/10.1061/(ASCE)0733-9437(2007)133:6(593).

Chang, W. J., and D. J. Hills. 1993. “Sprinkler Droplet Effects on Infiltration. II. Laboratory Study.” *J. Irrig. Drain Eng.*, 119(1): 157-169. https://doi.org/10.1061/(ASCE)0733-9437(1993)119:1(157).

Chen, P., B. Mirus, N. Lu, and J. W. Godt. 2017. “Effect of Hydraulic Hysteresis on Stability of Infinite Slopes under Steady Infiltration.” *J. Geotech. Geoenviron. Eng.,* 143(9): 04017041. https://doi.org/10.1061/(ASCE)GT.1943-5606.0001724.

Curtis, M. J., and V. P. Claassen. 2007. “Using Compost to Increase Infiltration and Improve the Revegetation of a Decomposed Granite Roadcut.” *J. Geotech. Geoenviron. Eng.,* 133(2): 215-218. https://doi.org/10.1061/(ASCE)1090-0241(2007)133:2(215).

Hartsig, T., and A. Szatko. 2012. “Performace Assessment of Two Stormwater Best Management Practices for Infiltration, Water Quality, and Vegetation Growth.” City of Omaha, Nebraska.

Kim, Y. K., and S. R. Lee. 2010. “Field Infiltration Characteristics of Natural Rainfall in Compacted Roadside Slopes.” *J. Geotech. Geoenviron. Eng.,* 136(1): 248-252. https://doi.org/10.1061/(ASCE)GT.1943-5606.0000160.

Lu, N., and C. Zhang. 2019. “Soil Sorptive Potential: Concept, Theory, and Verification”. *J. Geotech. Geoenviron. Eng.,* 2019, 145(4): 04019006. https://doi.org/10.1061/(ASCE)GT.1943-5606.0002025.

Menashe, E. 1998. “Vegetation and Erosion A Literature Survey.” Greenbelt Consulting

Morrow, S., M. Smolen, J. Stiegler, and J. Cole. 1994. “Using Vegetation for Erosion Control on Construction Sites.” Oklahoma Cooperative Extension Service

National Cooperative Highway Research Program (NCHRP). 2021. “NCHRP 25-41 – Volume Performance Tool V.1.0 for Windows.” [Microsoft Excel Spreadsheet] Last modified by UDOT: 2021

Natural Resources Conservation Service (NRCS). 2022. *Web Soil Survey.* https://websoilsurvey.sc.egov.usda.gov/App/WebSoilSurvey.aspx

Oorthuis, R., Vaunat, J., Hürlimann, M., Lloret, A., Moya, J., Puig-Polo, C., and A. Fraccica. 2021. “Effect of vegetation and slope orientation on water infiltration in a monitored embankment.” *EGU General Assembly 2021,* online, 19–30 Apr 2021, EGU21-7599, https://doi.org/10.5194/egusphere-egu21-7599, 2021.

Pitt, R., and J. Lantrip. 2000. "Infiltration Through Disturbed Urban Soils." *Journal of Water Management Modeling* R206-01. doi: I 0.14 796/JWMMR206-01.

Sajjan, A. K., Y. G. Agyei, and R. H. Sharma. 2015. “Modeling Grass-Cover Effects on Soil Erosion on Railway Embankment Steep Slopes.” *J. Hydrol. Eng.*, 20(9): 04014092. https://doi.org/10.1061/(ASCE)HE.1943-5584.0001127.

Smesrud, J. K., and J. S. Selker. 2001. “Effect of Soil-Particle Size Contrast on Capillary Barrier Performance.” *J. Geotech. Geoenviron. Eng.*, 127(10): 885-888. https://doi.org/10.1061/(ASCE)1090-0241(2001)127:10(885).

Stormont, J. C., and C. E. Anderson. 1999. “Capillary Barrier Effect from Underlying Coarser Soil Layer.” *J. Geotech. Geoenviron. Eng.*, 125(8): 641-648. https://doi.org/10.1061/(ASCE)1090-0241(1999)125:8(641).

Tami, D., H. Rahardjo, and E. C. Leong. 2004. “Effects of Hysteresis on Steady-State Infiltration in Unsaturated Slopes.” *J. Geotech. Geoenviron. Eng.*, 130(9): 956-967. https://doi.org/10.1061/(ASCE)1090-0241(2004)130:9(956).

Thompson, S. E., C. J. Harman, P. Heine, and G. G. Katul. 2010. “Vegetation-infiltration relationships across climatic and soil type gradients”. *J. Geophys.* Res. 115. G02023. doi:10.1029/2009JG001134.

Winston, R. J., W. F. Hunt, S. G. Kennedy, J. D. Wright, and M. S. Lauffer. 2012. “Field Evaluation of Storm-Water Control Measures for Highway Runoff Treatment.” *J. Environ. Eng.*, 138(1): 101-111. https://doi.org/10.1061/(ASCE)EE.1943-7870.0000454.

United States Department of Agriculture (USDA). 2017. “Rangeland Soil Quality Infiltration.”

Utah Department of Transportation (UDOT). 2021. “Stormwater Quality Design Manual.”

APPENDICES

Appendix A: 2-hr Data Curves

Configuration 1: 19” Embankment Fill

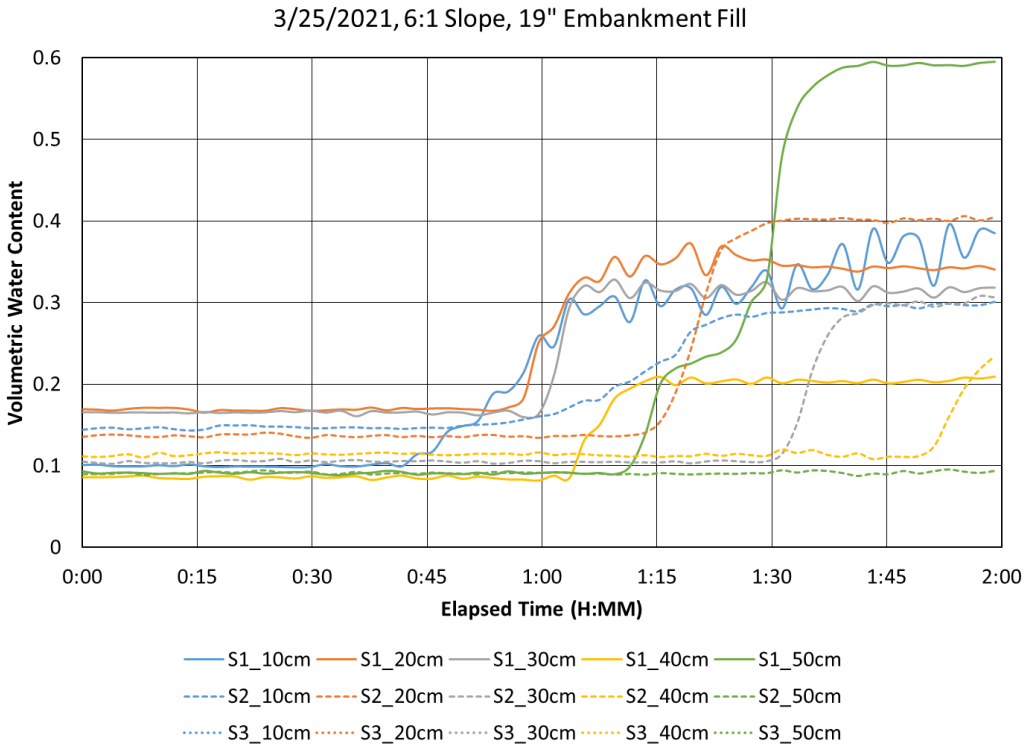

Fig. A1. 19” Embankment Fill 2-hr raw data at a 6:1 slope.

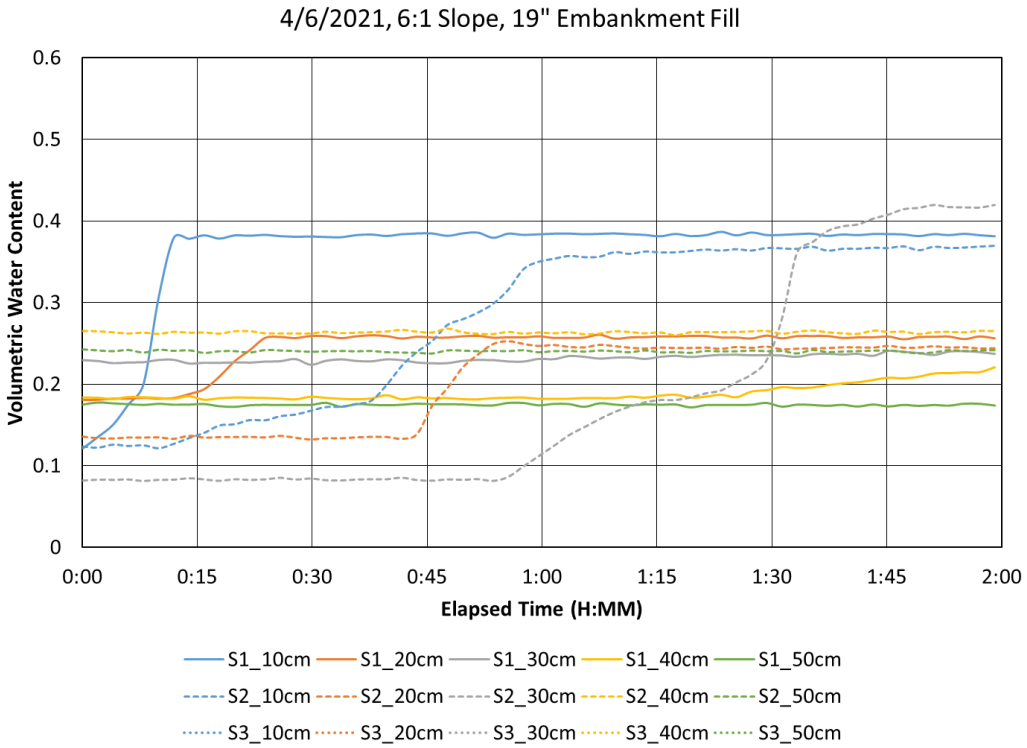

Fig. A2. 19" Embankment Fill 2-hr raw data at a 6:1 slope.

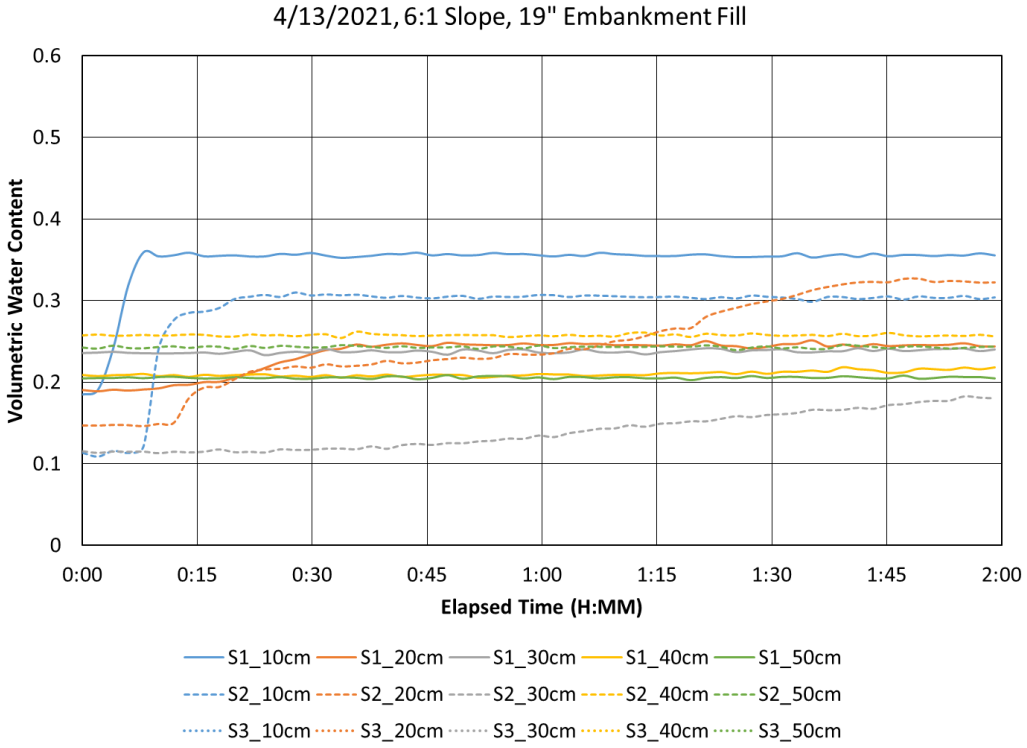

Fig. A3. 19" Embankment Fill 2-hr raw data at a 6:1 slope.

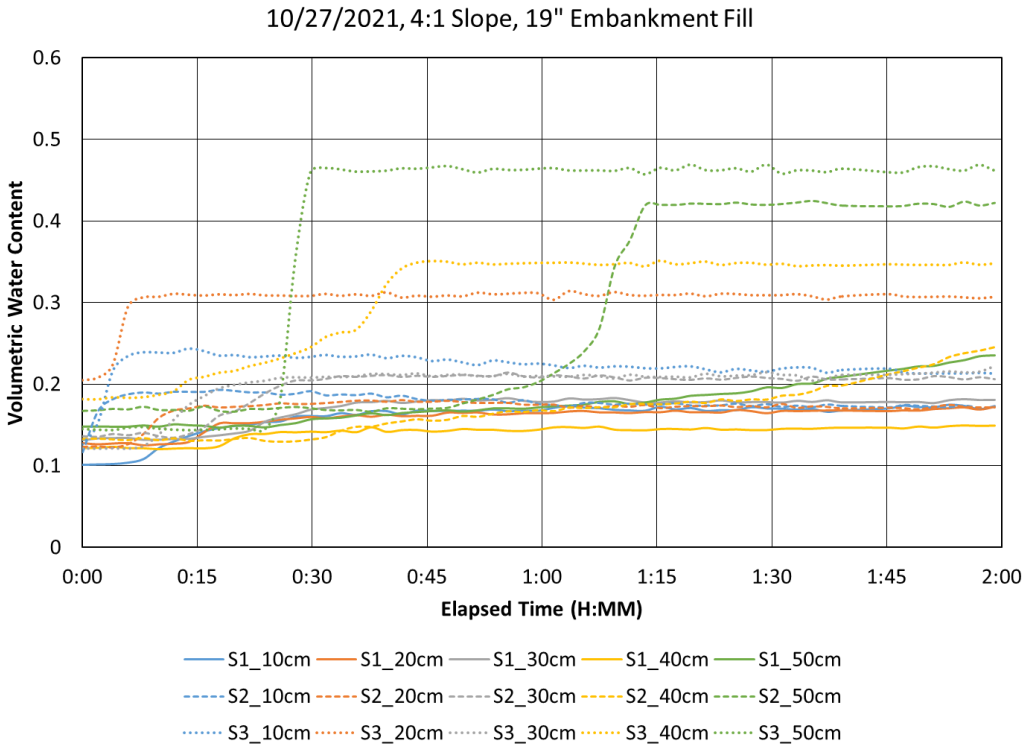

Fig. A4. 19" Embankment Fill 2-hr raw data at a 4:1 slope.

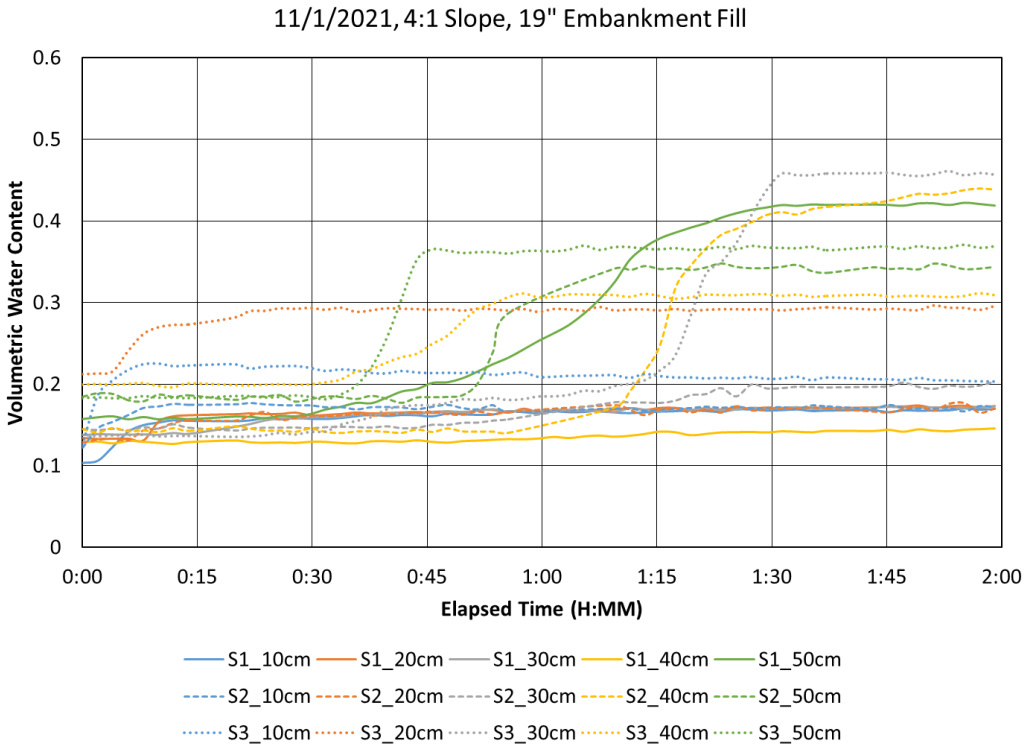

Fig. A5. 19" Embankment Fill 2-hr raw data at a 4:1 slope.

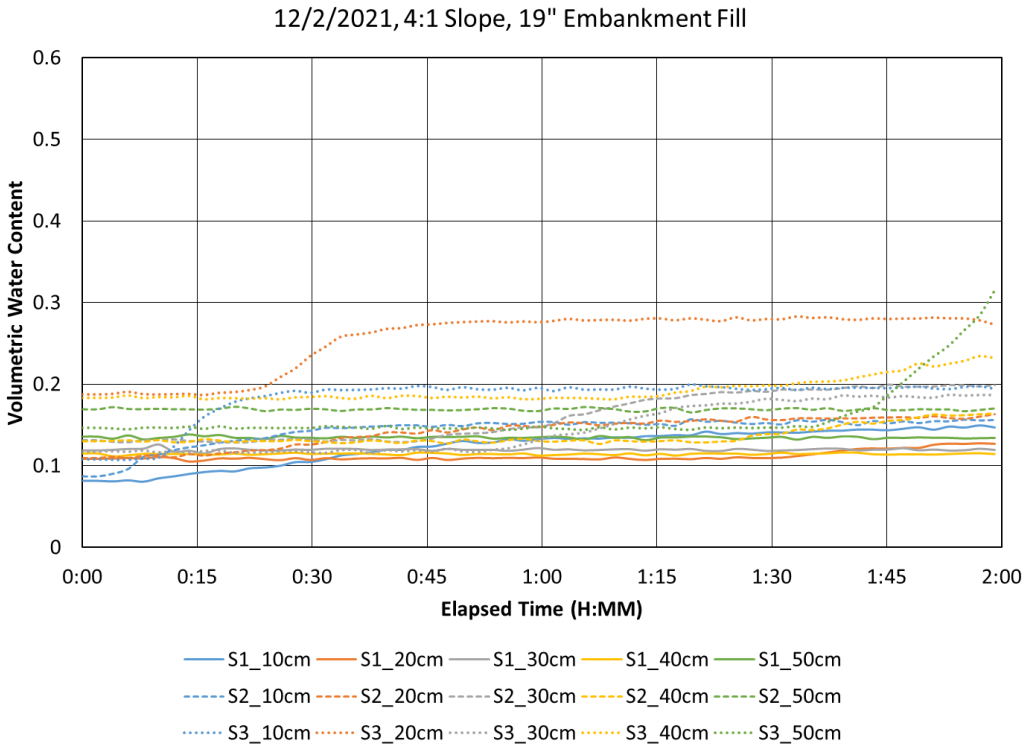

Fig. A6. 19" Embankment Fill 2-hr raw data at a 4:1 slope.

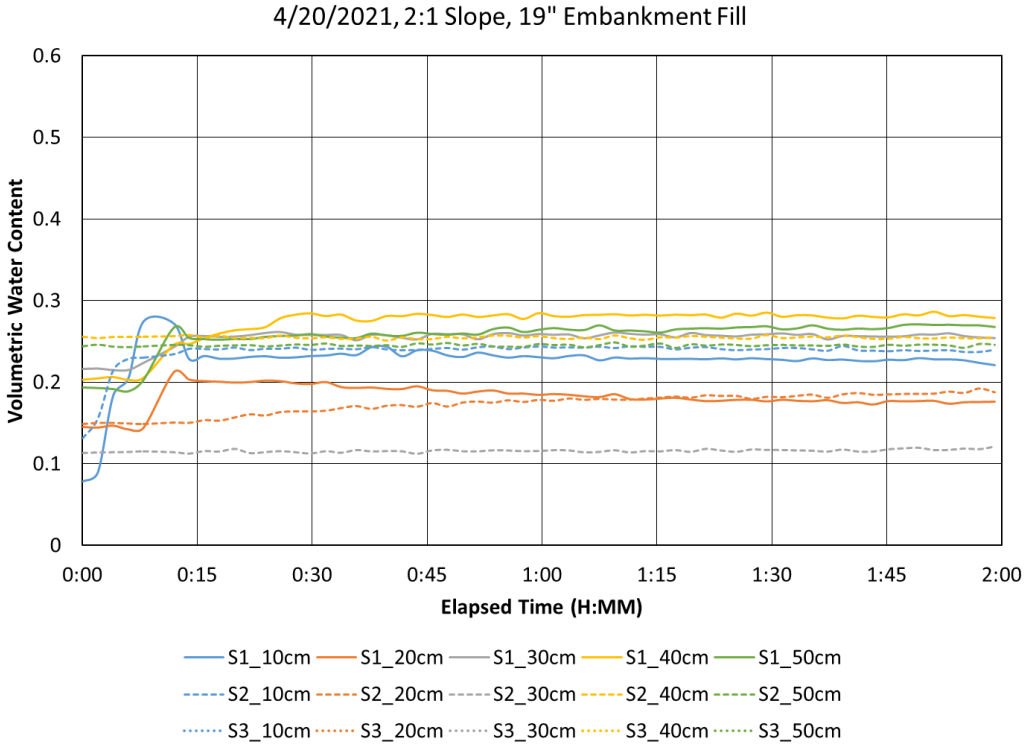

Fig. A7. 19" Embankment Fill 2-hr raw data at a 2:1 slope.

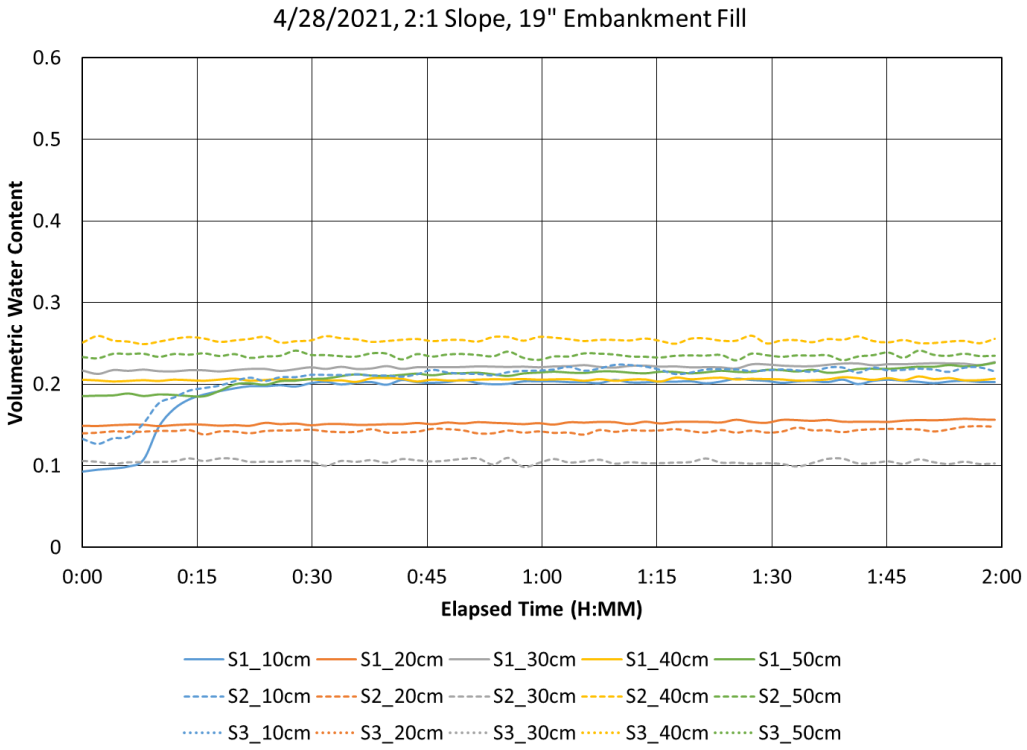

Fig. A8. 19" Embankment Fill 2-hr raw data at a 2:1 slope.

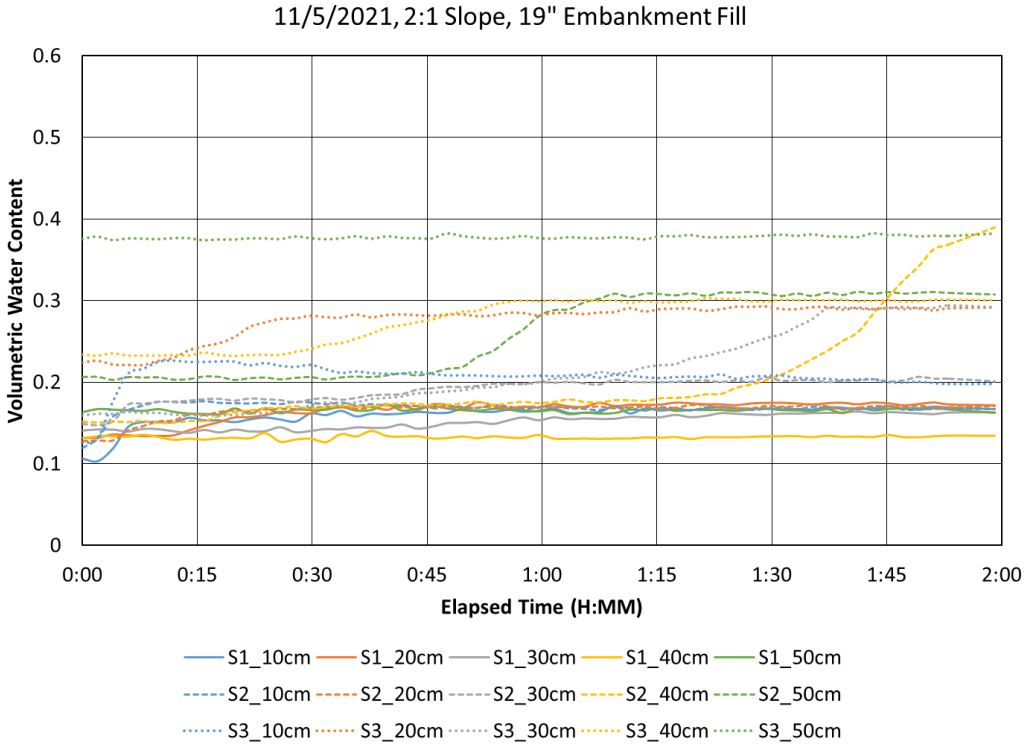

Fig. A9. 19" Embankment Fill 2-hr raw data at a 2:1 slope.

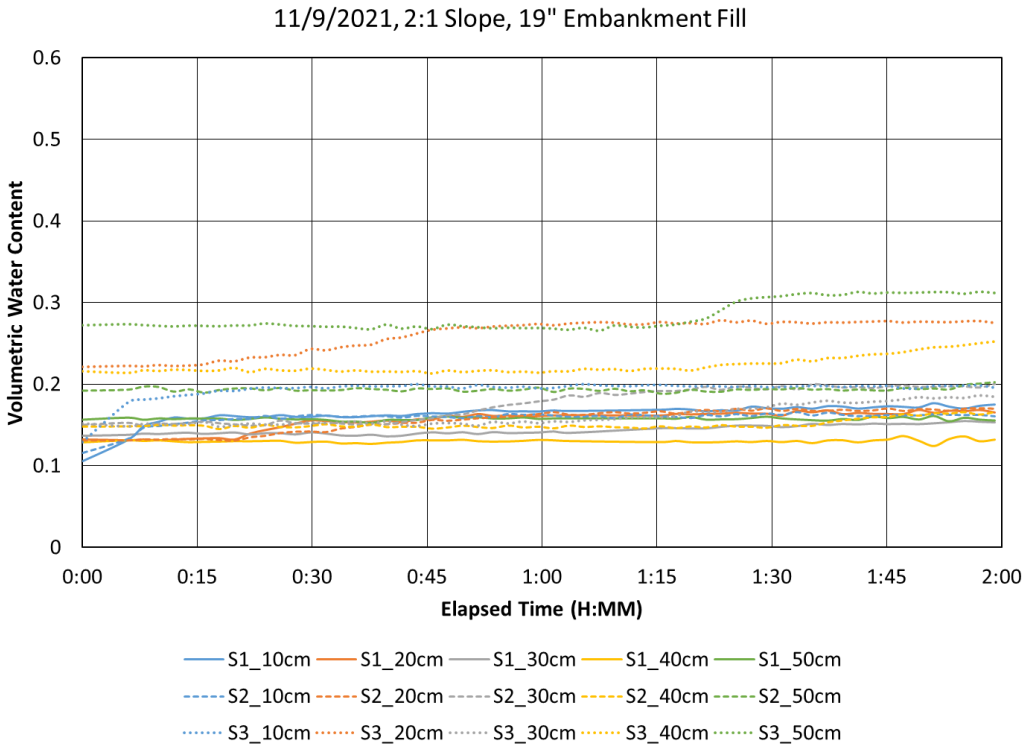

Fig. A10. 19” Embankment Fill 2-hr raw data at a 2:1 slope.

Configuration 2: 15” Embankment Fill 4” Topsoil

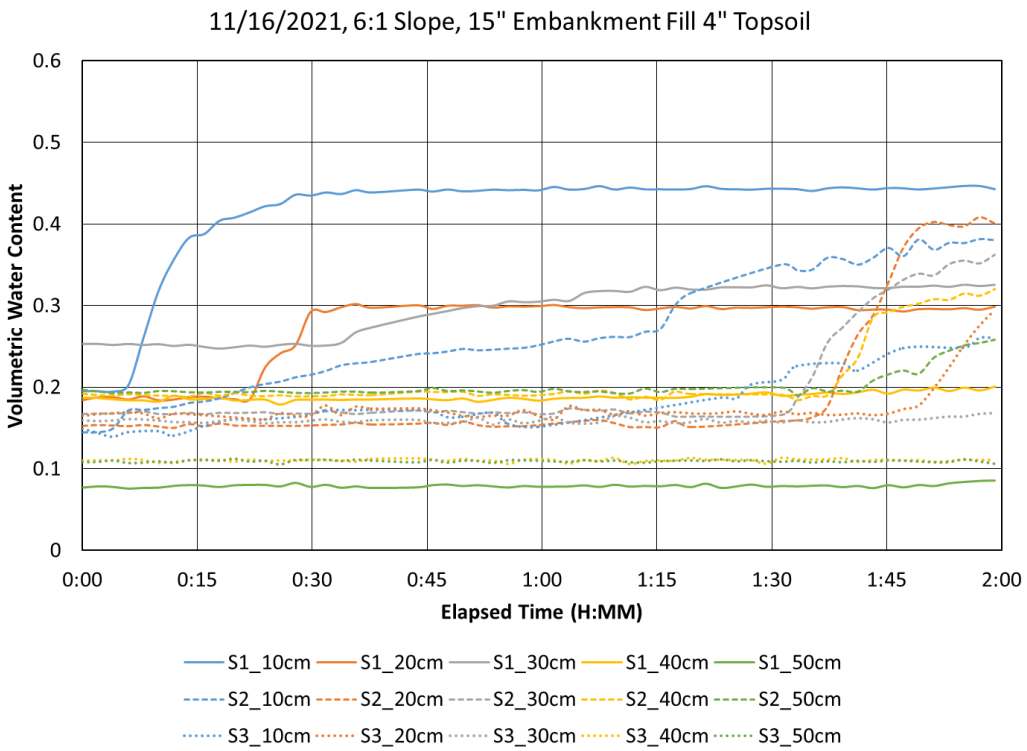

Fig. A11. 15” Embankment Fill 4” Topsoil 2-hr raw data at a 6:1 slope.

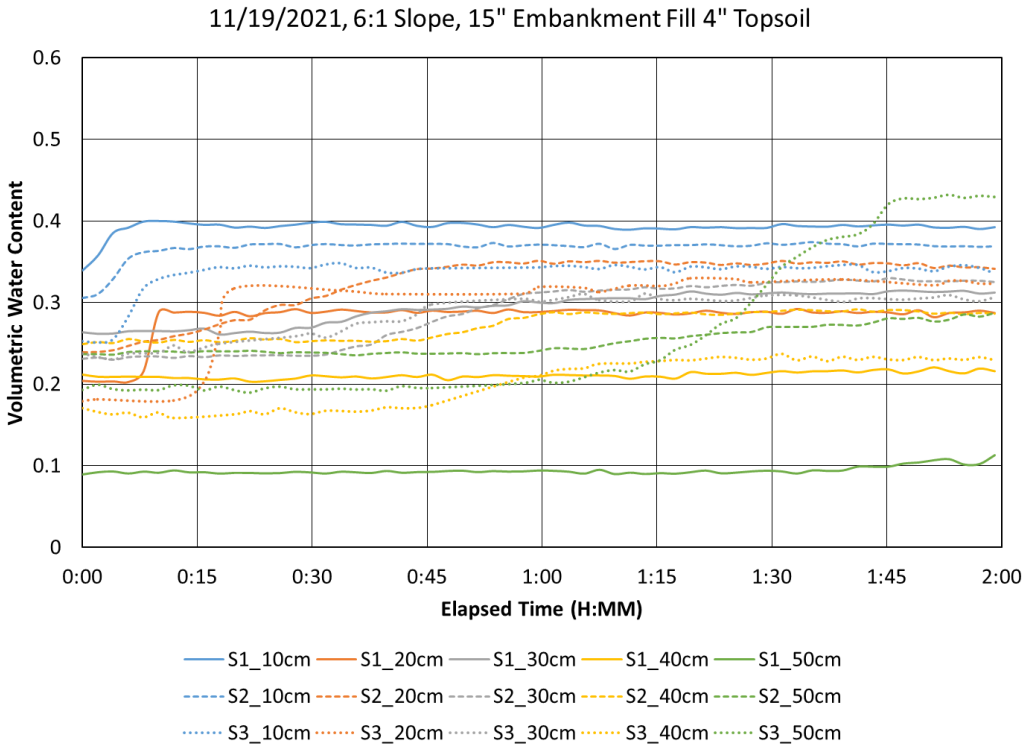

Fig. A12. 15" Embankment Fill 4" Topsoil 2-hr raw data at a 6:1 slope.

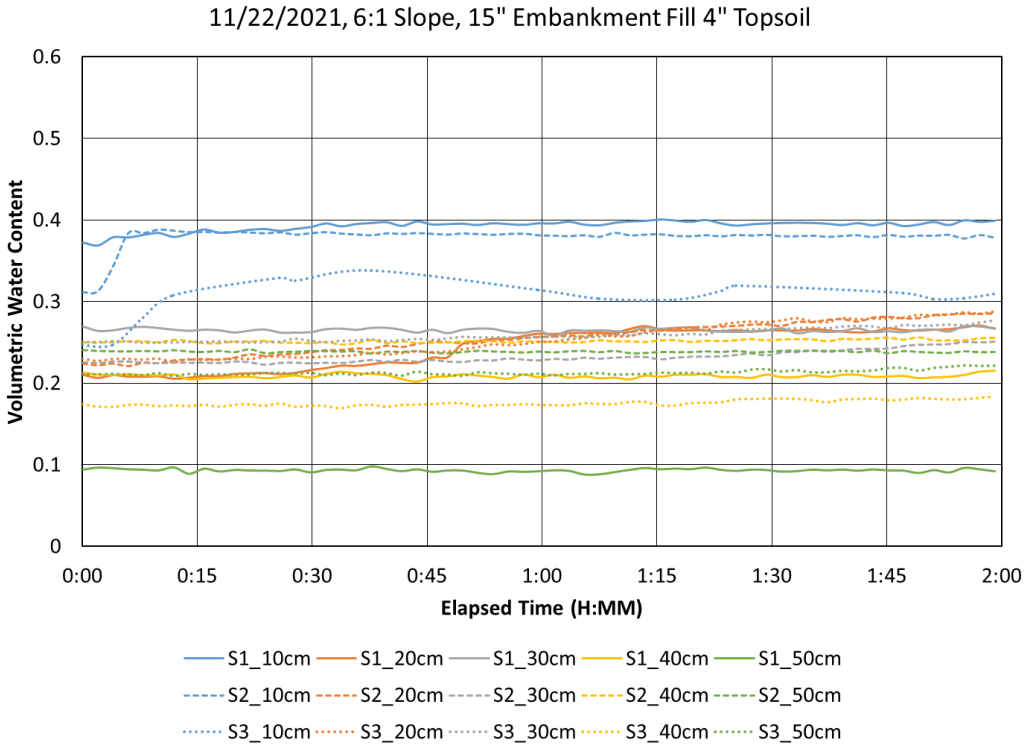

Fig. A13. 15" Embankment Fill 4" Topsoil 2-hr raw data at a 6:1 slope.

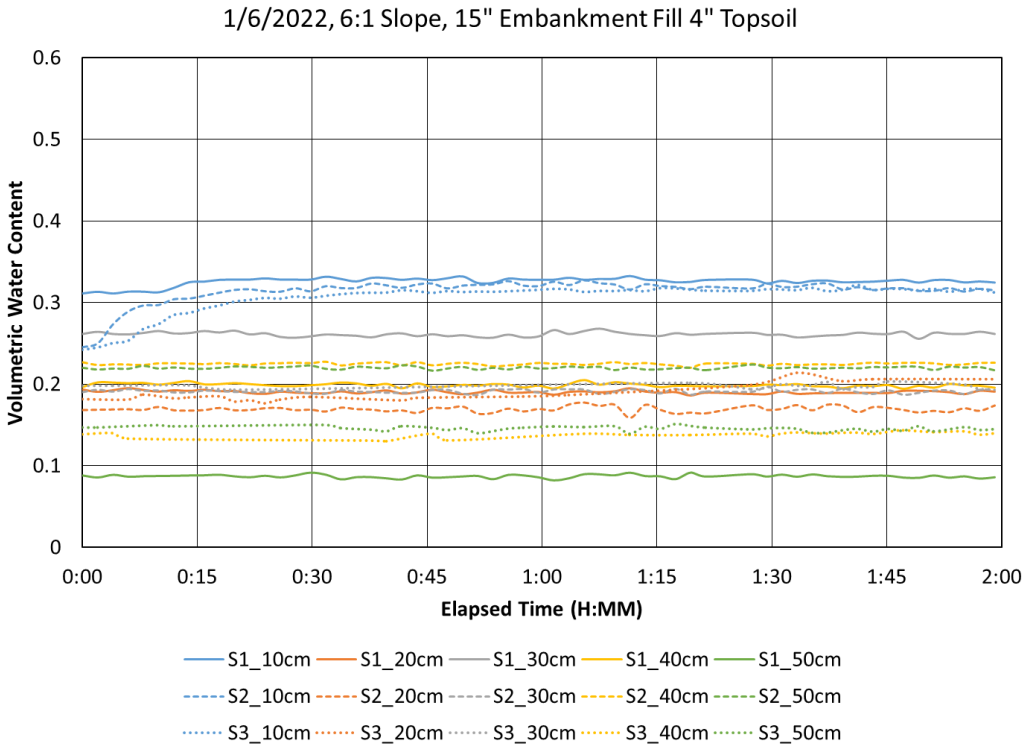

Fig. A14. 15" Embankment Fill 4" Topsoil 2-hr raw data at a 6:1 slope.

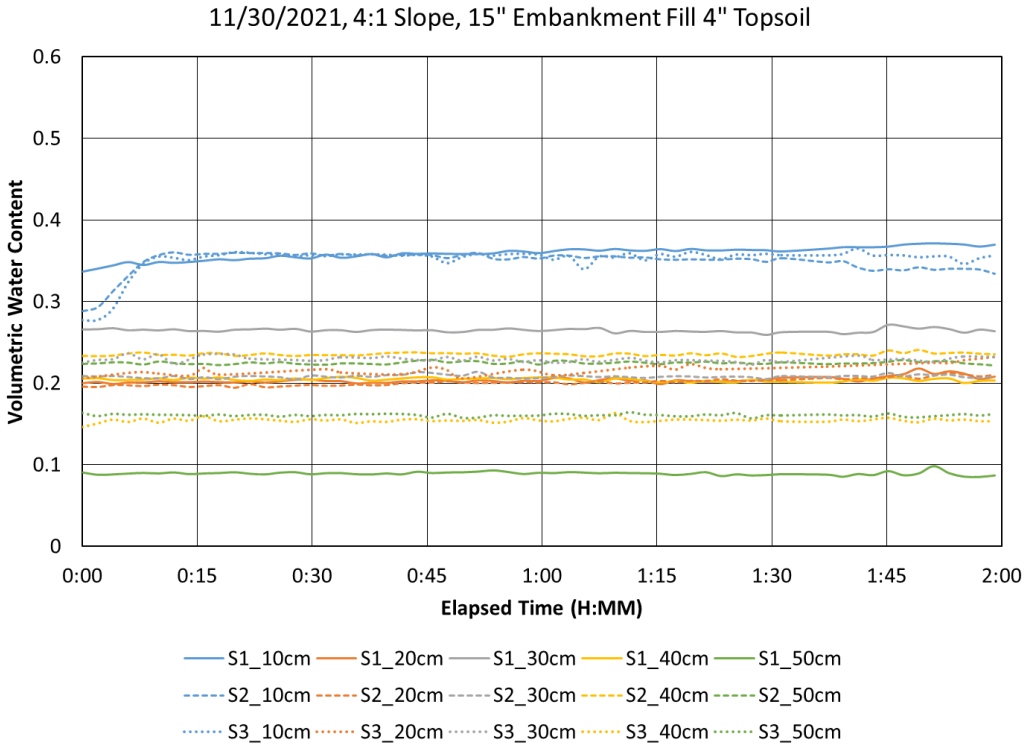

Fig. A15. 15" Embankment Fill 4" Topsoil 2-hr raw data at a 4:1 slope.

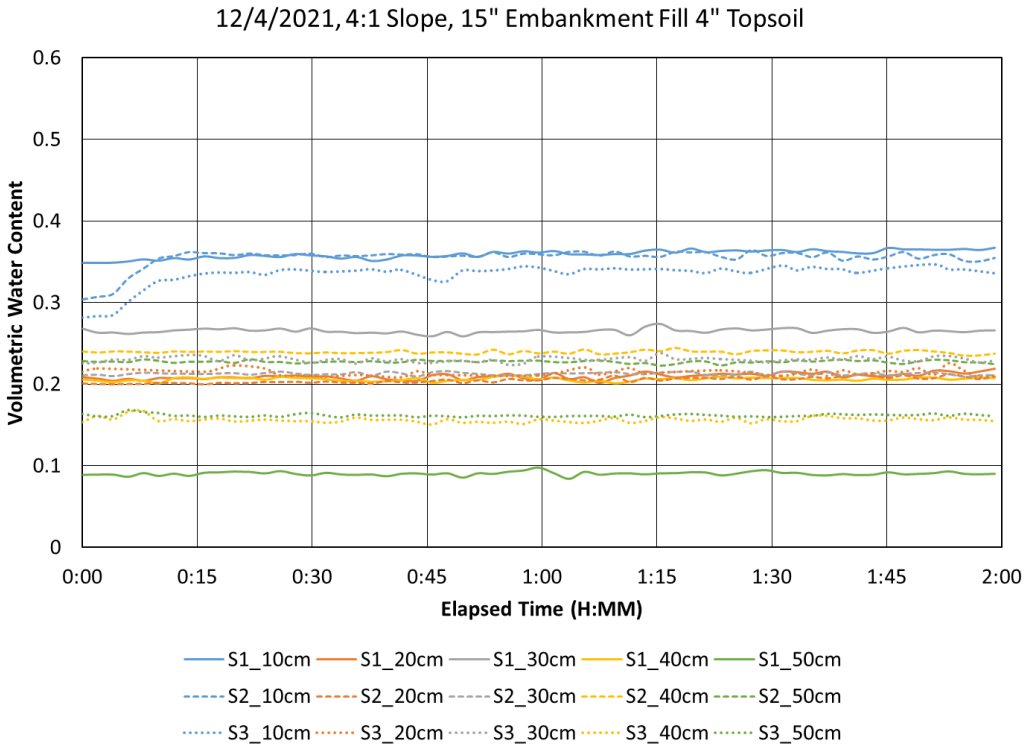

Fig. A16. 15" Embankment Fill 4" Topsoil 2-hr raw data at a 4:1 slope.

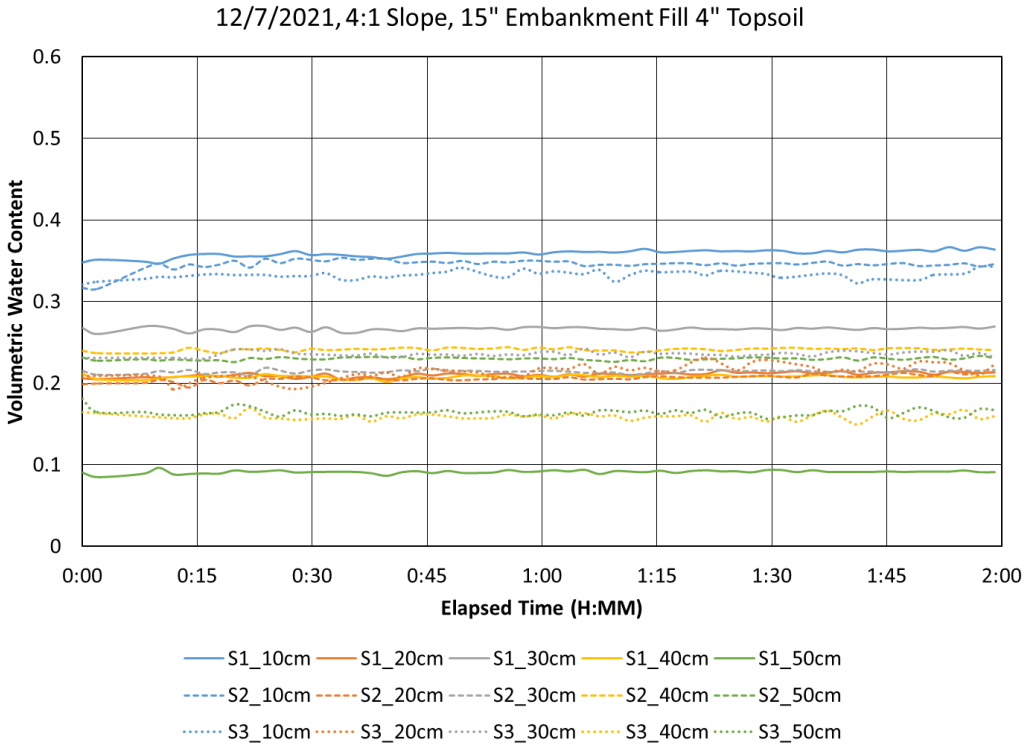

Fig. A17. 15" Embankment Fill 4" Topsoil 2-hr raw data at a 4:1 slope.

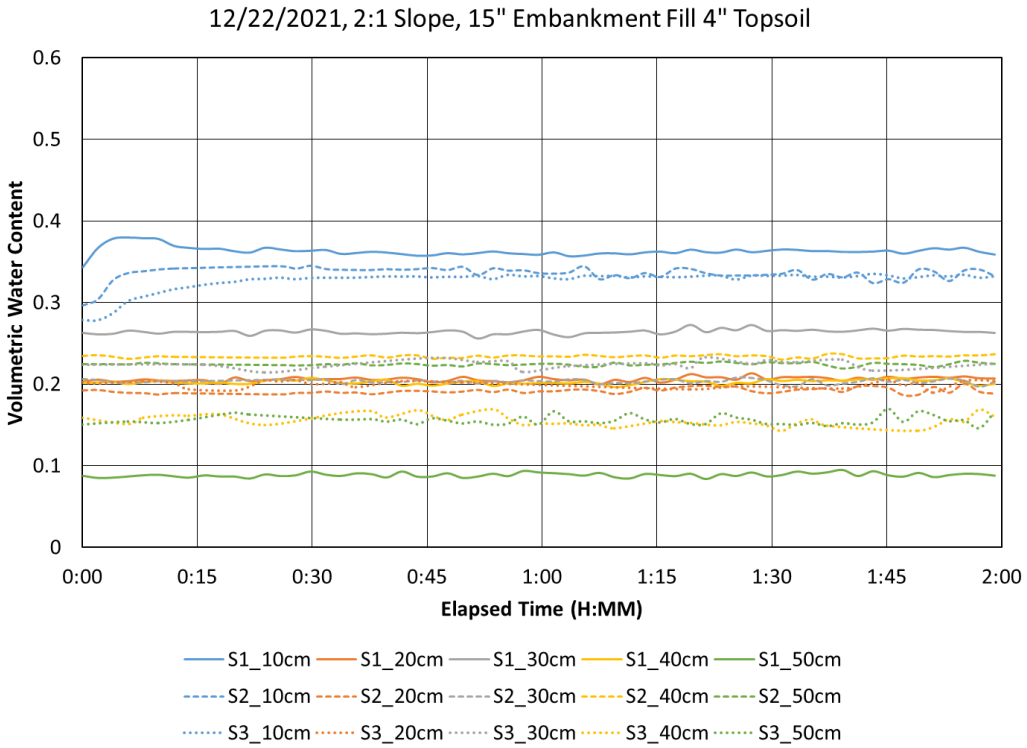

Fig. A18. 15” Embankment Fill 4” Topsoil 2-hr raw data at a 2:1 slope.

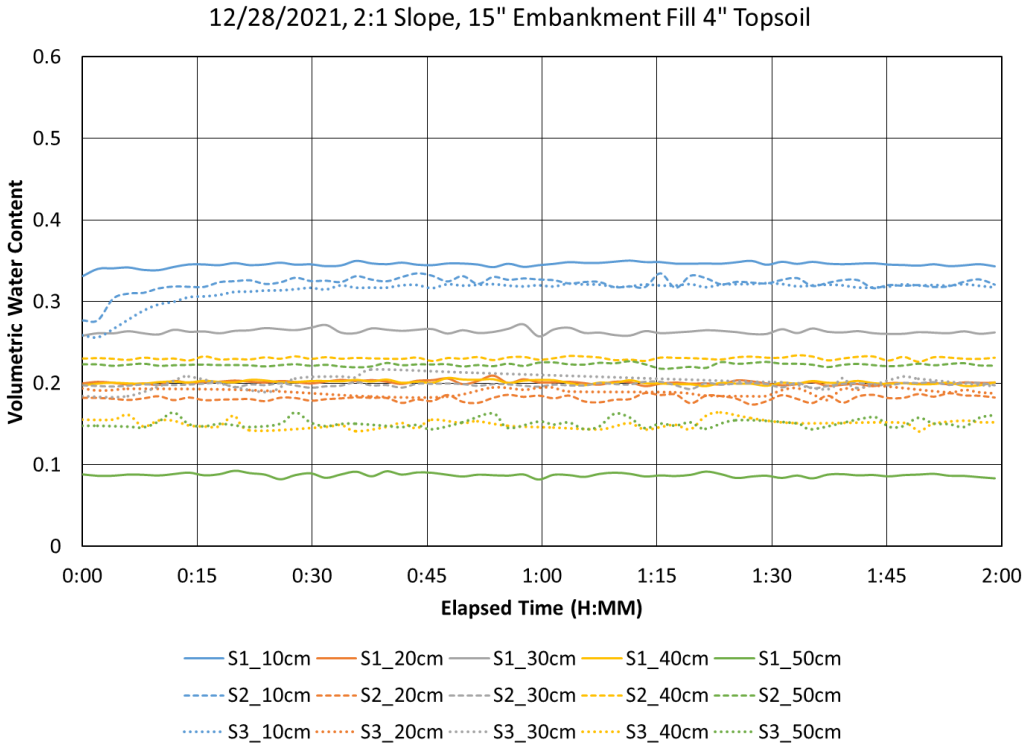

Fig. A19. 15” Embankment Fill 4” Topsoil 2-hr raw data at a 2:1 slope.

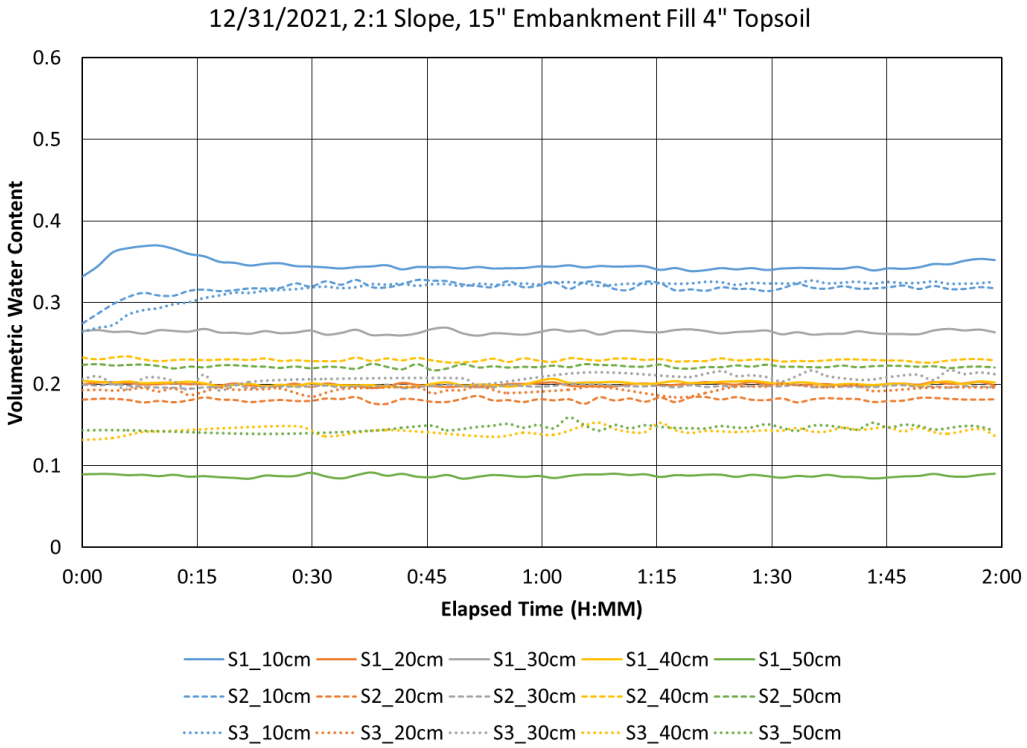

Fig. A20. 15” Embankment Fill 4” Topsoil 2-hr raw data at a 2:1 slope.

Configuration 3: 15” Embankment Fill 4” Topsoil with Vegetation

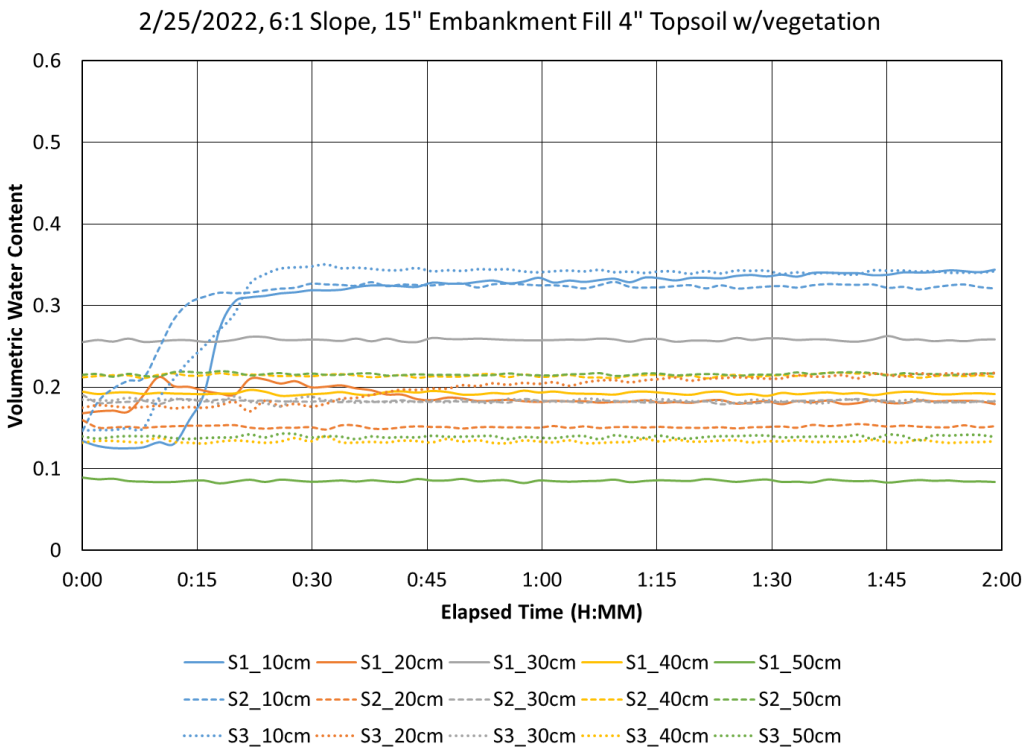

Fig. A21. 15” Embankment Fill 4” Topsoil w/vegetation 2-hr raw data at a 6:1 slope.

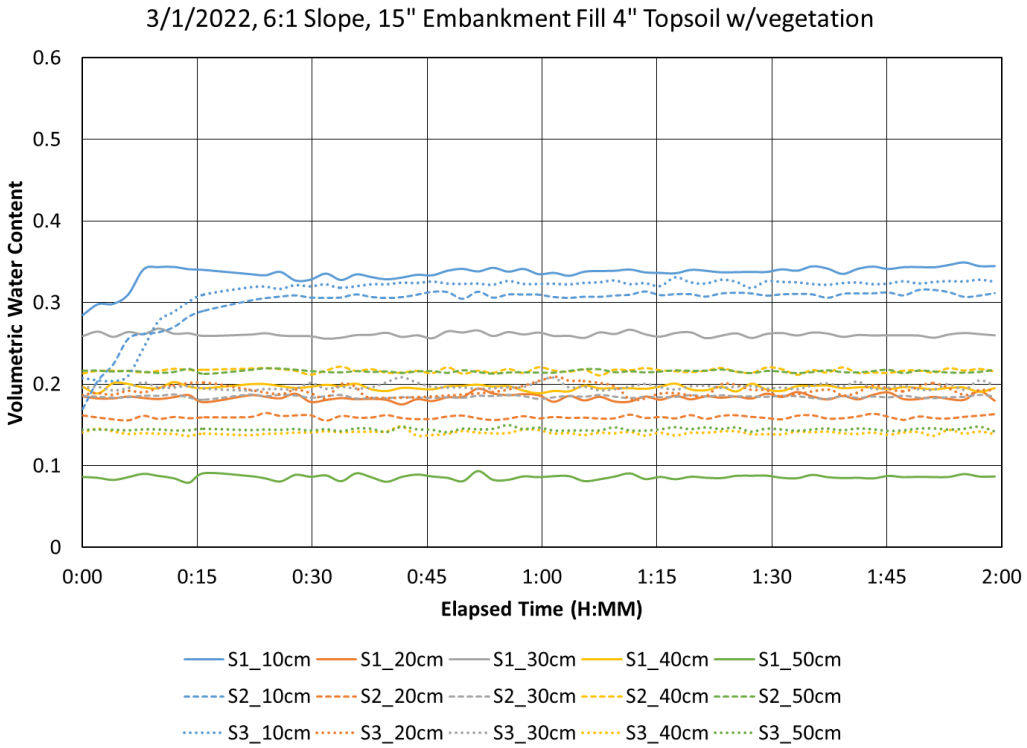

Fig. A22. 15" Embankment Fill 4" Topsoil w/vegetation 2-hr raw data at a 6:1 slope.

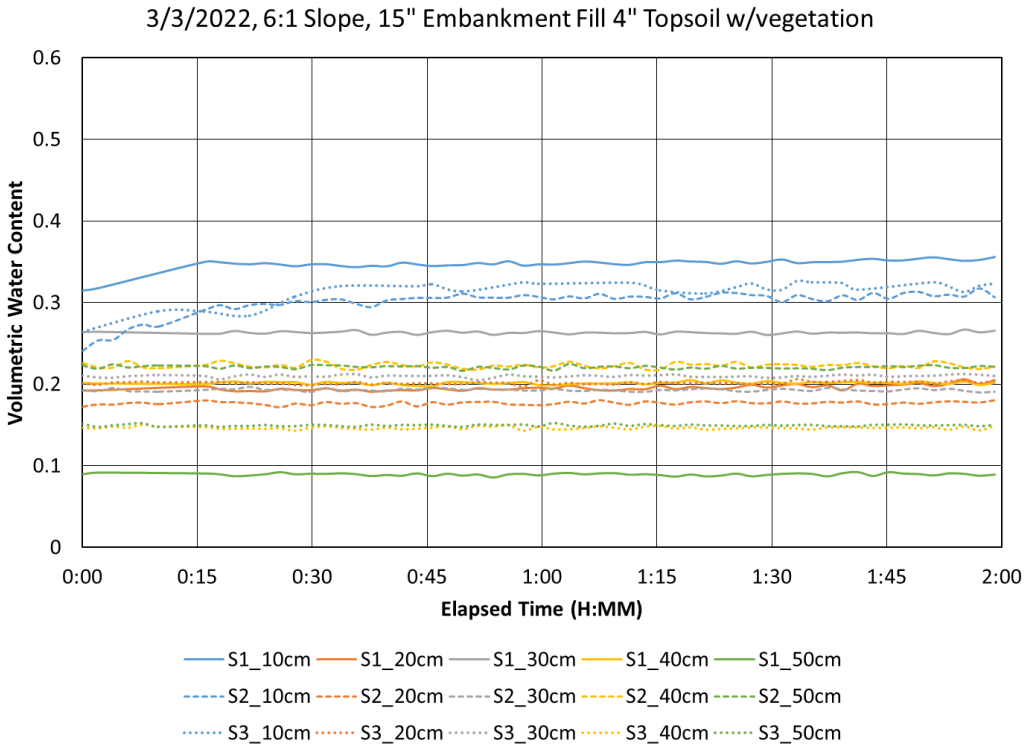

Fig. A23. 15" Embankment Fill 4" Topsoil w/vegetation 2-hr raw data at a 6:1 slope.

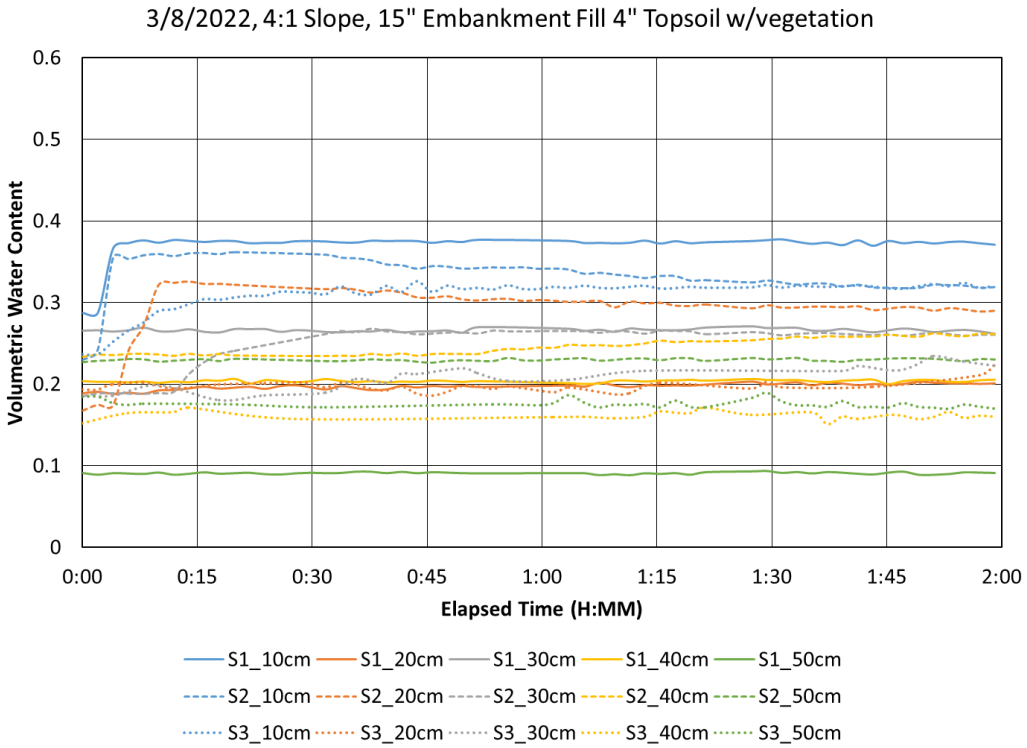

Fig. A24. 15" Embankment Fill 4" Topsoil w/vegetation 2-hr raw data at a 4:1 slope.

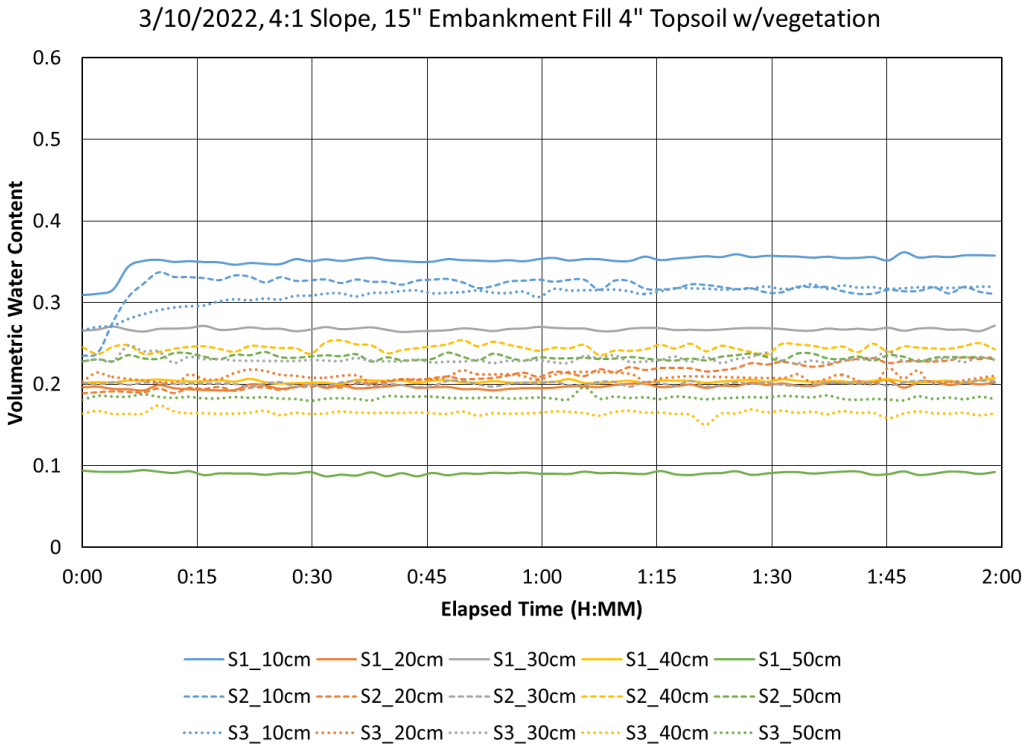

Fig. A25. 15" Embankment Fill 4" Topsoil w/vegetation 2-hr raw data at a 4:1 slope.

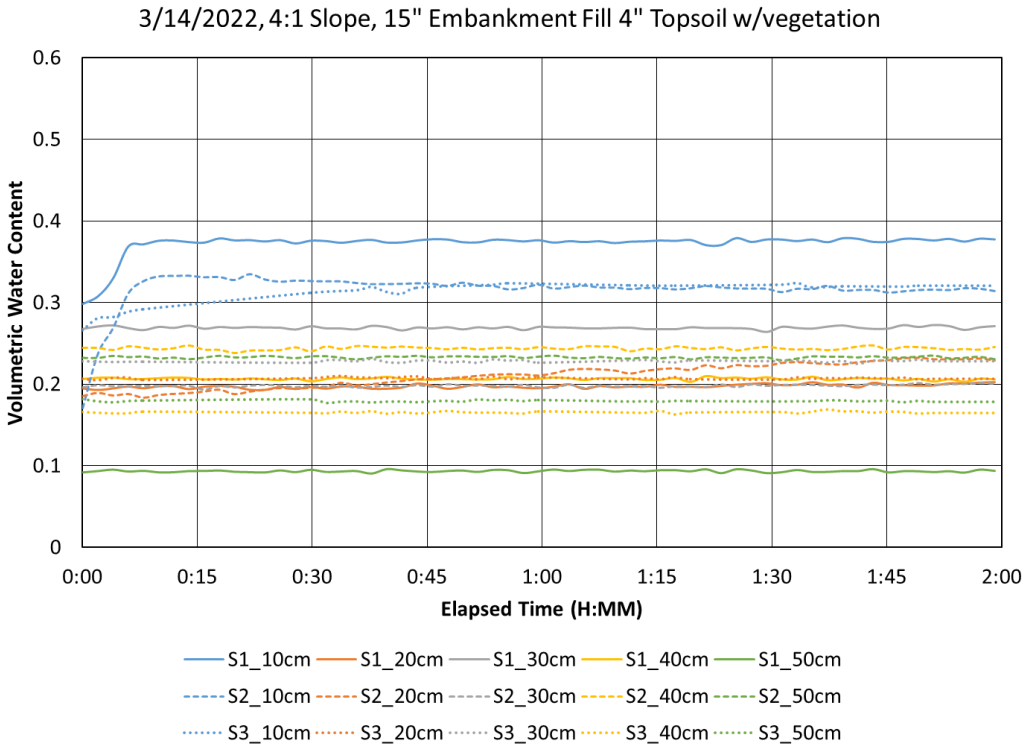

Fig. A26. 15" Embankment Fill 4" Topsoil w/vegetation 2-hr raw data at a 4:1 slope.

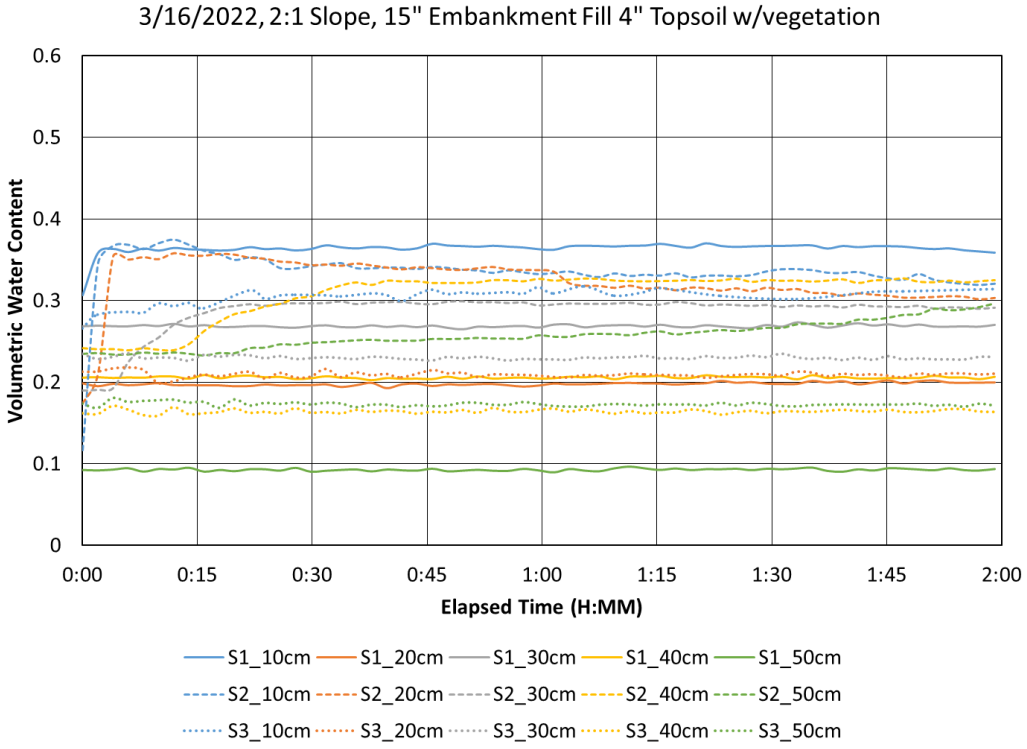

Fig. A27. 15" Embankment Fill 4" Topsoil w/vegetation 2-hr raw data at a 2:1 slope.

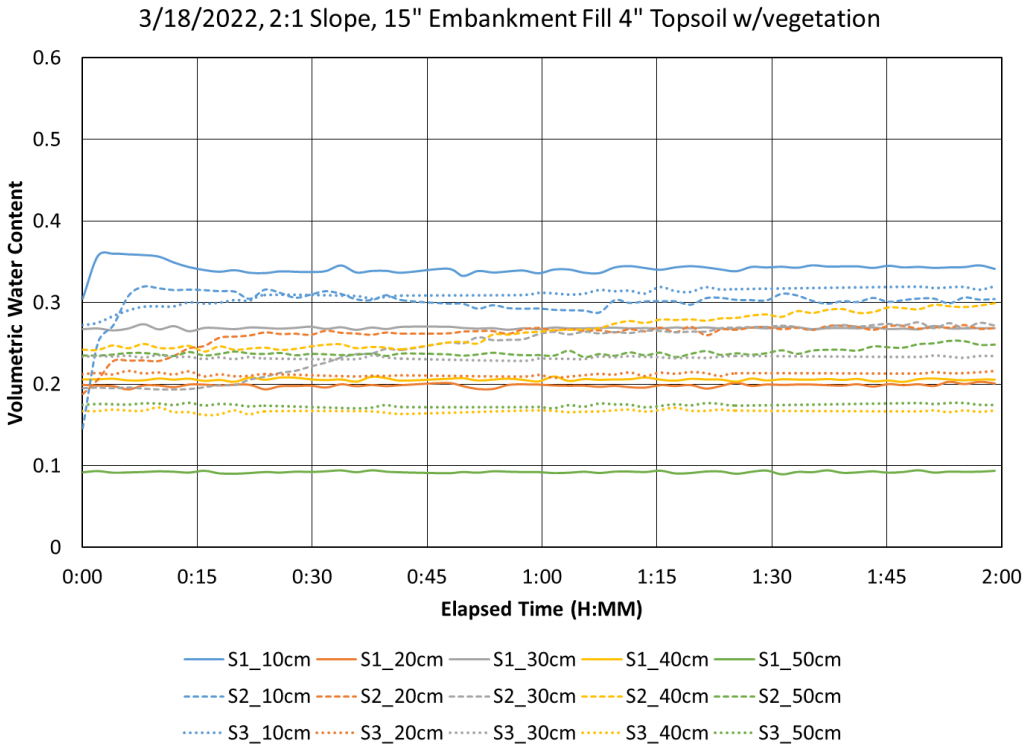

Fig. A28. 15” Embankment Fill 4” Topsoil w/vegetation 2-hr raw data at a 2:1 slope.

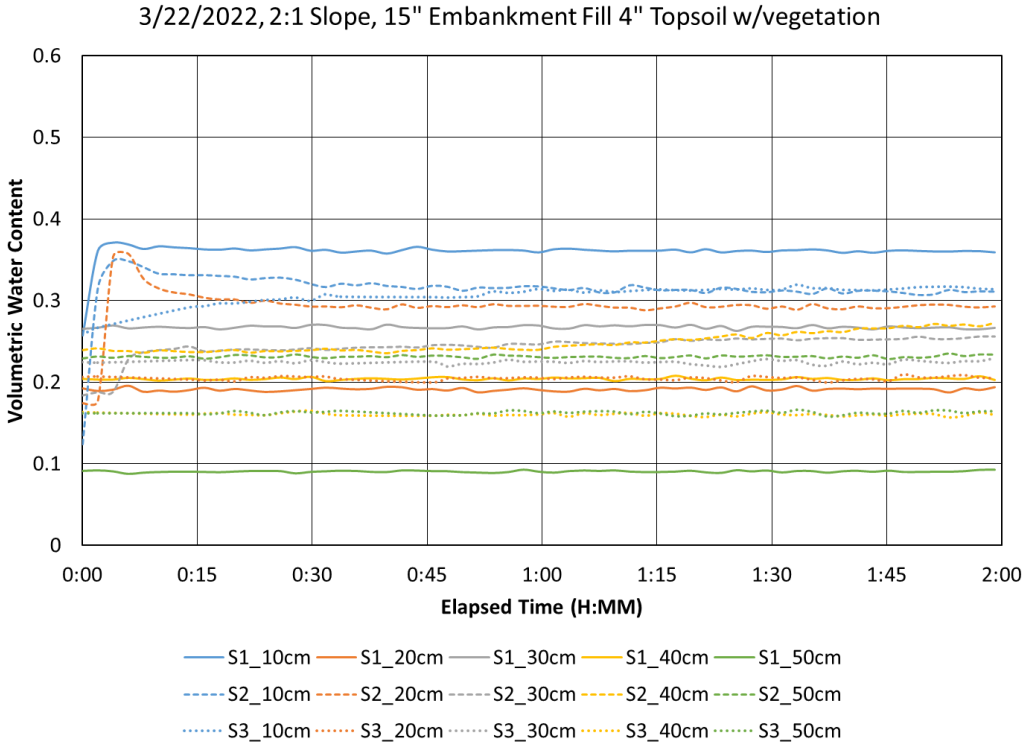

Fig. A29. 15” Embankment Fill 4” Topsoil w/vegetation 2-hr raw data at a 2:1 slope.

Configuration 4: 15” Embankment Fill 4” Amended Topsoil

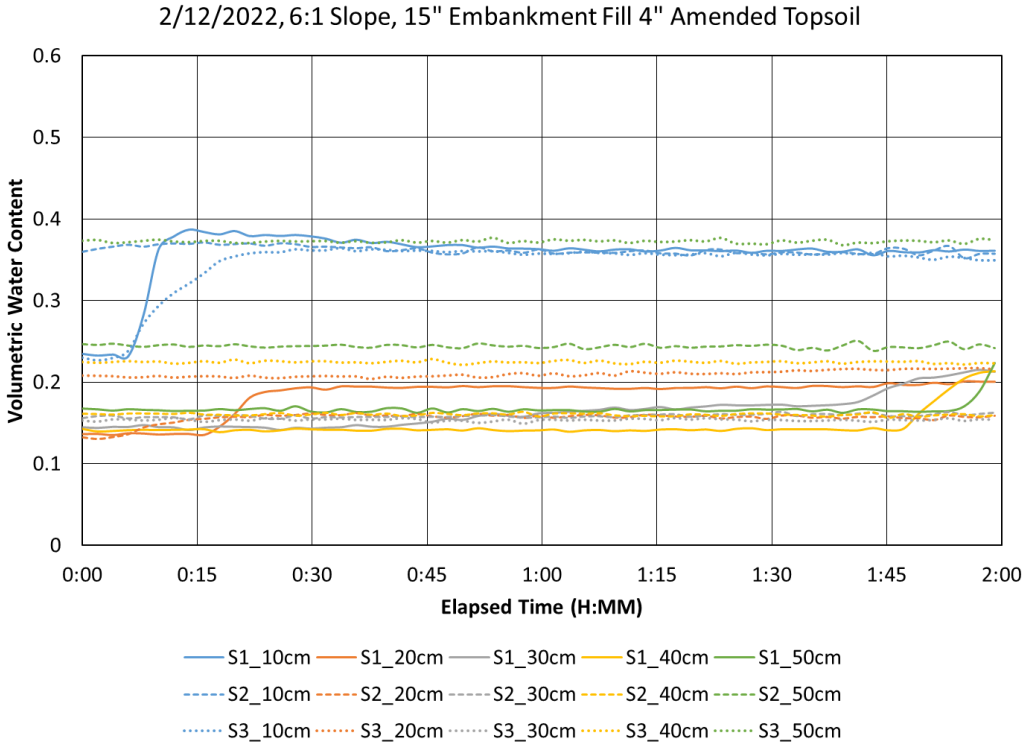

Fig. A30. 15” Embankment Fill 4” Amended Topsoil 2-hr raw data at a 6:1 slope.

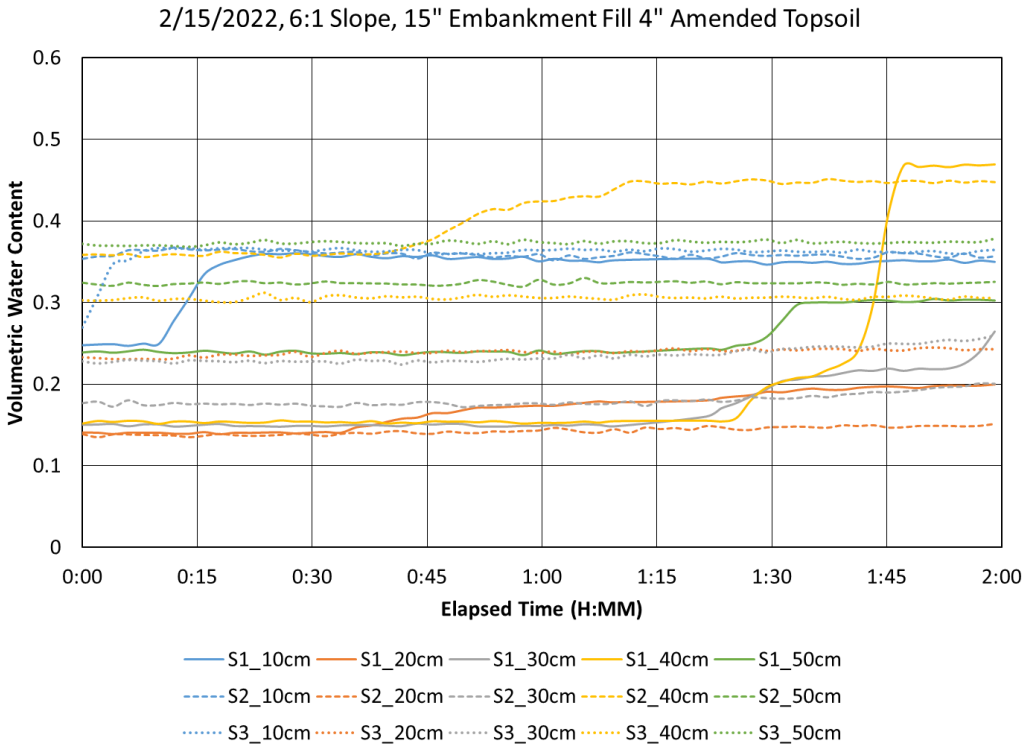

Fig. A31. 15" Embankment Fill 4" Amended Topsoil 2-hr raw data at a 6:1 slope.

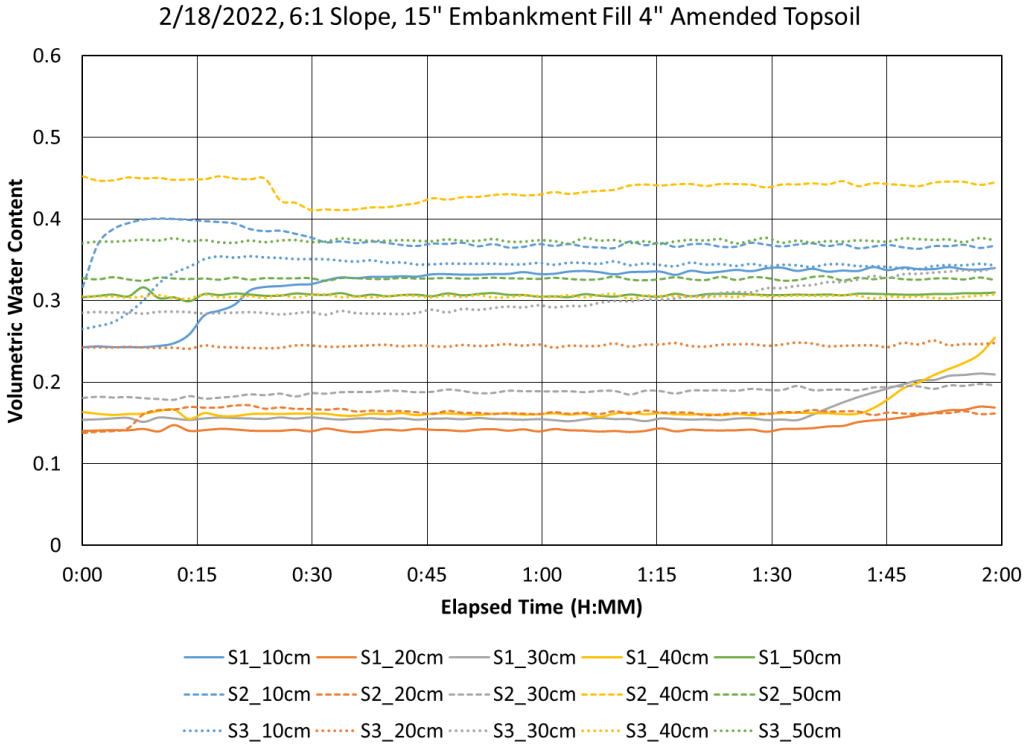

Fig. A32. 15" Embankment Fill 4" Amended Topsoil 2-hr raw data at a 6:1 slope.

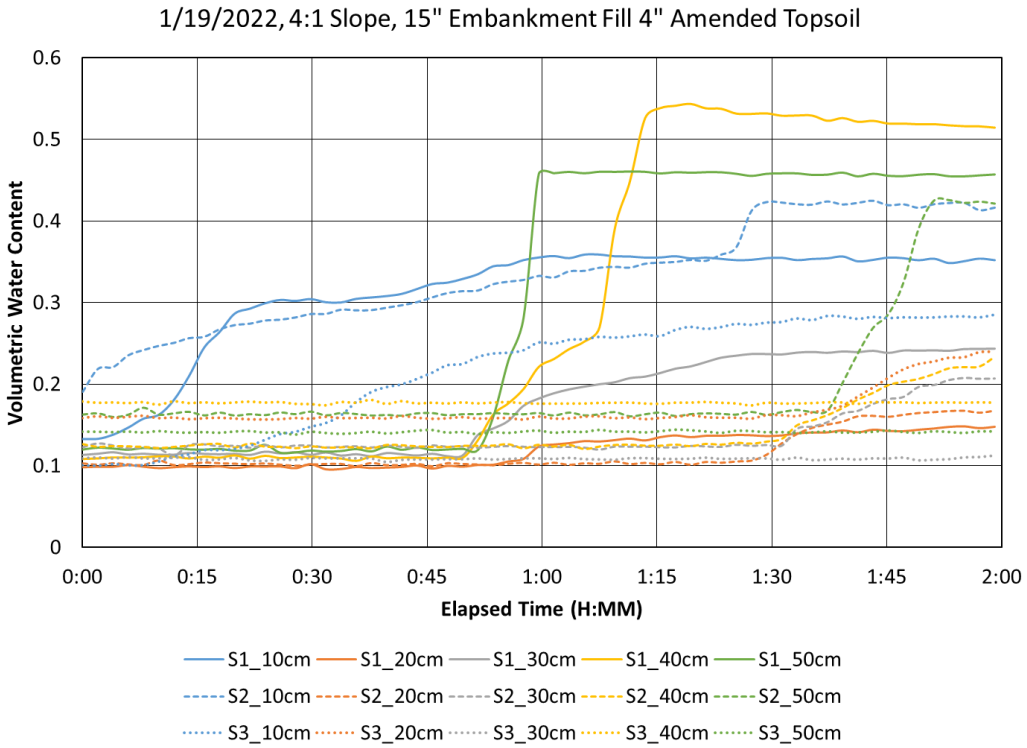

Fig. A33. 15" Embankment Fill 4" Amended Topsoil 2-hr raw data at a 4:1 slope.

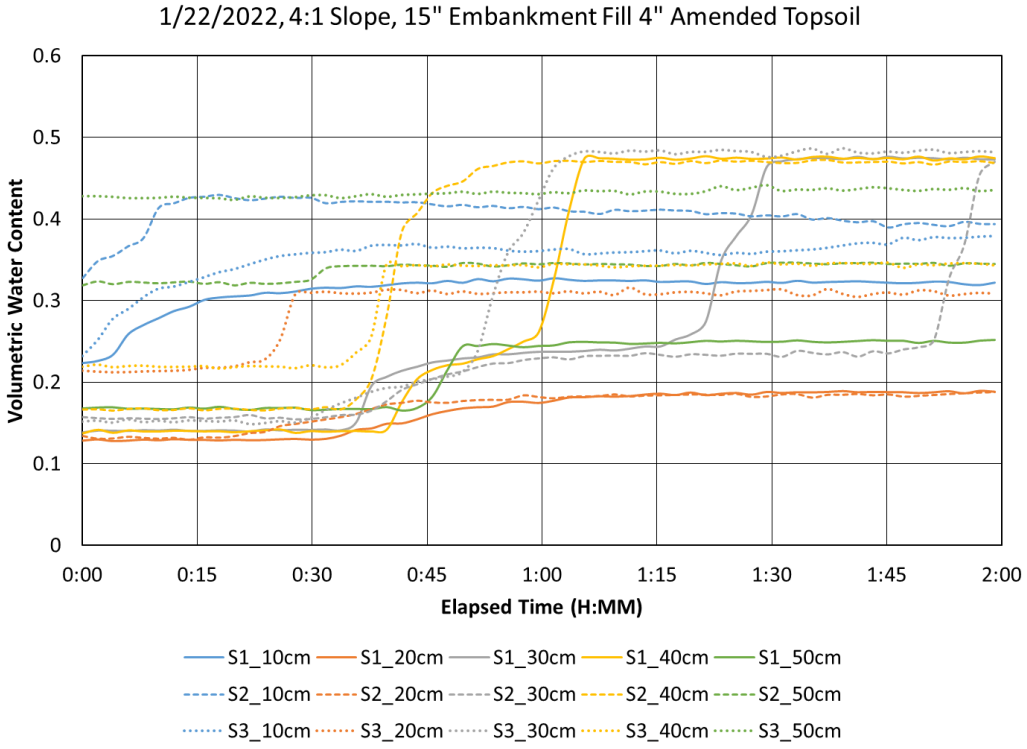

Fig. A34. 15" Embankment Fill 4" Amended Topsoil 2-hr raw data at a 4:1 slope.

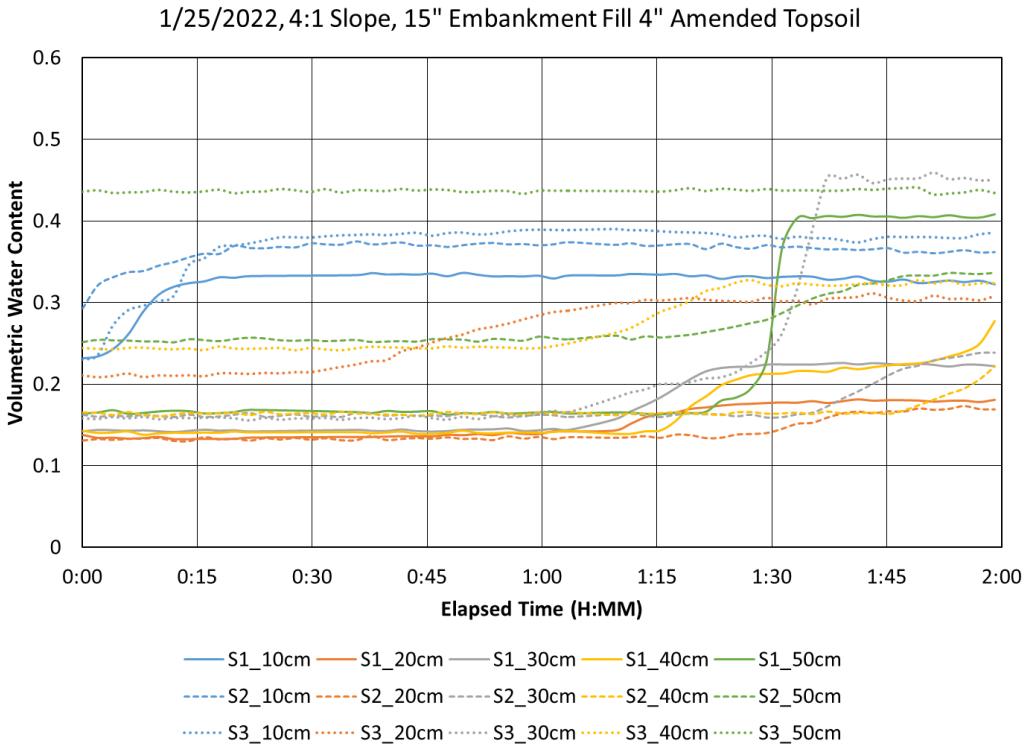

Fig. A35. 15” Embankment Fill 4” Amended Topsoil 2-hr raw data at a 4:1 slope.

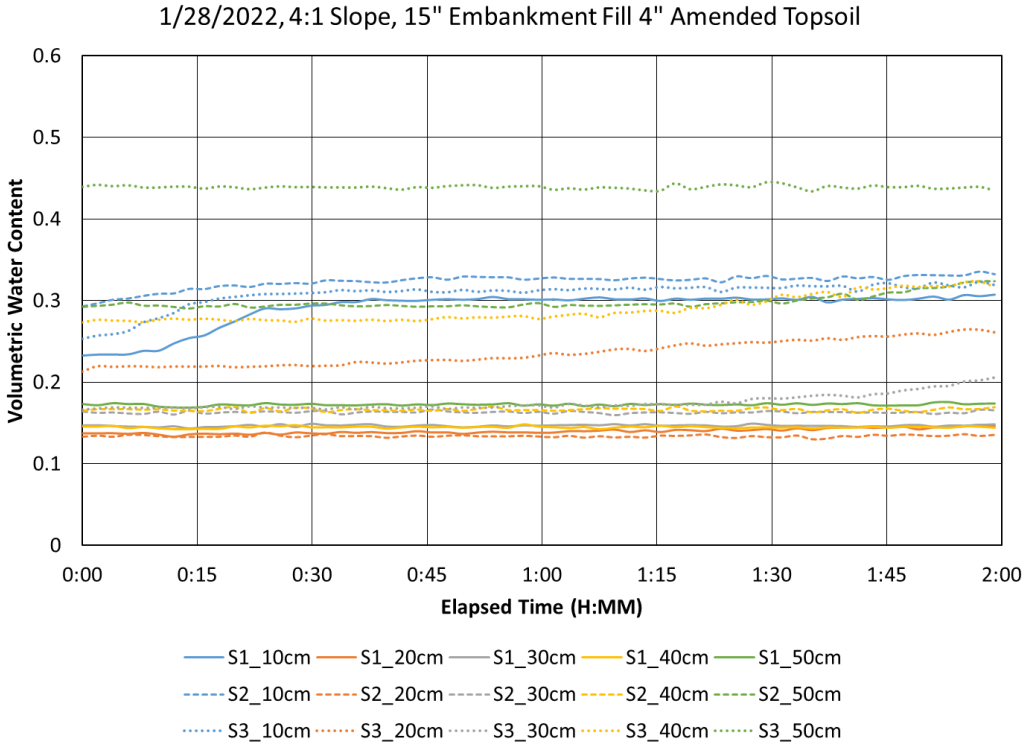

Fig. A36. 15” Embankment Fill 4” Amended Topsoil 2-hr raw data at a 2:1 slope.

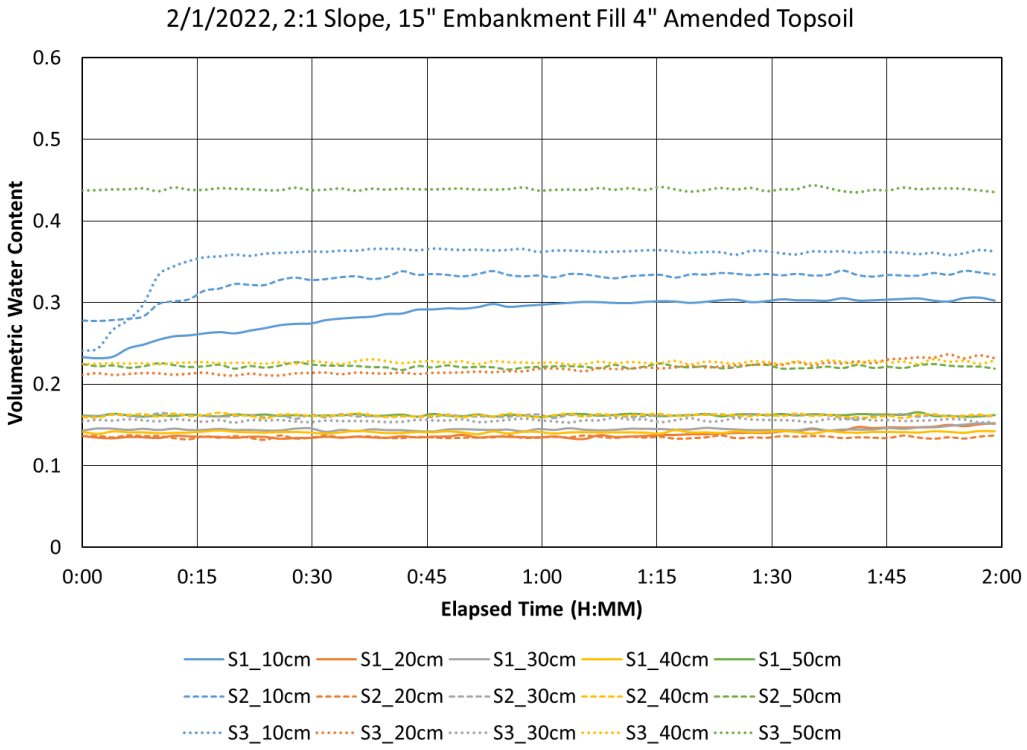

Fig. A37. 15” Embankment Fill 4” Amended Topsoil 2-hr raw data at a 2:1 slope.

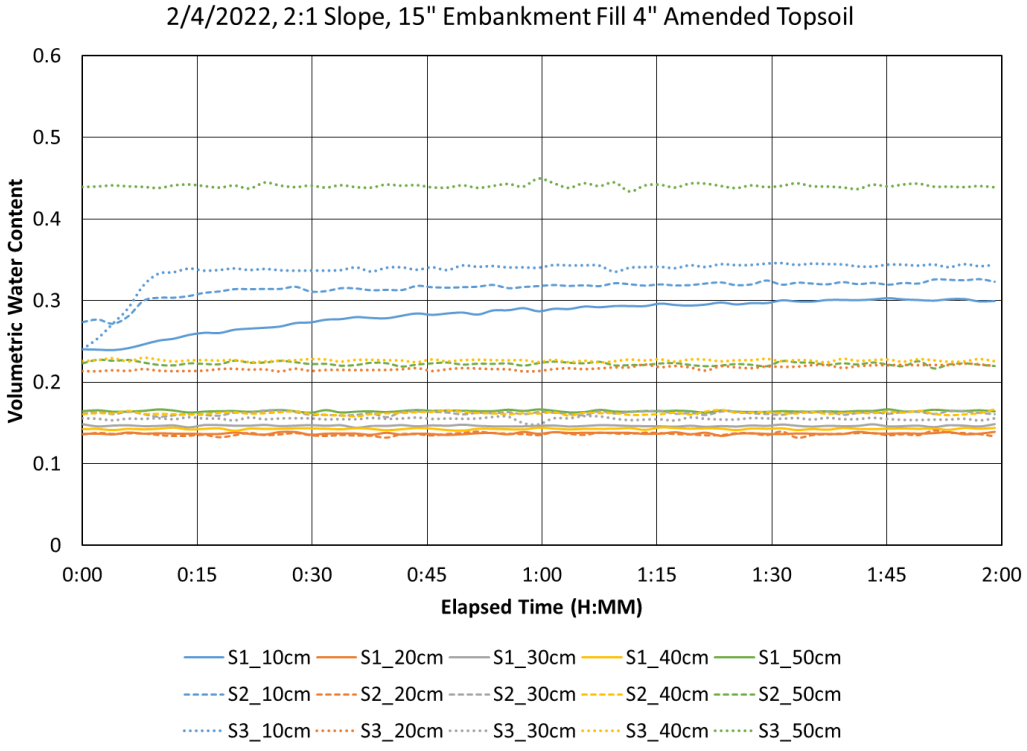

Fig. A38. 15” Embankment Fill 4” Amended Topsoil 2-hr raw data at a 2:1 slope.

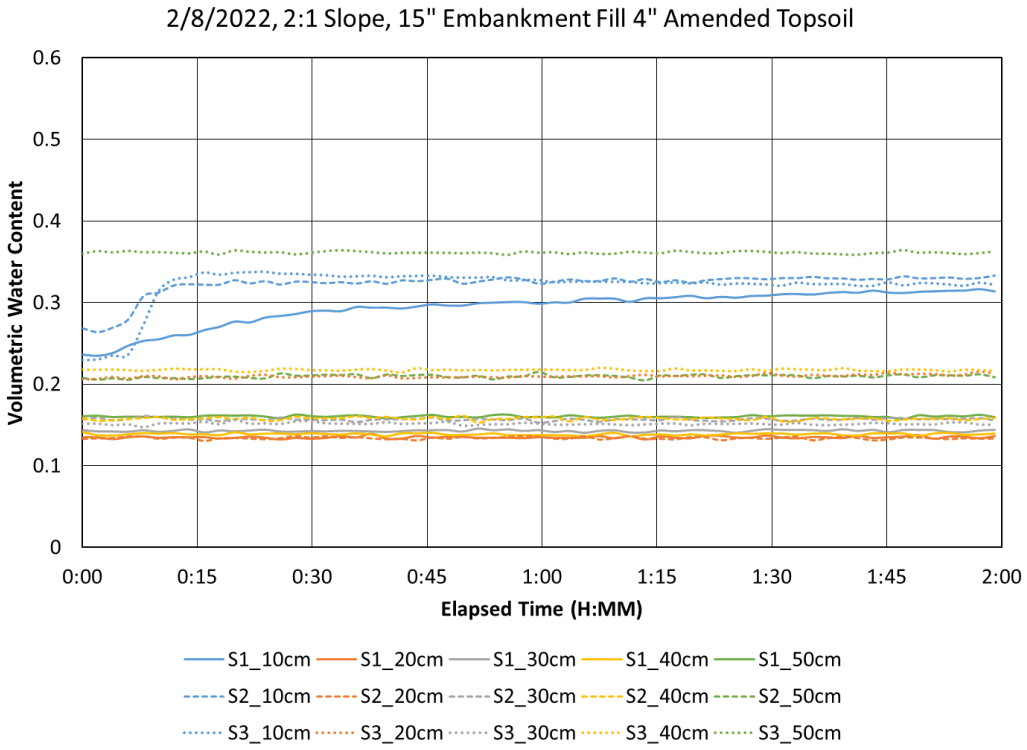

Fig. A39. 15” Embankment Fill 4” Amended Topsoil 2-hr raw data at a 2:1 slope.

Configuration 5: 15” Embankment Fill 4” Amended Topsoil with Vegetation

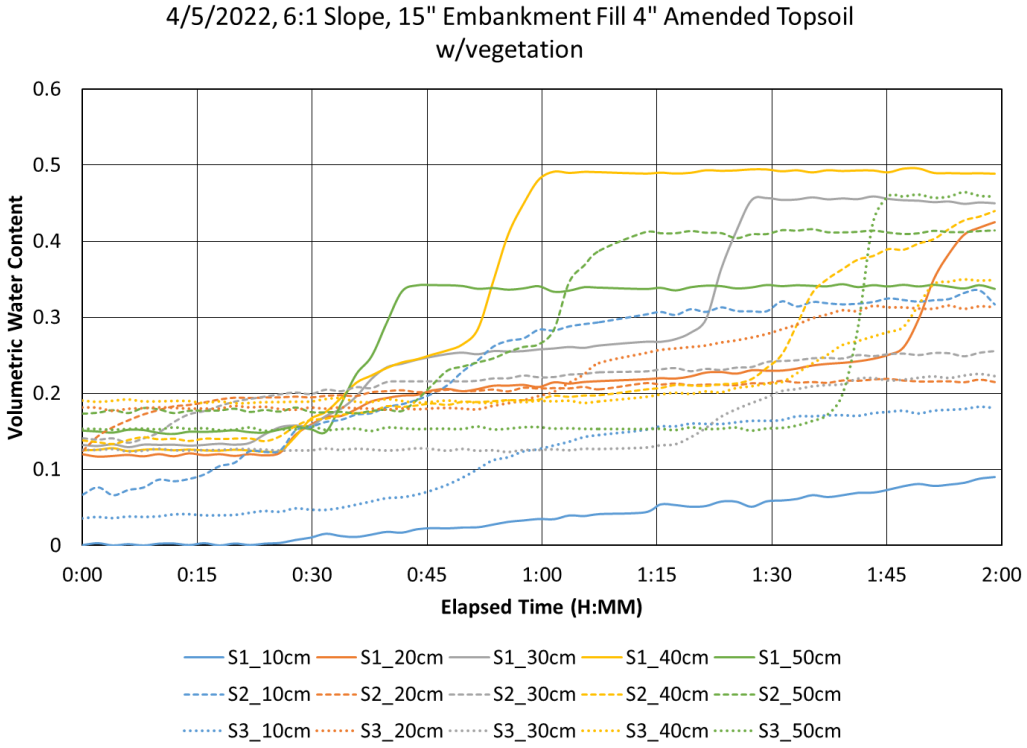

Fig. A40. 15” Embankment Fill 4” Amended Topsoil w/vegetation 2-hr raw data at a 6:1 slope.

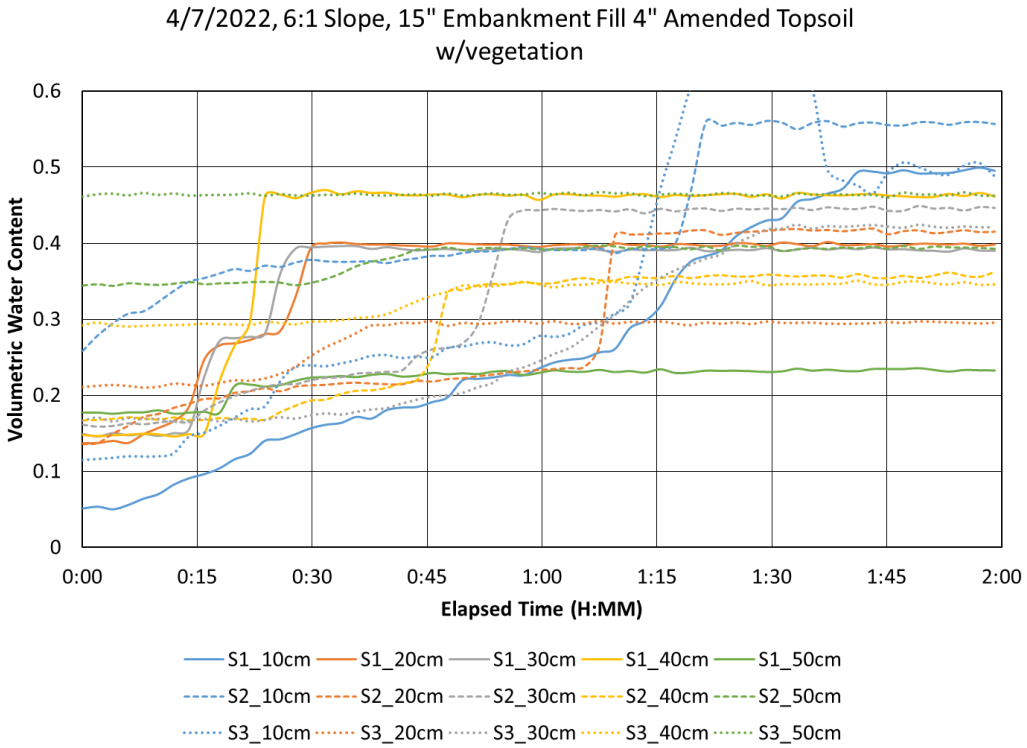

Fig. A41. 15" Embankment Fill 4" Amended Topsoil w/vegetation 2-hr raw data at a 6:1 slope.

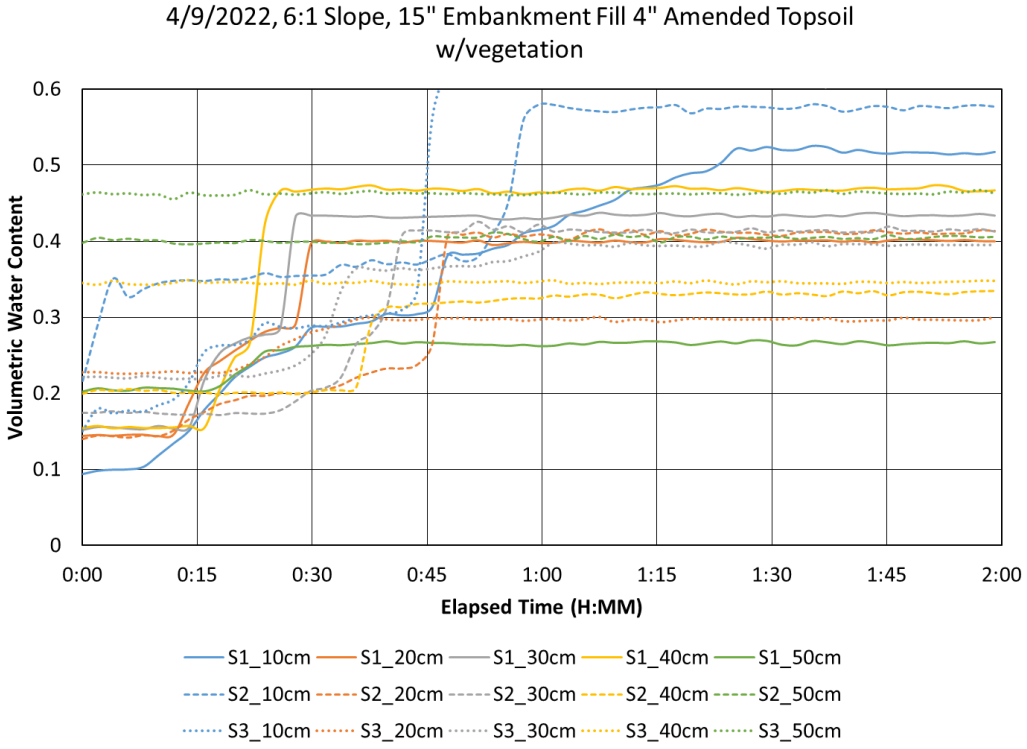

Fig. A42. 15" Embankment Fill 4" Amended Topsoil w/vegetation 2-hr raw data at a 6:1 slope.

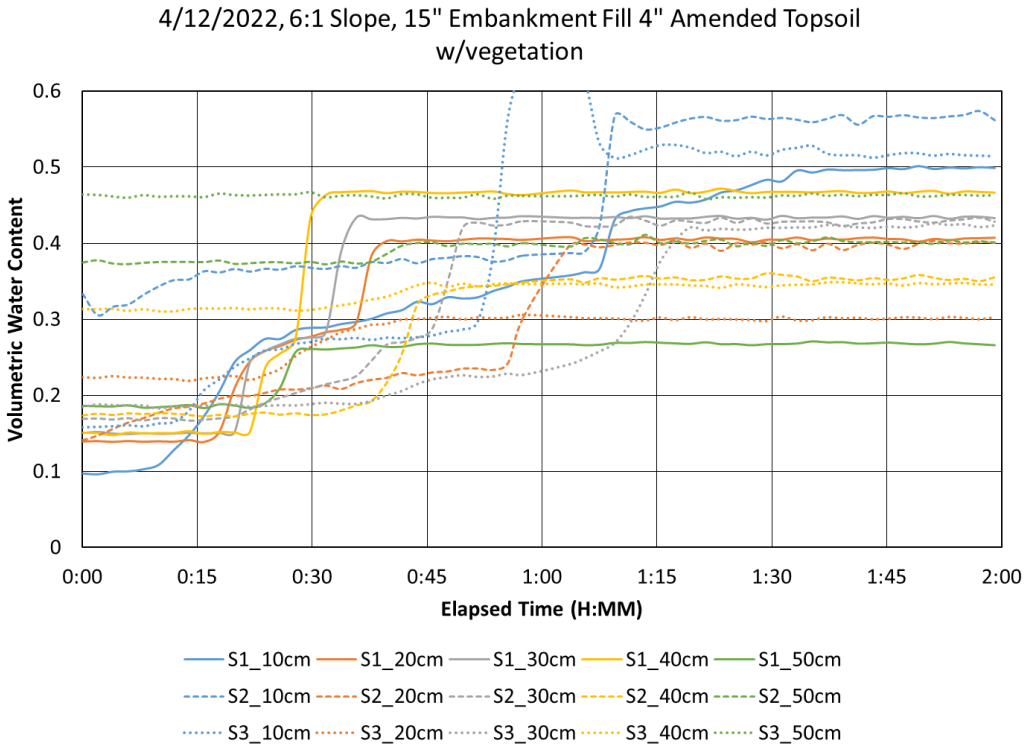

Fig. A43. 15" Embankment Fill 4" Amended Topsoil w/vegetation 2-hr raw data at a 6:1 slope.

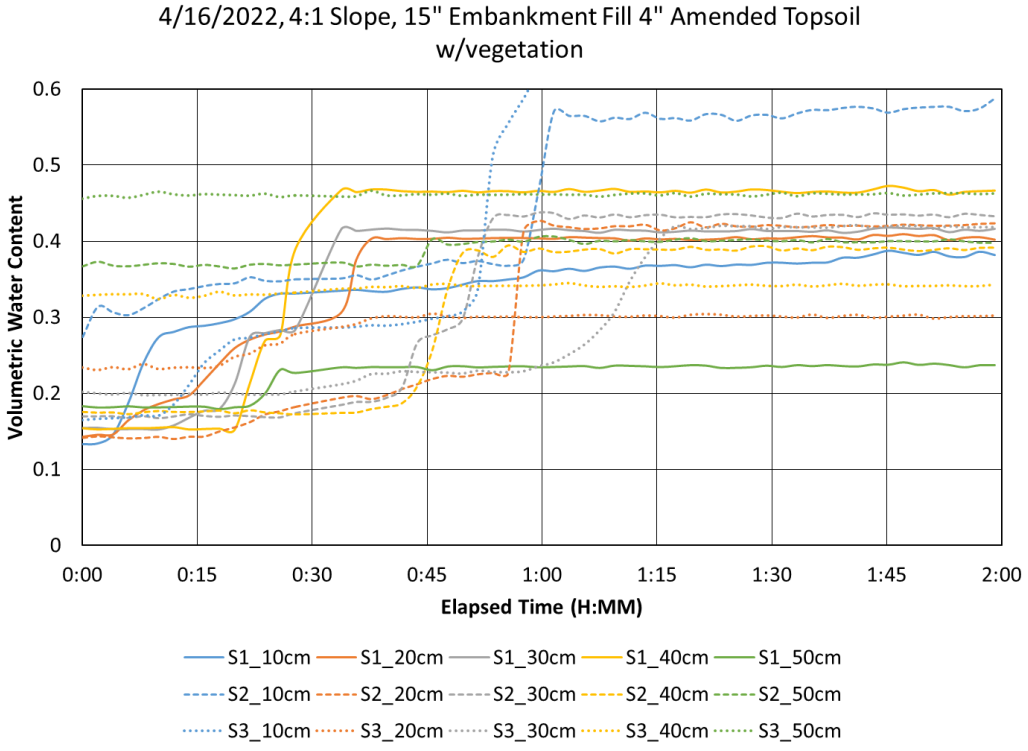

Fig. A44. 15" Embankment Fill 4" Amended Topsoil w/vegetation 2-hr raw data at a 4:1 slope.

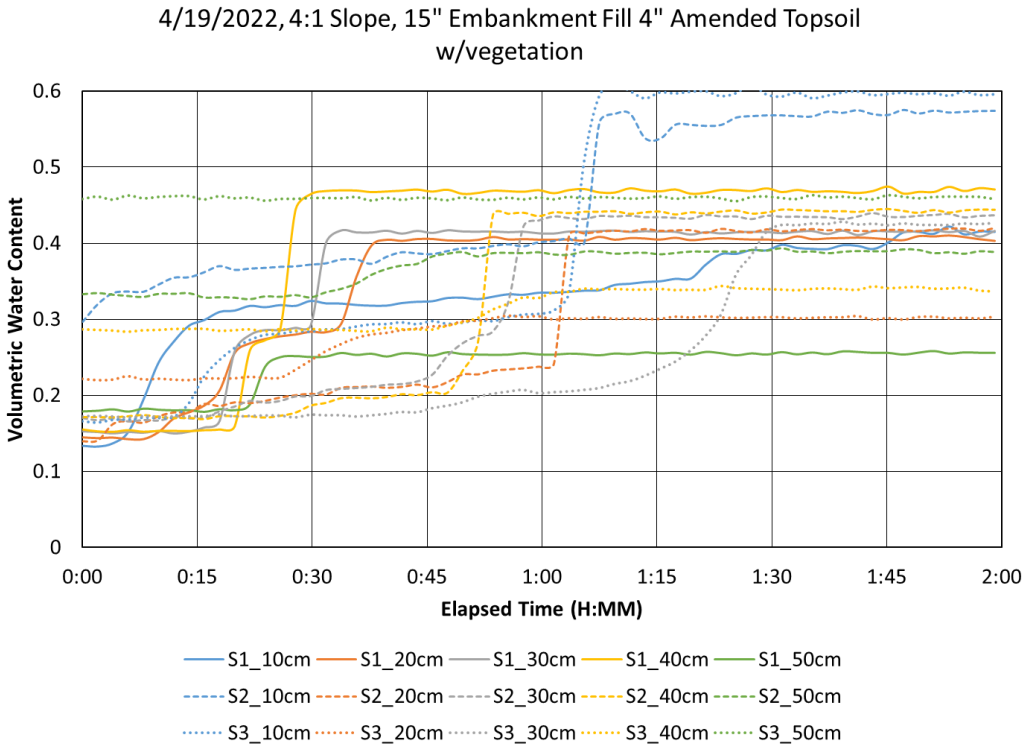

Fig. A45. 15" Embankment Fill 4" Amended Topsoil w/vegetation 2-hr raw data at a 4:1 slope.

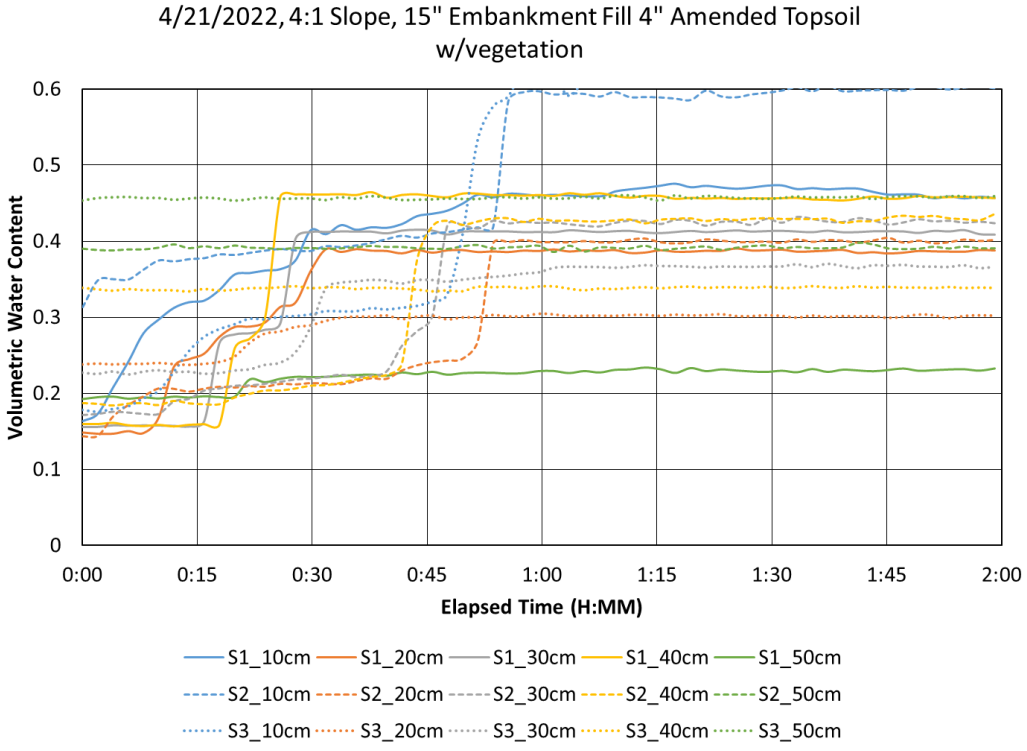

Fig. A46. 15" Embankment Fill 4" Amended Topsoil w/vegetation 2-hr raw data at a 4:1 slope.

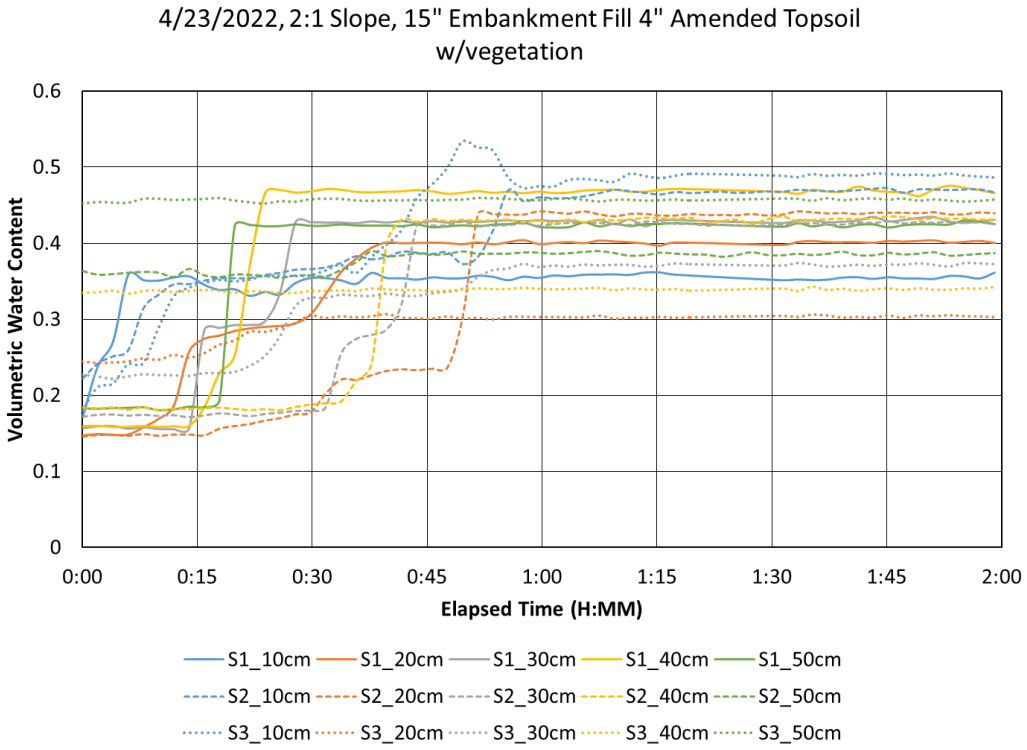

Fig. A47. 15" Embankment Fill 4" Amended Topsoil w/vegetation 2-hr raw data at a 2:1 slope.

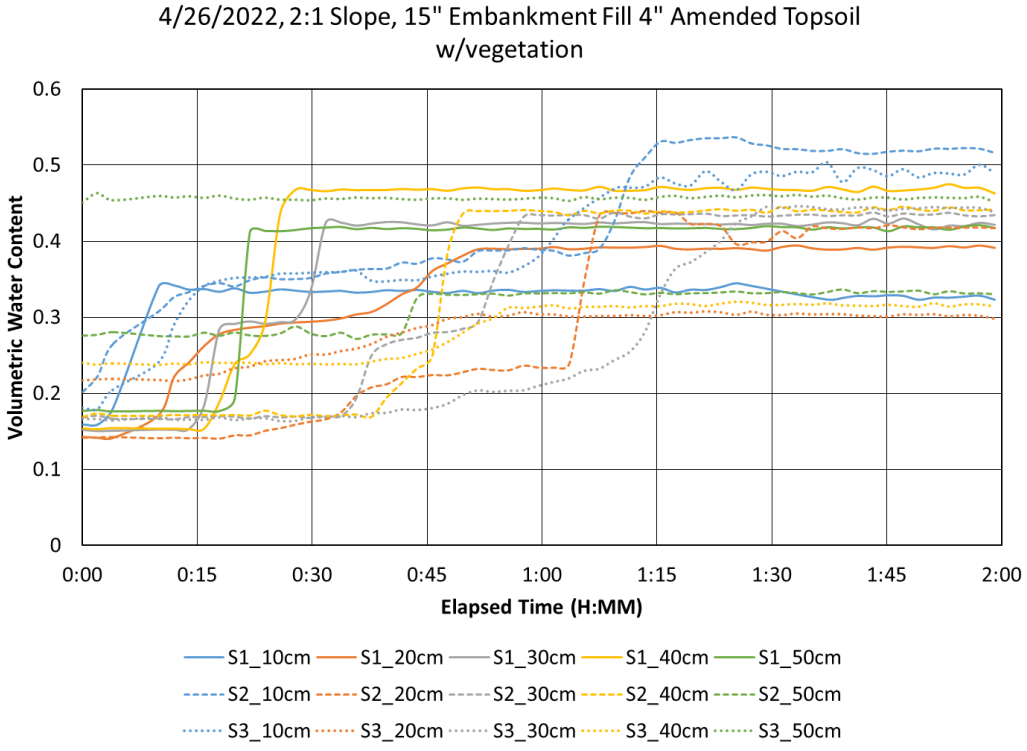

Fig. A48. 15" Embankment Fill 4" Amended Topsoil w/vegetation 2-hr raw data at a 2:1 slope.

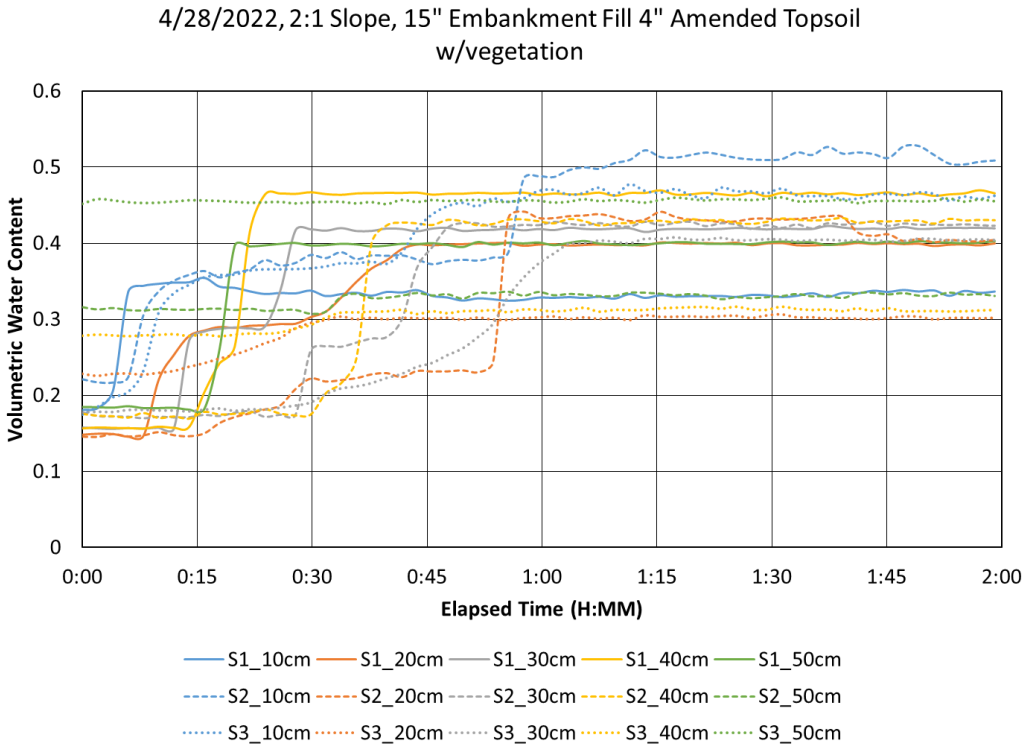

Fig. A49. 15” Embankment Fill 4” Amended Topsoil w/vegetation 2-hr raw data at a 2:1 slope.

Configuration 6: 15” Embankment Fill (6” Ripped) 4” Topsoil

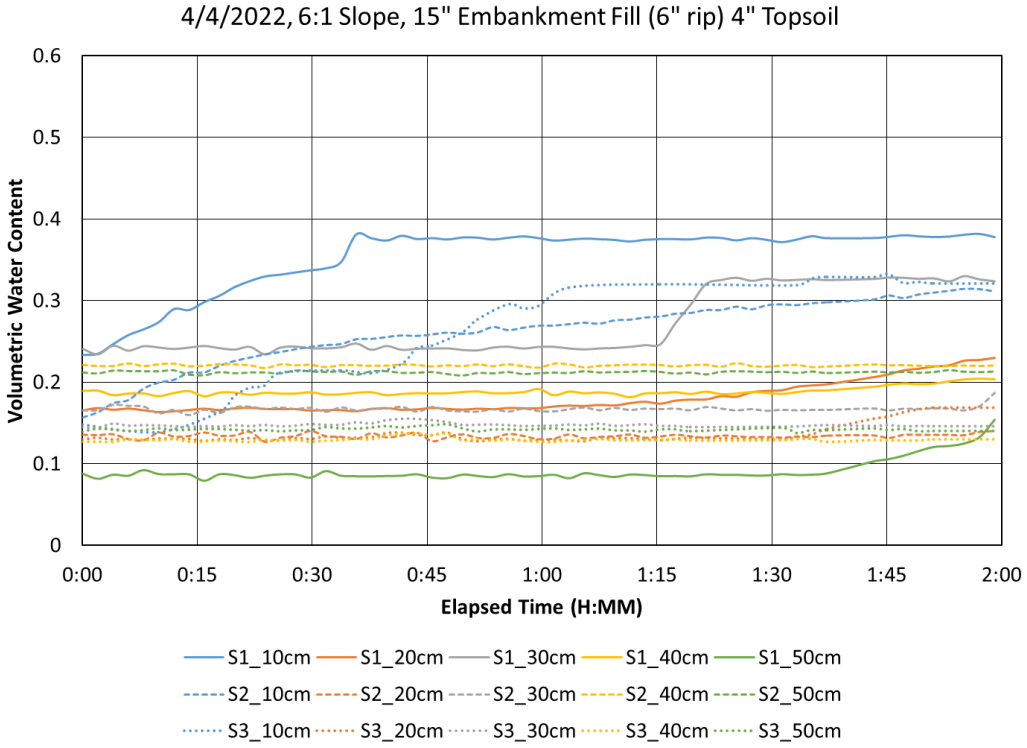

Fig. A50. 15” Embankment Fill (6” Ripped) 4” Amended Topsoil w/vegetation 2-hr raw data at a 6:1 slope.

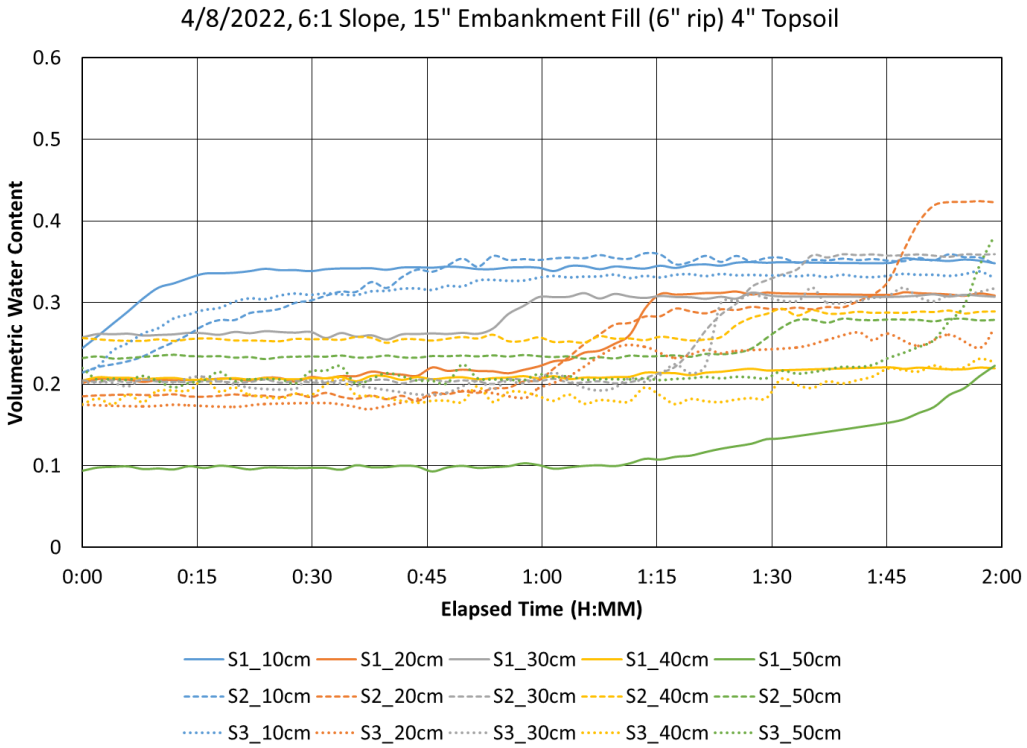

Fig. A51. 15” Embankment Fill (6” Ripped) 4” Amended Topsoil w/vegetation 2-hr raw data at a 6:1 slope.

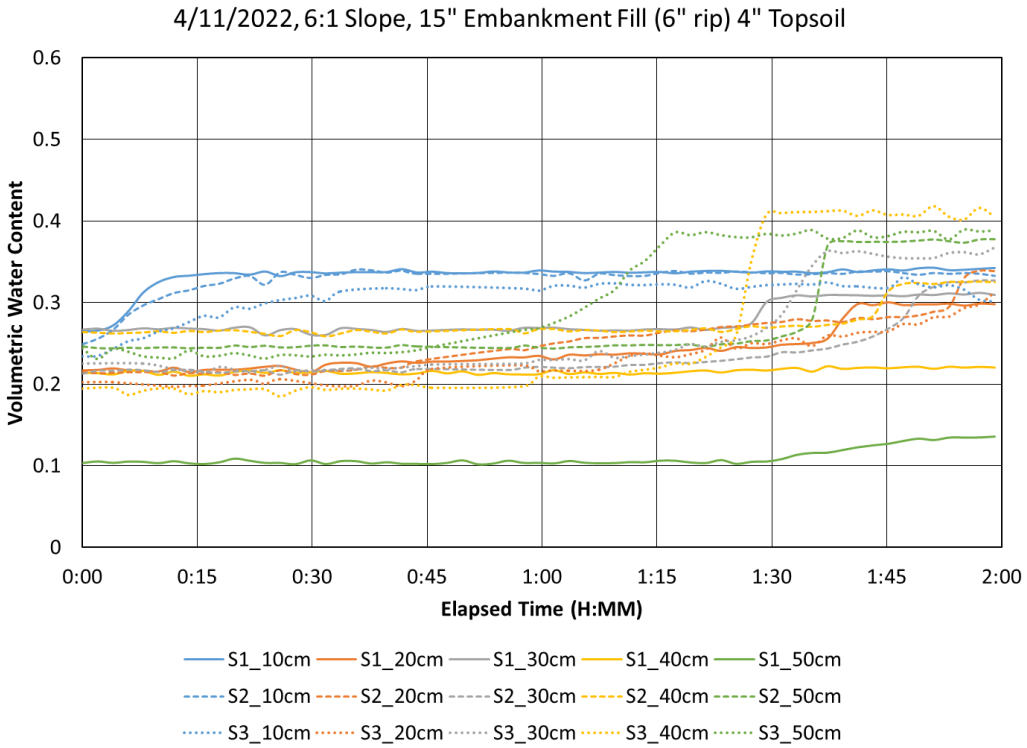

Fig. A52. 15” Embankment Fill (6” Ripped) 4” Amended Topsoil w/vegetation 2-hr raw data at a 6:1 slope.

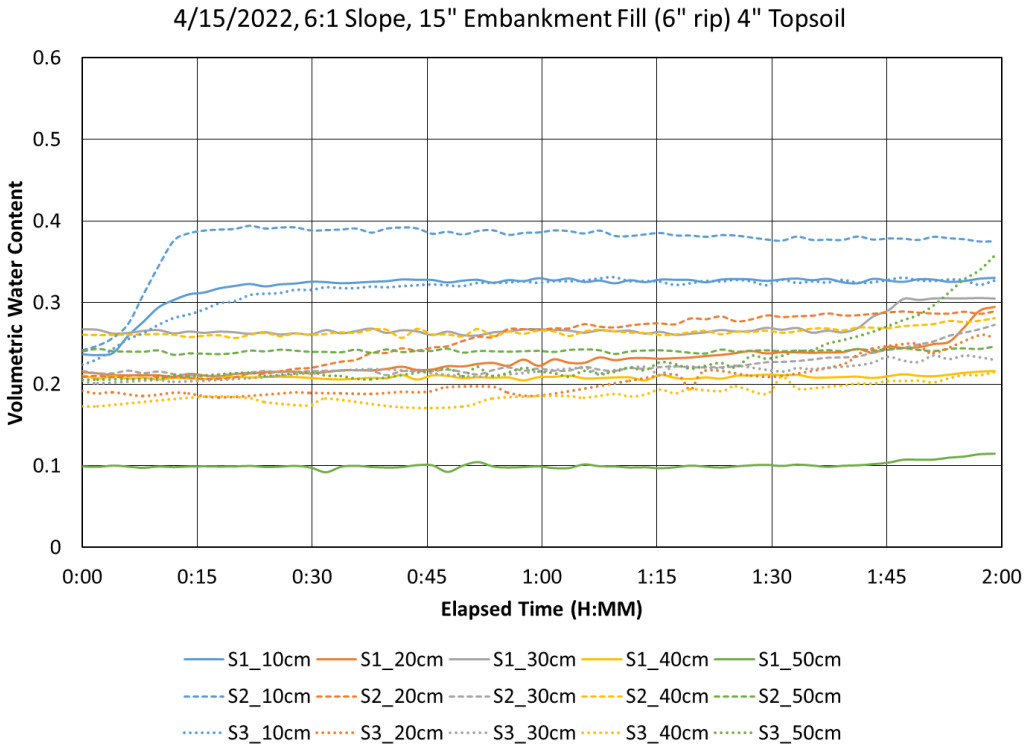

Fig. A53. 15” Embankment Fill (6” Ripped) 4” Amended Topsoil w/vegetation 2-hr raw data at a 6:1 slope.

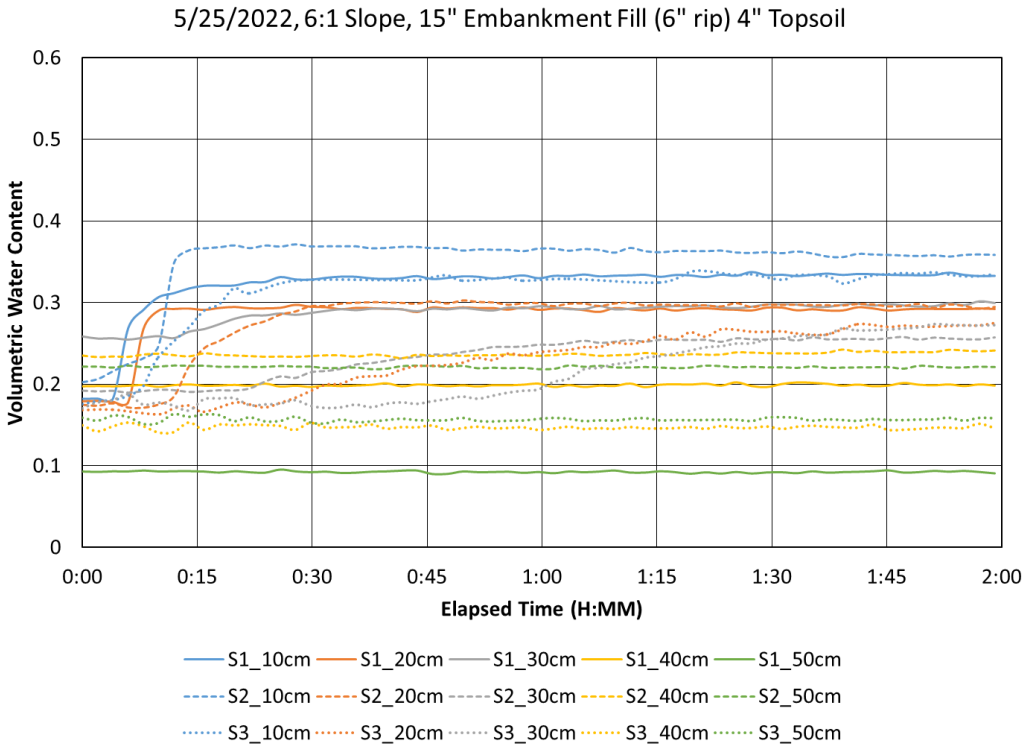

Fig. A54. 15” Embankment Fill (6” Ripped) 4” Amended Topsoil w/vegetation 2-hr raw data at a 6:1 slope.

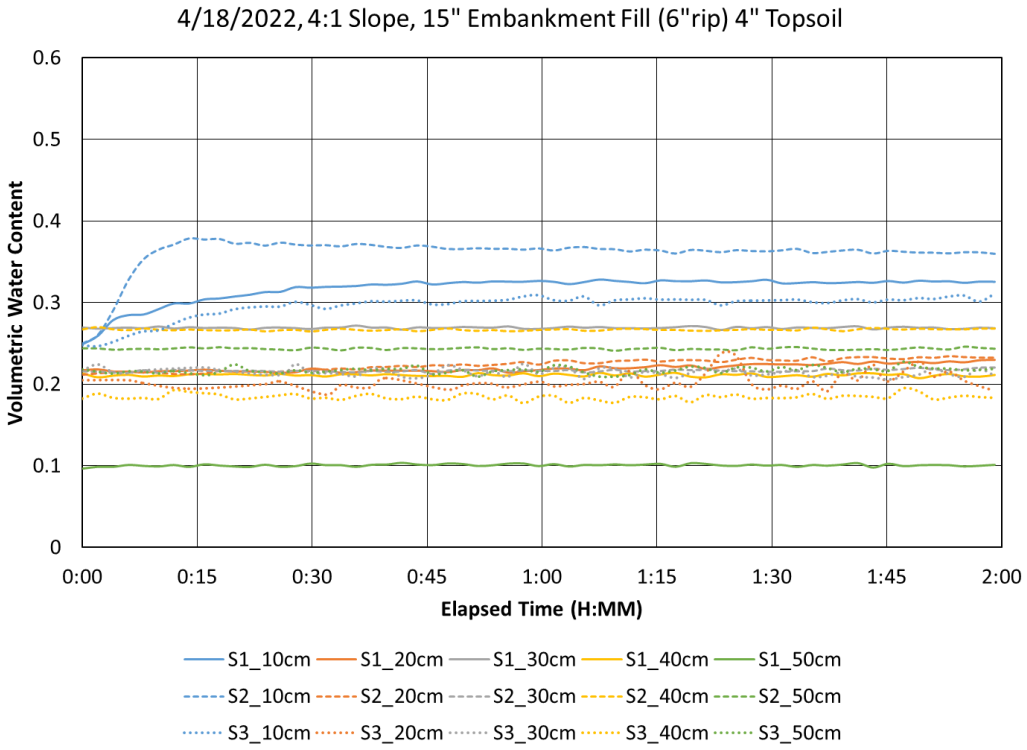

Fig. A55. 15" Embankment Fill (6" Ripped) 4" Amended Topsoil w/vegetation 2-hr raw data at a 4:1 slope.

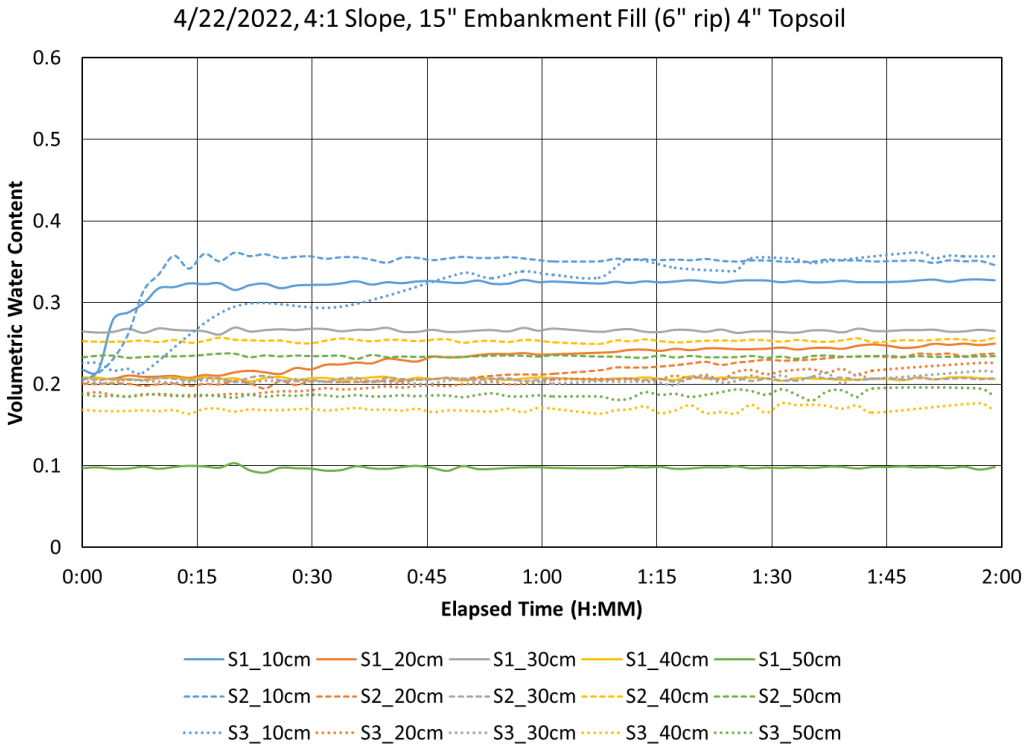

Fig. A56. 15" Embankment Fill (6" Ripped) 4" Amended Topsoil w/vegetation 2-hr raw data at a 4:1 slope.

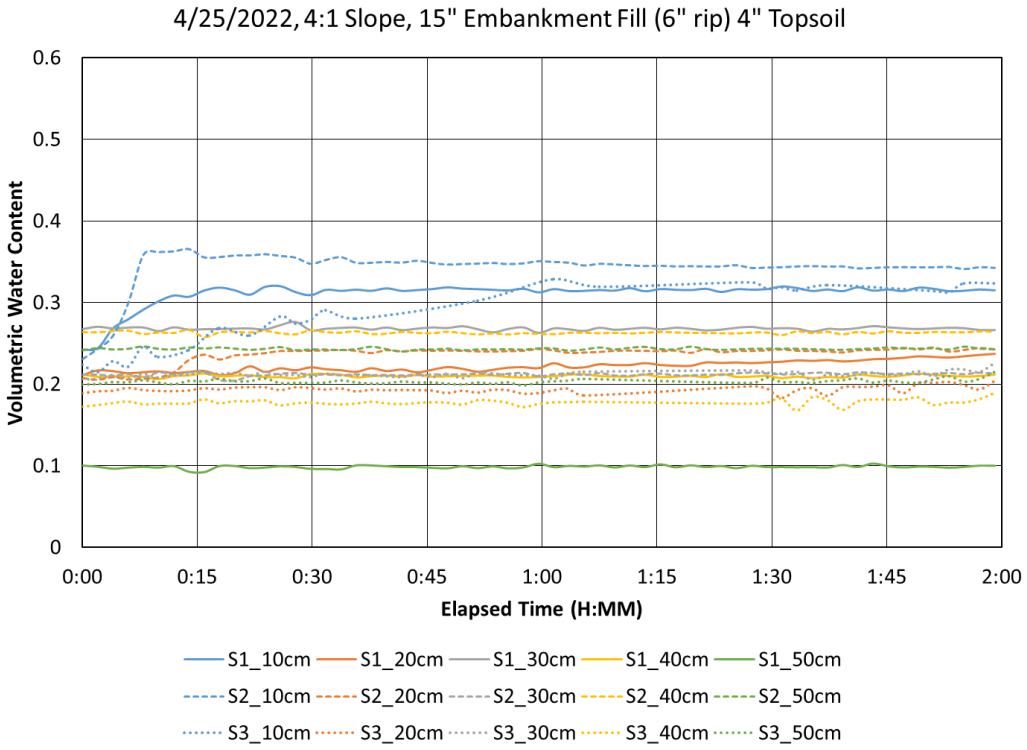

Fig. A57. 15" Embankment Fill (6" Ripped) 4" Amended Topsoil w/vegetation 2-hr raw data at a 4:1 slope.

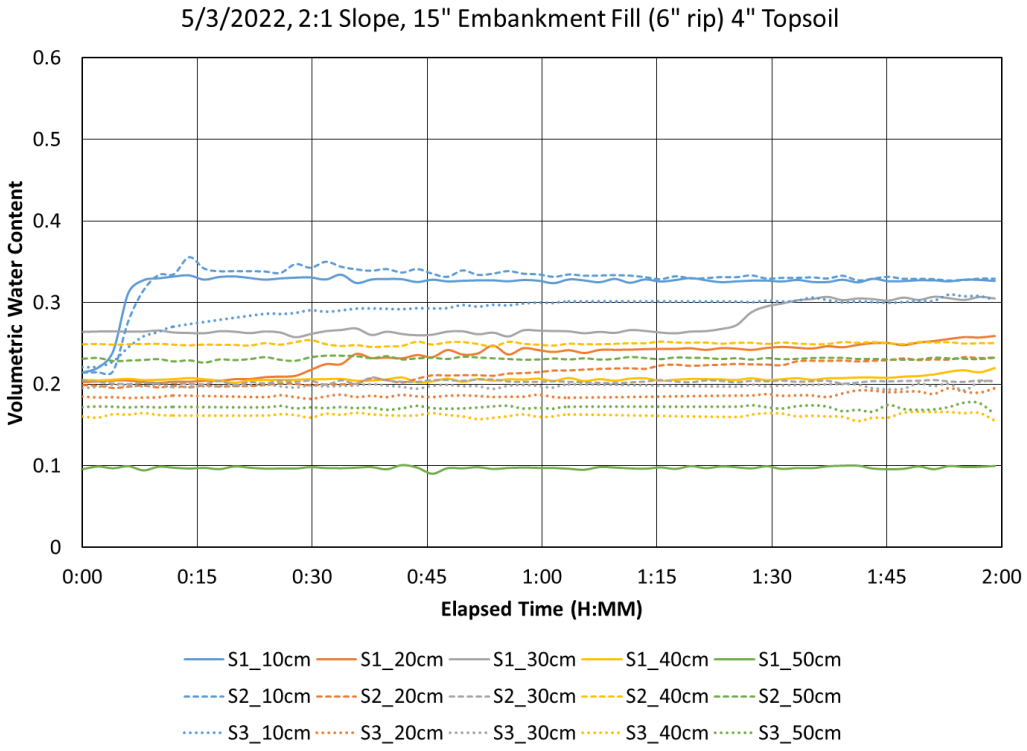

Fig. A58. 15" Embankment Fill (6" Ripped) 4" Amended Topsoil w/vegetation 2-hr raw data at a 2:1 slope.

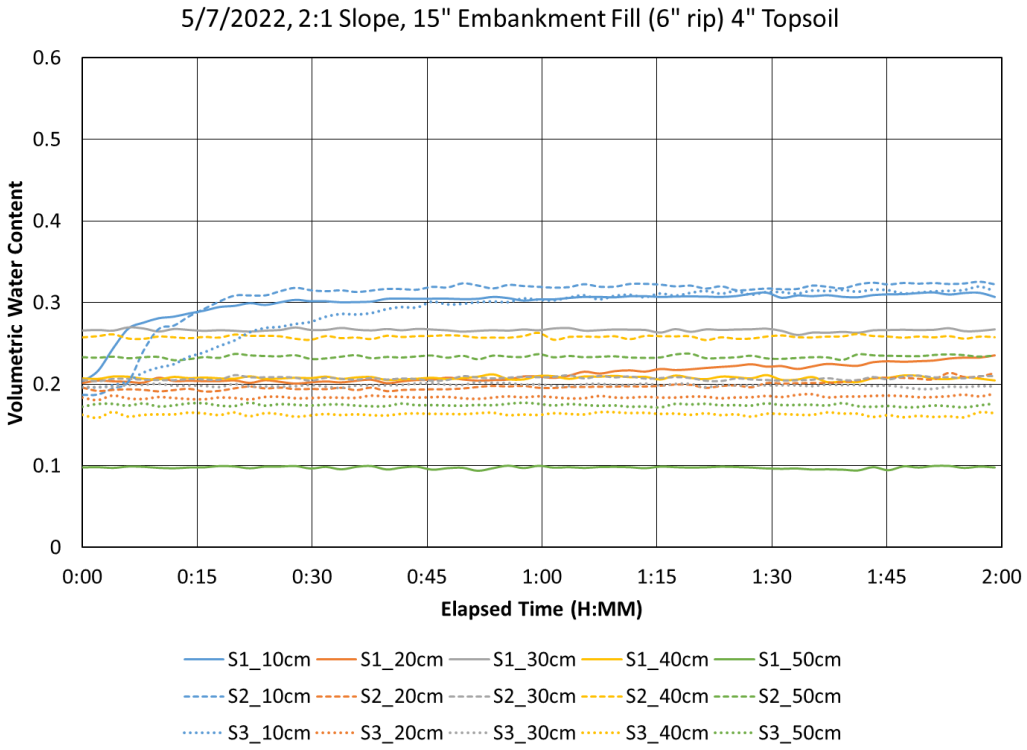

Fig. A59. 15” Embankment Fill (6” Ripped) 4” Amended Topsoil w/vegetation 2-hr raw data at a 2:1 slope.

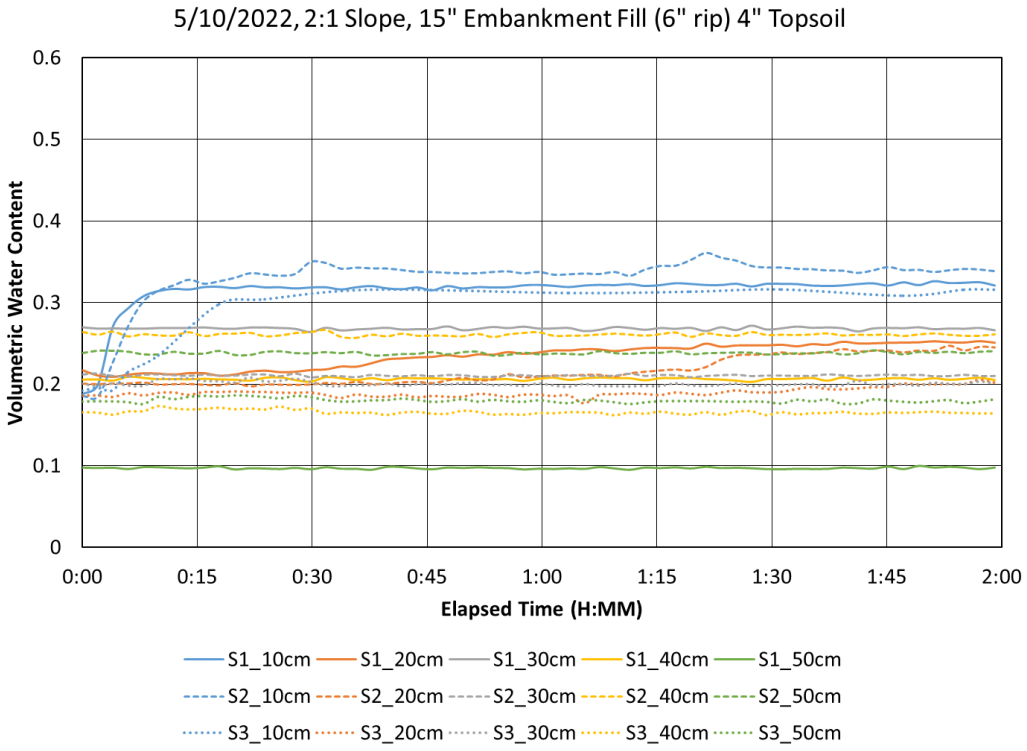

Fig. A60. 15” Embankment Fill (6” Ripped) 4” Amended Topsoil w/vegetation 2-hr raw data at a 2:1 slope.

Appendix B: Corrected 2-hr Data Curves

Configuration 1: 19” Embankment Fill

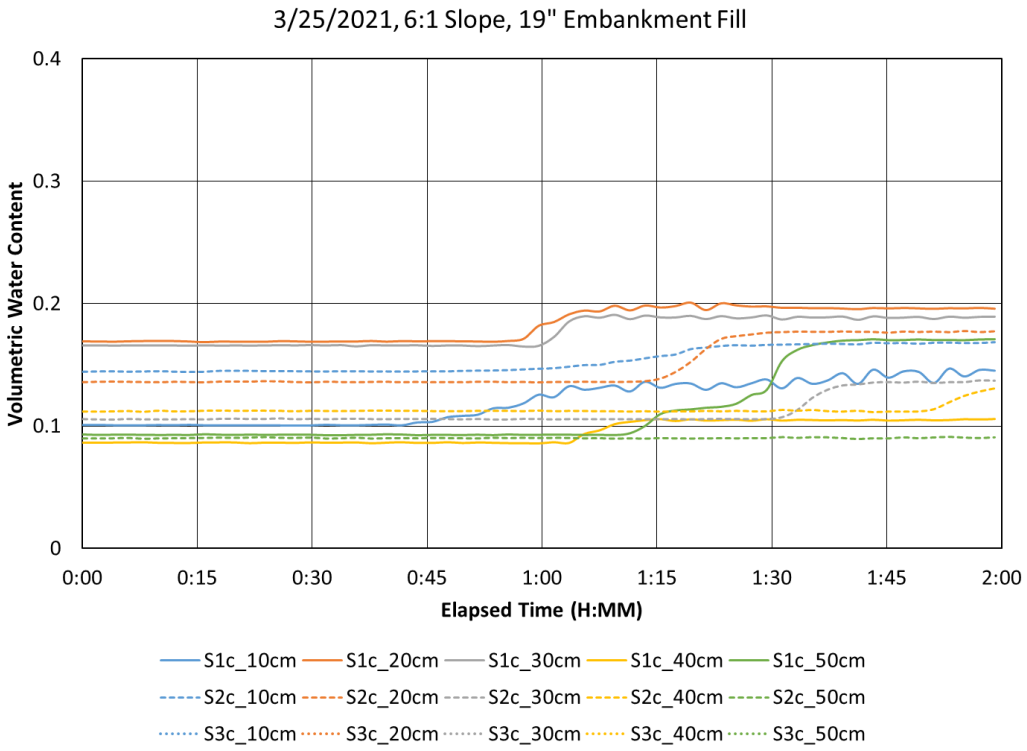

Fig. B1. 19” Embankment Fill 2-hr corrected data at a 6:1 slope.

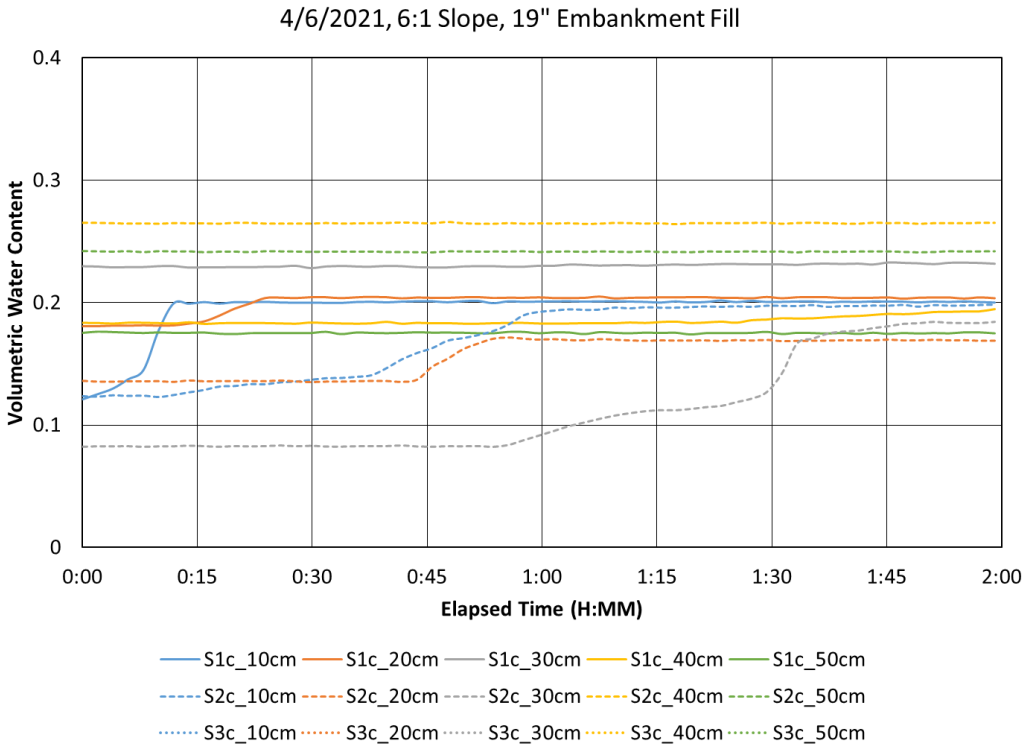

Fig. B2. 19” Embankment Fill 2-hr corrected data at a 6:1 slope.

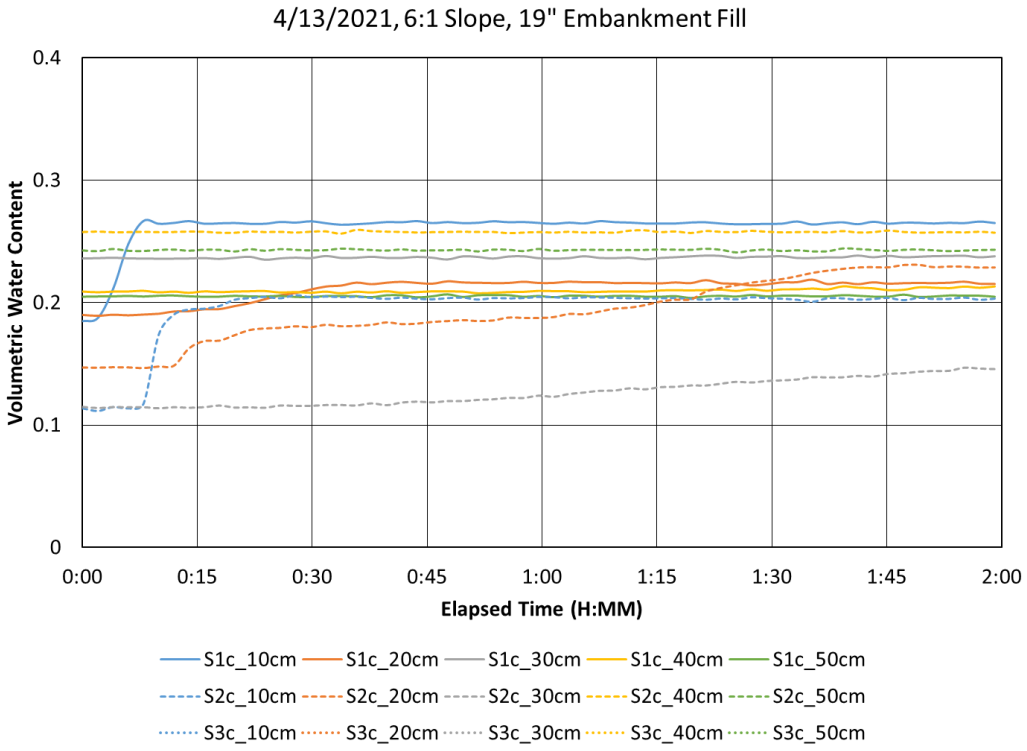

Fig. B3. 19” Embankment Fill 2-hr corrected data at a 6:1 slope.

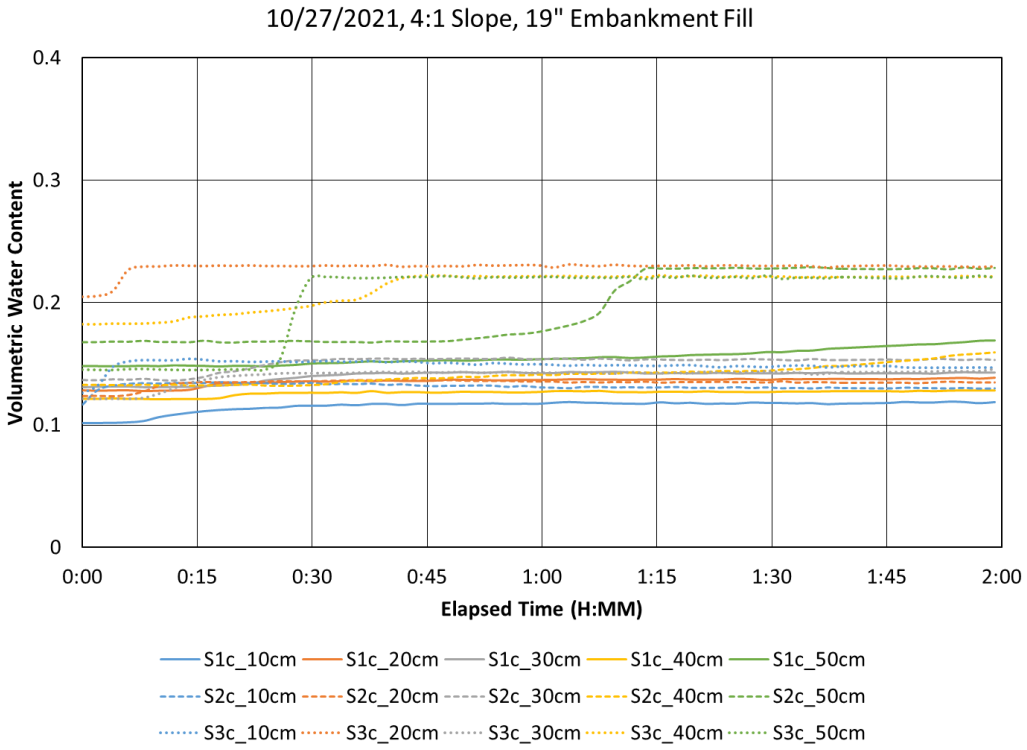

Fig. B4. 19" Embankment Fill 2-hr corrected data at a 4:1 slope.

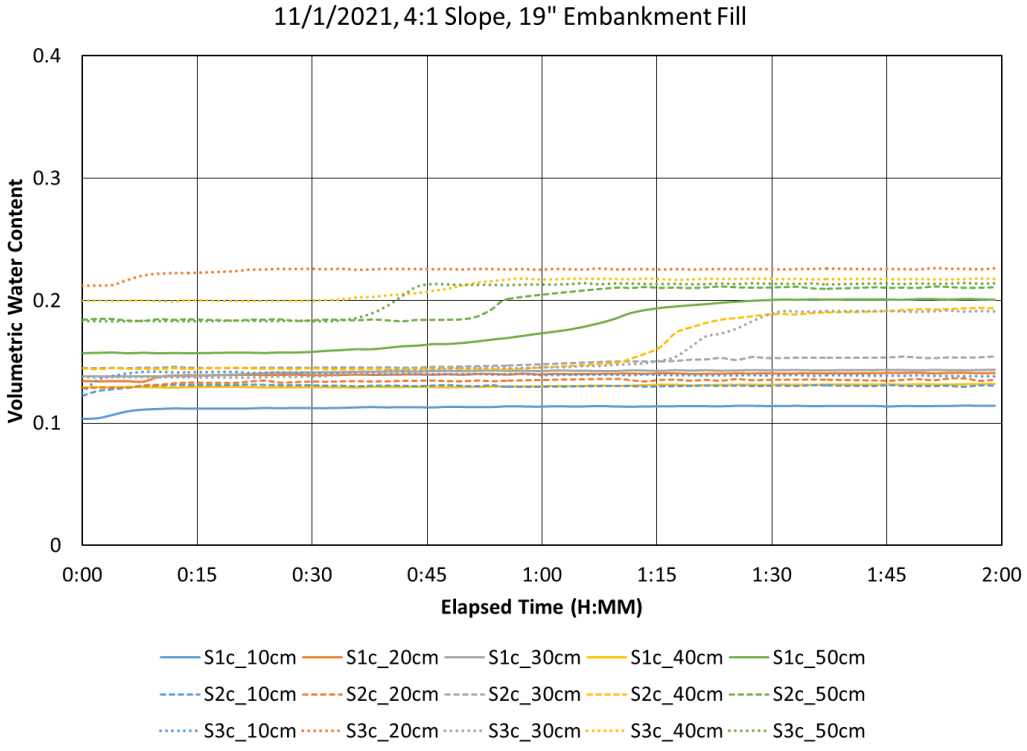

Fig. B5. 19" Embankment Fill 2-hr corrected data at a 4:1 slope.

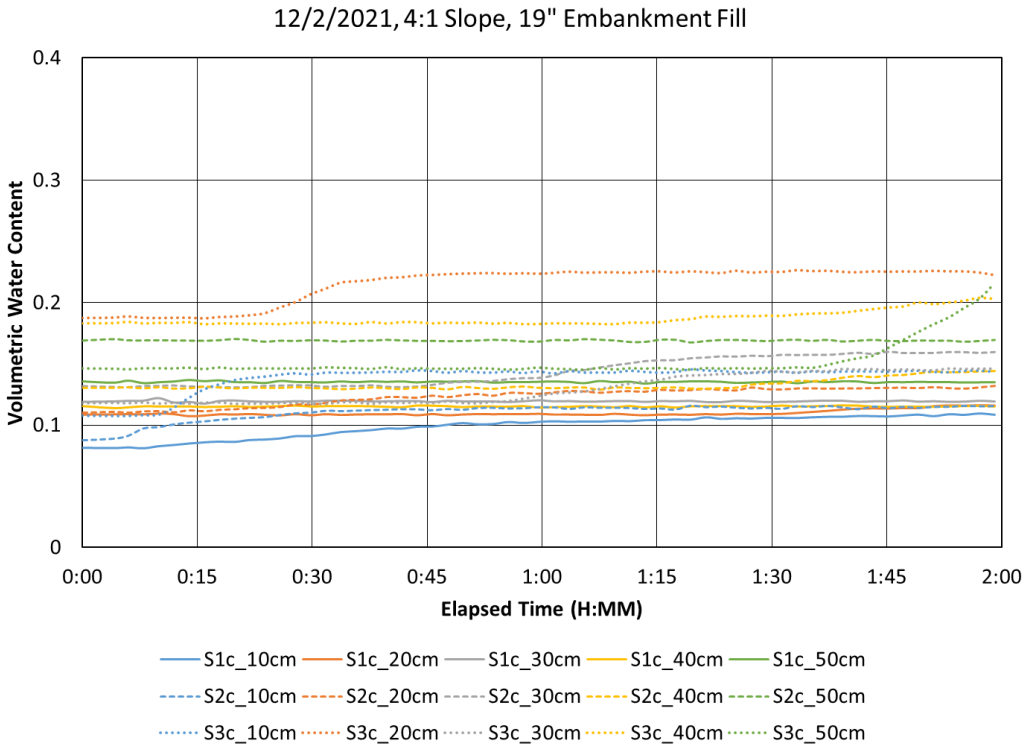

Fig. B6. 19" Embankment Fill 2-hr corrected data at a 4:1 slope.

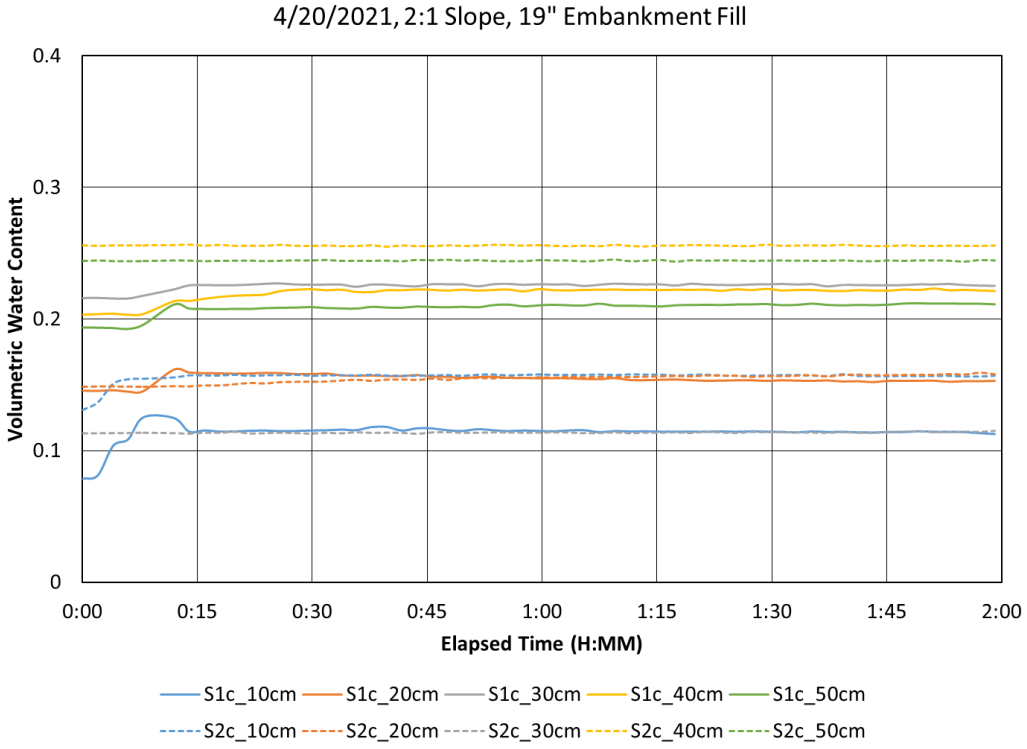

Fig. B7. 19" Embankment Fill 2-hr corrected data at a 2:1 slope.

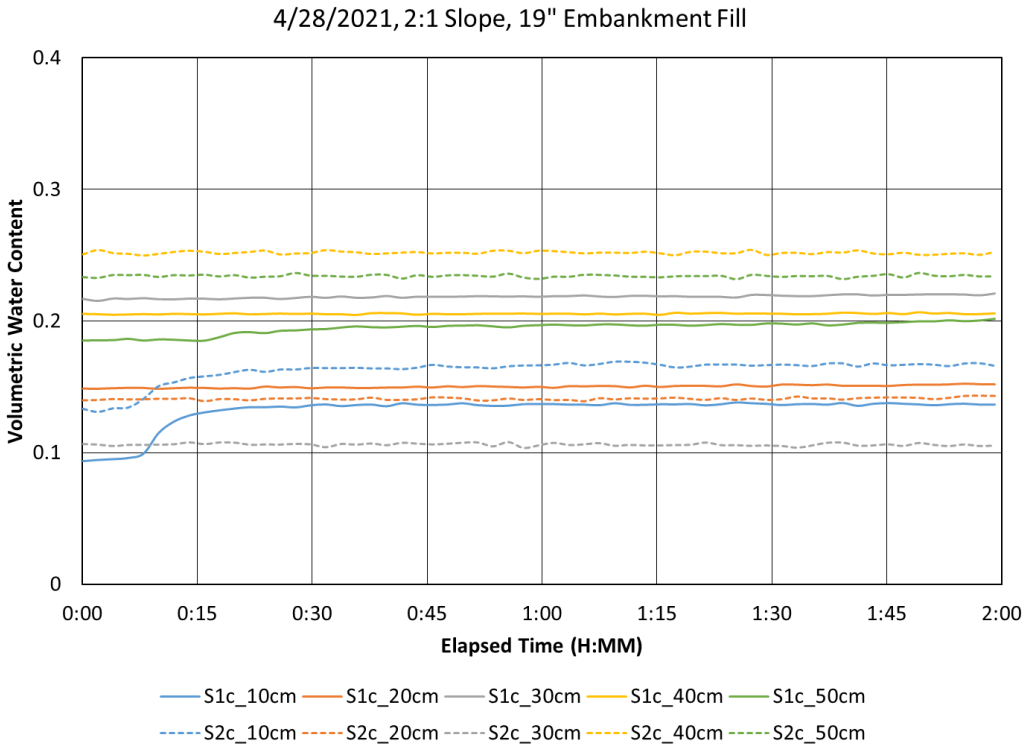

Fig. B8. 19" Embankment Fill 2-hr corrected data at a 2:1 slope.

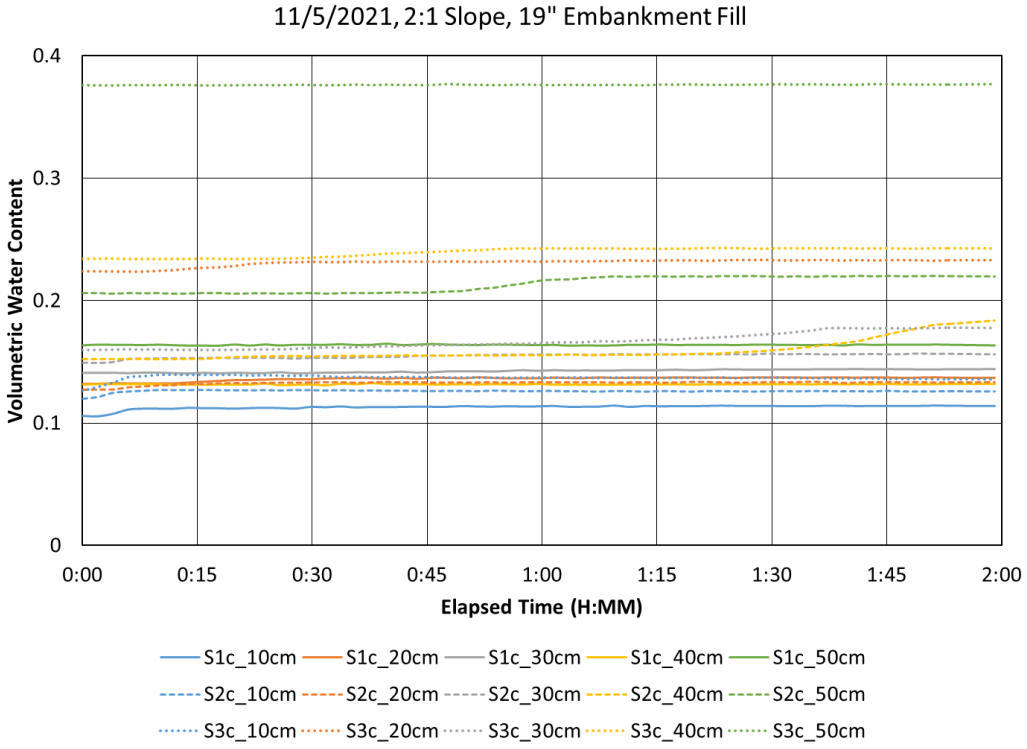

Fig. B9. 19" Embankment Fill 2-hr corrected data at a 2:1 slope.

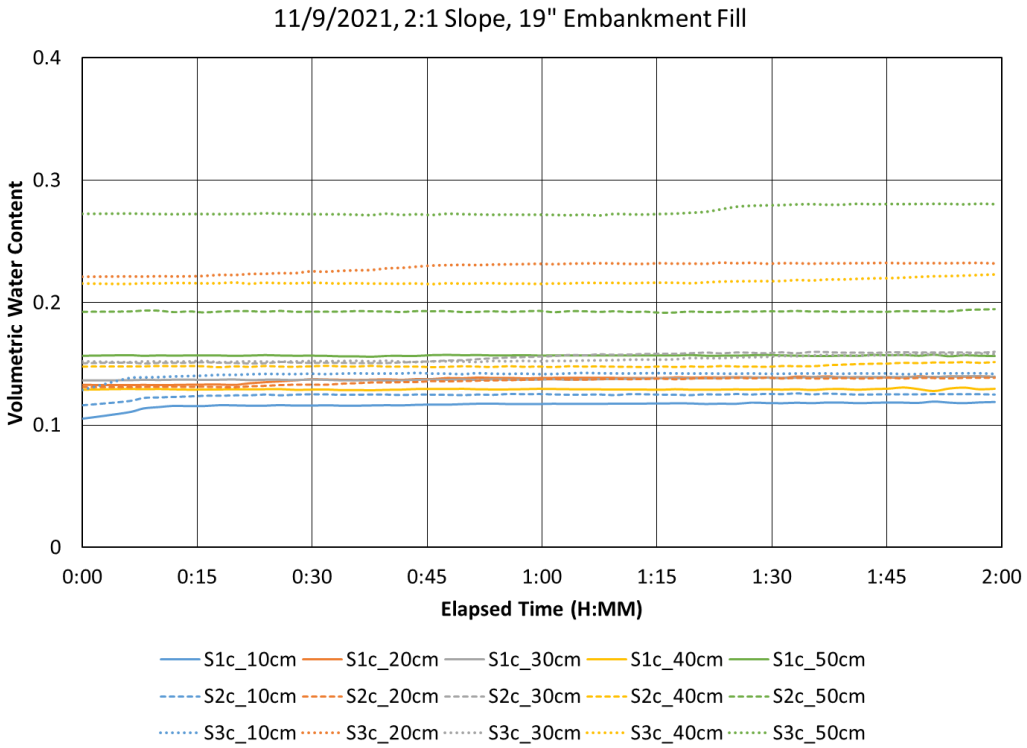

Fig. B10. 19” Embankment Fill 2-hr corrected data at a 2:1 slope.

Configuration 2: 15” Embankment Fill 4” Topsoil

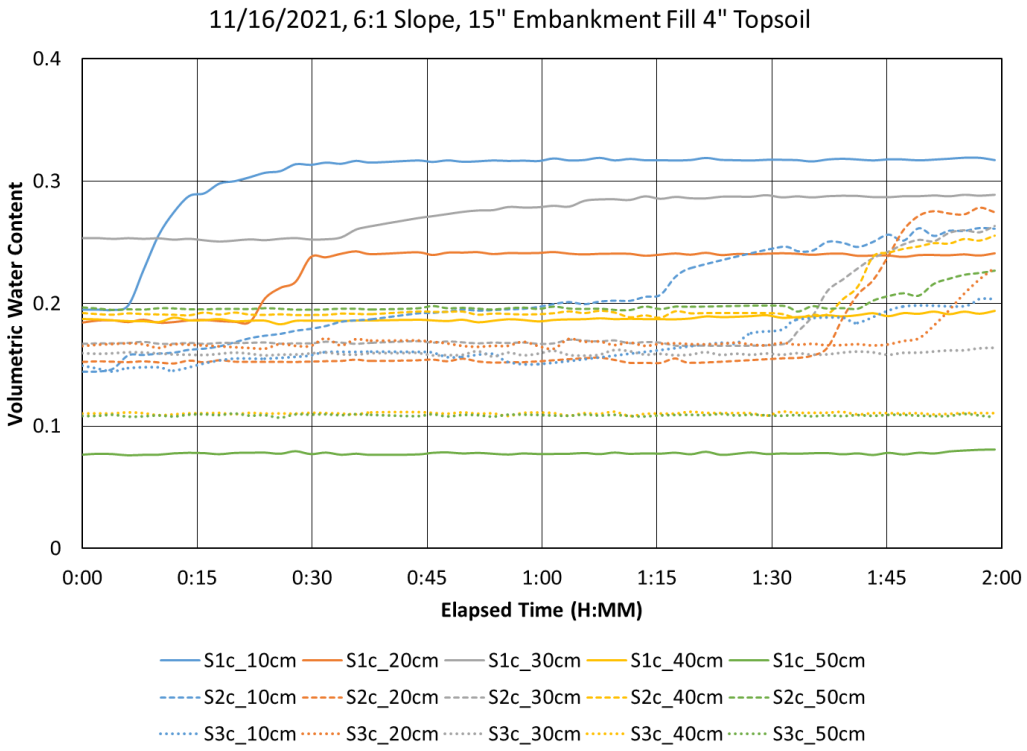

Fig. B11. 15” Embankment Fill 4” Topsoil 2-hr corrected data at a 6:1 slope.

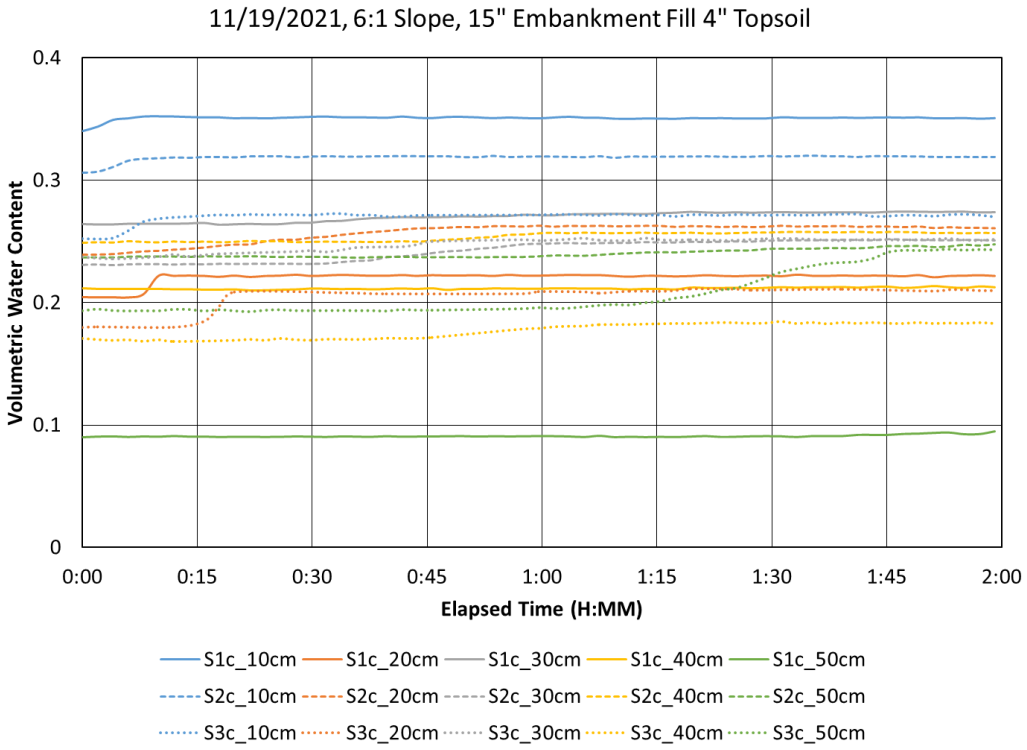

Fig. B12. 15" Embankment Fill 4" Topsoil 2-hr corrected data at a 6:1 slope.

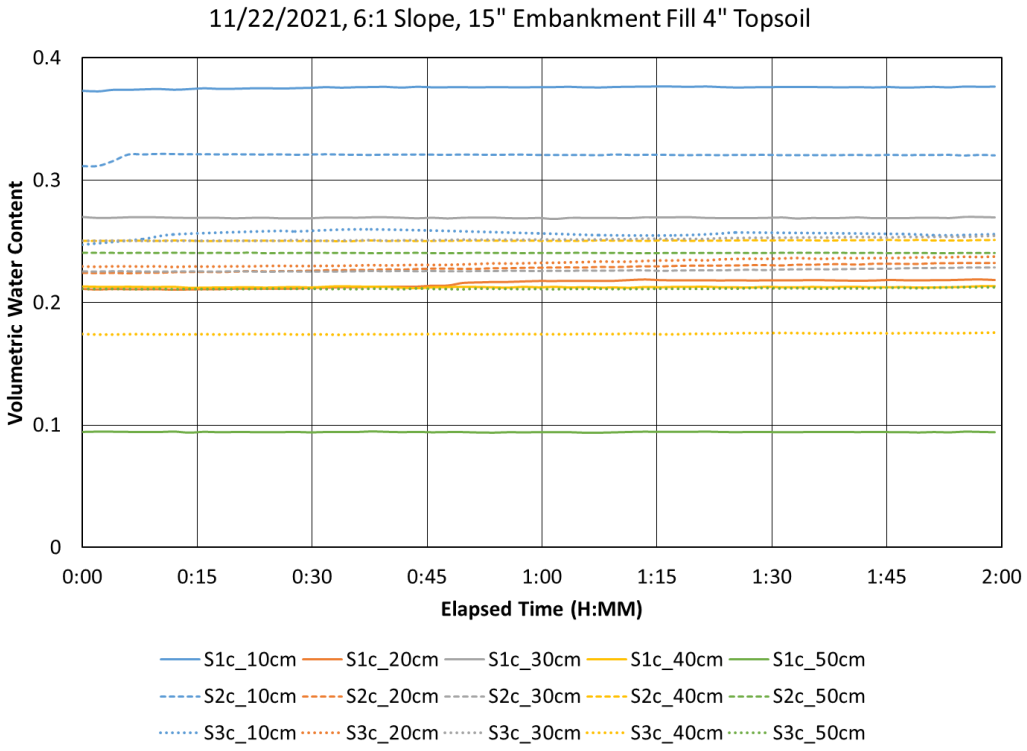

Fig. B13. 15" Embankment Fill 4" Topsoil 2-hr corrected data at a 6:1 slope.

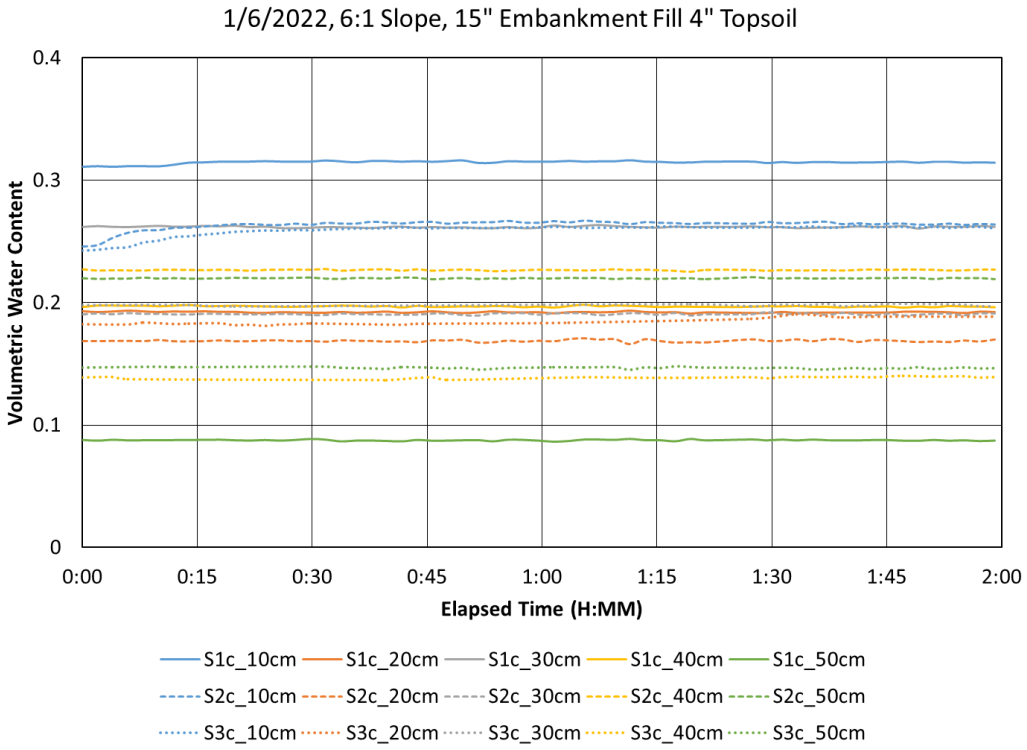

Fig. B14. 15" Embankment Fill 4" Topsoil 2-hr corrected data at a 6:1 slope.

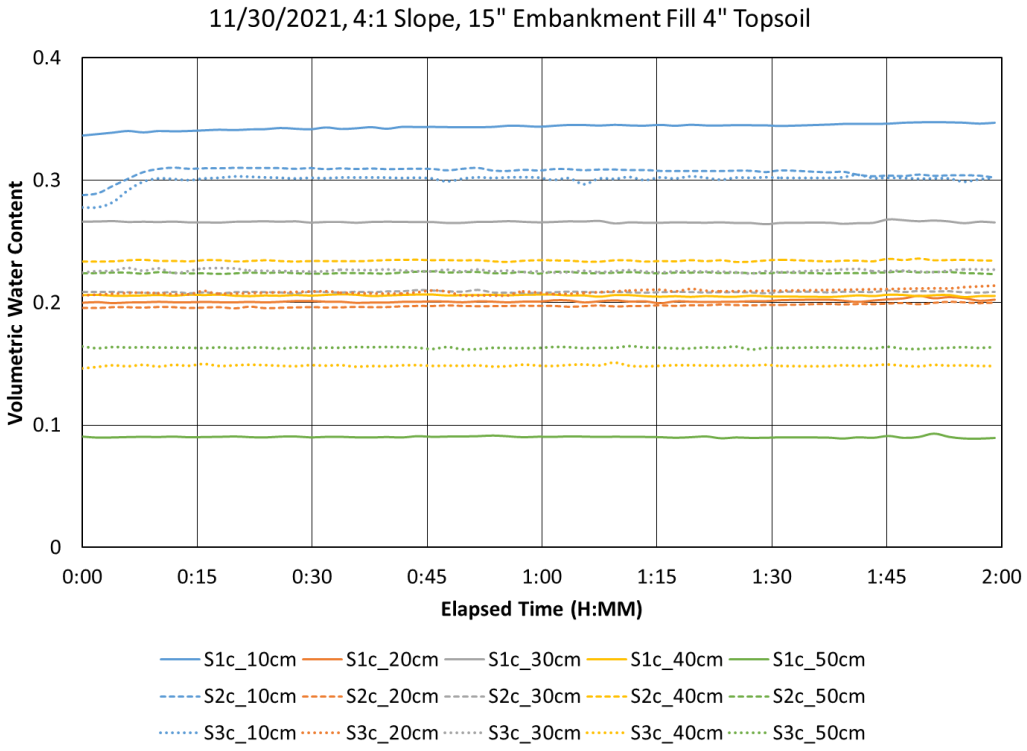

Fig. B15. 15" Embankment Fill 4" Topsoil 2-hr corrected data at a 4:1 slope.

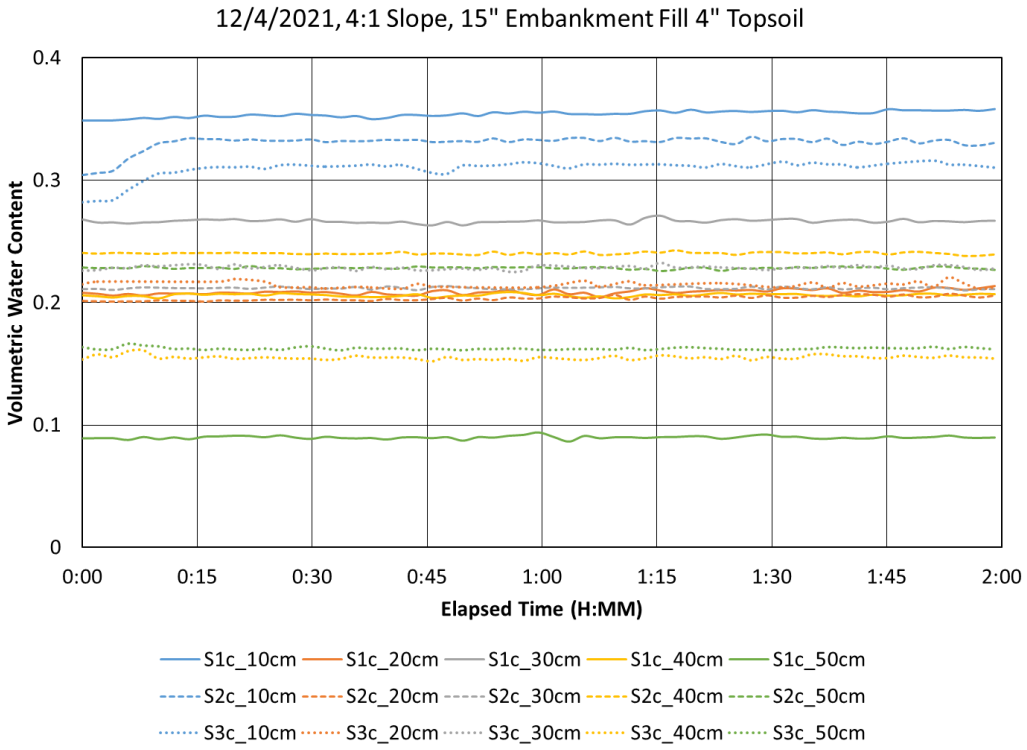

Fig. B16. 15” Embankment Fill 4” Topsoil 2-hr corrected data at a 4:1 slope.

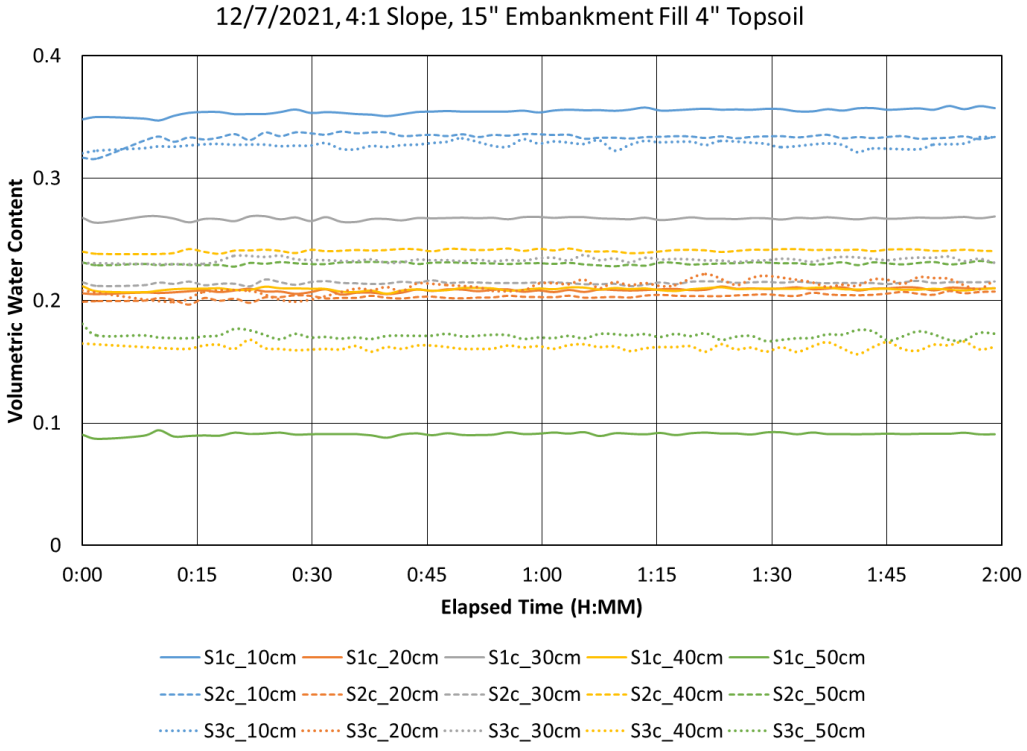

Fig. B17. 15” Embankment Fill 4” Topsoil 2-hr corrected data at a 4:1 slope.

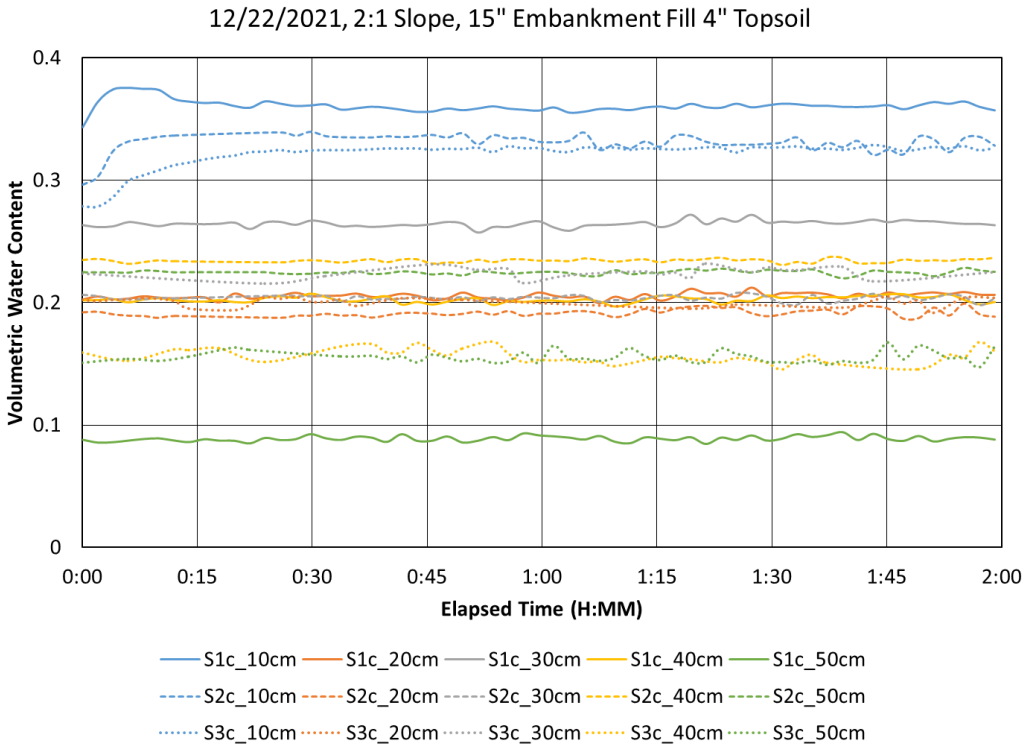

Fig. B18. 15” Embankment Fill 4” Topsoil 2-hr corrected data at a 2:1 slope.

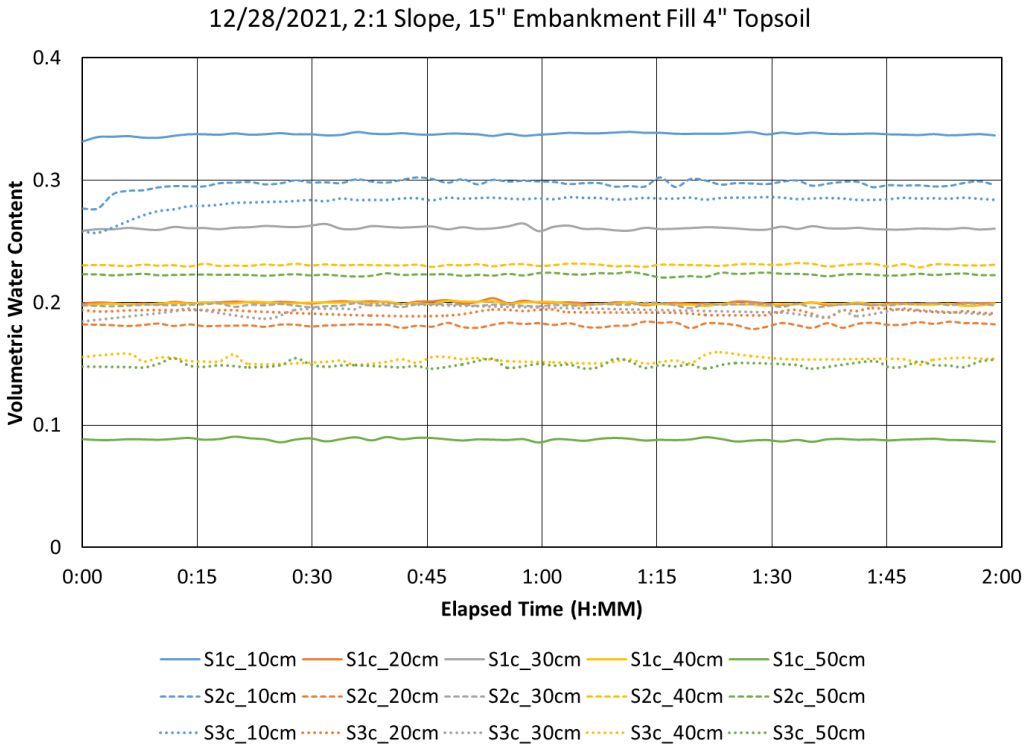

Fig. B19. 15” Embankment Fill 4” Topsoil 2-hr corrected data at a 2:1 slope.

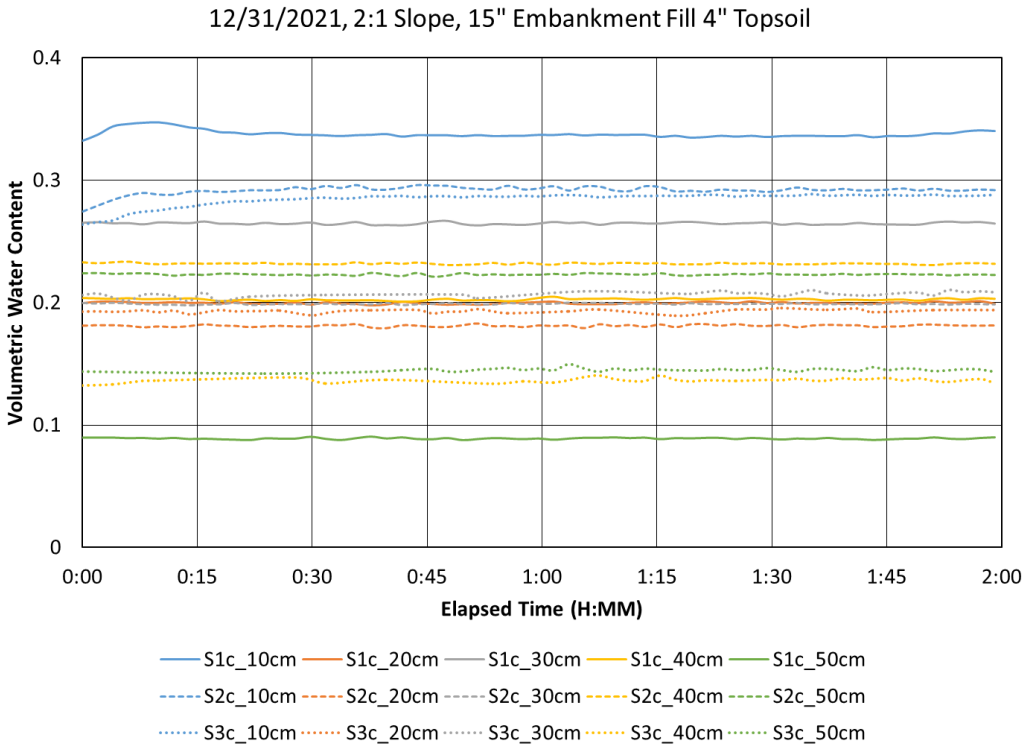

Fig. B20. 15” Embankment Fill 4” Topsoil 2-hr corrected data at a 2:1 slope.

Configuration 3: 15” Embankment Fill 4” Topsoil with Vegetation

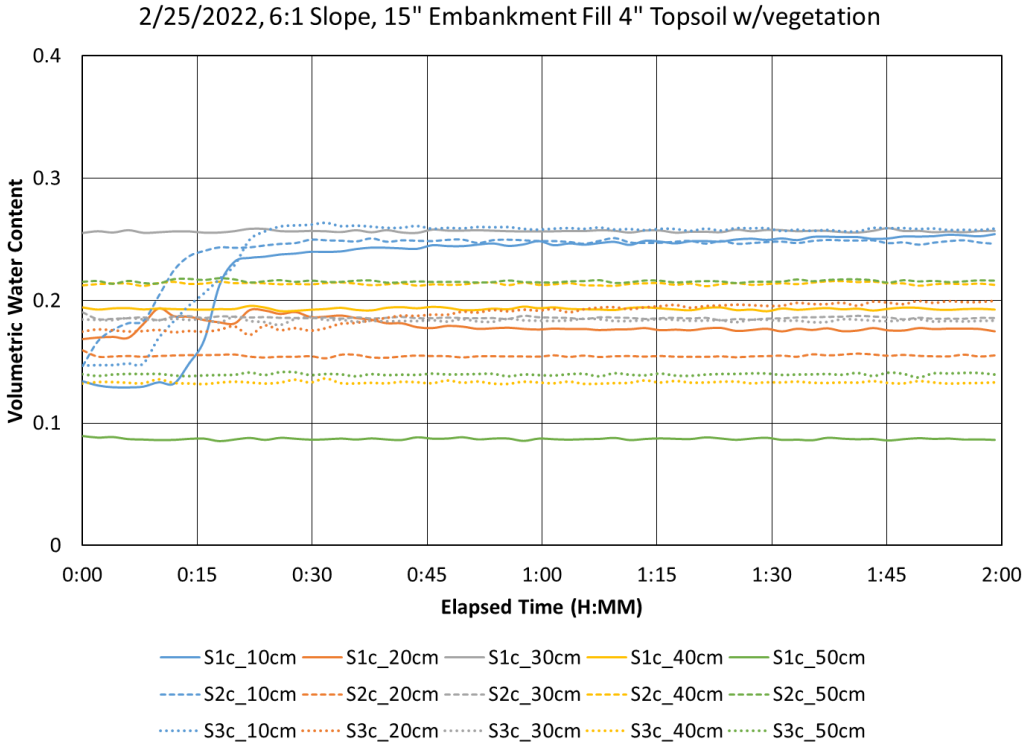

Fig. B21. 15” Embankment Fill 4” Topsoil w/vegetation 2-hr corrected data at a 6:1 slope.

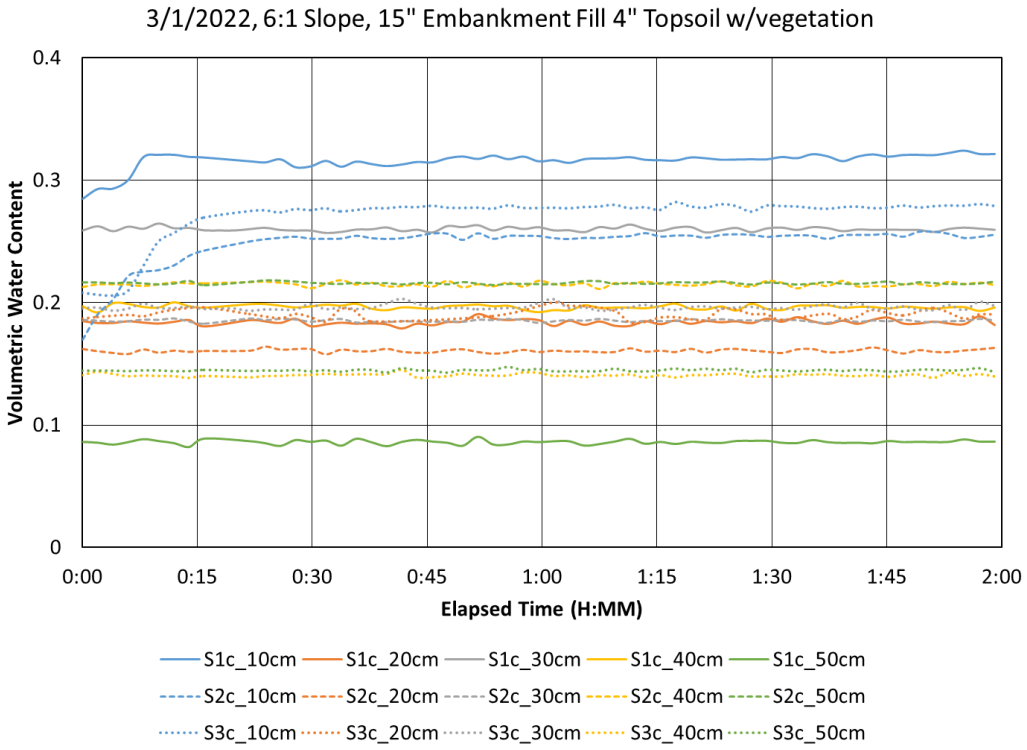

Fig. B22. 15" Embankment Fill 4" Topsoil w/vegetation 2-hr corrected data at a 6:1 slope.

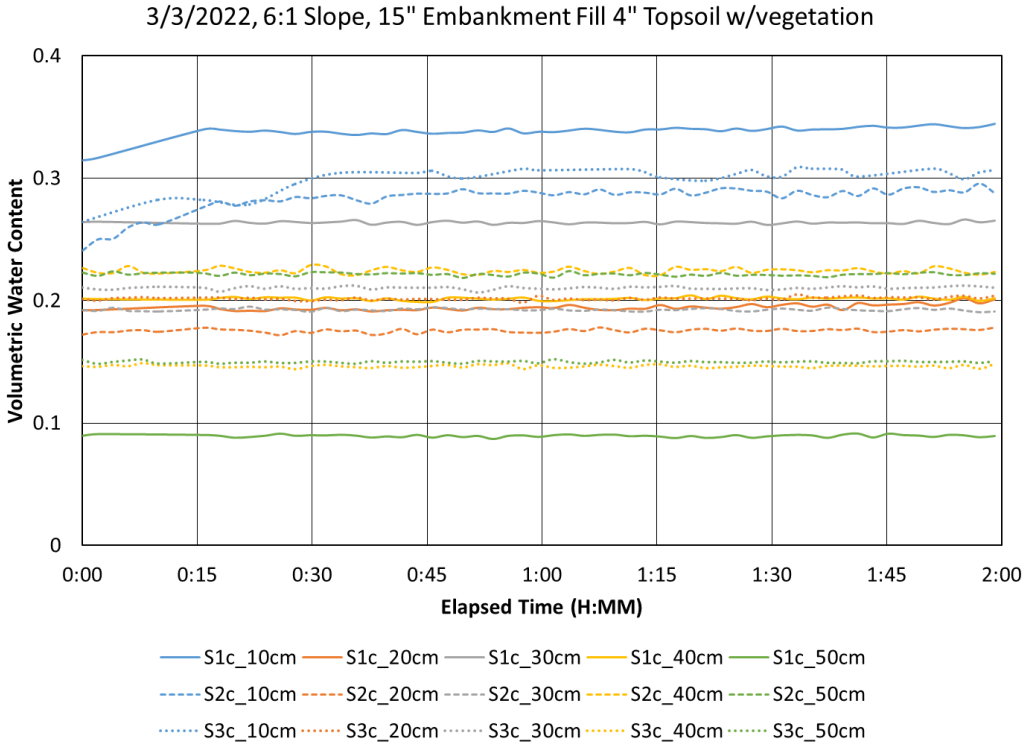

Fig. B23. 15" Embankment Fill 4" Topsoil w/vegetation 2-hr corrected data at a 6:1 slope.

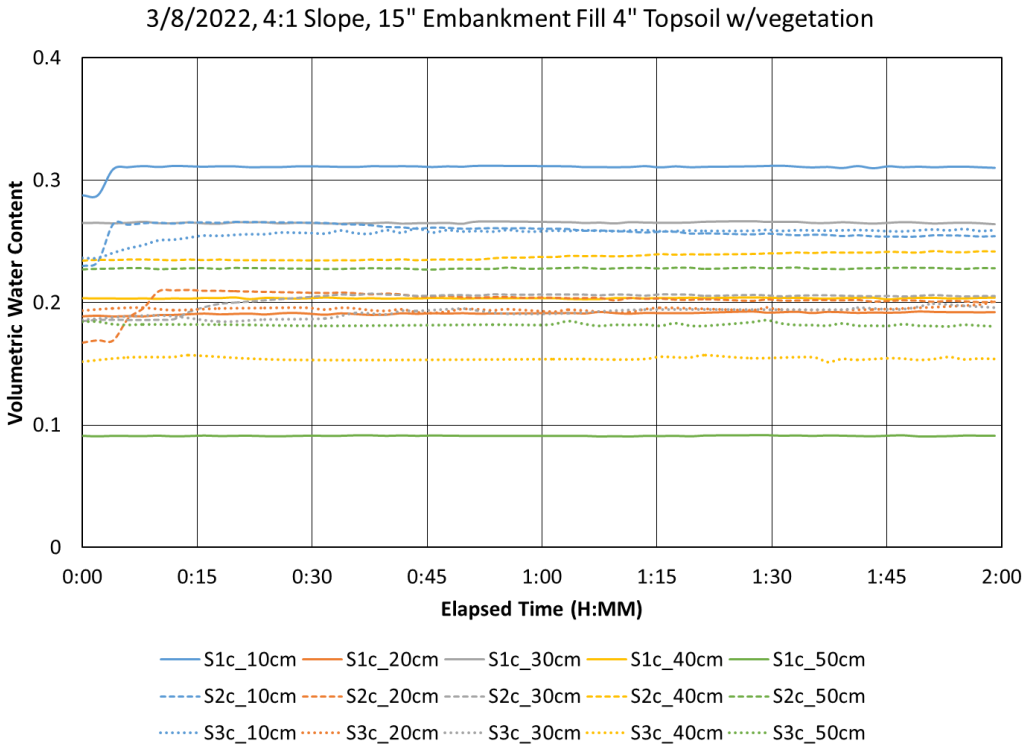

Fig. B24. 15" Embankment Fill 4" Topsoil w/vegetation 2-hr corrected data at a 4:1 slope.

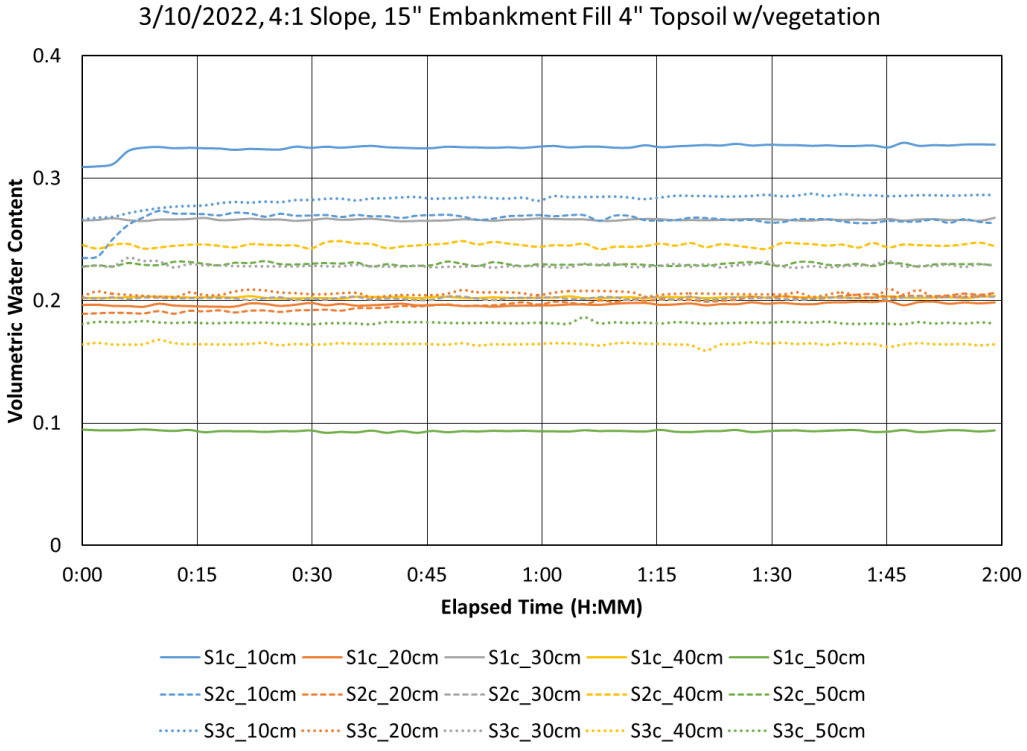

Fig. B25. 15" Embankment Fill 4" Topsoil w/vegetation 2-hr corrected data at a 4:1 slope.

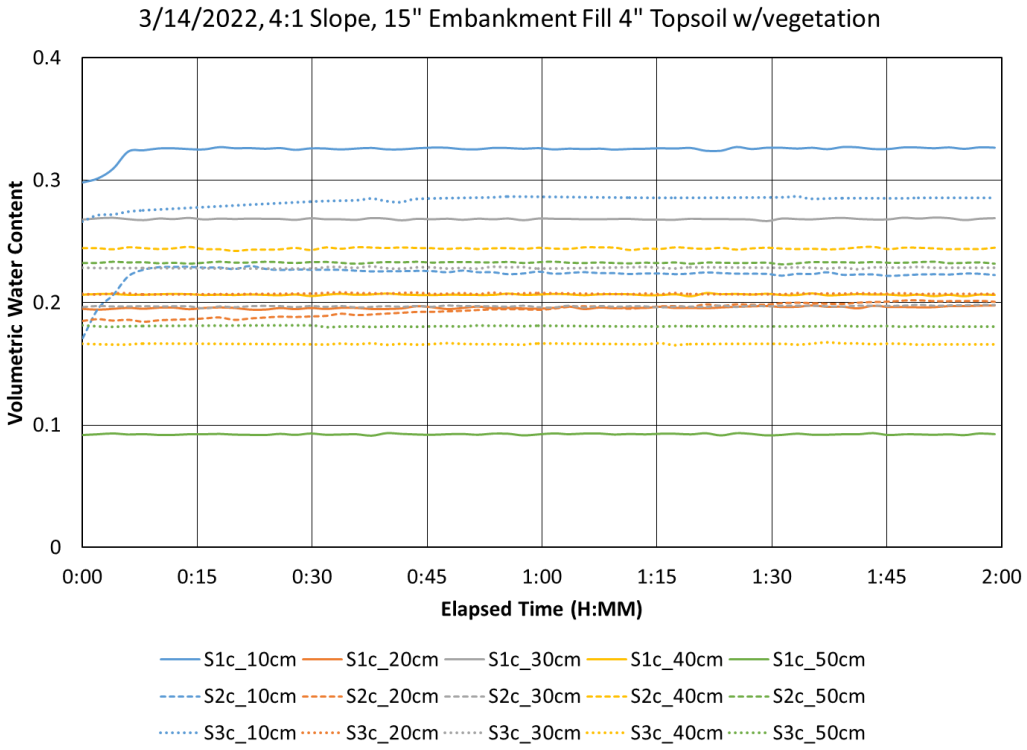

Fig. B26. 15" Embankment Fill 4" Topsoil w/vegetation 2-hr corrected data at a 4:1 slope.

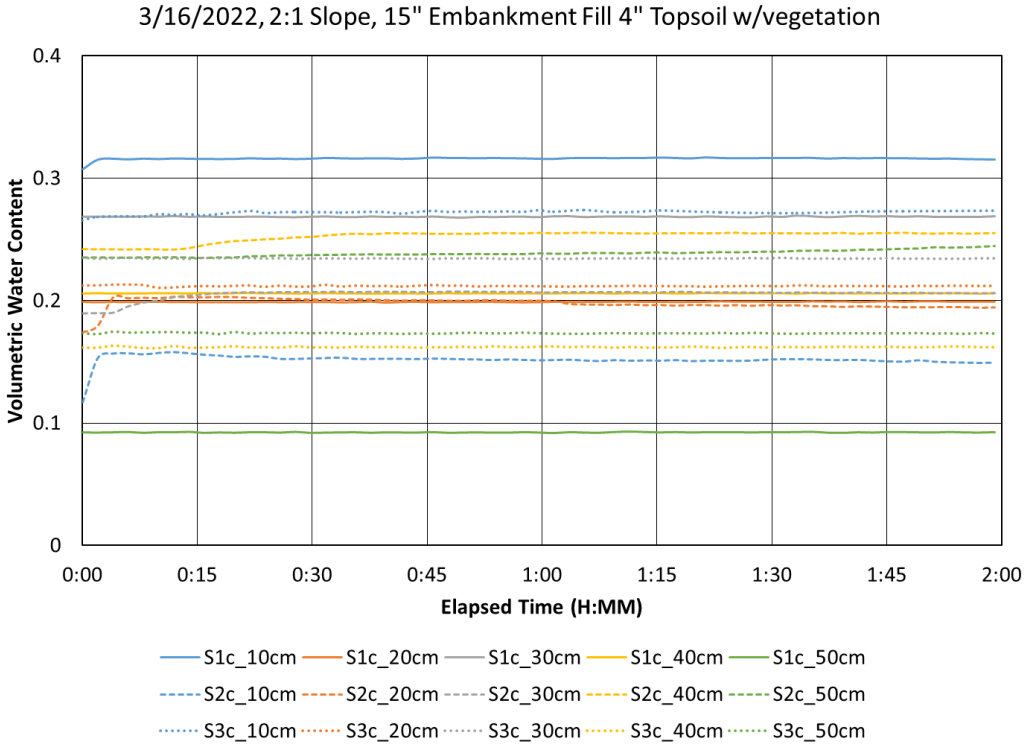

Fig. B27. 15" Embankment Fill 4" Topsoil w/vegetation 2-hr corrected data at a 2:1 slope.

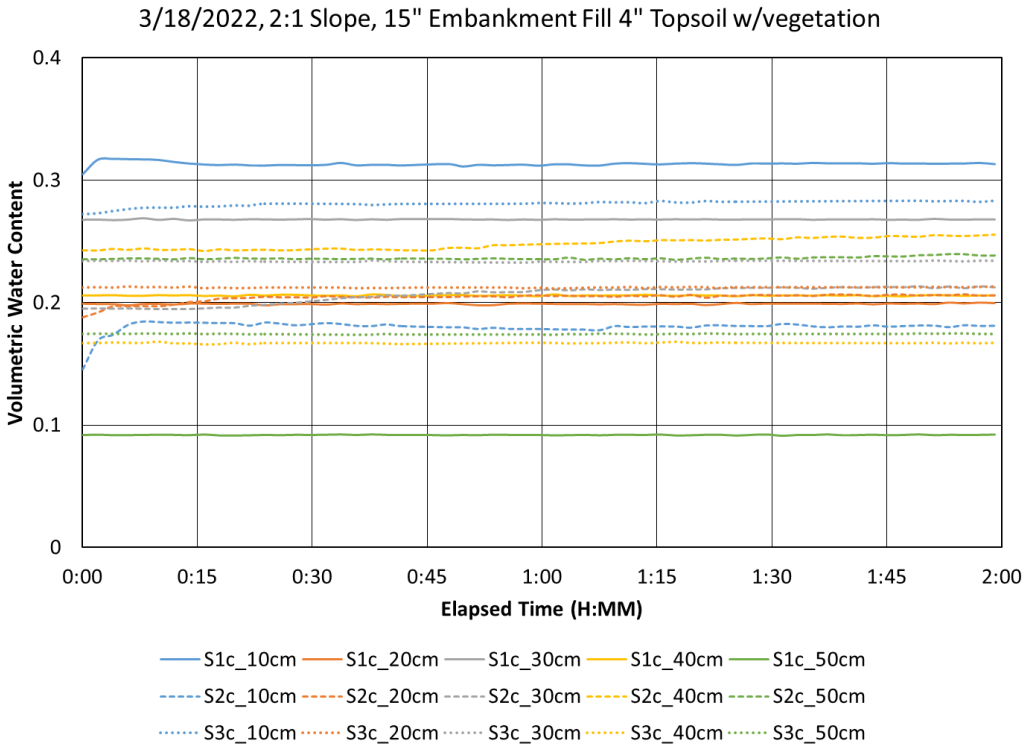

Fig. B28. 15" Embankment Fill 4" Topsoil w/vegetation 2-hr corrected data at a 2:1 slope.

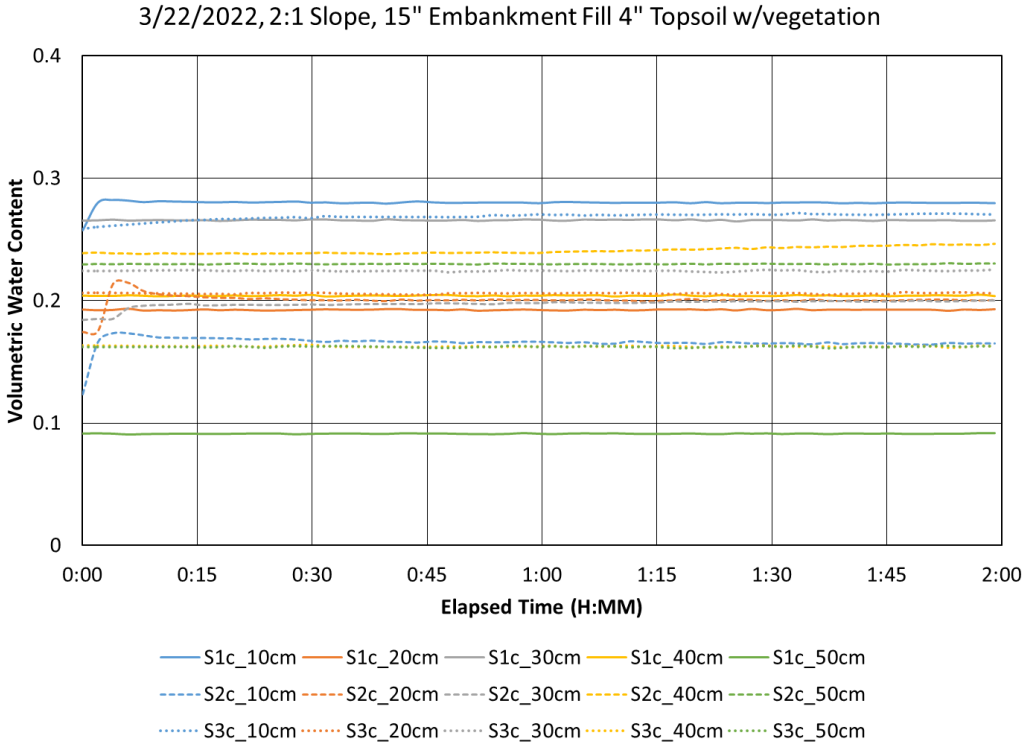

Fig. B29. 15" Embankment Fill 4" Topsoil w/vegetation 2-hr corrected data at a 2:1 slope.

Configuration 4: 15” Embankment Fill 4” Amended Topsoil

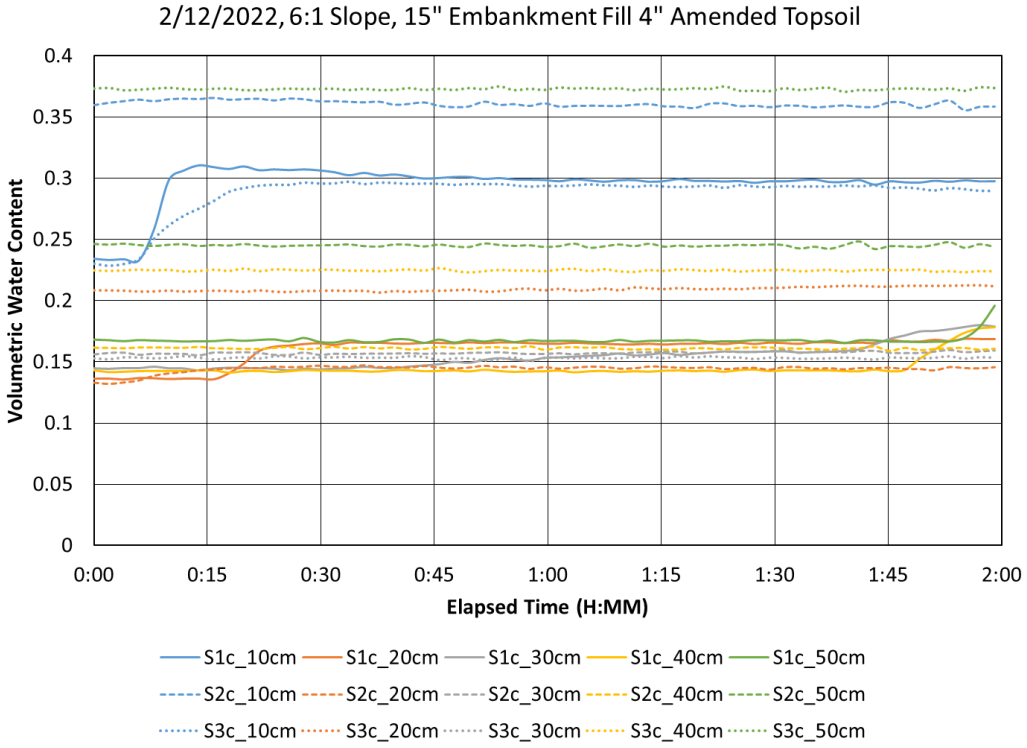

Fig. B30. 15” Embankment Fill 4” Amended Topsoil 2-hr corrected data at a 6:1 slope.

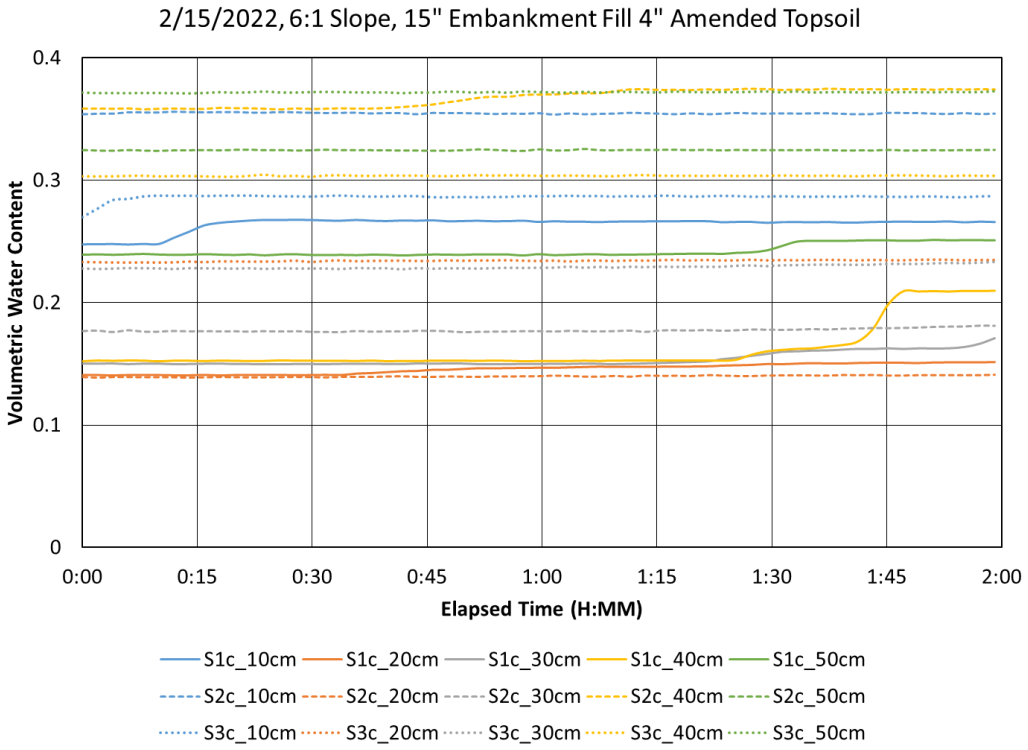

Fig. B31. 15" Embankment Fill 4" Amended Topsoil 2-hr corrected data at a 6:1 slope.

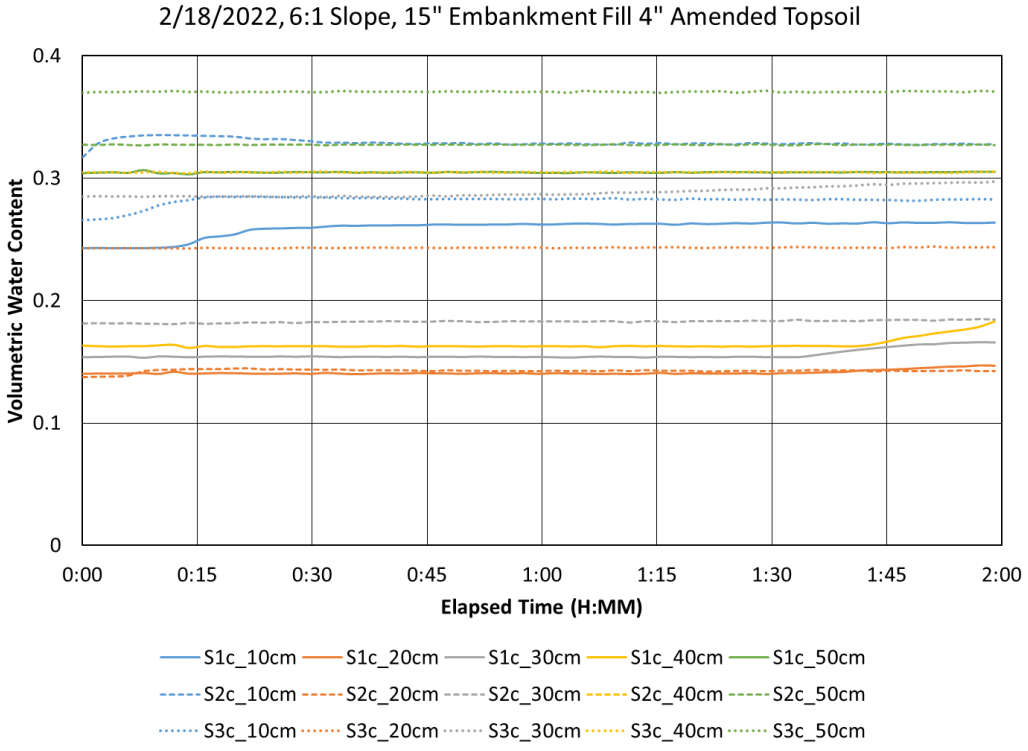

Fig. B32. 15" Embankment Fill 4" Amended Topsoil 2-hr corrected data at a 6:1 slope. Note: S3c_40 exceeds 0.4.

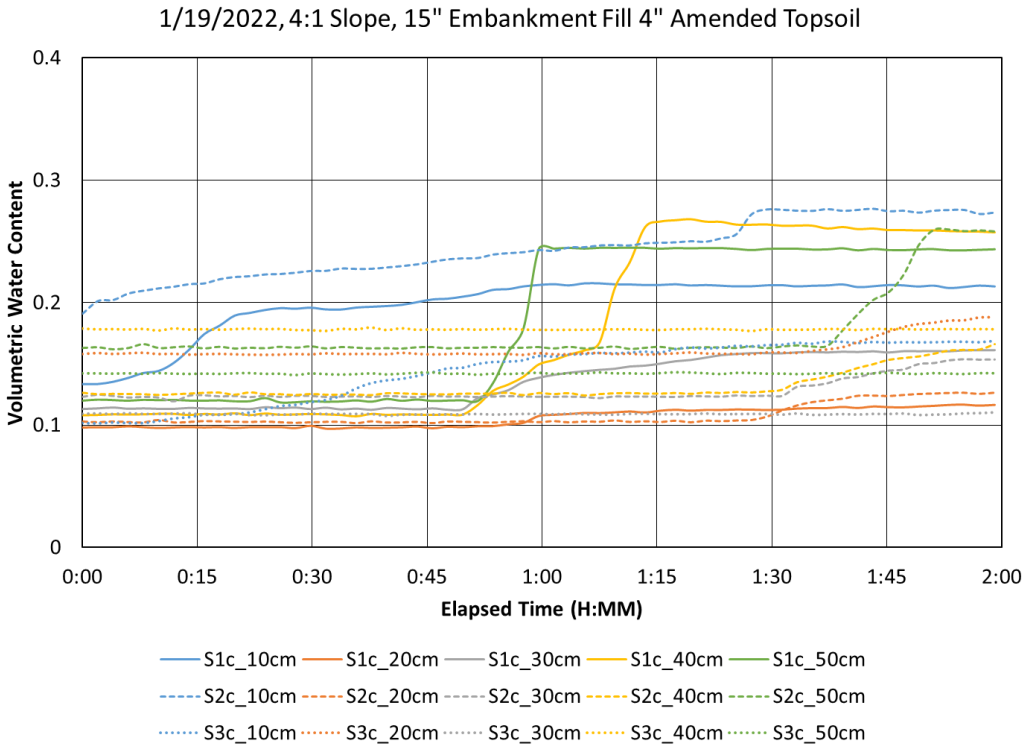

Fig. B33. 15" Embankment Fill 4" Amended Topsoil 2-hr corrected data at a 4:1 slope.

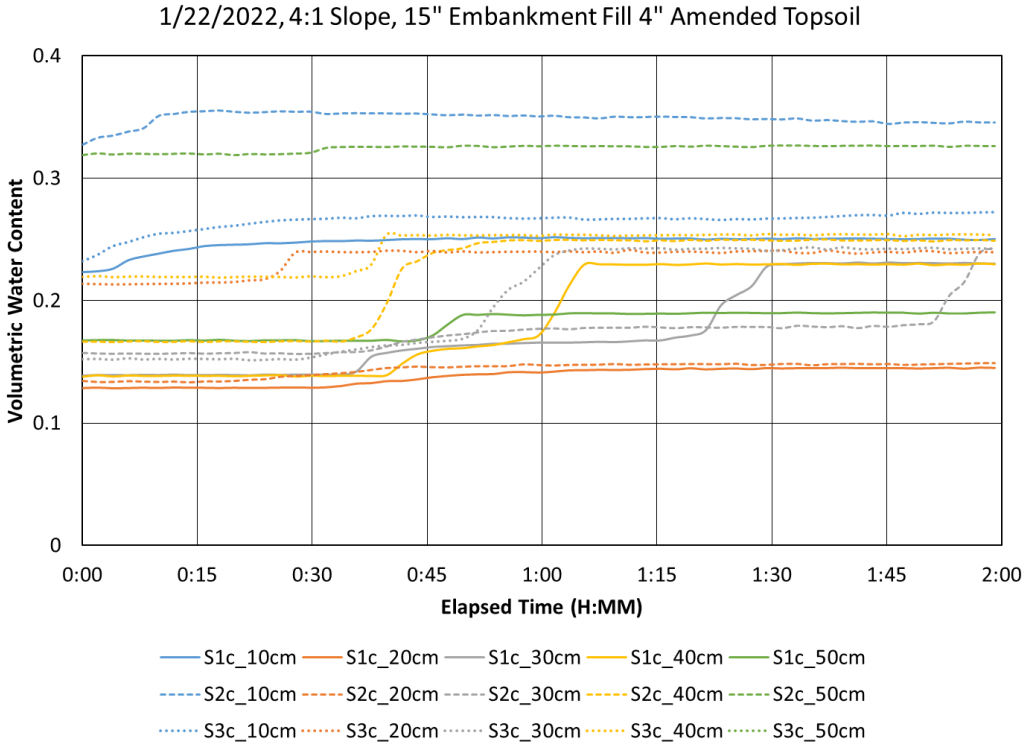

Fig. B34. 15" Embankment Fill 4" Amended Topsoil 2-hr corrected data at a 4:1 slope.

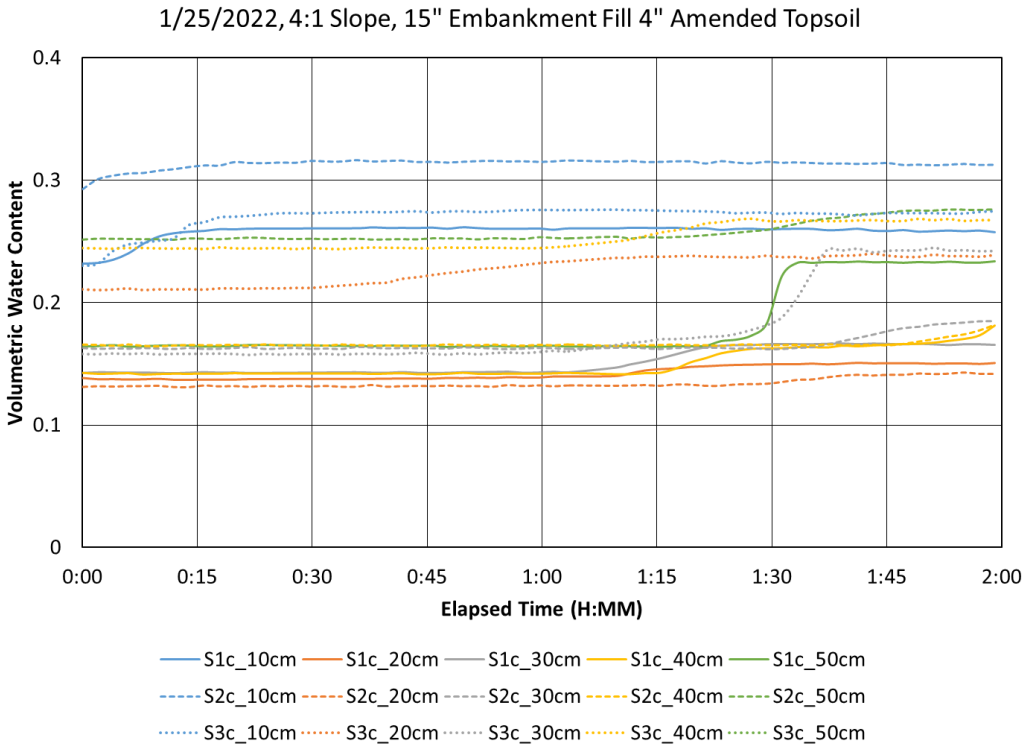

Fig. B35. 15” Embankment Fill 4” Amended Topsoil 2-hr corrected data at a 4:1 slope.

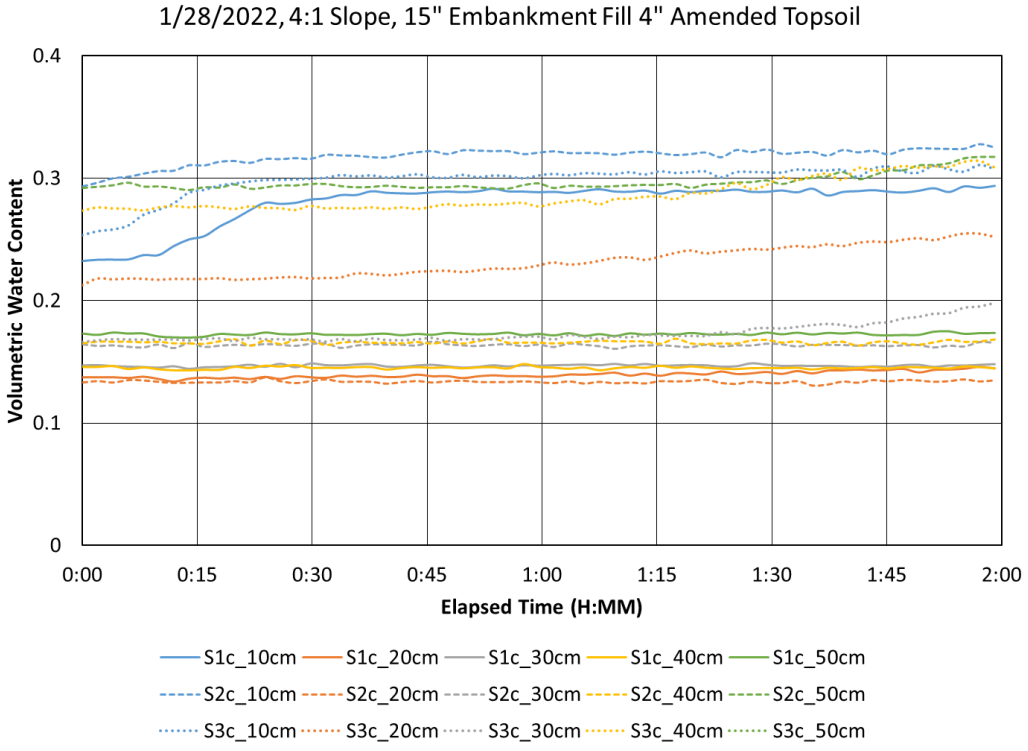

Fig. B36. 15” Embankment Fill 4” Amended Topsoil 2-hr corrected data at a 4:1 slope.

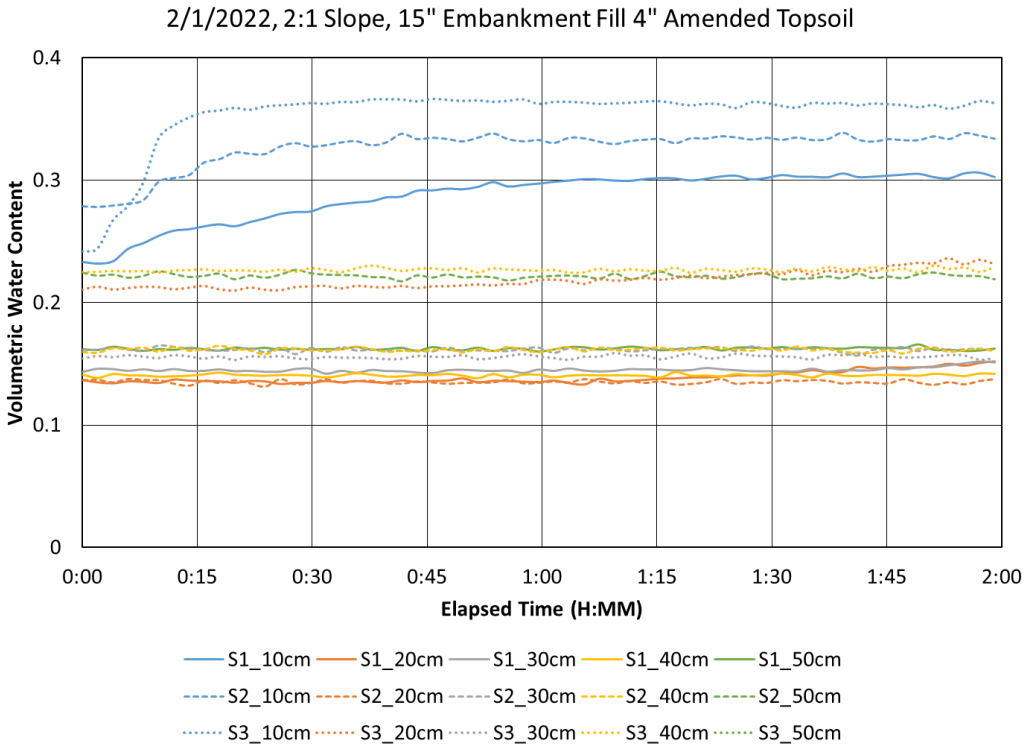

Fig. B37. 15" Embankment Fill 4" Amended Topsoil 2-hr corrected data at a 2:1 slope. Note: S3c_50cm exceeds 0.4.

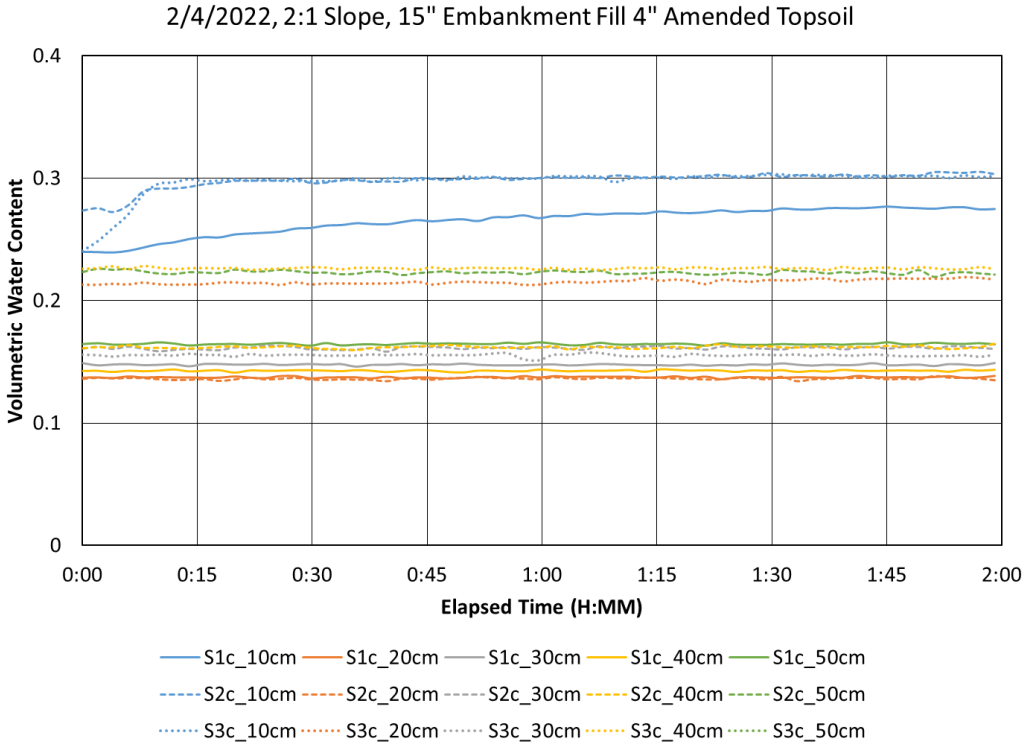

Fig. B38. 15" Embankment Fill 4" Amended Topsoil 2-hr corrected data at a 2:1 slope. Note: S3c_50cm exceeds 0.4.

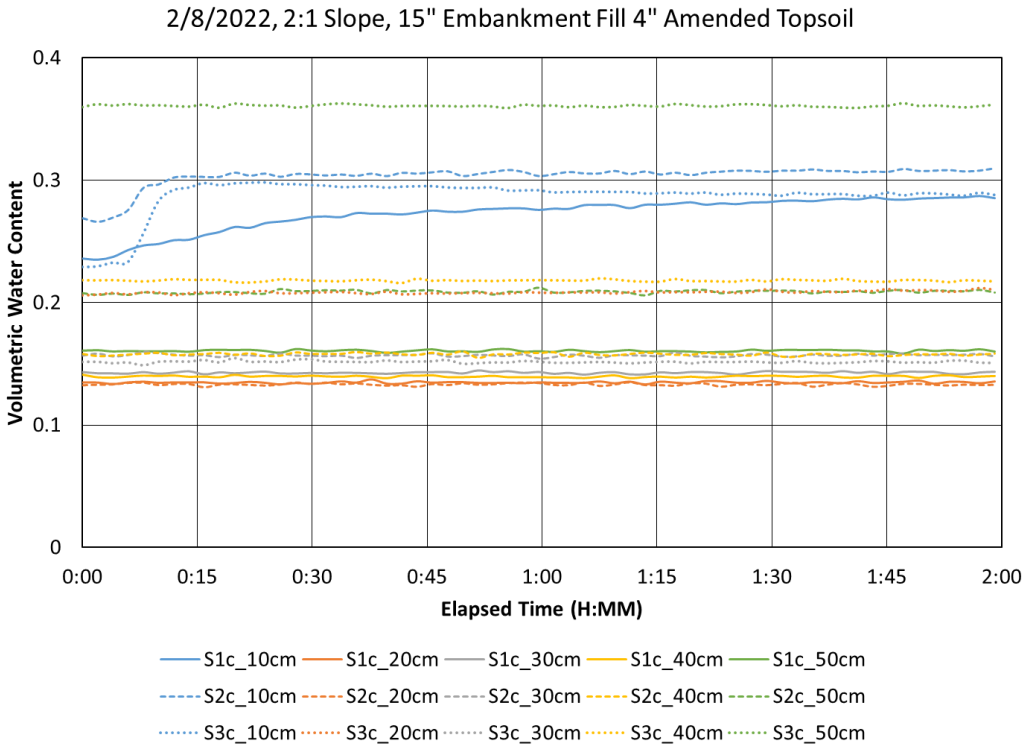

Fig. B39. 15” Embankment Fill 4” Amended Topsoil 2-hr corrected data at a 2:1 slope.

Configuration 5: 15” Embankment Fill 4” Amended Topsoil with Vegetation

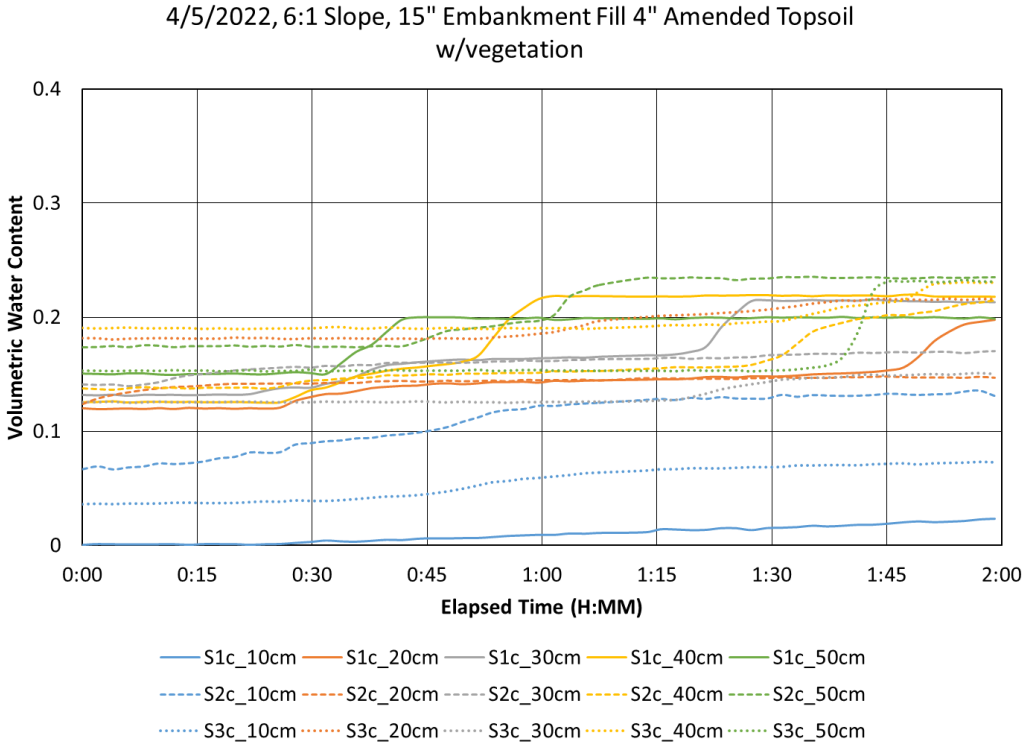

Fig. B40. 15” Embankment Fill 4” Amended Topsoil w/vegetation 2-hr corrected data at a 6:1 slope.

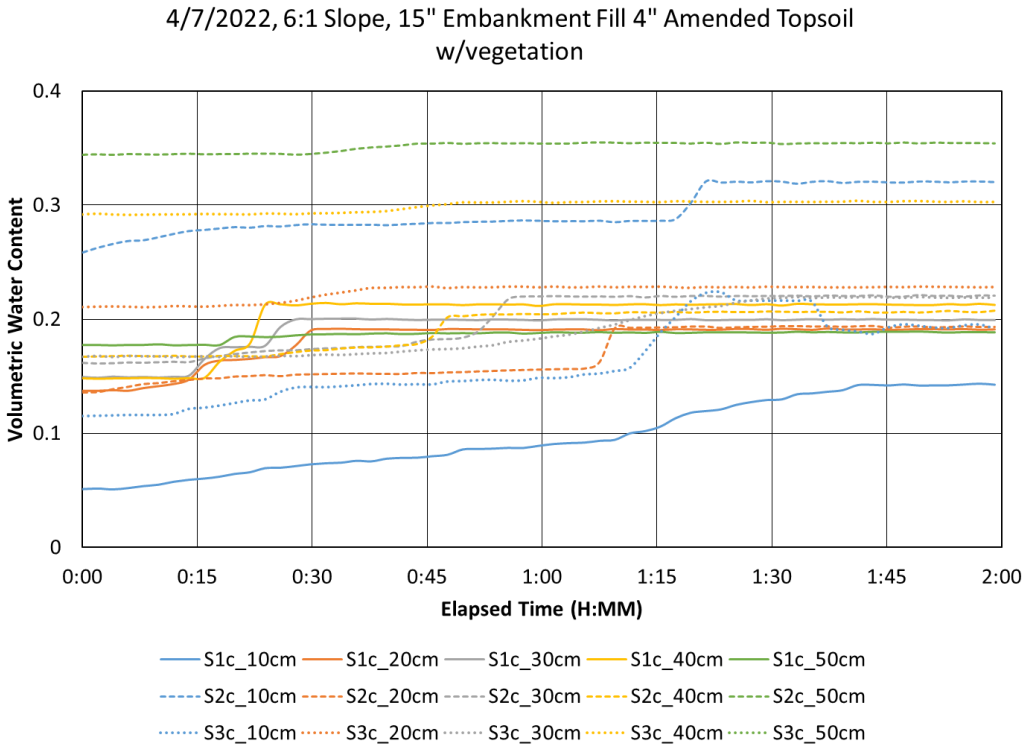

Fig. B41. 15" Embankment Fill 4" Amended Topsoil w/vegetation 2-hr corrected data at a 6:1 slope. Note: S3c_50cm exceeds 0.4.

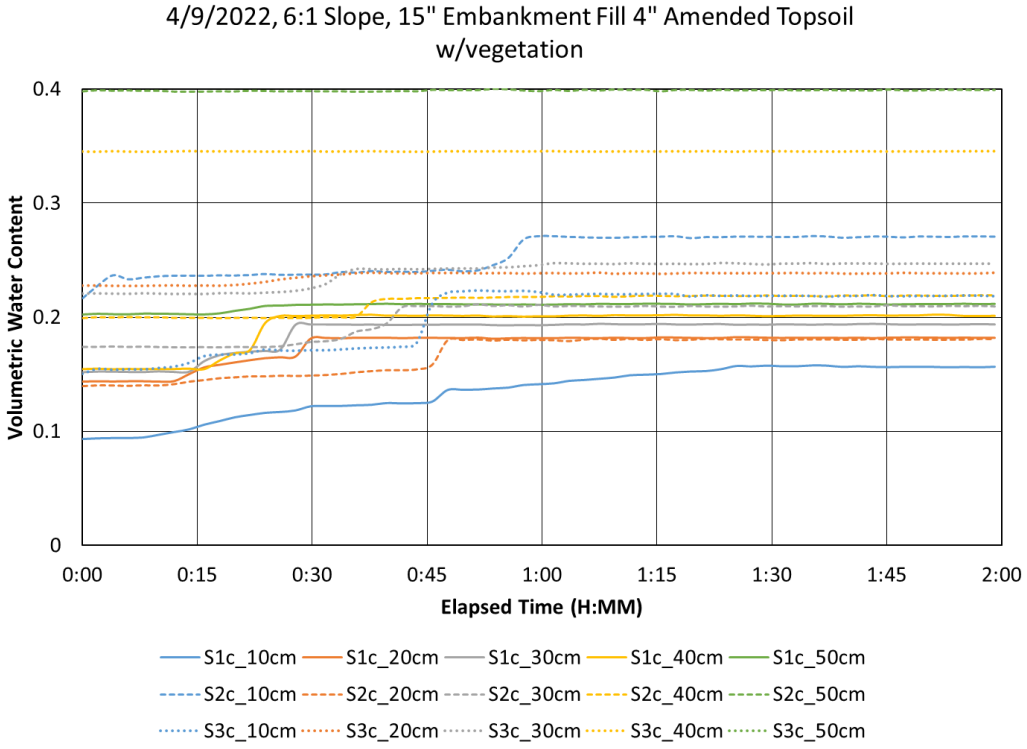

Fig. B42. 15" Embankment Fill 4" Amended Topsoil w/vegetation 2-hr corrected data at a 6:1 slope. Note: S3c_50cm exceeds 0.4.

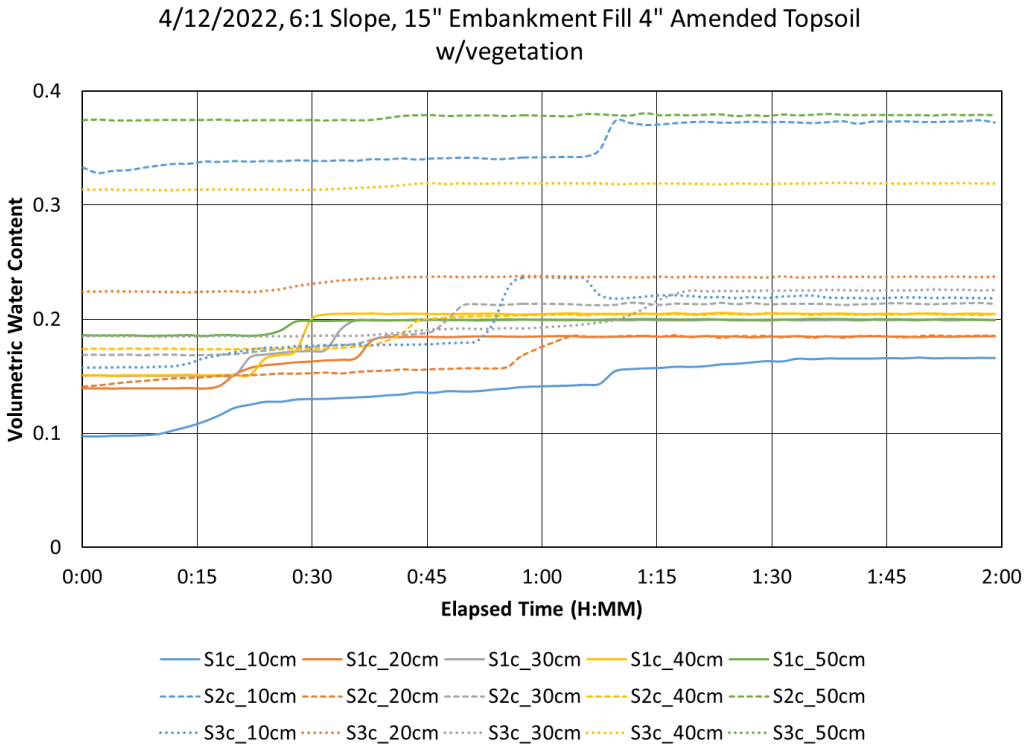

Fig. B43. 15" Embankment Fill 4" Amended Topsoil w/vegetation 2-hr corrected data at a 4:1 slope. Note: S3c_50cm exceeds 0.4.

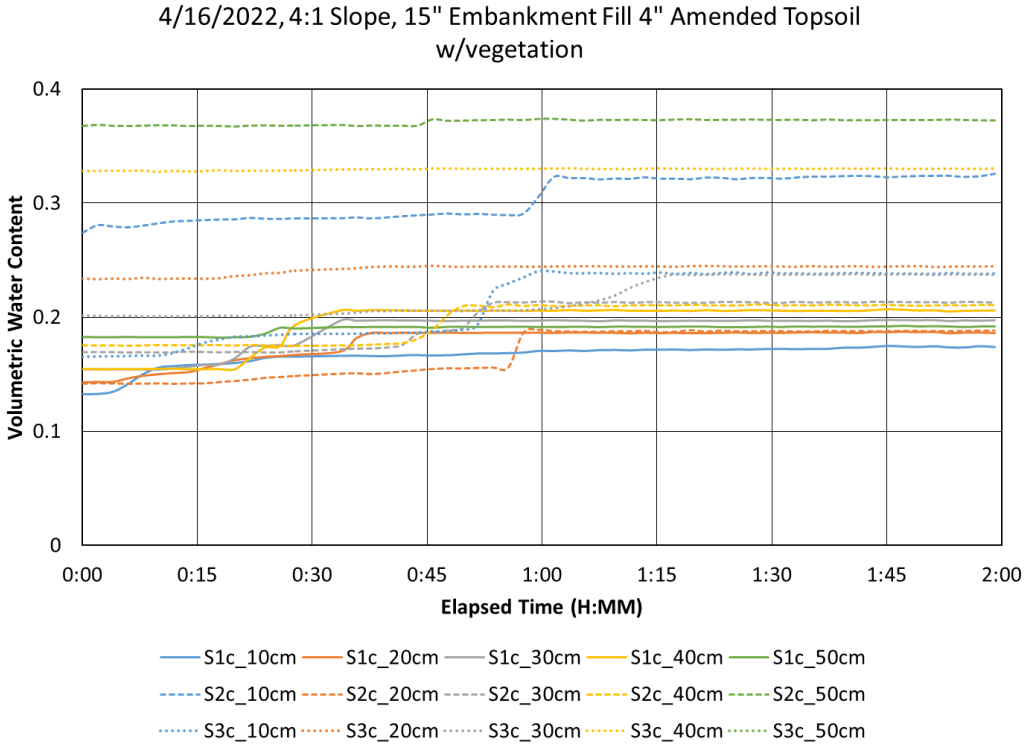

Fig. B44. 15" Embankment Fill 4" Amended Topsoil w/vegetation 2-hr corrected data at a 6:1 slope. Note: S3c_50cm exceeds 0.4.

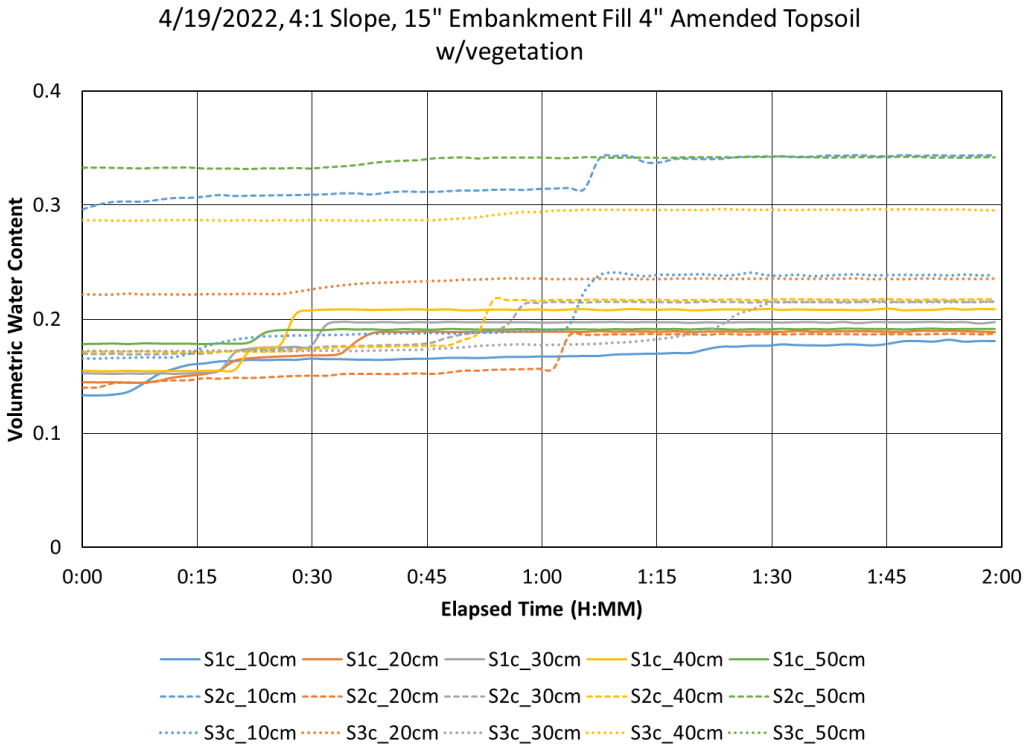

Fig. B45. 15" Embankment Fill 4" Amended Topsoil w/vegetation 2-hr corrected data at a 4:1 slope. Note: S3c_50cm exceeds 0.4.

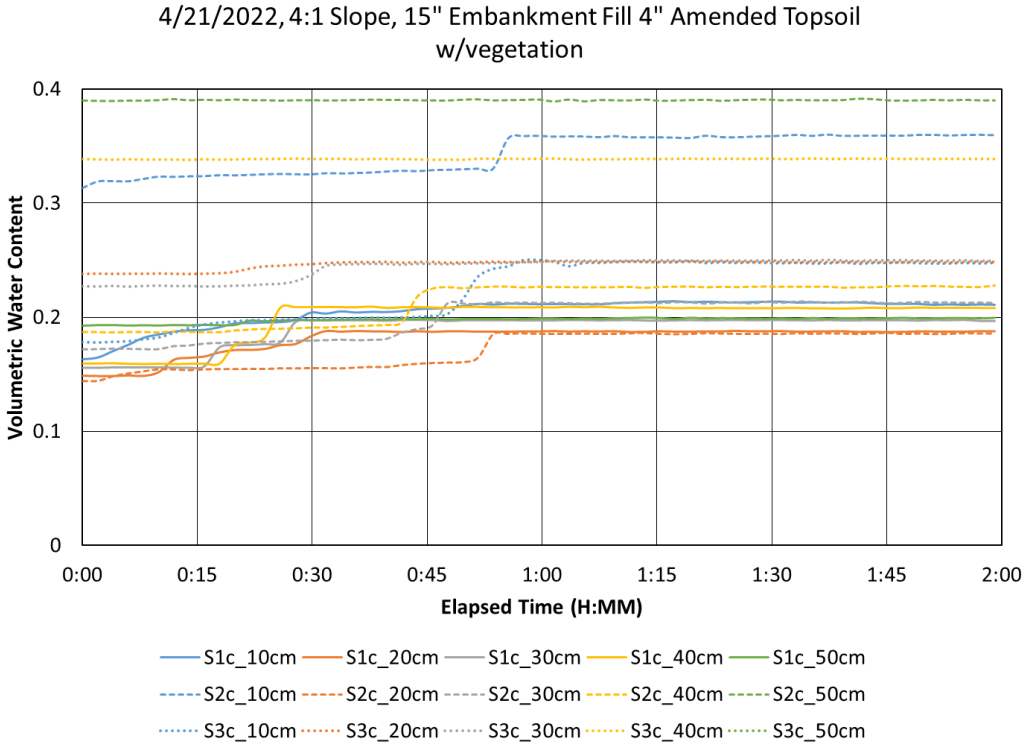

Fig. B46. 15" Embankment Fill 4" Amended Topsoil w/vegetation 2-hr corrected data at a 4:1 slope. Note: S3c_50cm exceeds 0.4.

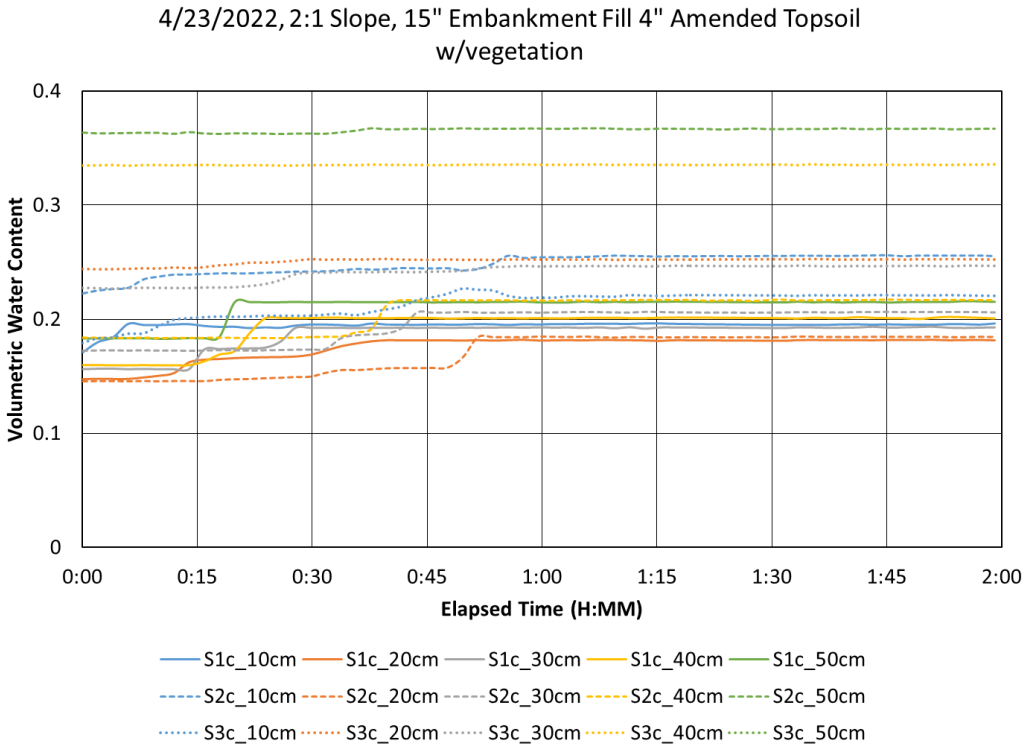

Fig. B47. 15" Embankment Fill 4" Amended Topsoil w/vegetation 2-hr corrected data at a 2:1 slope. Note: S3c_50cm exceeds 0.4.

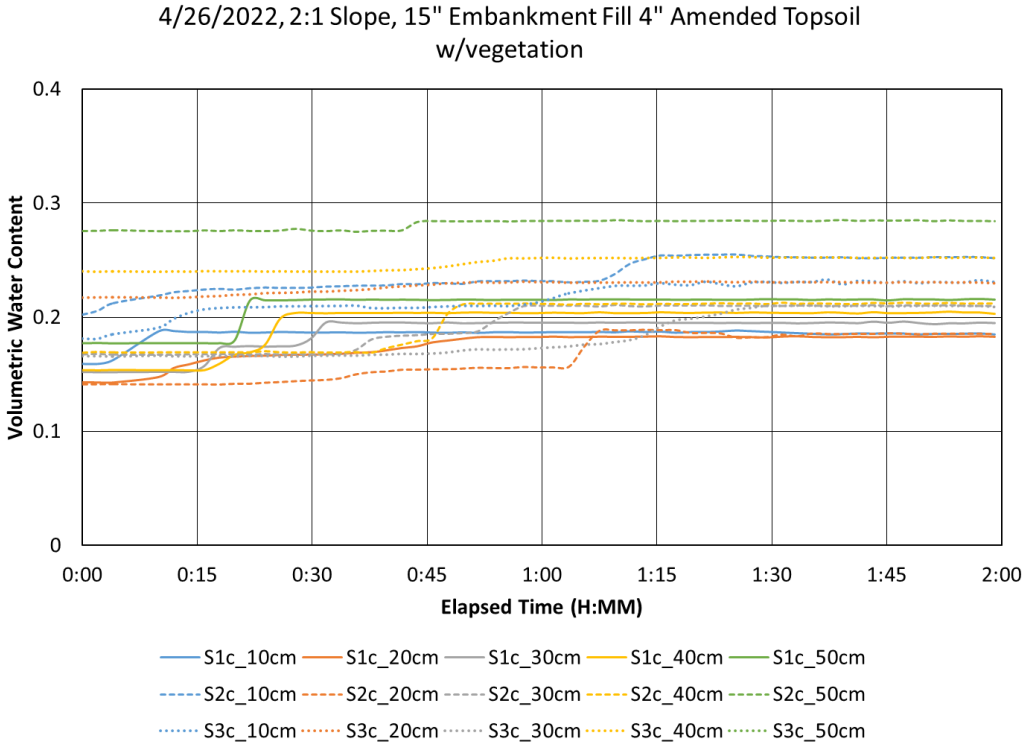

Fig. B48. 15" Embankment Fill 4" Amended Topsoil w/vegetation 2-hr corrected data at a 2:1 slope. Note: S3c_50cm exceeds 0.4.

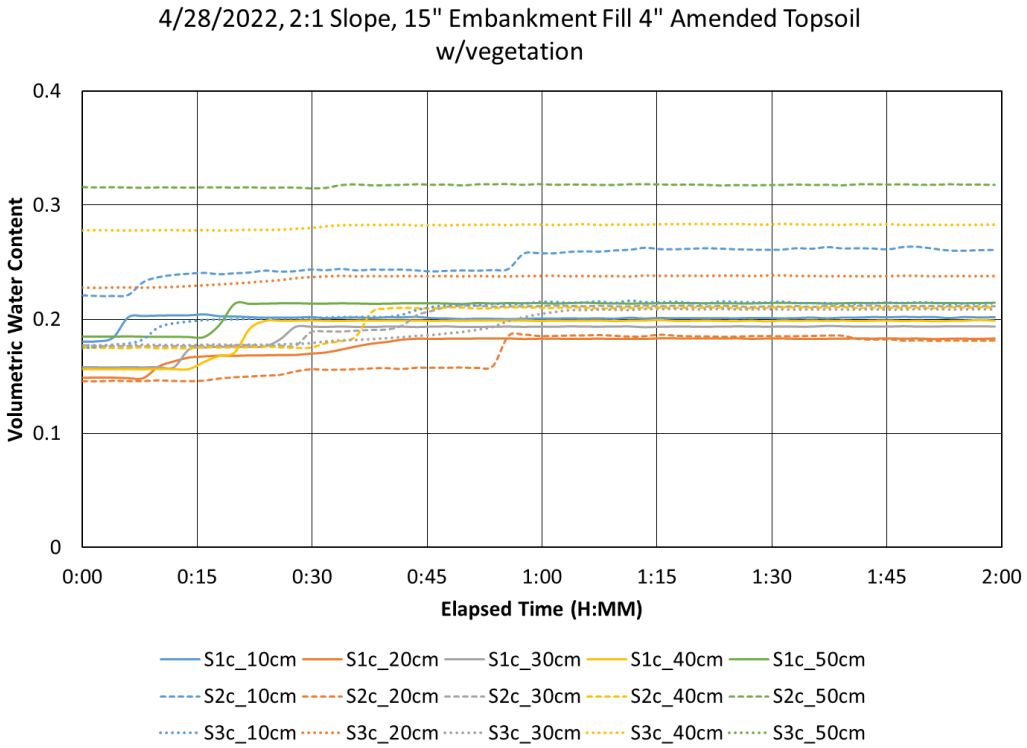

Fig. B49. 15” Embankment Fill 4” Amended Topsoil w/vegetation 2-hr corrected data at a 2:1 slope. Note: S3c_50cm exceeds 0.4.

Configuration 6: 15” Embankment Fill (6” Ripped) 4” Topsoil

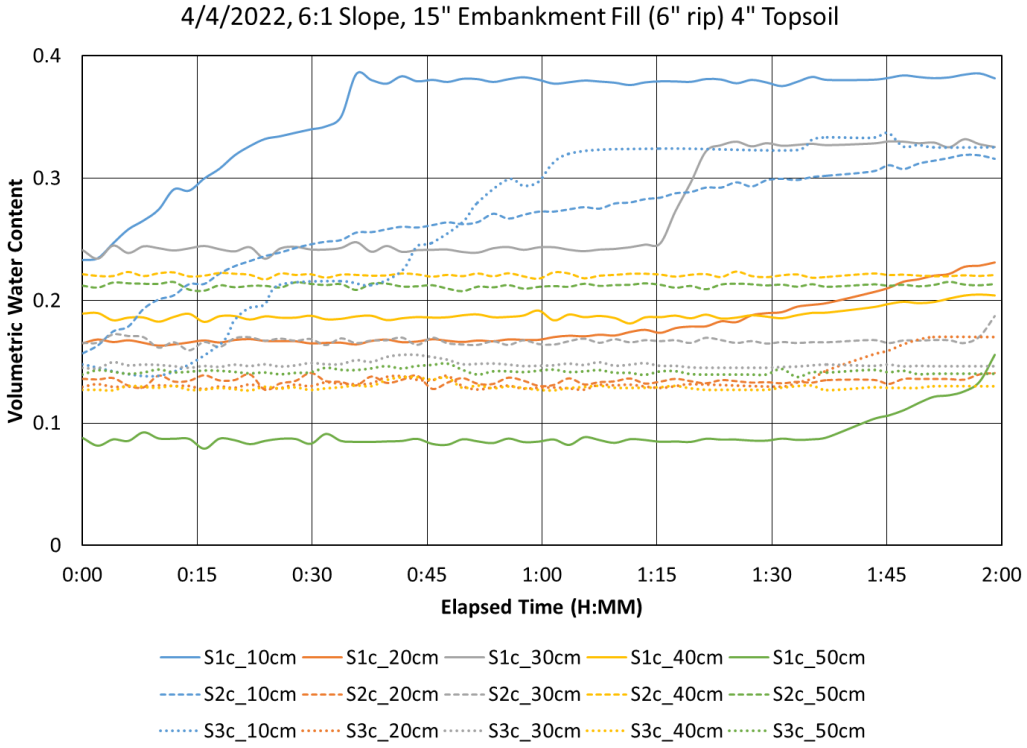

Fig. B50. 15” Embankment Fill (6” Ripped) 4” Topsoil 2-hr corrected data at a 6:1 slope.

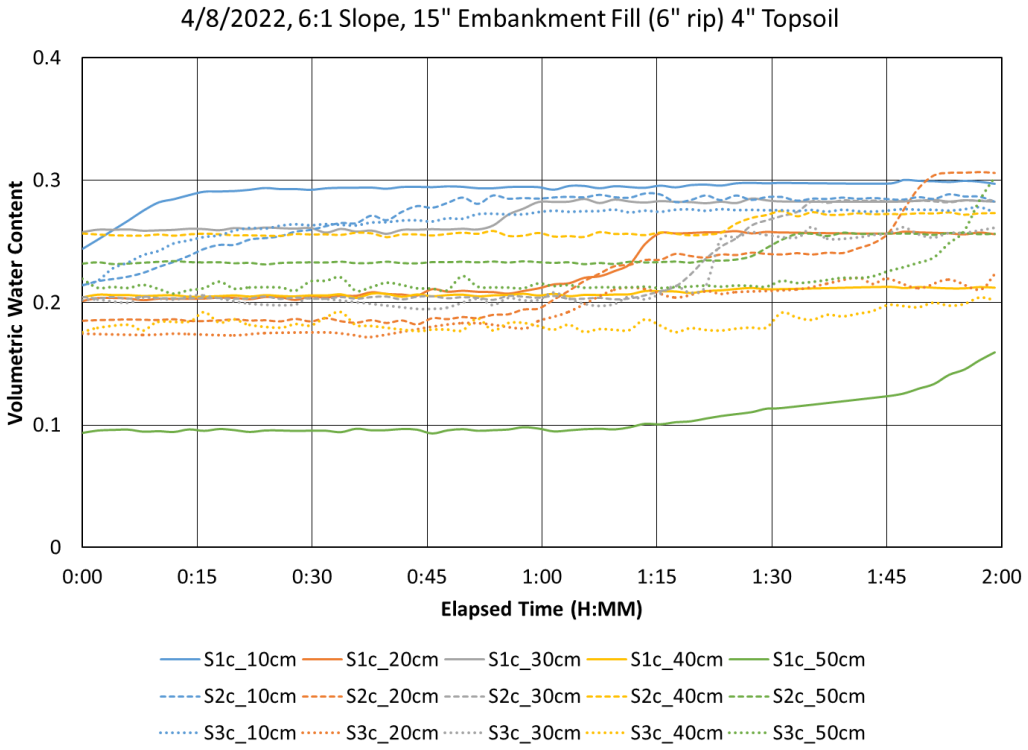

Fig. B51. 15” Embankment Fill (6” Ripped) 4” Topsoil 2-hr corrected data at a 6:1 slope.

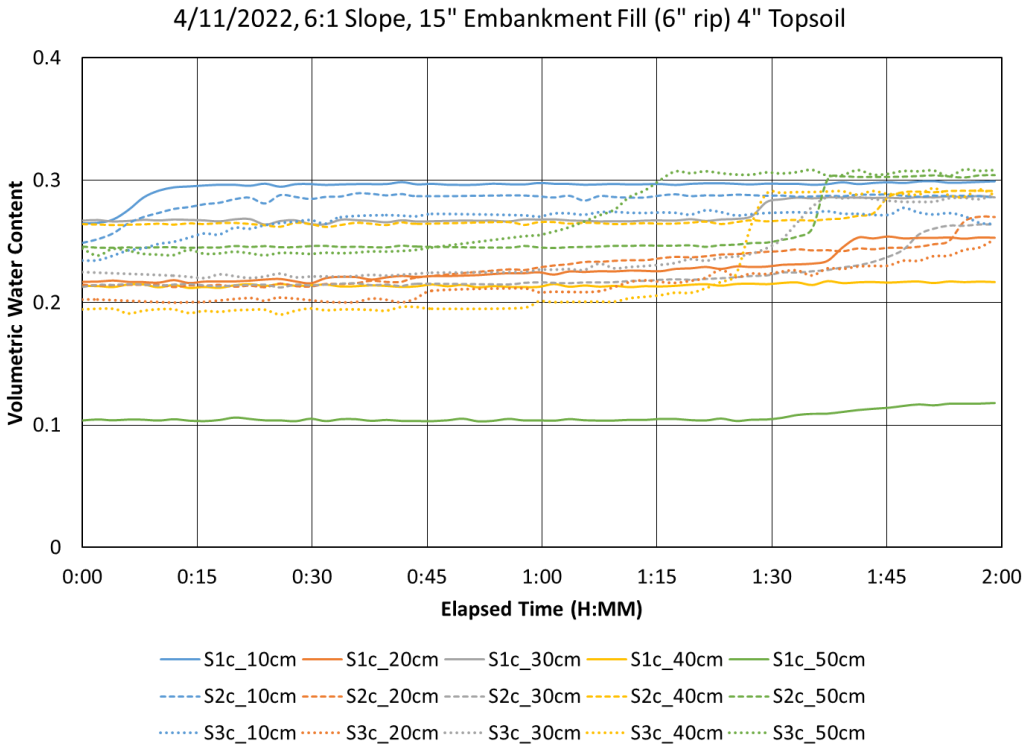

Fig. B52. 15” Embankment Fill (6” Ripped) 4” Topsoil 2-hr corrected data at a 6:1 slope.

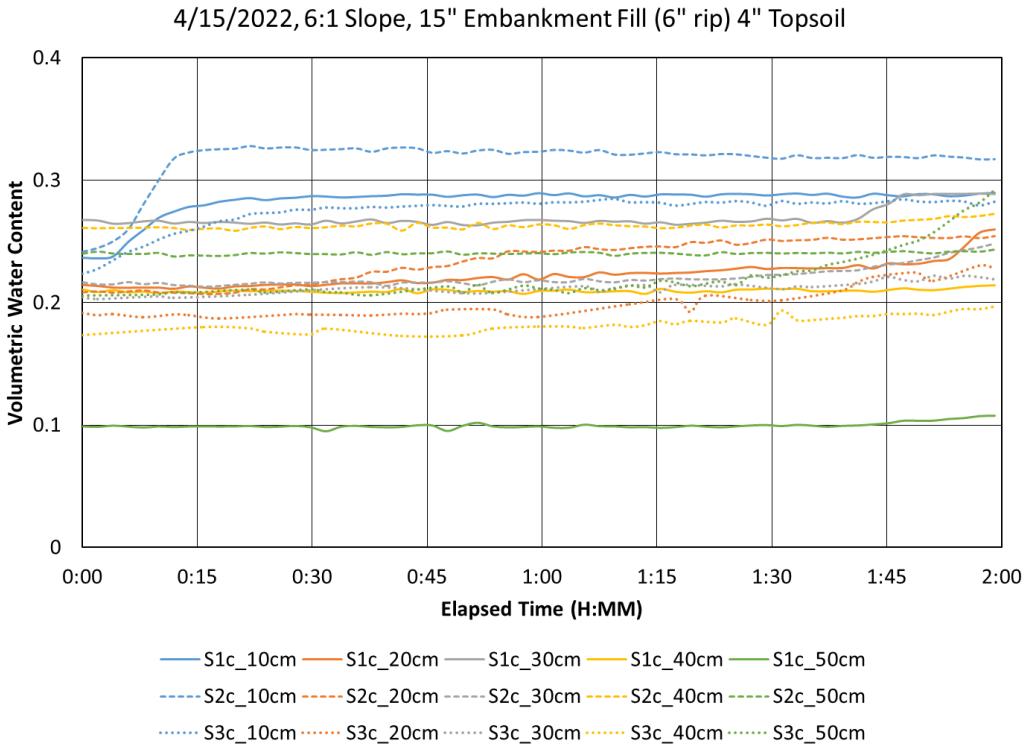

Fig. B53. 15” Embankment Fill (6” Ripped) 4” Topsoil 2-hr corrected data at a 6:1 slope.

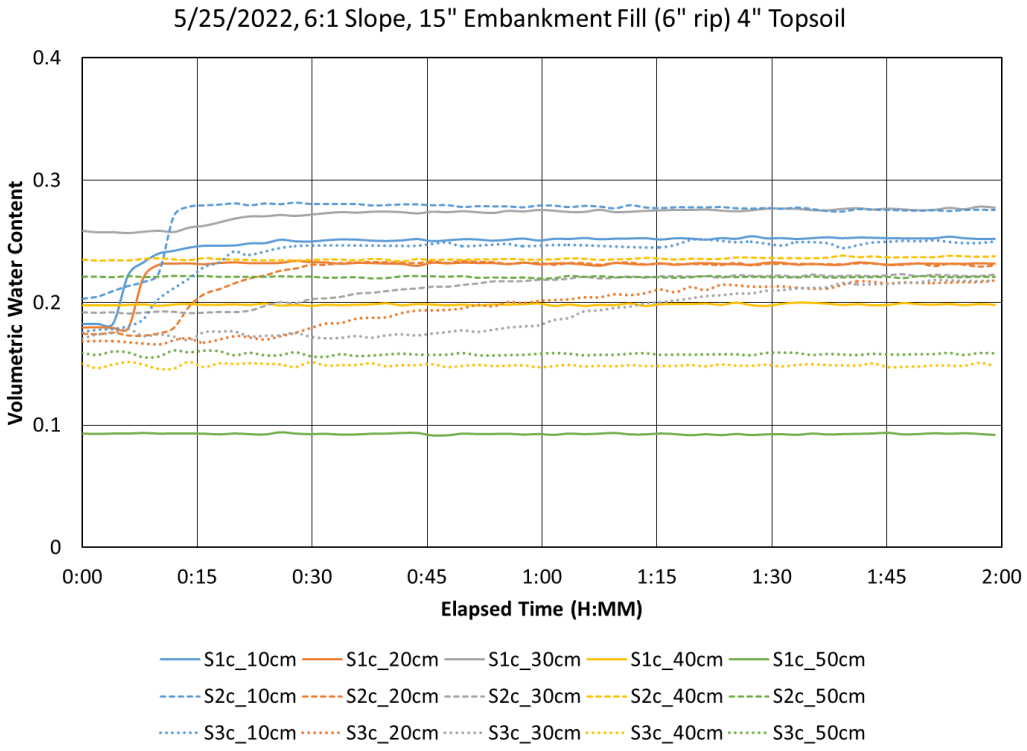

Fig. B54. 15” Embankment Fill (6” Ripped) 4” Topsoil 2-hr corrected data at a 6:1 slope.

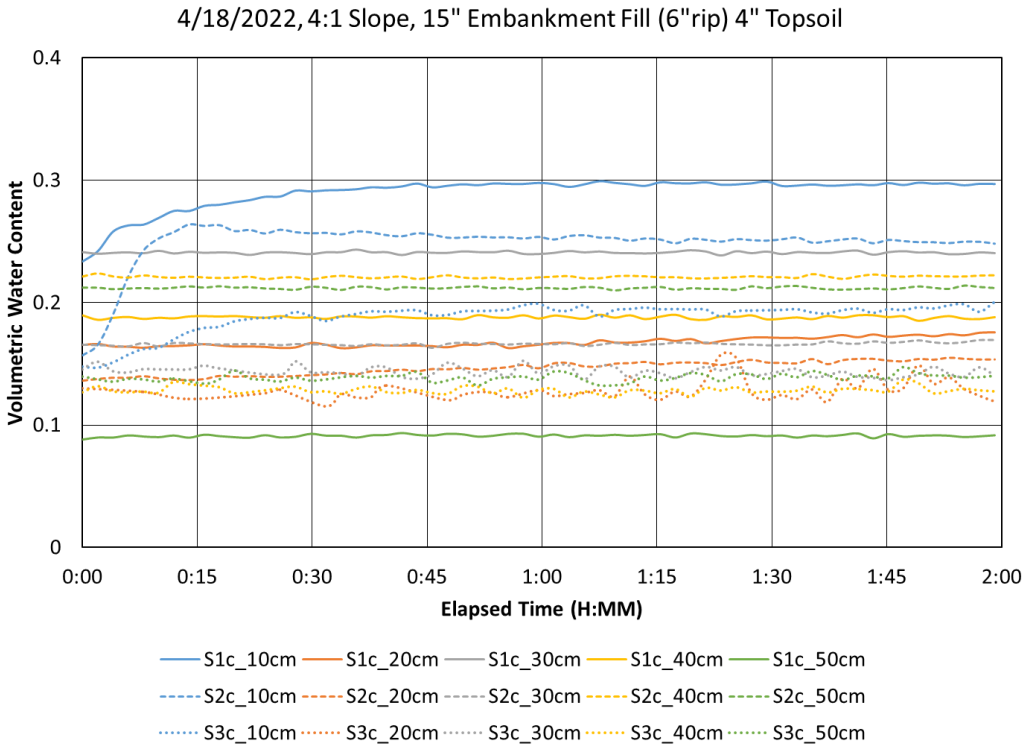

Fig. B55. 15” Embankment Fill (6” Ripped) 4” Topsoil 2-hr corrected data at a 4:1 slope.

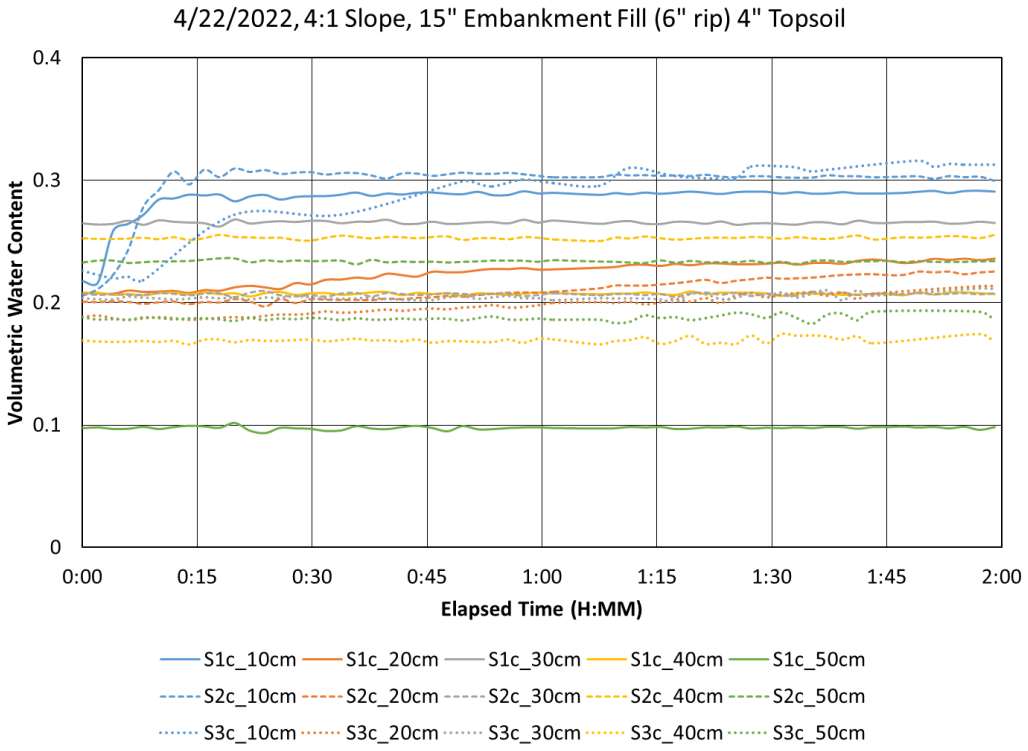

Fig. B56. 15” Embankment Fill (6” Ripped) 4” Topsoil 2-hr corrected data at a 4:1 slope.

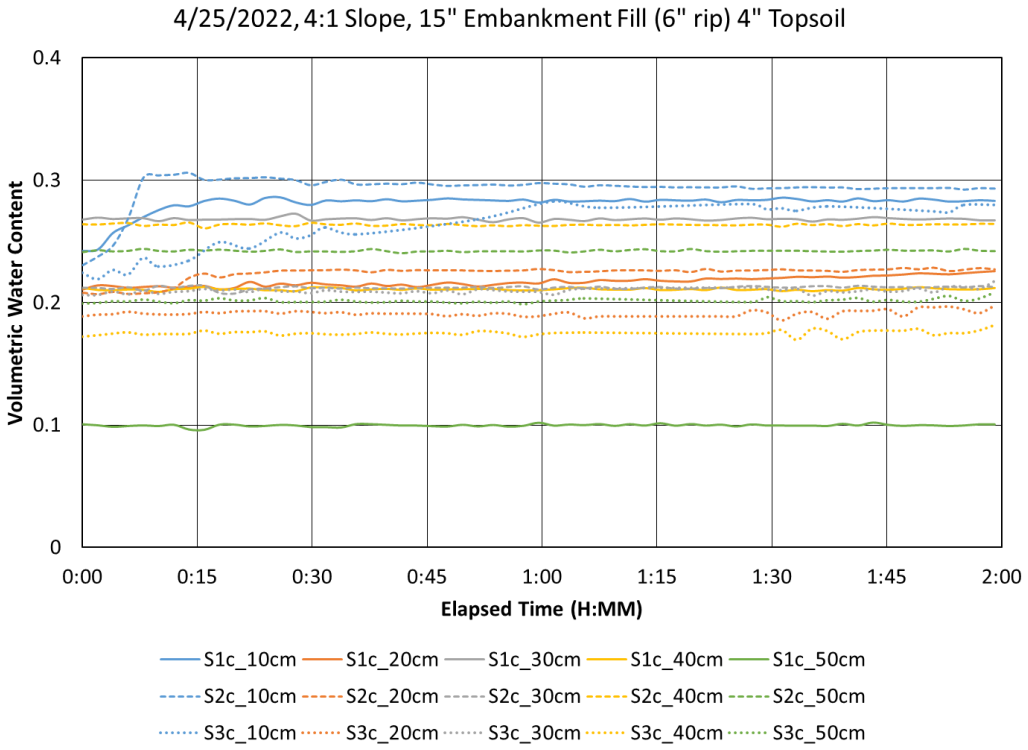

Fig. B57. 15” Embankment Fill (6” Ripped) 4” Topsoil 2-hr corrected data at a 4:1 slope.

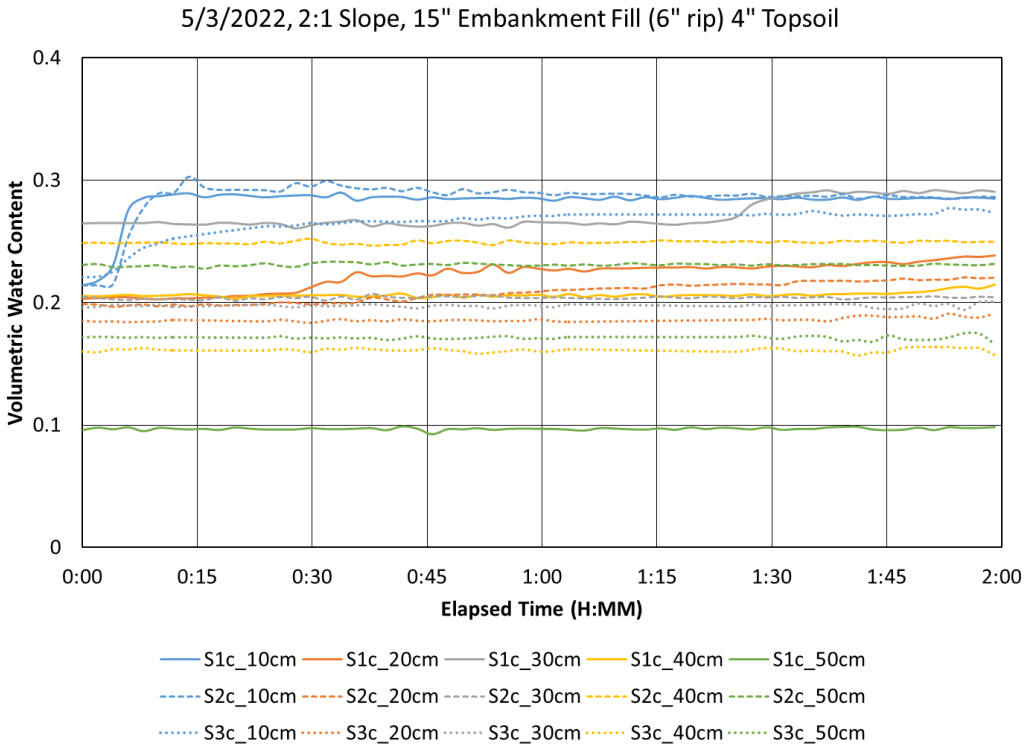

Fig. B58. 15” Embankment Fill (6” Ripped) 4” Topsoil 2-hr corrected data at a 2:1 slope.

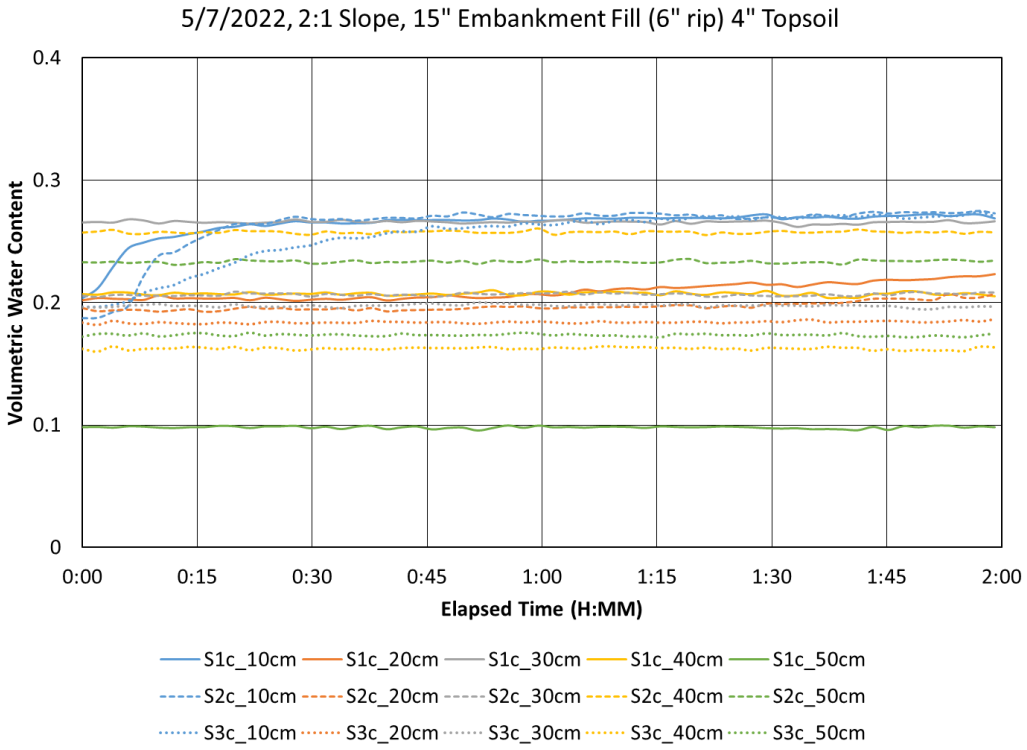

Fig. B59. 15” Embankment Fill (6” Ripped) 4” Topsoil 2-hr corrected data at a 2:1 slope.

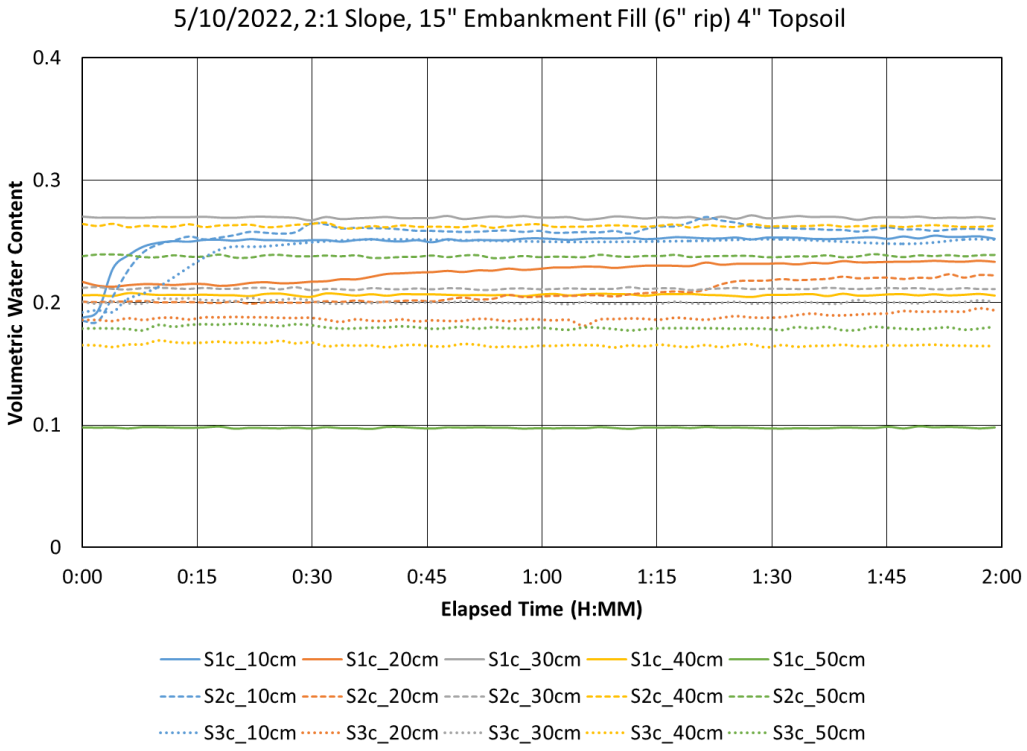

Fig. B60. 15” Embankment Fill (6” Ripped) 4” Topsoil 2-hr corrected data at a 2:1 slope.

Appendix C: Infiltration Data Curves

Configuration 1: 19” Embankment Fill

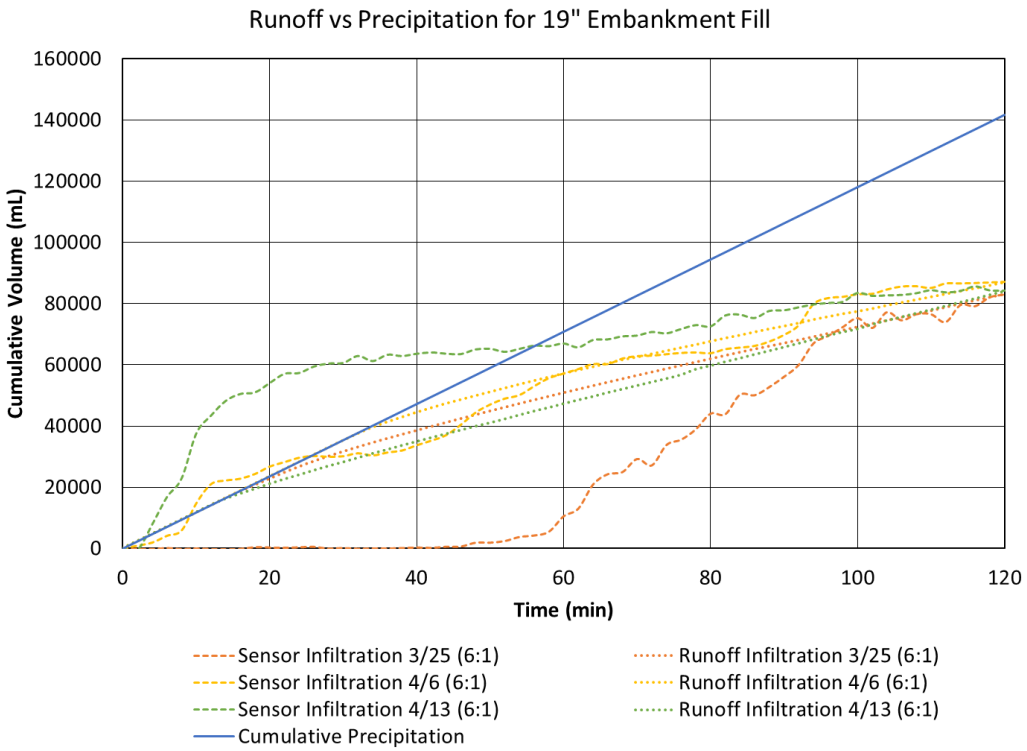

Fig. C1. 19” Embankment Fill 2-hr infiltration data for multiple tests at a 6:1 slope.

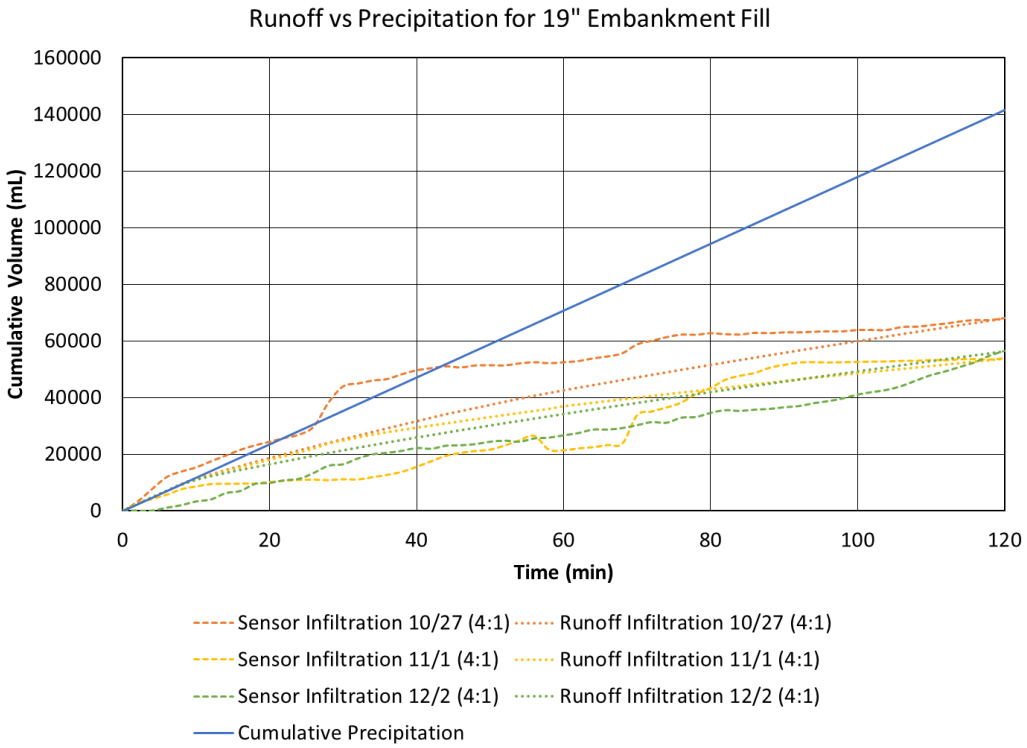

Fig. C2. 19" Embankment Fill 2-hr infiltration data for multiple tests at a 4:1 slope.

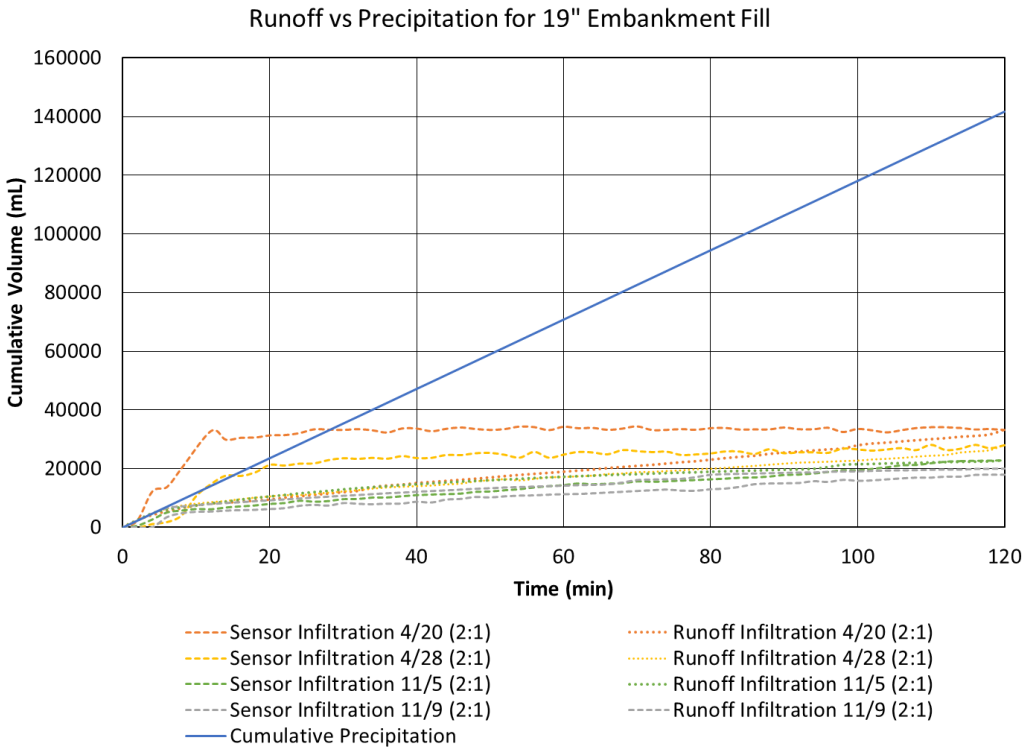

Fig. C3. 19" Embankment Fill 2-hr infiltration data for multiple tests at a 2:1 slope.

Configuration 2: 15” Embankment Fill 4” Topsoil

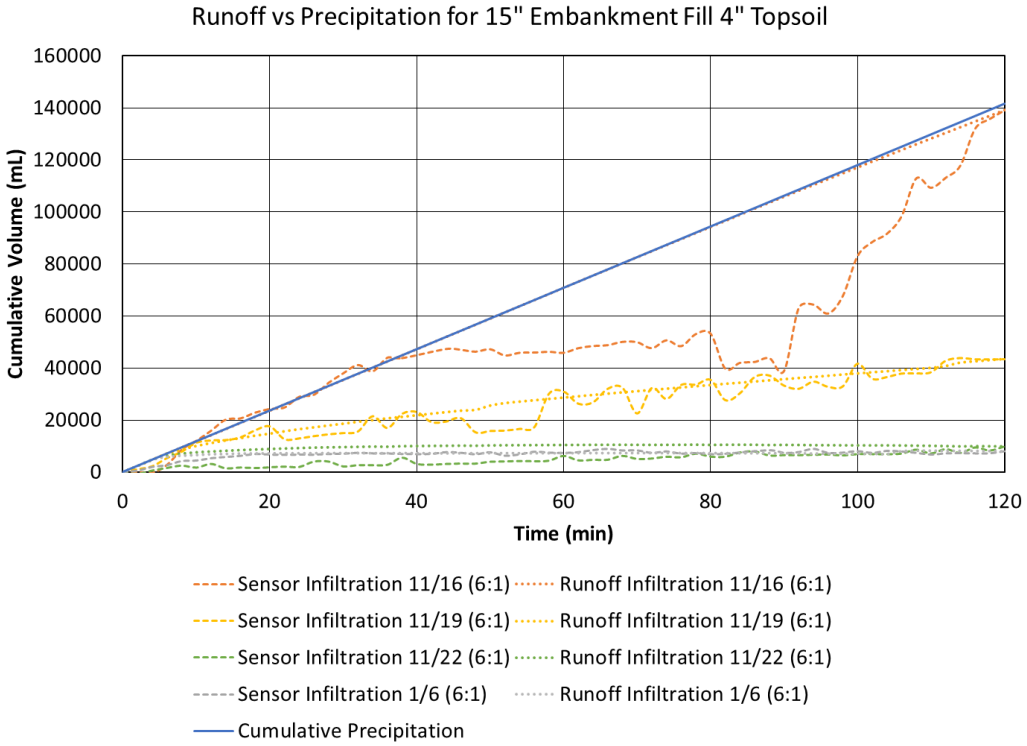

Fig. C4. 15” Embankment Fill 4” Topsoil 2-hr infiltration data for multiple tests at a 6:1 slope.

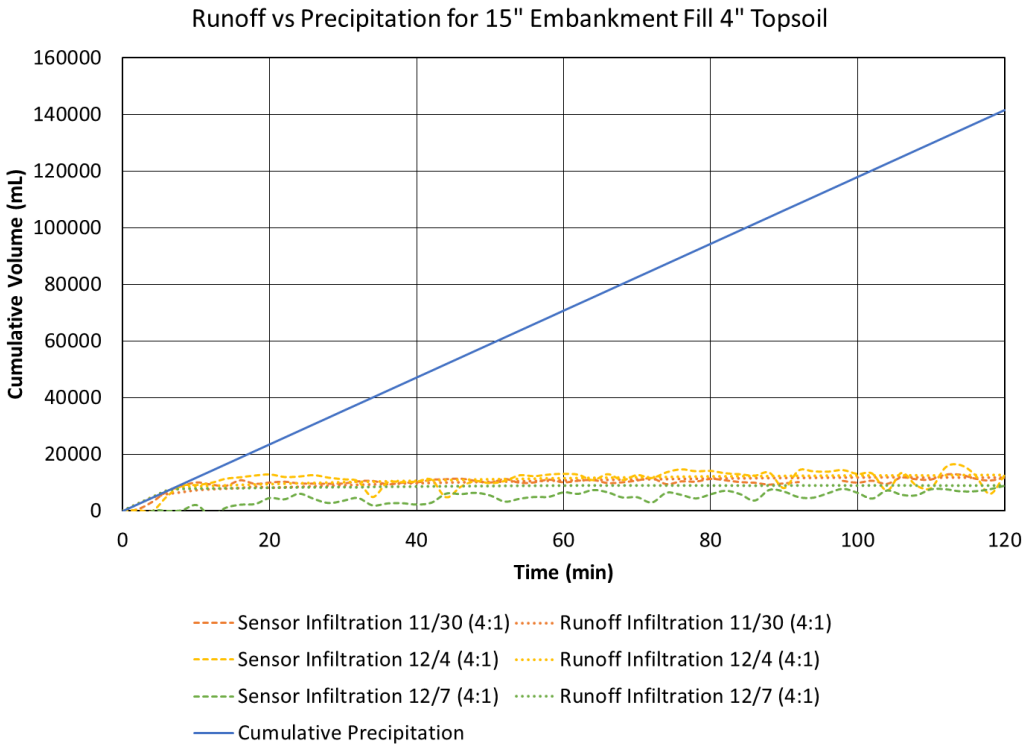

Fig. C5. 15” Embankment Fill 4” Topsoil 2-hr infiltration data for multiple tests at a 4:1 slope.

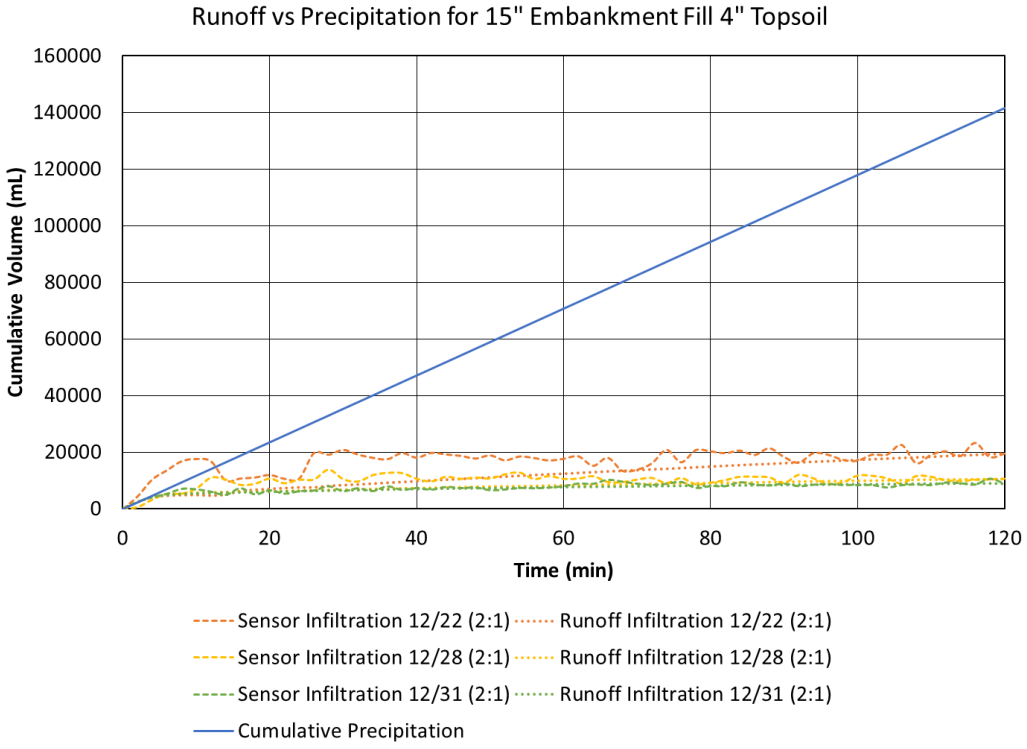

Fig. C6. 15” Embankment Fill 4” Topsoil 2-hr infiltration data for multiple tests at a 2:1 slope.

Configuration 3: 15” Embankment Fill 4” Topsoil with Vegetation

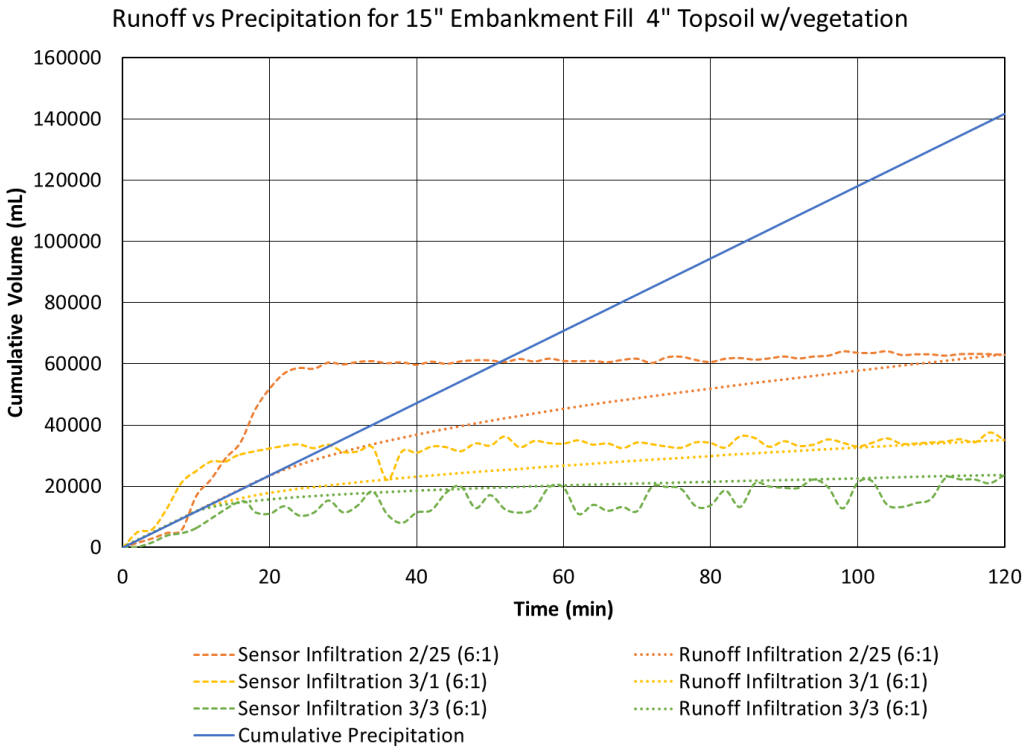

Fig. C7. 15” Embankment Fill 4” Topsoil w/vegetation 2-hr infiltration data for multiple tests at a 6:1 slope.

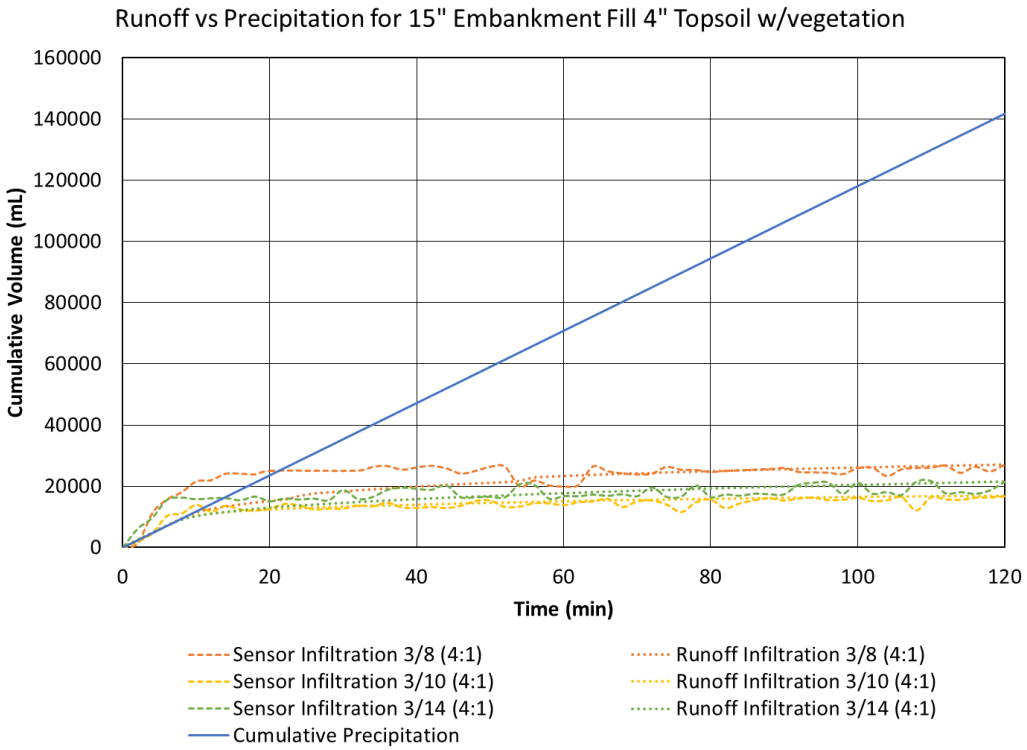

Fig. C8. 15" Embankment Fill 4" Topsoil w/vegetation 2-hr infiltration data for multiple tests at a 4:1 slope.

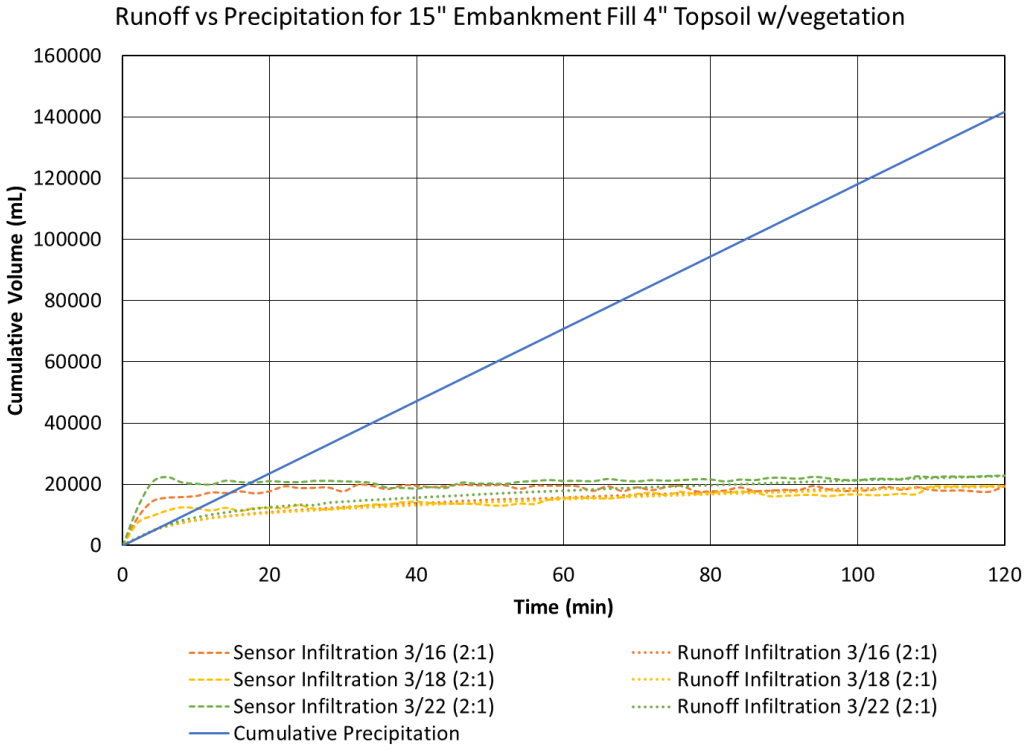

Fig. C9. 15" Embankment Fill 4" Topsoil w/vegetation 2-hr infiltration data for multiple tests at a 2:1 slope.

Configuration 4: 15” Embankment Fill 4” Amended Topsoil

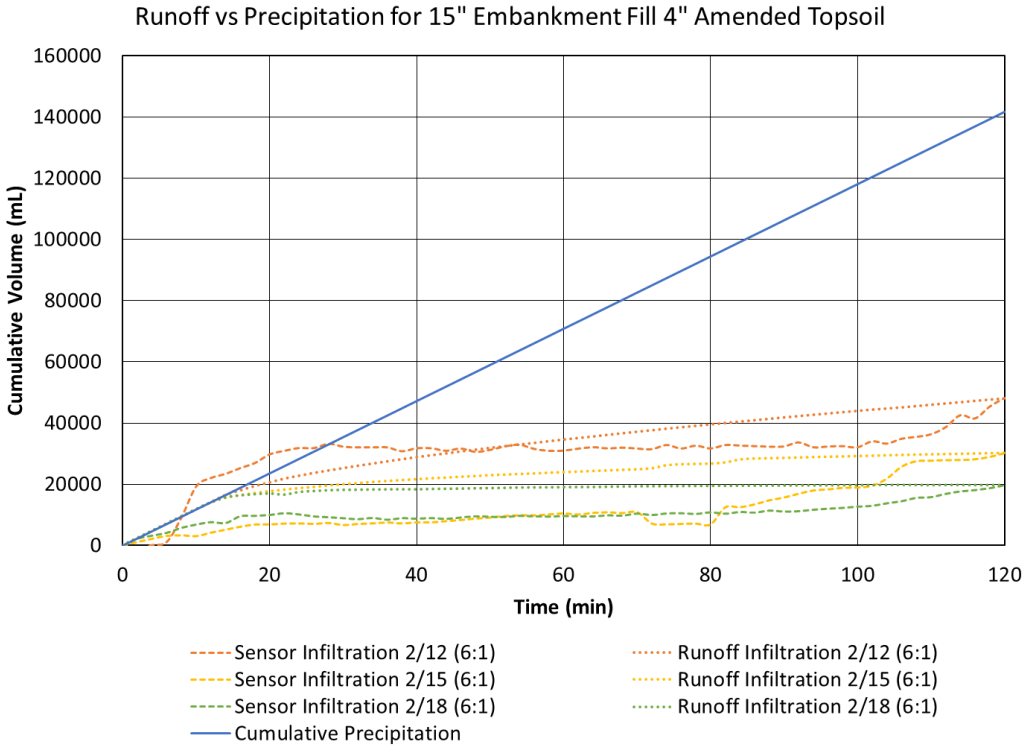

Fig. C10. 15” Embankment Fill 4” Amended Topsoil 2-hr infiltration data for multiple tests at a 6:1 slope.

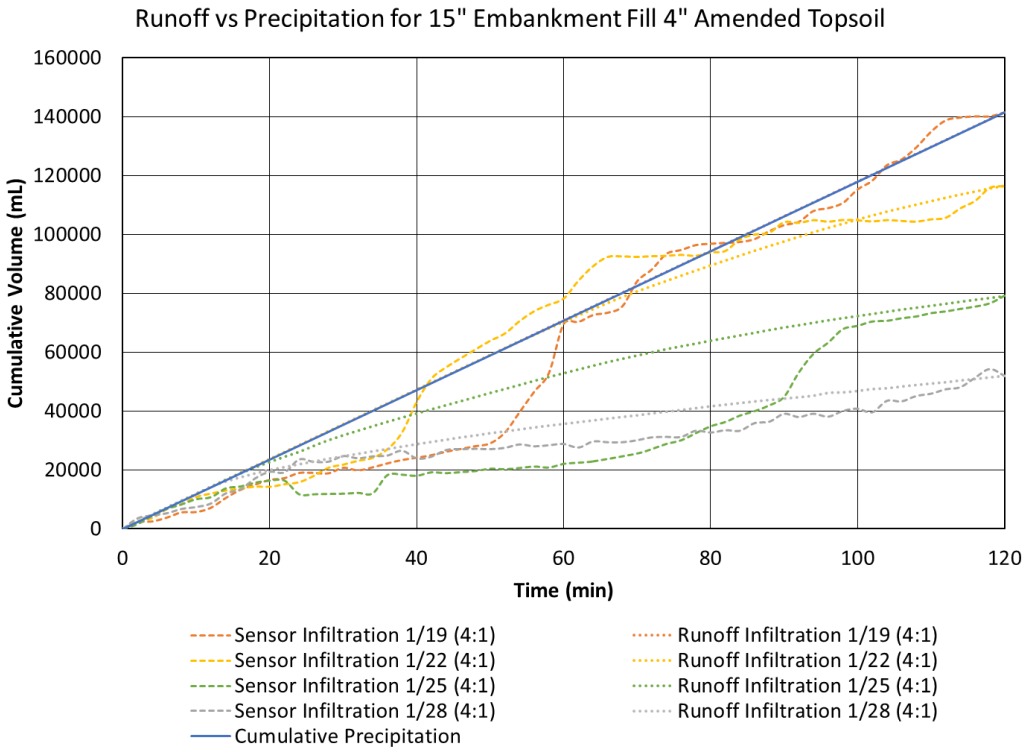

Fig. C11. 15" Embankment Fill 4" Amended Topsoil 2-hr infiltration data for multiple tests at a 4:1 slope.

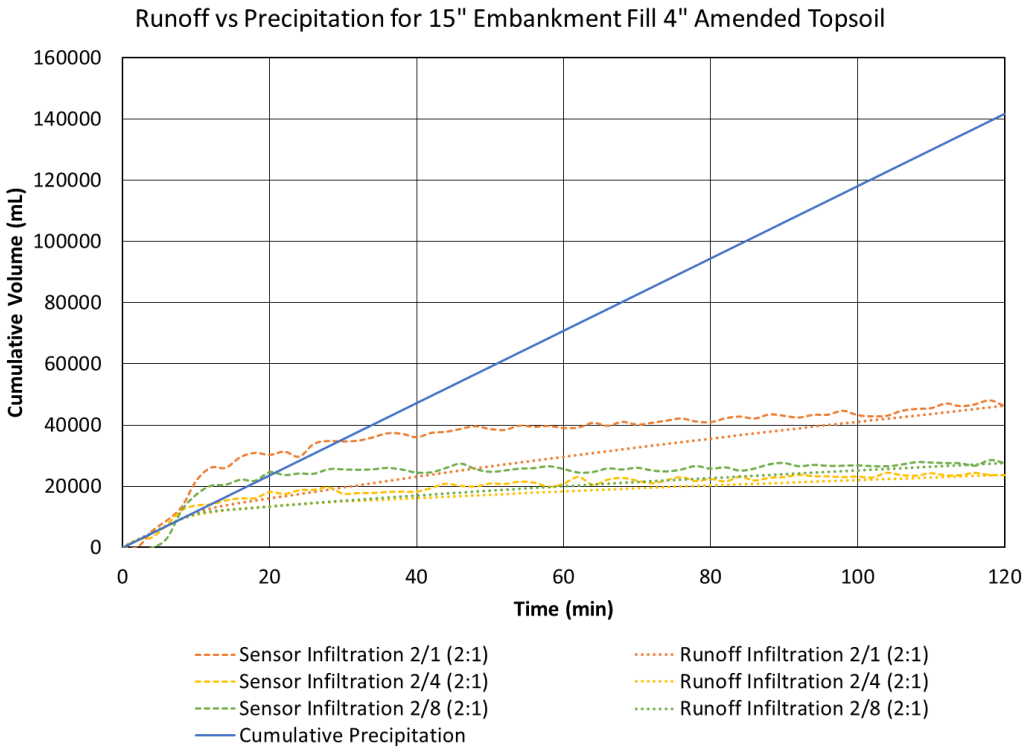

Fig. C12. 15" Embankment Fill 4" Amended Topsoil 2-hr infiltration data for multiple tests at a 2:1 slope.

Configuration 5: 15” Embankment Fill 4” Amended Topsoil with Vegetation

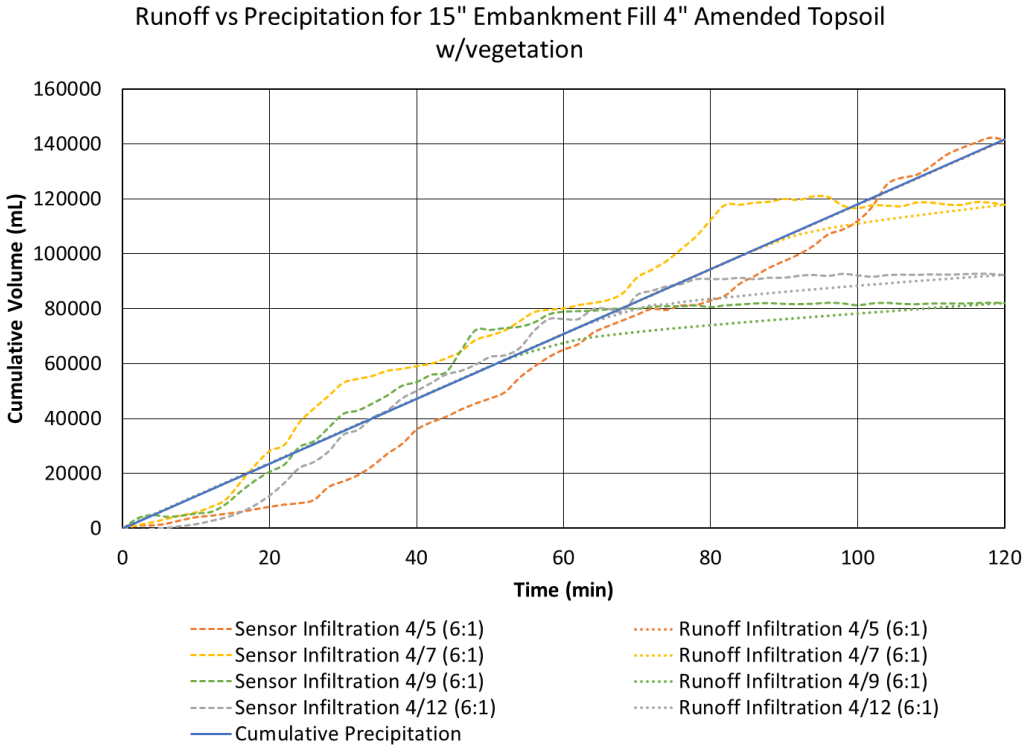

Fig. C13. 15” Embankment Fill 4” Amended Topsoil w/vegetation 2-hr infiltration data for multiple tests at a 6:1 slope.

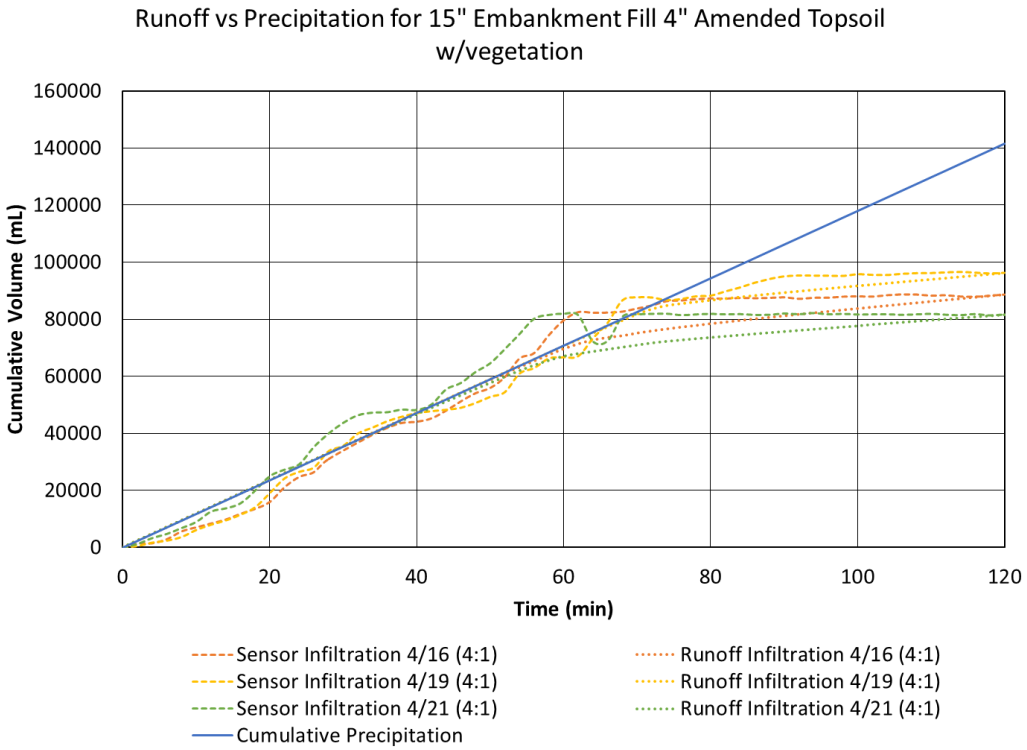

Fig. C14. 15" Embankment Fill 4" Amended Topsoil w/vegetation 2-hr infiltration data for multiple tests at a 4:1 slope.

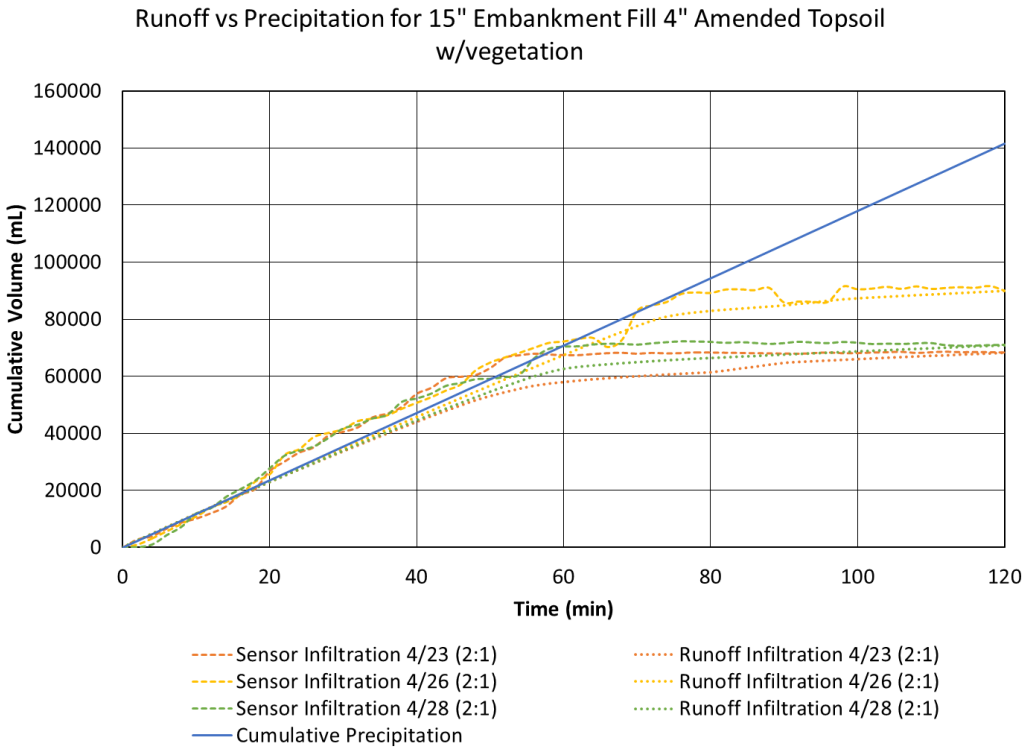

Fig. C15. 15" Embankment Fill 4" Amended Topsoil w/vegetation 2-hr infiltration data for multiple tests at a 2:1 slope.

Configuration 6: 15” Embankment Fill (6” Ripped) 4” Topsoil

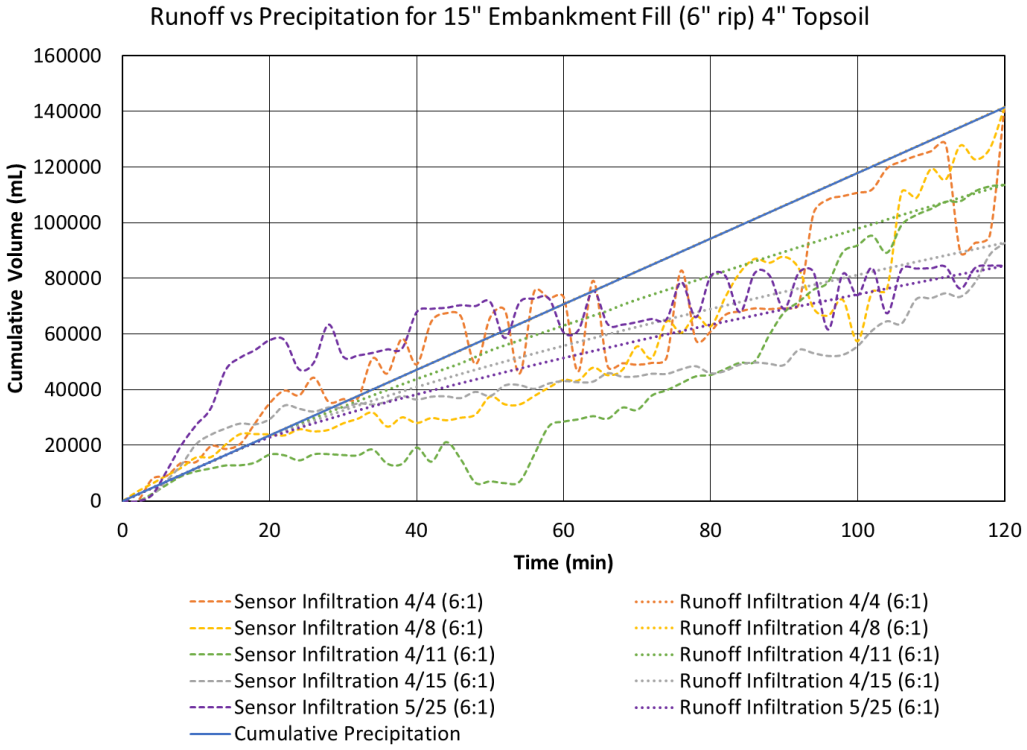

Fig. C16. 15” Embankment Fill (6” Ripped) 4” Topsoil 2-hr infiltration data for multiple tests at a 6:1 slope.

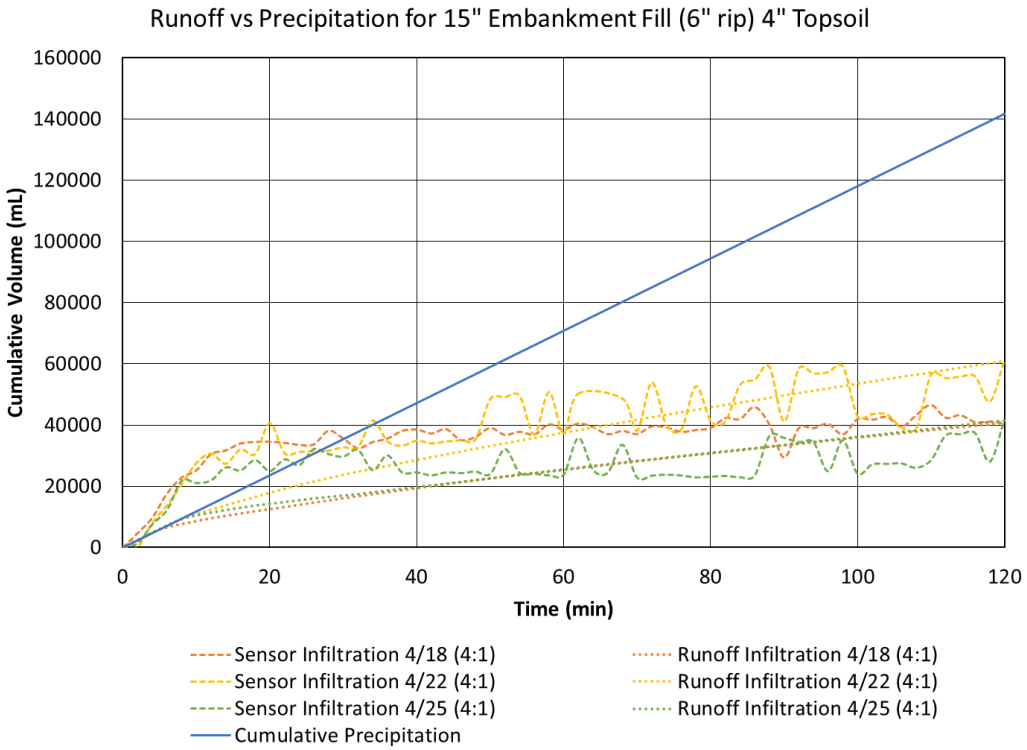

Fig. C17. 15” Embankment Fill (6” Ripped) 4” Topsoil 2-hr infiltration data for multiple tests at a 4:1 slope.

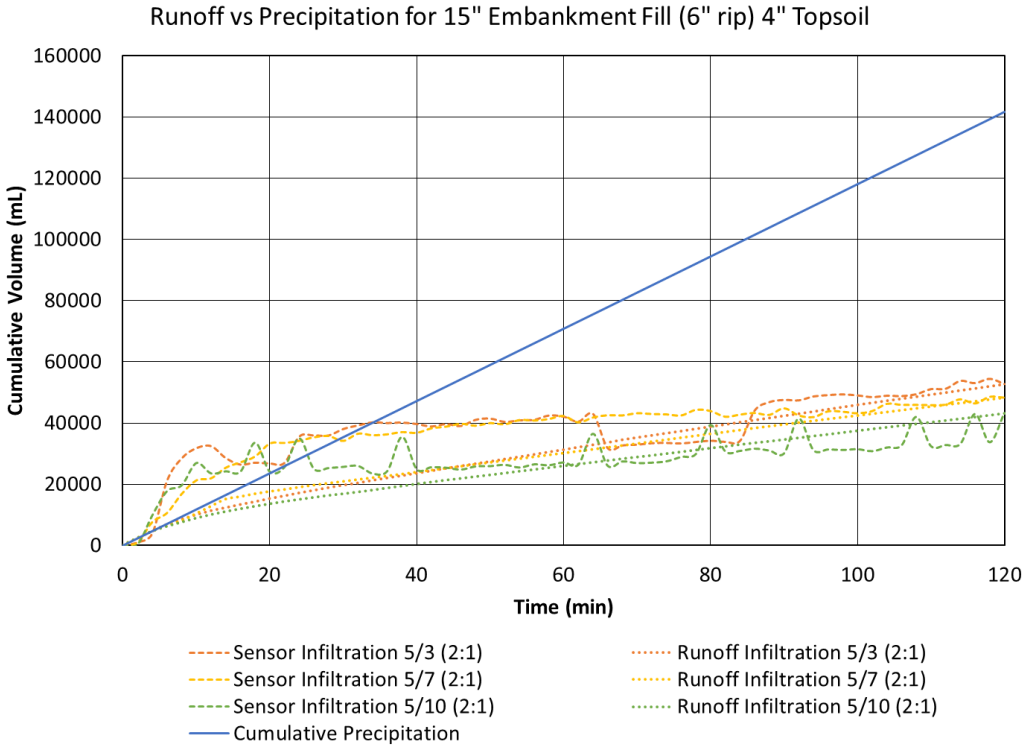

Fig. C18. 15” Embankment Fill (6” Ripped) 4” Topsoil 2-hr infiltration data for multiple tests at a 2:1 slope.

Appendix D: Correction Factor Table

Table D1. Calculated correction factors for each test.

	19" Embankment Fill			15" Embankment Fill 4" Topsoil			15" Embankment Fill 4" Topsoil w/vegetation		
Slope	Correction Factor	Slope Average	Total Average	Correction Factor	Slope Average	Total Average	Correction Factor	Slope Average	Total Average
6:1	0.16	0.31	0.27	0.26	0.28	0.42	0.57	0.63	0.39
6:1	0.30			0.49			0.60		
6:1	0.47			0.21			0.71		
6:1				0.14					
6:1									
4:1	0.24	0.27		0.31	0.47		0.27	0.34	
4:1	0.17			0.52			0.37		
4:1	0.41			0.57			0.36		
4:1									
2:1	0.24	0.24		0.88	0.57		0.16	0.20	
2:1	0.39			0.44			0.23		
2:1	0.13			0.40			0.22		
2:1	0.19								

	15" Embankment Fill 4" Amended Topsoil			15" Embankment Fill 4" Amended Topsoil w/vegetation			15" Embankment Fill (6" Rips) 4" Topsoil		
Slope	Correction Factor	Slope Average	Total Average	Correction Factor	Slope Average	Total Average	Correction Factor	Slope Average	Total Average
6:1	0.50	0.30	0.48	0.26	0.20	0.17	1.03	0.60	0.62
6:1	0.18			0.21			0.51		
6:1	0.22			0.15			0.44		
6:1				0.17			0.56		
6:1							0.47		
4:1	0.37	0.44		0.17	0.17		0.83	0.69	
4:1	0.27			0.17			0.67		
4:1	0.29			0.16			0.56		
4:1	0.82								
2:1	0.89	0.71		0.13	0.14		0.63	0.58	
2:1	0.59			0.16			0.63		
2:1	0.64			0.14			0.48		
2:1									

Appendix E: Summary Tables

Configuration 1: 19” Embankment Fill

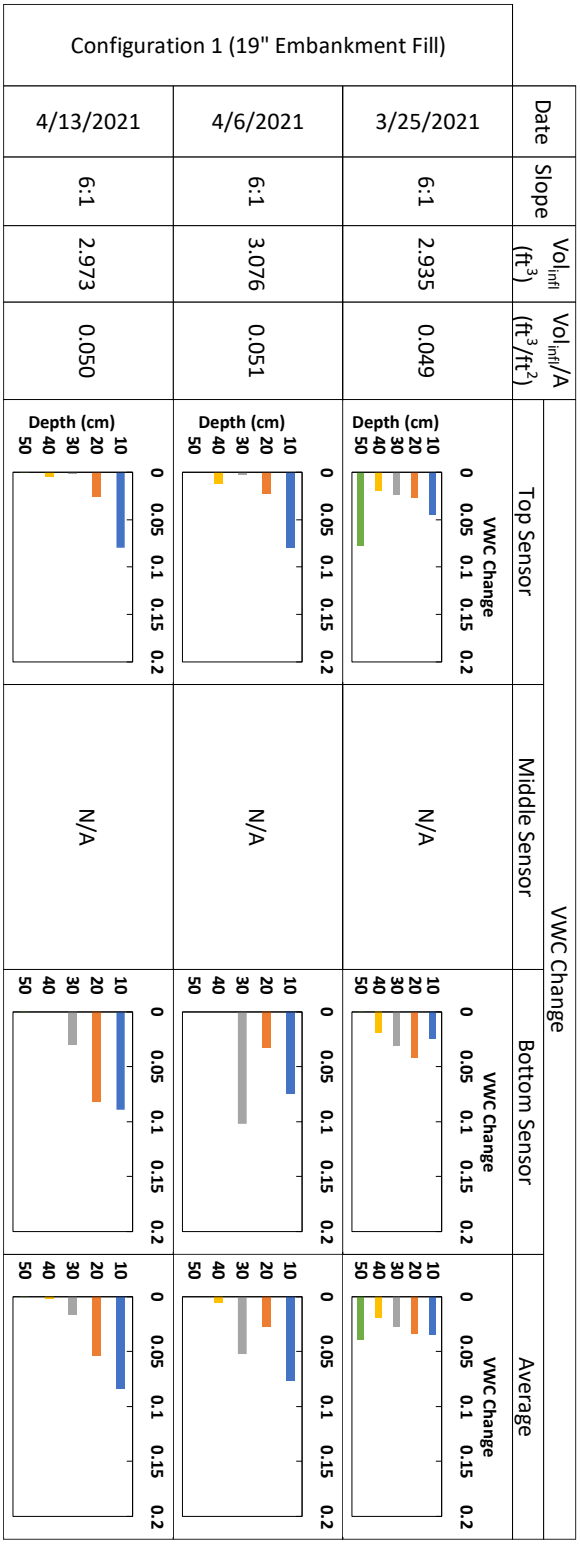

Fig. E1. 19” Embankment Fill VWC Change summary table for all tests at a 6:1 slope.

	Date	Slope	Vol_{infl} (ft^3)	Vol_{infl}/A (ft^3/ft^2)	VWC Change			
					Top Sensor	Middle Sensor	Bottom Sensor	Average
Configuration 1 (19" Embankment Fill)	10/27/2021	4:1	2.401	0.040	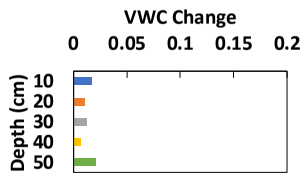	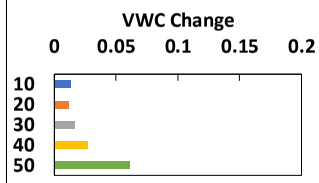	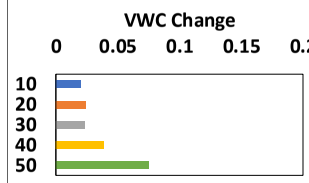	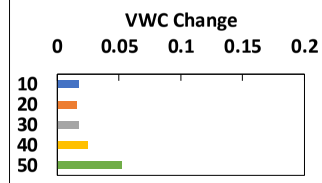
	11/1/2021	4:1	1.903	0.032	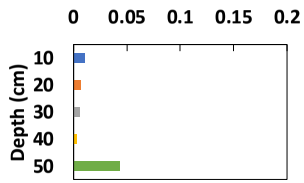	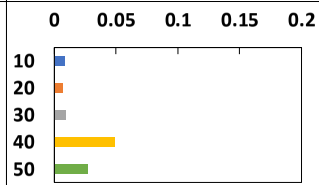	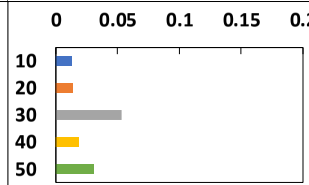	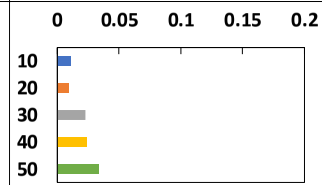
	12/2/2021	4:1	1.990	0.033	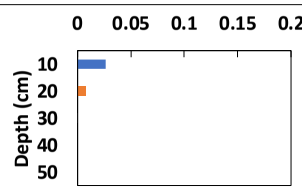	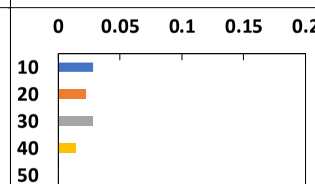	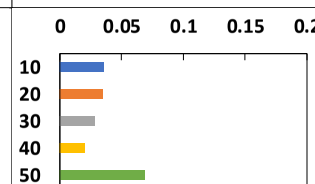	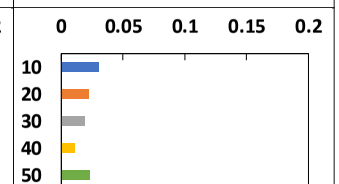

Fig. E2. 19” Embankment Fill VWC Change summary table for all tests at a 4:1 slope.

	Date	Slope	Vol_{infl} (ft^3)	Vol_{infl}/A (ft^3/ft^2)	VWC Change			
					Top Sensor	Middle Sensor	Bottom Sensor	Average
Configuration 1 (19" Embankment Fill)	4/20/2021	2:1	1.173	0.020	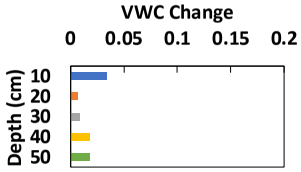	N/A	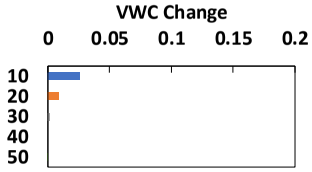	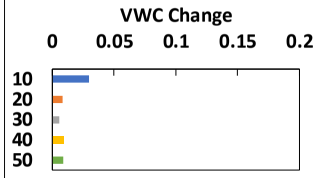
	4/28/2021	2:1	0.990	0.017	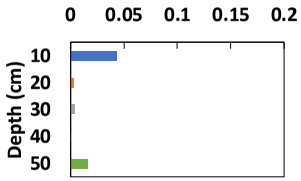	N/A	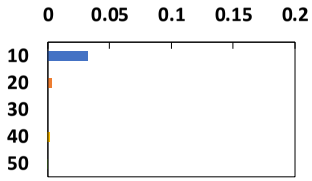	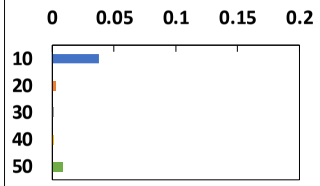
	11/5/2021	2:1	0.807	0.013	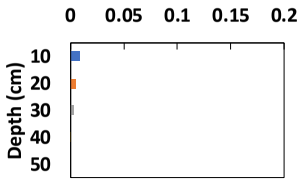	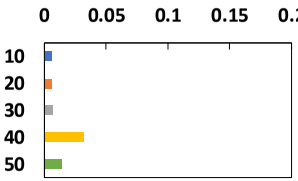	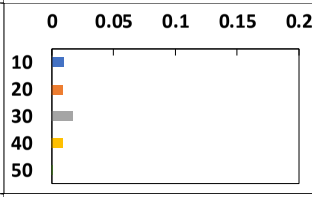	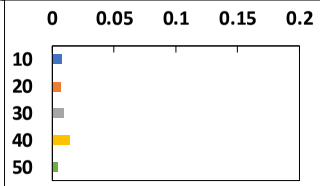
	11/9/2021	2:1	0.631	0.011	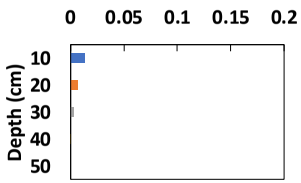	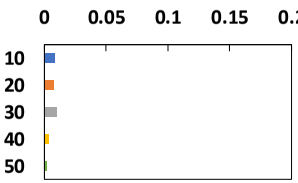	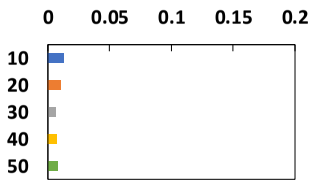	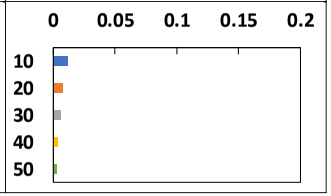

Fig. E3. 19" Embankment Fill VWC Change summary table for all tests at a 2:1 slope.

Configuration 2: 15” Embankment Fill 4” Topsoil

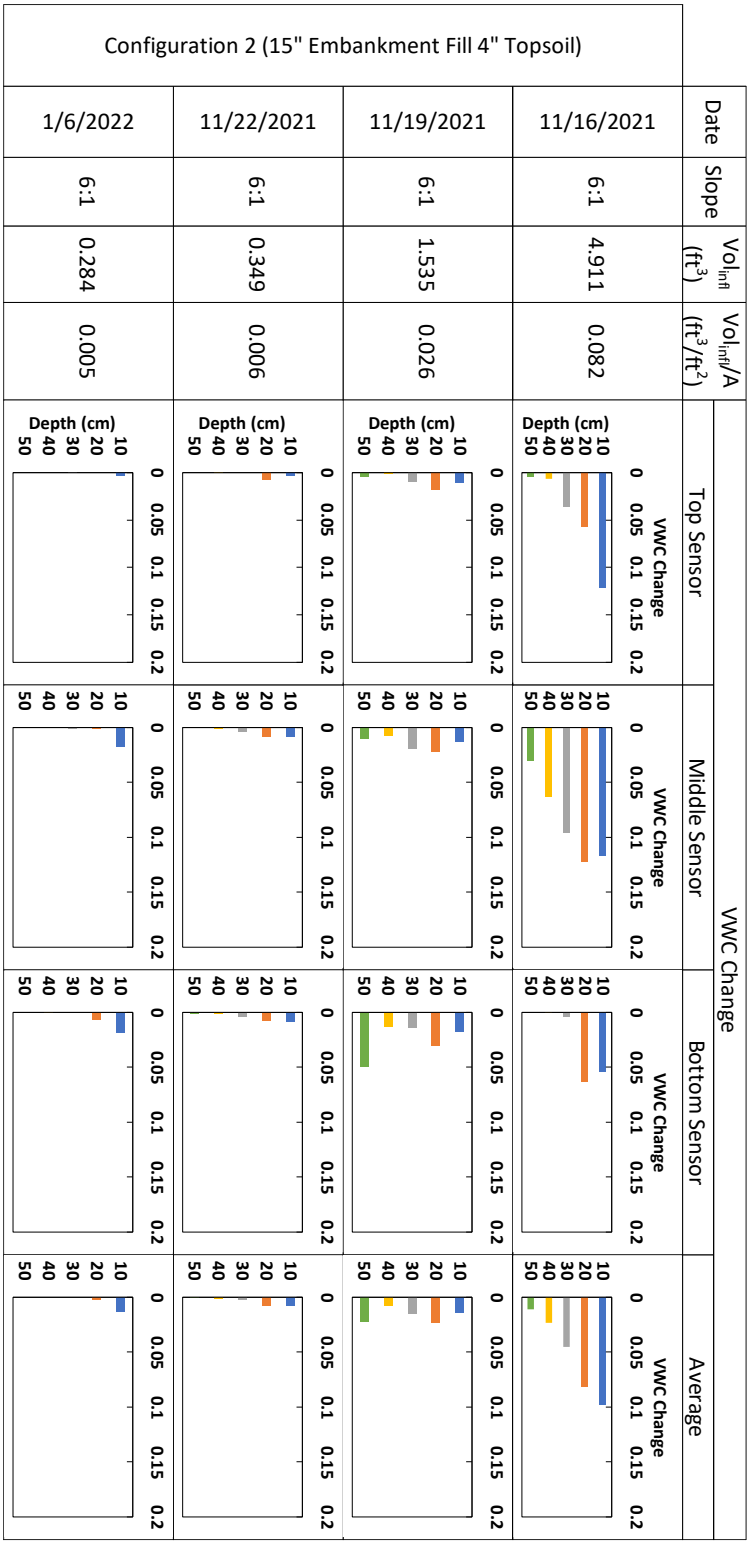

Fig. E4. 14” Embankment Fill 4” Topsoil VWC Change summary table for all tests at a 6:1 slope.

	Date	Slope	Vol_{infl} (ft^3)	Vol_{infl}/A (ft^3/ft^2)	VWC Change			
					Top Sensor	Middle Sensor	Bottom Sensor	Average
Configuration 2 (15" Embankment Fill 4" Topsoil)	11/30/2021	4:1	0.412	0.007	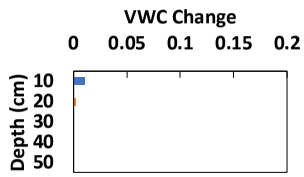	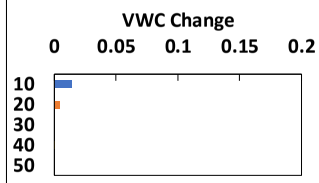	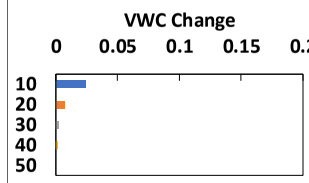	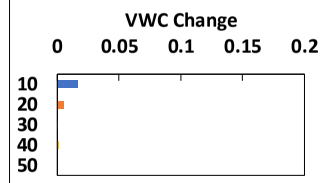
	12/4/2021	4:1	0.446	0.007	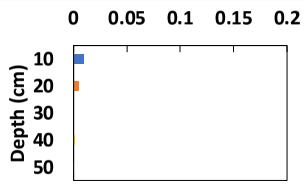	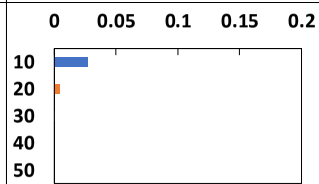	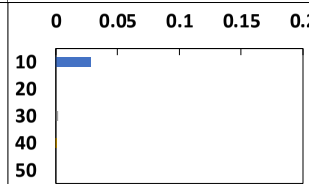	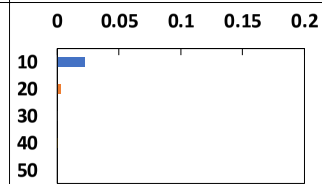
	12/7/2021	4:1	0.314	0.005	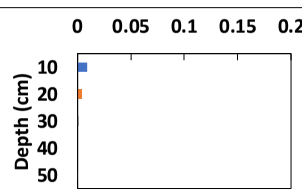	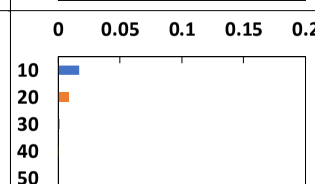	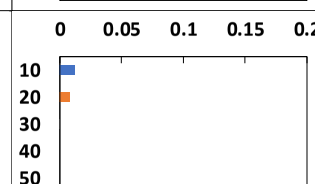	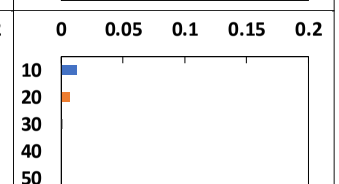

Fig. E5. 14" Embankment Fill 4" Topsoil VWC Change summary table for all tests at a 4:1 slope.

	Date	Slope	Vol_{infl} (ft^3)	Vol_{infl}/A (ft^3/ft^2)	VWC Change			
					Top Sensor	Middle Sensor	Bottom Sensor	Average
Configuration 2 (15" Embankment Fill 4" Topsoil)	12/22/2021	2:1	0.688	0.011	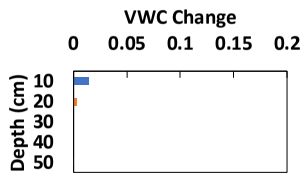	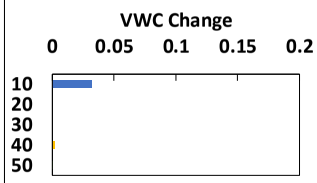	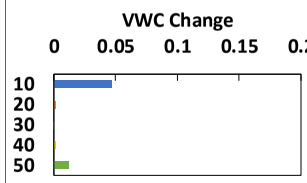	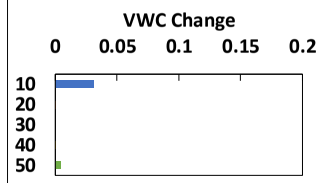
	12/28/2021	2:1	0.373	0.006	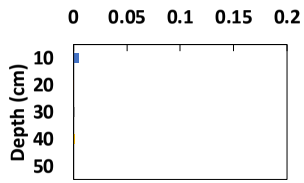	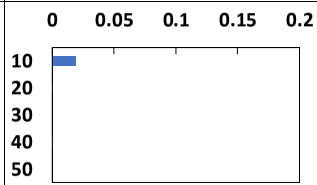	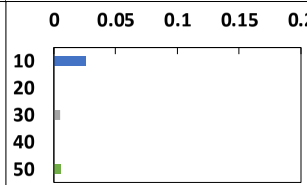	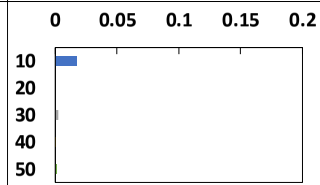
	12/31/2021	2:1	0.316	0.005	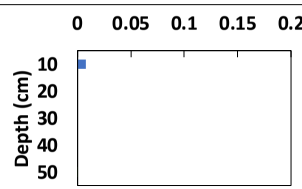	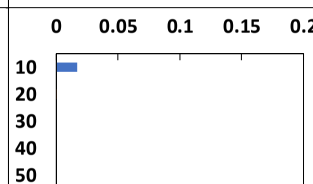	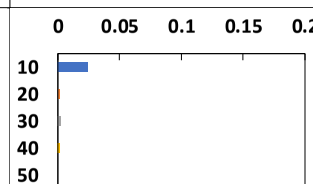	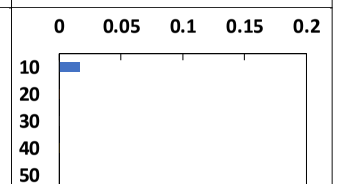

Fig. E6. 14” Embankment Fill 4” Topsoil VWC Change summary table for all tests at a 2:1 slope.

Configuration 3: 15” Embankment Fill 4” Topsoil with Vegetation

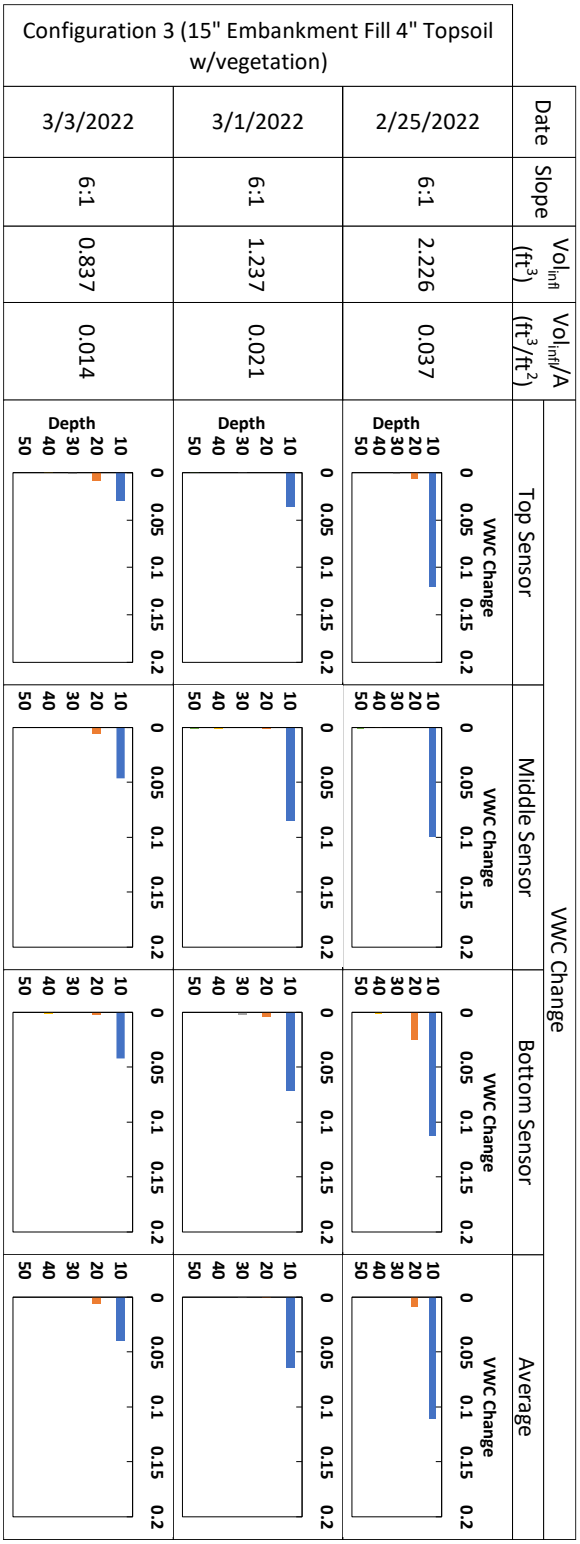

Fig. E7. 14” Embankment Fill 4” Topsoil w/vegetation VWC Change summary table for all tests at a 6:1 slope.

	Date	Slope	Vol_{infl} (ft^3)	Vol_{infl}/A (ft^3/ft^2)	VWC Change			
					Top Sensor	Middle Sensor	Bottom Sensor	Average
Configuration 3 (15" Embankment Fill 4" Topsoil w/vegetation)	3/8/2022	4:1	0.959	0.016	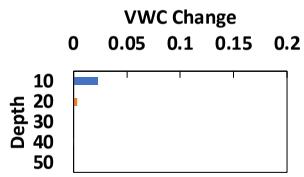	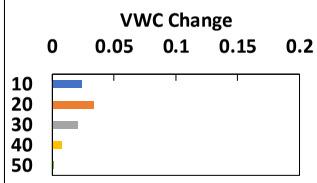	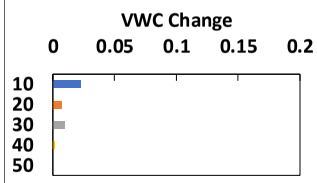	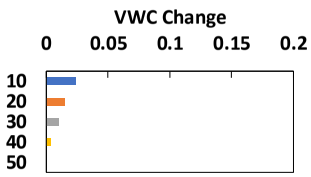
	3/10/2022	4:1	0.593	0.010	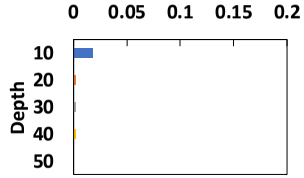	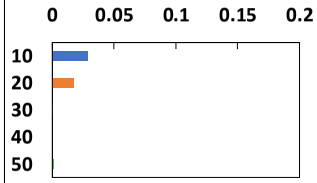	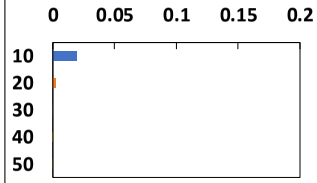	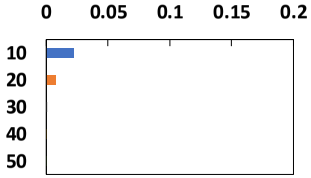
	3/14/2022	4:1	0.758	0.013	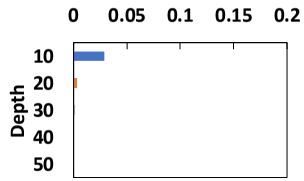	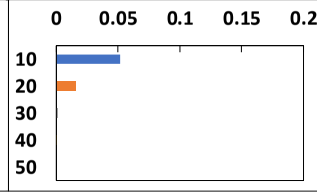	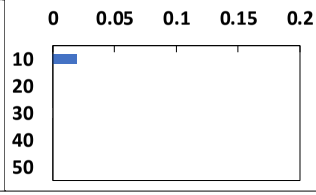	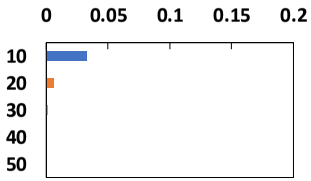

Fig. E8. 14” Embankment Fill 4” Topsoil w/vegetation VWC Change summary table for all tests at a 4:1 slope.

Configuration 3 (15" Embankment Fill 4" Topsoil w/vegetation)								
Date	Slope	Vol_{Infl} (ft^3)	Vol_{Infl}/A (ft^3/ft^2)	VWC Change				
				Top Sensor	Middle Sensor	Bottom Sensor	Average	
3/16/2022	2:1	0.685	0.011					
3/18/2022	2:1	0.687	0.011					
3/22/2022	2:1	0.805	0.013					

Fig. E9. 14” Embankment Fill 4” Topsoil w/vegetation VWC Change summary table for all tests at a 2:1 slope.

Configuration 4: 15” Embankment Fill 4” Amended Topsoil

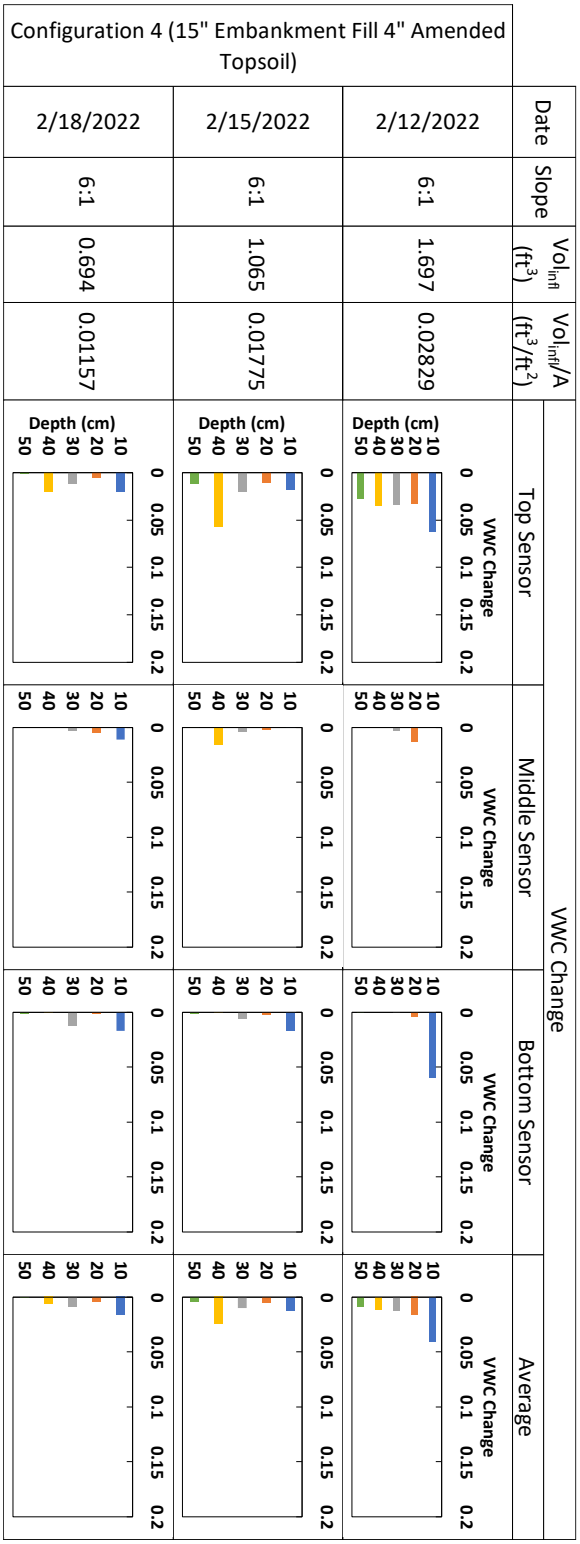

Fig. E10. 14” Embankment Fill 4” Amended Topsoil VWC Change summary table for all tests at a 6:1 slope.

	Date	Slope	Vol_{infl} (ft^3)	Vol_{infl}/A (ft^3/ft^2)	VWC Change			
					Top Sensor	Middle Sensor	Bottom Sensor	Average
Configuration 4 (15" Embankment Fill 4" Amended Topsoil)	1/19/2022	4:1	5.000	0.08333	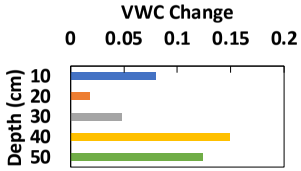	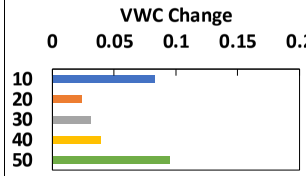	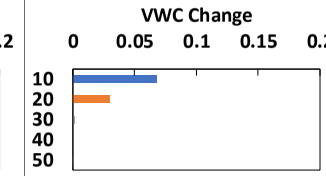	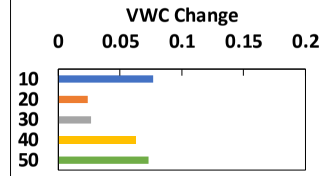
	1/22/2022	4:1	4.112	0.06854	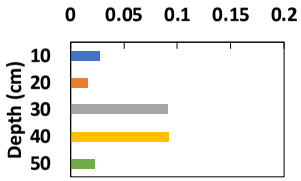	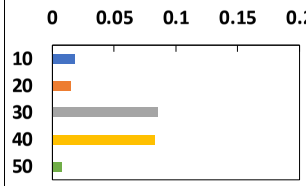	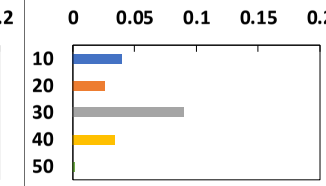	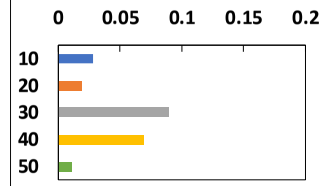
	1/25/2022	4:1	2.796	0.04659	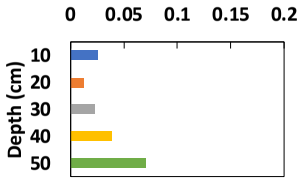	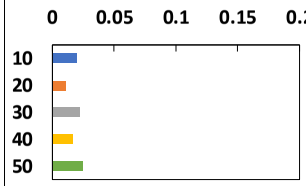	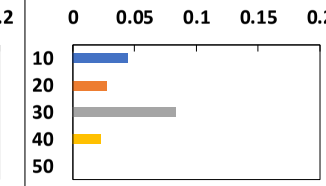	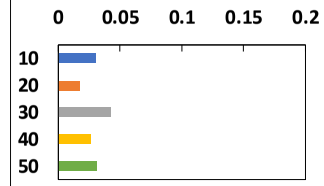
	1/28/2022	4:1	1.836	0.0306	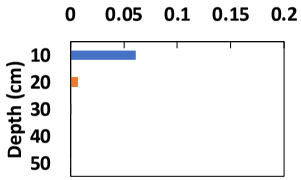	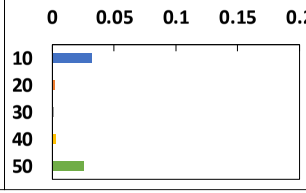	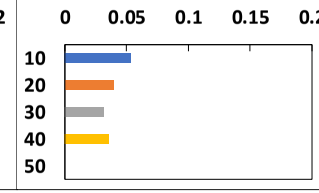	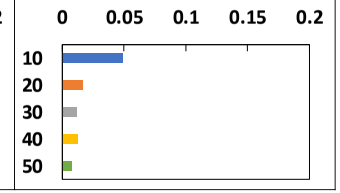

Fig. E11. 14” Embankment Fill 4” Amended Topsoil VWC Change summary table for all tests at a 4:1 slope.

	Date	Slope	Vol_{infl} (ft^3)	Vol_{infl}/A (ft^3/ft^2)	VWC Change			
					Top Sensor	Middle Sensor	Bottom Sensor	Average
Configuration 4 (15" Embankment Fill 4" Amended Topsoil)	2/1/2022	2:1	1.635	0.02725	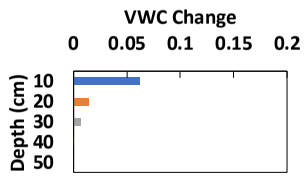	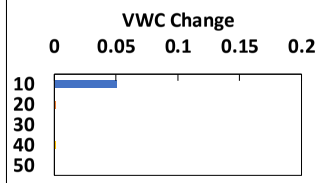	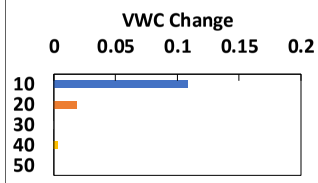	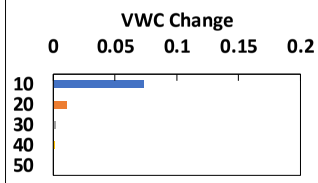
	2/4/2022	2:1	0.835	0.01392	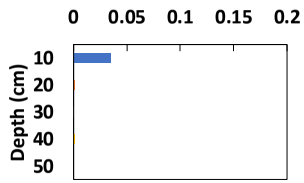	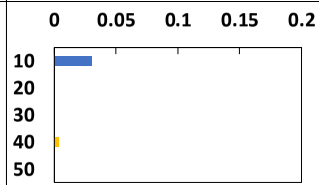	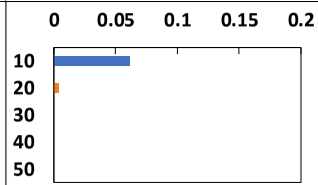	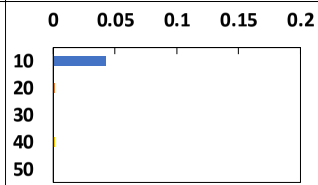
	2/8/2022	2:1	0.972	0.01621	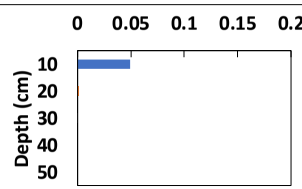	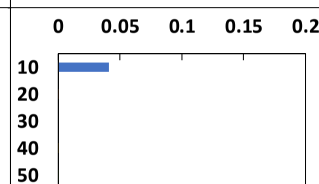	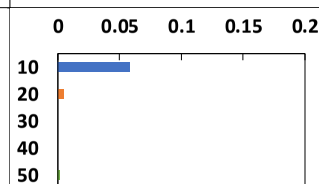	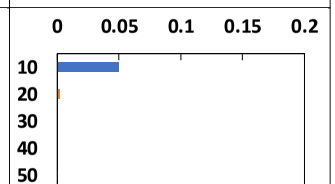

Fig. E12. 14” Embankment Fill 4” Amended Topsoil VWC Change summary table for all tests at a 2:1 slope.

Configuration 5: 15” Embankment Fill 4” Amended Topsoil with Vegetation

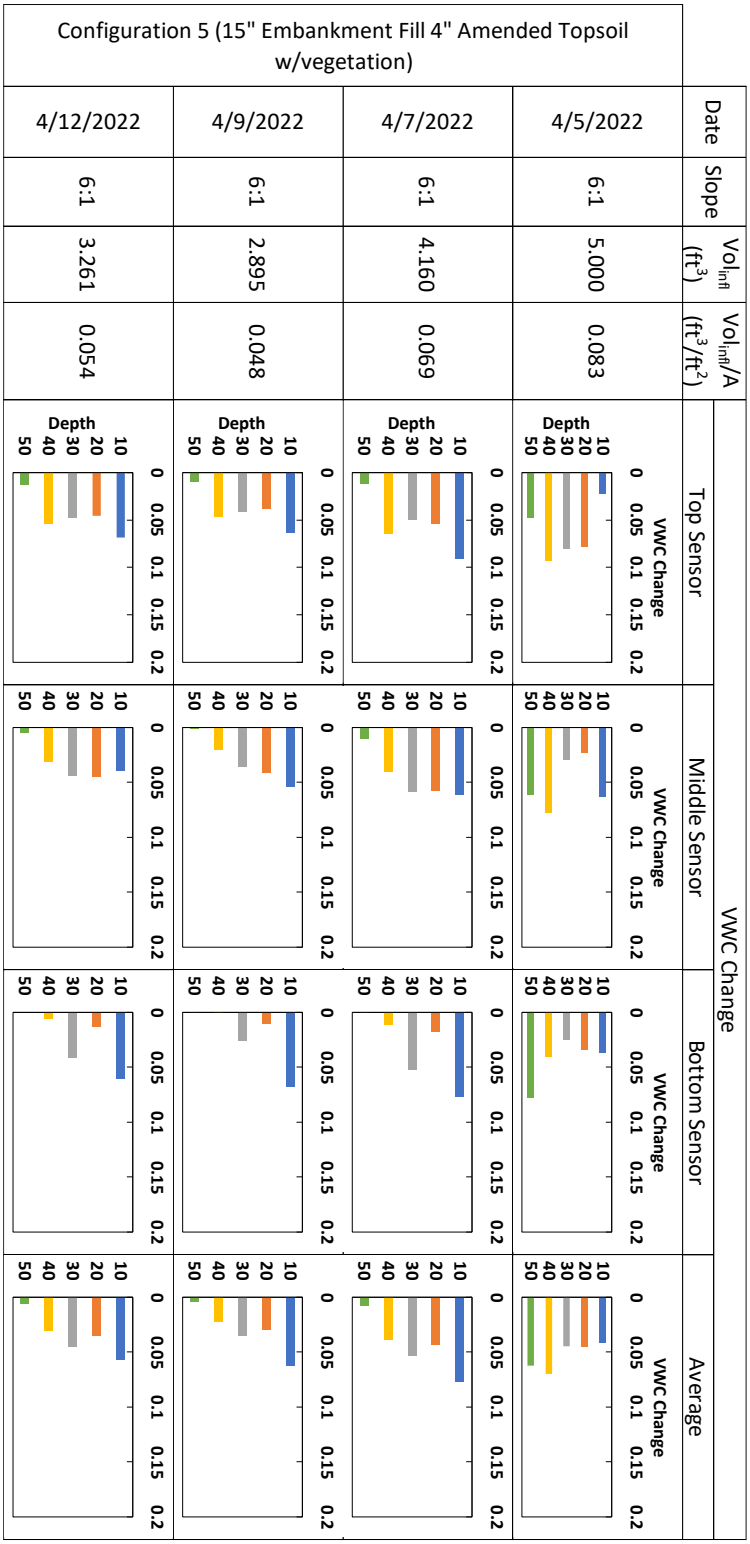

Fig. E13. 14” Embankment Fill 4” Amended Topsoil w/vegetation VWC Change summary table for all tests at a 6:1 slope.

	Date	Slope	Vol_{infl} (ft^3)	Vol_{infl}/A (ft^3/ft^2)	VWC Change			
					Top Sensor	Middle Sensor	Bottom Sensor	Average
Configuration 5 (15" Embankment Fill 4" Amended Topsoil w/vegetation)	4/16/2022	4:1	3.128	0.052	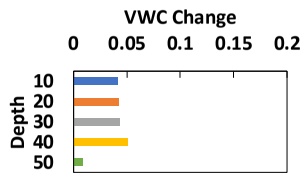	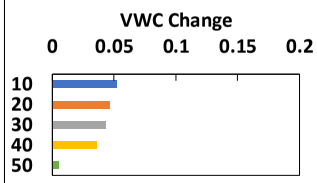	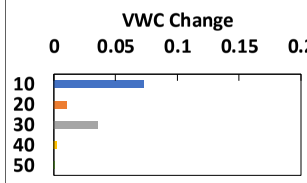	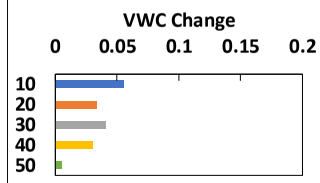
	4/19/2022	4:1	3.398	0.057	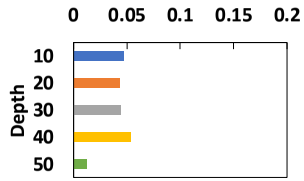	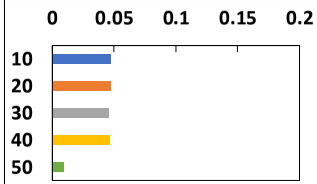	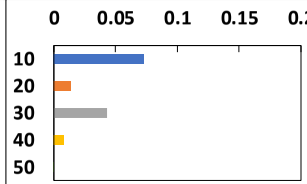	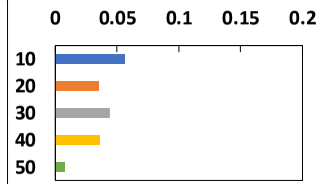
	4/21/2022	4:1	2.882	0.048	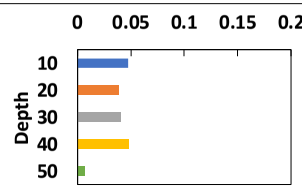	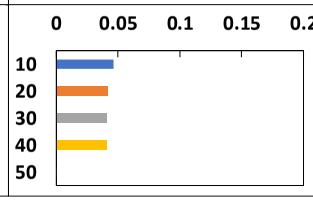	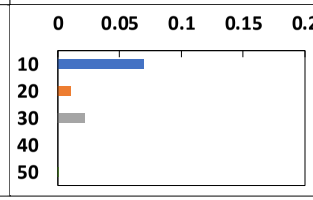	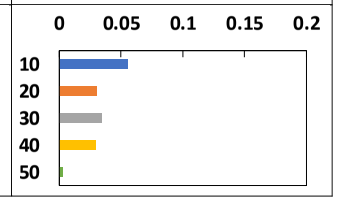

Fig. E14. 14” Embankment Fill 4” Amended Topsoil w/vegetation VWC Change summary table for all tests at a 4:1 slope.

	Date	Slope	Vol_{infl} (ft^3)	Vol_{infl}/A (ft^3/ft^2)	VWC Change			
					Top Sensor	Middle Sensor	Bottom Sensor	Average
Configuration 5 (15" Embankment Fill 4" Amended Topsoil w/vegetation)	4/23/2022	2:1	2.412	0.040	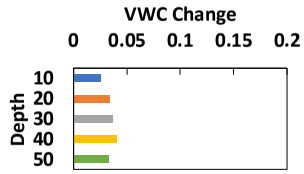	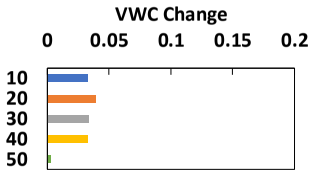	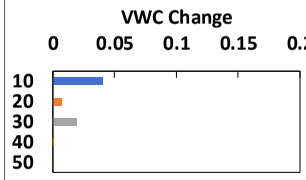	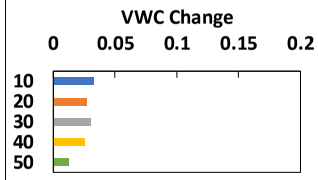
	4/26/2022	2:1	3.178	0.053	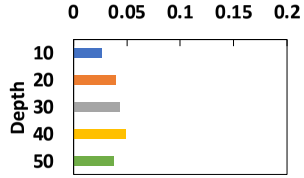	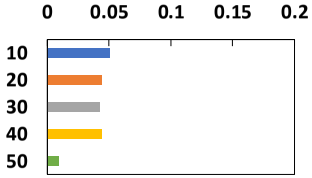	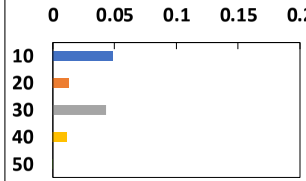	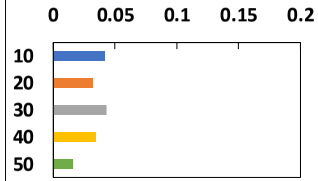
	4/28/2022	2:1	2.505	0.042	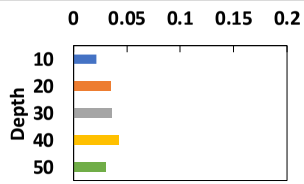	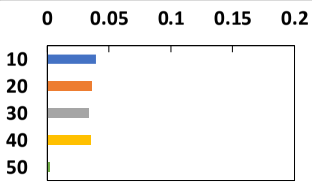	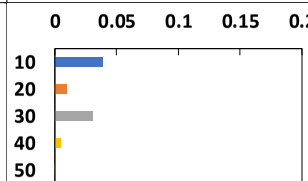	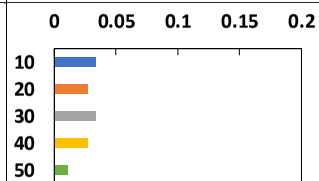

Fig. E15. 14” Embankment Fill 4” Amended Topsoil w/vegetation VWC Change summary table for all tests at a 2:1 slope.

Configuration 6: 15” Embankment Fill (6” Ripped) 4” Topsoil

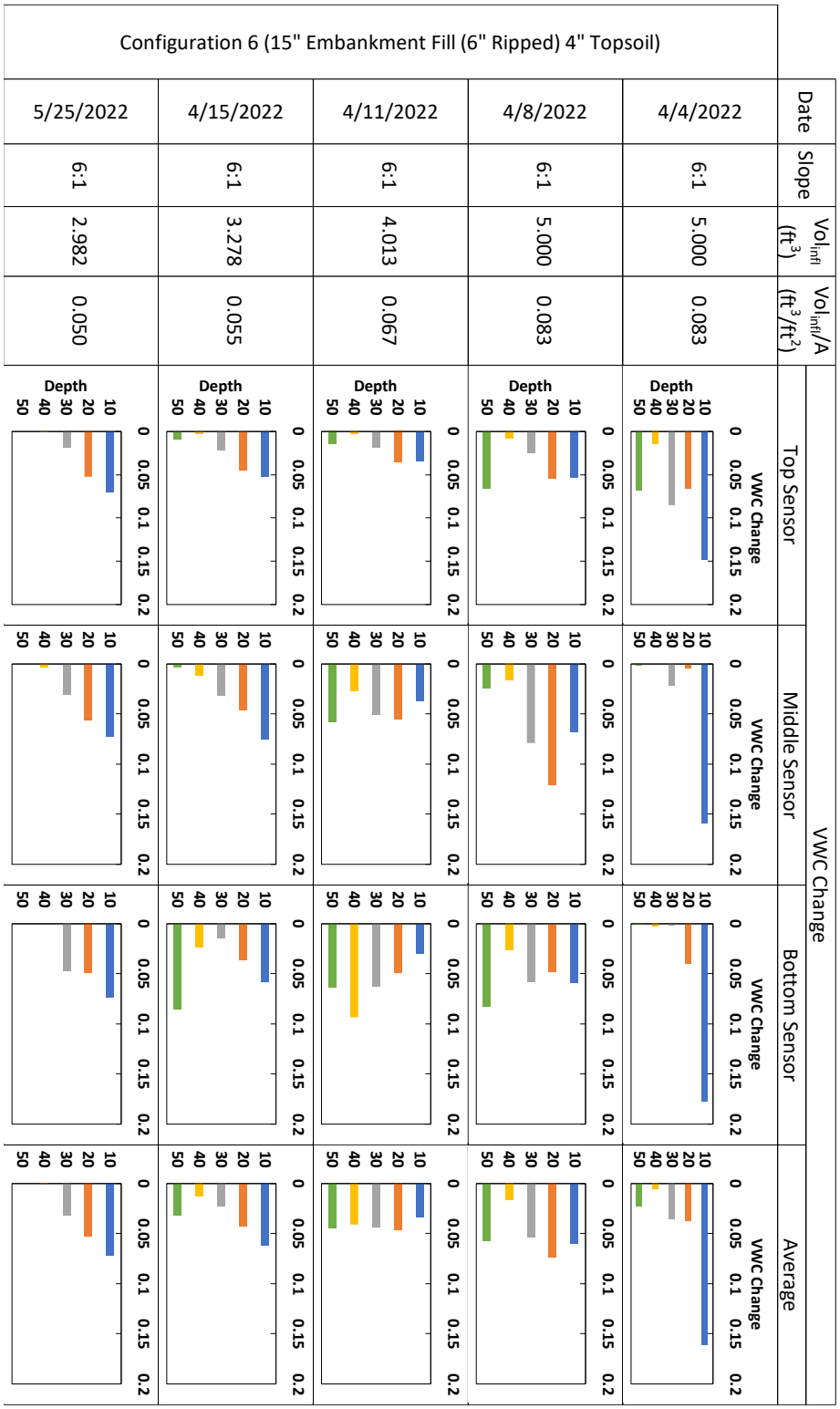

Fig. E16. 14” Embankment Fill (6” Ripped) 4” Topsoil VWC Change summary table for all tests at a 6:1 slope.

	Date	Slope	Vol_{infl} (ft^3)	Vol_{infl}/A (ft^3/ft^2)	VWC Change			
					Top Sensor	Middle Sensor	Bottom Sensor	Average
Configuration 6 (15" Embankment Fill (6" Ripped) 4" Topsoil)	4/18/2022	4:1	1.437	0.024	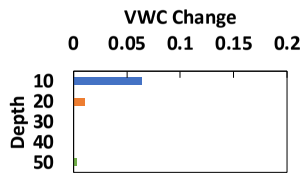	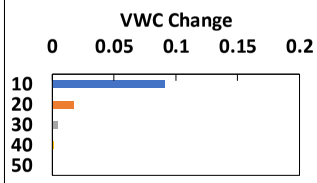	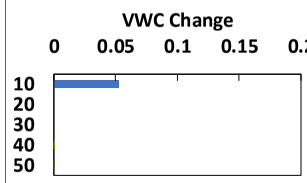	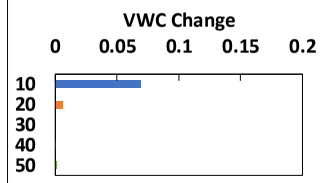
	4/22/2022	4:1	2.156	0.036	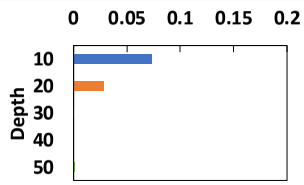	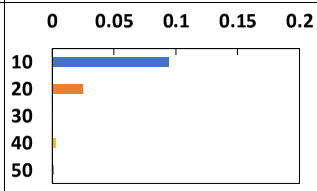	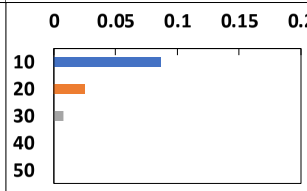	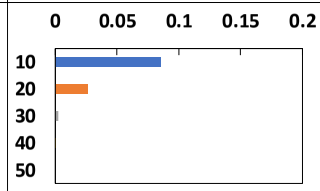
	4/25/2022	4:1	1.466	0.024	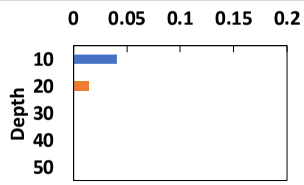	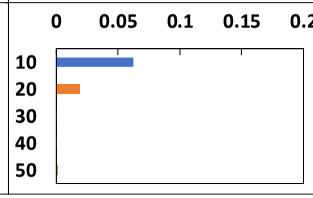	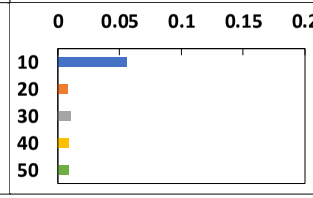	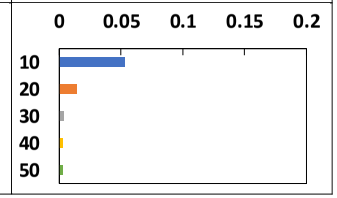

Fig. E17. 14” Embankment Fill (6” Ripped) 4” Topsoil VWC Change summary table for all tests at a 4:1 slope.

	Date	Slope	Vol_{infl} (ft^3)	Vol_{infl}/A (ft^3/ft^2)	VWC Change			
					Top Sensor	Middle Sensor	Bottom Sensor	Average
Configuration 6 (15" Embankment Fill (6" Ripped) 4" Topsoil)	5/3/2022	2:1	1.859	0.031	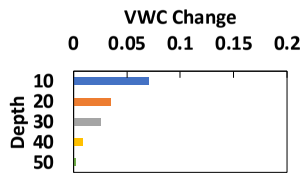	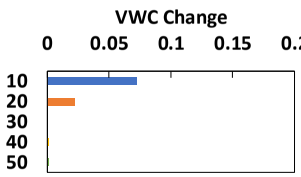	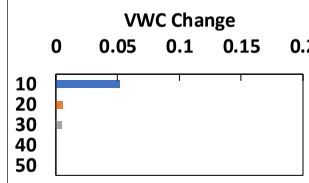	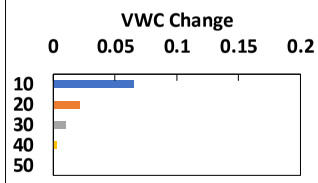
	5/7/2022	2:1	1.705	0.028	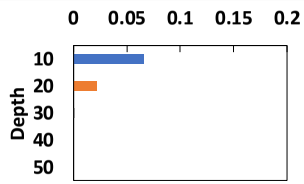	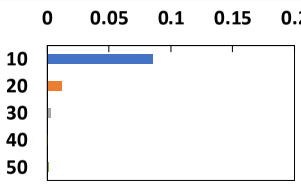	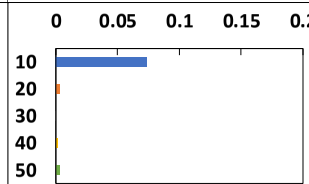	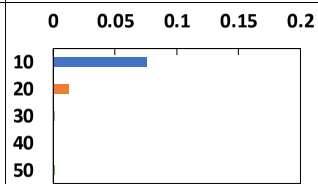
	5/10/2022	2:1	1.528	0.025	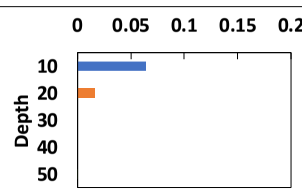	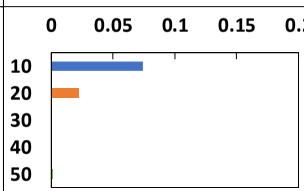	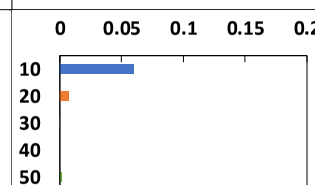	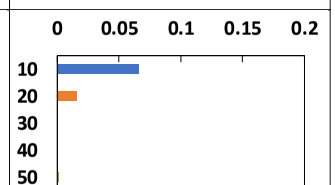

Fig. E18. 14” Embankment Fill (6” Ripped) 4” Topsoil VWC Change summary table for all tests at a 2:1 slope.